Regulation of Autophagy by Acetyl Coenzime A : From the Mechanisms to a Revised Definition of Caloric Restriction Mimetics

Federico Pietrocola

UNIVERSITE PARIS SUD

ÉCOLE DOCTORALE 418
DE CANCÉROLOGIE

Laboratoire : UMR1138 Apoptosis, Cancer & Immunity

THESE

Présentée et soutenue publiquement par

FEDERICO PIETROCOLA

Le 2 septembre 2015

REGULATION OF AUTOPHAGY BY ACETYL COENZIME A: FROM THE MECHANISMS TO A REVISED DEFINITION OF CALORIC RESTRICTION MIMETICS

Composition du jury

Directeur de thèse	Pr. Guido KROEMER	Directeur de Recherche UMR1138 (CRC Paris)
Rapporteur	Pr. Pascal FERRE Dr. Patricia BOYA	Directeur CRC (CRC Paris) Directeur de Laboratoire (CIB-CSIC-Madrid)
Examinateur	Pr. Jose M. FUENTES RODRIGUEZ Pr. Laurence ZITVOGEL Dr. Maria Chiara MAIURI	Directeur de Laboratoire (UNEX Caceres) Directeur de Recherche UMR1015 (IGR Villejuif) Chargé de Recherche UMR1138 (CRC Paris)

INDEX

ABBREVIATIONS

2-DG = 2-DeoxyGlucose

4EBP1 = Eukaryotic translation initiation factor 4E Binding Protein 1

ACAC = Acetyl CoA Carboxylase

AcCoA = AcetylCoA

ACLY = ATP Citrate Lyase

ACO1 = Aconitase 1

ACSS = Acyl-CoA Synthetase Short-chain family

Akt = v-Akt murine thymoma viral oncogene homolog 1

ALDH = Aldehyde Dehydrogenase

AMBRA1 = Activating Molecule in BECN-1 Regulated Autophagy protein 1

AMP = Adenosine MonoPhosphate

AMPK = Adenosine MonoPhosphate-activated Protein Kinase

APP = Aβ-extracellular amyloid plaques derived from Amyloid Precursor Protein

ATF4 = Activating Transcription Factor 4

ATG = Autophagy related

ATP = Adenosine TriPhosphate

Bak = BCL2-antagonist/killer

Bax = BCL2-associated X protein

BCAA = Branched-Chain Amino Acids

BCAT1 = Branched-Chain amino Acid Transaminase 1

BCKD = Branched-Chain α-Ketoacid Dehydrogenase

Bcl-2 = member B-cell lymphoma 2

BDH1 = 3-HydroxyButyrate Dehydrogenase, type 1

BECN1 = Beclin-1

BNIP3 = BCL2/adenovirus E1B 19kDa interacting Protein 3-like

JNK1 = c-Jun N-terminal Kinase 1

CAMMK2 = Calcium/calmodulin-dependent protein Kinase *2*

CLEAR = Coordinate Lysosome Expression And Regulation

CMA = Chaperone Mediated Autophagy

CNS = Central Nervous System

CoA = Coenzyme A

CPT1 = Carnitine PalmitoylTransferase 1

CR = Caloric Restriction

CRAT = Carnitine O-AcetylTransferase

CRM = Caloric Restriction Mimetics

CS = Citrate Synthase

DAMP = Damage-Associated Molecular Pattern molecules

DCA = Dichloroacetate

DEPTOR = DEP domanin containing MTOR-interacting protein

DFCP1 = Double FYVE Containing Protein 1

DLAT = DihydroLipoamide S-AcetylTransferase

DLD = DihydroLipoamide Dehydrogenase

DR = Dietary Restriction

EGFR = Epithelial Growth Factor Receptor

EIF2AK3 = Eukaryotic translation Initiation Factor 2-Alpha Kinase 3

eIF2α = eukaryotic translation Initiation Factor 2 alpha

ER = Endoplasmic Reticulum

ERGIC = ER-Golgi Intermediate Compartment

FIP200 = FAK family kinase activating protein of 200 kDa

FOXO1 = Forkhead box O1

GAAC = General Amino Acids Control

GAG = Glycosaminoglycans

GAP = Guanosine triphosphatase Activating Protein

GATOR = GAP activity towards Rag

GFP = Green Fluorescent Protein

GH = Growth Hormone

GLS = Glutaminase

GOT2 = Glutamic-Oxaloacetic Transaminase 2

GTP = Guanosine TriPhosphate

HSC70 = Heat Shock Cognate 70

HDAC = Histone Deacetylases

HFD = High Fat Diet

HIF1-α = Hypoxia Inducible Factor 1-alpha

HAT = Histone AcetylTransferases

HK-II = Hexokinase-II

HPV = Human Papilloma Virus

ICD = Immunogenic Cell Death

IDH1 = Isocitrate Dehydrogenase 1

IGF-1 = Insulin Growth Factor -1

IGFBP = Insulin-like Growth Factor Binding Protein

Ikkβ = Inhibitor of kappa light polypeptide gene enhancer in B-cells, kinase beta I

IL = Interleukin

KAT = Lysine acetyltransferases

Keap1 = Kelch-like ECH-associated protein 1

LAMP-2A = Lysosome-Associated Membrane Protein 2

ESCRT = Endosomal Sorting Complex Required for Transport

LIR = LC3 Interacting

LKB1 = Liver Kinase B1

LRRK2 = Leucine-Rich Repeat Kinase 2

MAM = Mitochondria-Associated Membrane

MAPK = Mitogen-Activated Protein Kinase

MDH1 = Malate Dehydrogenase 1

ME = Malic Enzyme

MEF = Mouse Embryo Fibroblast

mETC = mitochondrial Electron Transport Chain

MPC = Mitochondrial Pyruvate Carrier

mTORC1 = mammalian Target Of Rapamycin Complex 1

MVB = Multivescicolar Body

NAD = Nicotinamide Dinucleotide

NADH = Nicotinamide Adenine Dinucleotide

NADP = Nicotinamide Dinucleotide Phosphate

NAMPT = Nicotinamide Phosphoribosyltransferase

NBR1 = Neighbor of BRCA1 gene 1

Nrf2 = Nuclear Factor, Erythroid 2-Like 2

OIS = Oncogene Induced Senescence

OXCT1 = 3-Oxoacid CoA Transferase 1

OXPHOS = Oxidative Phosphorylation

PAMP = Pathogen-Associated Molecular Patterns

PDH = Pyruvate Dehydrogenase

PDHX = Pyruvate Dehydrogenase complex, component X

PDK = Pyruvate Dehydrogenase Kinase

PDP = Pyruvate Dehydrogenase Phosphatase

PE = PhosphatidylEthanolamine

PGC-1α = Proliferator-activated receptor Gamma Coactivator 1-alpha

PI3KIII = Class III Phosphatidylinositol-3 Kinase

PINK1 = PTEN Induced putative Kinase 1

PKD = Protein Kinase D

PNPLA5 = Patatin-like phospholipase domain containing 5

PRAS40 = Proline-Rich Akt Substrate of 40 kilodaltons

PTEN = Phosphatase and Tensin homolog

RAPTOR = Regulatory Associated Protein of mTOR

RB1CC1 = RB-1 inducible Coiled-Coil 1

RHEB = Ras Homolog Enriched in Brain

ROS = Reactive Oxygen Species

RTK = Receptor Tyrosine Kinases

SCD1 = Stearoyl-CoA Desaturase

SILAC = Stable Isotope Labeling with Aminoacids in cell Culture

siRNA = small interfering RNA

SIRT1 = Sirtuin 1

SLC = Solute carrier

SQSTM1 = Sequestosome 1

SREBP2 = Sterol Regulatory Element Binding Protein 2

TAB1 = Inhibitors TGF-beta activated kinase 1/ MAP3K7 binding protein 1

TAK1 = Transforming growth factor beta-activated kinase 1

TCA = Tricarboxylic Acid

TFEB = Transcription Factor EB

TSC = Tuberous Sclerosis Complex

ULK1 = UNC51-like Ser/Thr kinases

UPR = Unfolded Protein Response

UVRAG = UV Radiation resistance-Associated Gene

VDAC1 = Voltage-Dependent Anion Channel 1

ZKSCAN3 = Zinc finger with KRAB and SCAN domains 3

I. SUMMARY

Autophagy is a self-digestion process in which cell degrades its own components in order to maintain homeostasis in basal conditions. In absence of nutrients, autophagy is activated and promotes cell survival by providing energetic substrates to sustain stressful condition. Autophagy and metabolism crosstalk at different levels; a drop in energy-rich metabolites, such as ATP and NADH, is detected by cellular sensors (AMPK and SIRT1 respectively) and leads to autophagy activation. Here, we define a further regulatory level of starvation-induced autophagy. In this work, we show that nutrient deprivation is characterized by a rapid depletion of Acetyl CoA, a major integrator of the nutritional status at the crossroads of fat, sugar, and protein catabolism.

Decrease in AcCoA is accompanied by the commensurate reduction in overall protein acetylation levels as well as by autophagy induction. Manipulations designed to increase or reduce cytosolic levels of AcCoA, either targeting mitochondrial synthesis or its transport in the cytoplasm, resulted in the suppression or induction of autophagy both in cultured cells and in mice tissues. Depletion of AcCoA directly impacts on the activity of cellular KATs, which use AcCoA as substrate for acetylating proteins. We showed that a drop in AcCoA specifically reduces the activity of EP300; this KAT was indeed required for the suppression of autophagy by high AcCoA levels, thus behaving as the sensor of cytosolic AcCoA levels. In turn, EP300 controls autophagy by inhibiting key autophagic proteins. Altogether, our results indicate that cytosolic AcCoA functions as a central metabolic regulator of autophagy, thus delineating AcCoA-centered pharmacological strategies that allow for the therapeutic manipulation of autophagy. Indeed, nutrient deprivation and caloric restriction are known to play pro-healthy and longevity promoting effects. Nonetheless, CR-based strategies are hardly suitable in clinical settings. Here, we propose a new biochemical definition of Caloric Restriction Mimetics, compounds that mimic the positive effects of nutrient starvation. In our setting,

a CRM is a compound able to reduce protein acetylation through distinct but convergent mechanisms: first, by decreasing AcCoA levels, second by directly inhibiting KATs, third by the activation of protein deacetylases. This results in the execution of a cellular program ultimately leading to CR-related pro-healthy effects, including but not limited to autophagy.

Keywords: acetylation, caloric restriction, coffee, macroautophagy, metabolism, polyphenols, spermidine, starvation

L'autophagie est un processus d'autodigestion dans lequel la cellule dégrade ses propres composants dans le but de maintenir l'homéostasie dans ses conditions basales. En absence de nutriments, l'autophagie est activée et favorise la survie cellulaire en fournissant des substrats énergétiques résistant aux conditions de stress. Autophagie et métabolisme communiquent à différents niveaux; une baisse en métabolites richement énergétiques, tels qu'en ATP et en NADH, est détectée par des senseurs cellulaires (AMPK et SIRT1 respectivement) et mène à l'activation de l'autophagie. Ici, nous définissons un niveau supplémentaire de régulation de l'autophagie induite par le jeûne. Dans ce travail, nous montrons que cette privation en nutriments est caractérisée par une diminution rapide de l'Acétyl CoA, intégrateur majeur de l'état nutritionnel au carrefour du catabolisme des graisses, des sucres et des protéines. La baisse en AcCoA s'accompagne de la réduction proportionnelle des niveaux généraux d'acétylation des protéines ainsi que par l'induction de l'autophagie. Les manipulations destinées à augmenter ou diminuer les niveaux cytosoliques d'AcCoA, ciblant soit la synthèse mitochondriale soit son transport dans le cytoplasme, résultent en la suppression ou l'induction de l'autophagie aussi bien dans les cultures cellulaires que dans les tissus

de souris. La déplétion en AcCoA impacte directement l'activité des KATs utilisant l'AcCoA comme substrat pour l'acétylation protéique. Nous avont montré que cette baisse en AcCoA réduit spécifiquement l'activité de EP300; cette KAT est en effet nécessaire à la suppression de l'autophagie à des niveaux élevés d'AcCoA, se comportant ainsi comme le senseur des niveaux cytosoliques d'AcCoA. A son tour, EP300 contrôle l'autophagie en inhibant les protéines autophagiques clés. Dans l'ensemble, nos résultats illustrent les fonctions de l'AcCoA cytosolique comme régulateur métabolique central de l'autophagie, délimitant ainsi des stratégies pharmacologiques centrées sur l'AcCoA qui permettent la manipulation thérapeutique de l'autophagie. En effet, la privation en nutriments et la restriction calorique sont connues pour jouer un rôle positif sur la santé et la longévité en promouvant leurs effets. Néanmoins, les stratégies basées sur la restriction calorique sont difficilement applicables en clinique. Ici, nous proposons une nouvelle définition biochimique des Mimétiques de la Restriction Calorique, composés imitant l'effet positif du jeûne. Dans notre contexte, un MRC est un composé capable de réduire l'acétylation protéique par des mécanismes distincts mais convergents: premièrement, par diminution des niveaux d'AcCoA, deuxièmement par inhibition directe des KATs, et enfin, par activation des protéines déacétylases. Ces résultats de l'exécution d'un programme cellulaire conduisent finalement à des effets pro-santé liés à la restriction calorique incluant mais non limités à l'autophagie.

Mots Clefs: acétylation, restriction calorique, café, macroautophagie, métabolisme, polyphenoles, spermidine, jeun

II. INTRODUCTION

A. GENERAL PRINCIPLES OF THE AUTOPHAGIC PATHWAYS

Under the term autophagy (from the Greek "αὐτός" oneself and "φαγεῖν" to eat) fall different cellular processes culminating into the delivery of cytoplasmic material to lysosomes for its degradation by acidic hydrolases. The macromolecular building blocks, deriving from this lytic event, are then used to fuel bioenergetics reactions necessary for maintaining cellular fitness. In particular, three forms of this process have been described so far: Chaperone Mediated Autophagy (CMA), Microautophagy and Macroautophagy.

These cellular phenomena differ among them for the modality and the selectivity of the cargo to be delivered to lysosomes. In CMA, cytosolic proteins, bearing the pentapeptidic KFERQ-motif, are selectively recognized by the chaperone heat shock cognate 70 (HCS70) and co-chaperones system; after interacting with the lysosomal receptor Lysosome-associated membrane protein 2 (LAMP-2A), the unfolded proteins translocate into the lysosmal lumen (Kaushik and Cuervo, 2012). Microautophagy allows the degradation of cytosolic components by direct invagination of lysosomal membrane and membrane remodeling, during this process involves, as for late endosome system, the formation of multivesicular body (MVB) in which cargos are engulfed (Sahu et al., 2011). This system is based on endosomal sorting complex required for transport (ESCRT) -I and -III and the chaperone HSC70 but not on LAMP-2A. Conversely, macroautophagy implicates the sequestration of distinct cargos into a characteristic double-membrane vescicle defined as autophagosome, which eventually fuse with the lysosomal membrane for the degradation and recycling of its content. The formation and the maturation of the autophagosome occur in different steps and they are orchestrated by a series of autophagy related proteins (Mizushima et al., 2011), whose roles will be examined in

detail in this dissertation. Although these three processes have been demonstrated to play a role in physiological and pathological settings (Mizushima et al., 2008), macroautophagy (herein simply defined as autophagy) is thought to be the major type of autophagy in cells.

Autophagy represents a housekeeping mechanism adopted with the purpose of maintaining cellular homeostasis via turnover of organelles and long-lived proteins, hence ensuring the removal of potential harmful entities. For this reason, autophagy occurs in all cells (Mizushima and Komatsu, 2011) at a baseline (yet-cell-specific) level; getting rid of 'cellular garbage' does not entirely reflect the plasticity of this process. Effectively, autophagic rate can dramatically increase as a consequence of the alteration of cellular *status quo*. Examples of stressful conditions able to induce autophagy include (but they are not limited to) nutrient deprivation (Mizushima et al., 2010), hypoxic stress (Bellot et al., 2009), a large panel of cytotoxic agents (Kroemer et al., 2010) and invading pathogens (Levine and Deretic, 2007).

Based on these premises, it appears evident as autophagy works mainly as a pro-survival pathway intervening to avoid cellular demise. Notwithstanding this consideration, in the recent past, the presence of autophagic vacuoli in dying cells led to the association of this process to a regulated cell death type (type II cell death or autophagic cell death), mainly based on morphological observations. It is now accepted that, except in particular settings (*i.e.* developmental program in flies (Nezis et al., 2009); (Mohseni et al., 2009)) or cancer cells lacking apoptotic mediators (Baehrecke, 2005), the definition of autophagic cell death should be applied to phenomena of cellular demise which can be *bona fine* inhibited by the silencing or the chemical inhibition of autophagic essential genes (Baehrecke, 2005).

In 2013, Levine's group has described, *in vitro* and in hippocampal hypoxic neurons *in vivo*, a new form of autophagic regulated cell death, defined as autosis (Liu et al., 2013). Autosis is triggered by a sustained stress produces by an autophagy inducing peptide as well as long-term nutrient deprivation and can be blocked upon genetic or pharmacological inhibition of autophagy. Interestingly, this phenomenon relies on the presence of Na^+/K^+-ATPase on plasma membrane and can hence be inhibited by cardiac glycosides. Whether Na^+/K^+-ATPase dependency is a common feature of autophagic cell death modes remains to be clarified.

B. MECHANISMS AND REGULATION OF AUTOPHAGOSOME FORMATION

Autophagy is an evolutionary conserved process characterized by the presence of a peculiar double-membrane organelle: the autophagosome. The autophagosome surrounds portions of cytoplasm and undergoes progressive maturation for acquiring lytic property after fusion with lysosome (hence forming a so-called autophagolysosome) and for the degradation of its substrates (Boya et al., 2013). Autophagosome biogenesis has been object of extensive studies in yeast Cvt pathway (Kim and Klionsky, 2000), which led to the identification of 37 autophagy related ATG genes involved in this process (Kim and Klionsky, 2000). In this section, only ATG genes participating in mammalian autophagy will be objet of discussion.

Autophagosome formation represents a *sine-qua non* step in the autophagic reaction and can be functionally divided into three distinct phases: initiation, nucleation and expansion. For brevity, we will analyze in detail the core pathway of autophagosome formation, composed of 4 main molecular actors: (i) Atg1/Ulk complex, (ii) Beclin-1 (BECN1)/Class III phosphatidylinositol-3 kinase (PI3K), (iii) the Ubiquitin-like conjugation system and (iv) a series of proteins involved in the fusion of autophagosome with lysosome. The regulation of autophagosome formation is resumed in Figure 1.

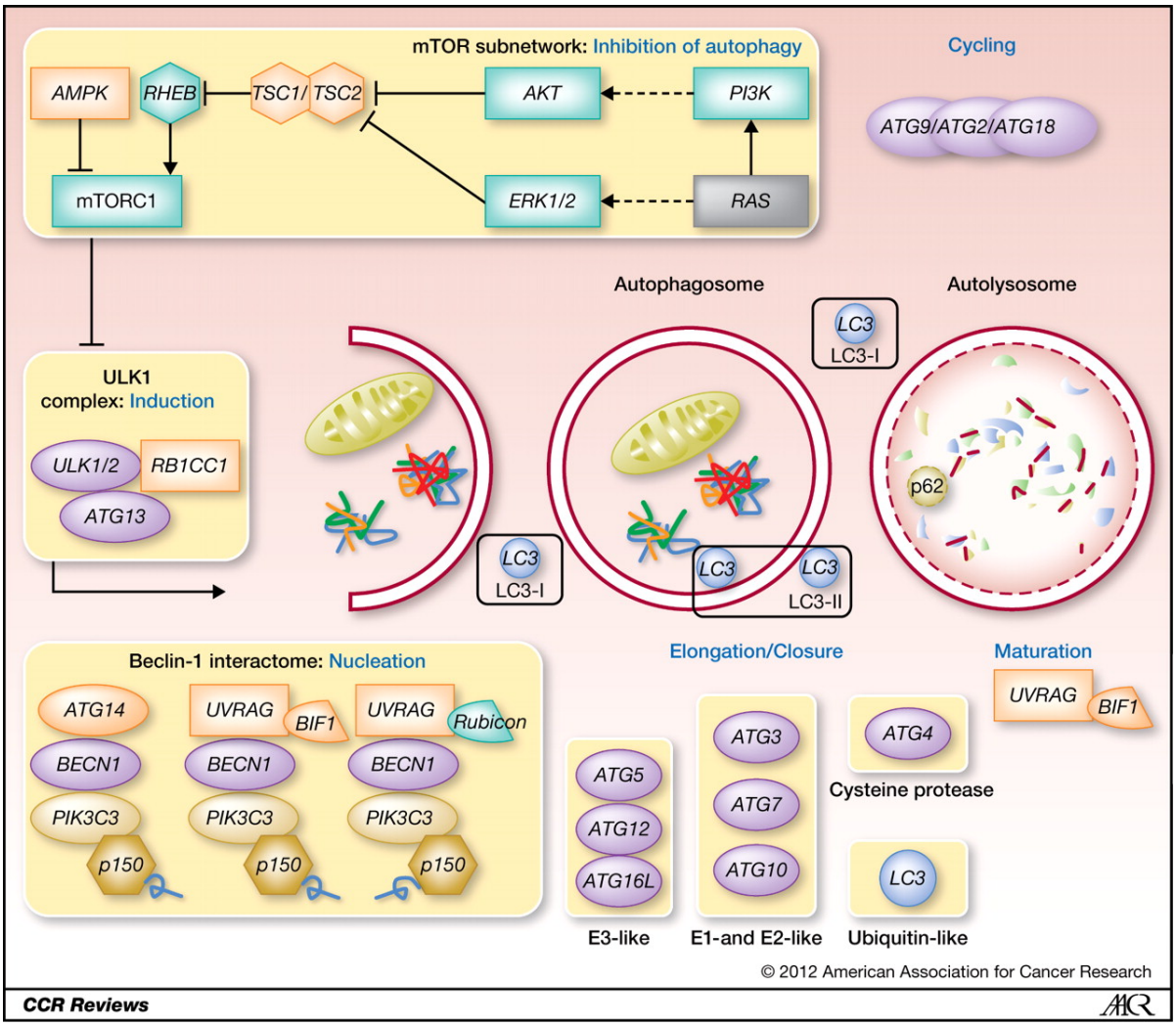

Figure 1. (Lebovitz et al., 2012). Scheme depicting molecular actors involved in different steps of autophagosome formation.

At the top of this hierarchic system is placed the ULK-complex, necessary for the initiation phase of autophagy (He and Klionsky, 2009). This complex is formed by UNC51-like Ser/Thr kinases ULK1 (ortholog of yeast Atg1 protein) and ULK-2, ATG13, FAK family kinase activating protein of 200 kDa (FIP200) and ATG101. ULK1/2 kinases are activated by nutrient deprivation signals and phosphorylate ATG13 and FIP200 for promoting autophagy initiation (Chan, 2009). ULK complex represents the major regulatory hub of autophagy initiation: its function is placed downstream the control of mammalian Target of Rapamycin complex 1 (mTORC1), integrator of energetic inputs deriving from insulin signaling and amino acids availability into translation and activation of anabolic processes as well as master repressor of autopahgy (Jewell et al., 2013). mTORC1 (composed of mTOR1, RAPTOR, mLST8/GβL and the inhibitor proteins DEPTOR and PRAS40) (Sengupta et al., 2010) retains Ser/Thr kinase activity and interacts-with and phosphorylates at inhibitory sites ULK1/2 and ATG13 thus promoting their dissociation and hence limiting autophagy induction in nutrient-rich condition (Hosokawa et al., 2009). Upon inhibition of mTORC1 by starvation, kinase activity of ULK towards its interactors, is unleashed and triggers autophagy (Jung et al., 2009), (Hosokawa et al., 2009)). The central role of ULK in starvation-induced autophagy is confirmed by the fact that mouse embryonic fibroblasts (MEFs) ULK1/2$^{-/-}$ are unable to mount an autophagic response in response to nutrient deprivation (Alers et al., 2012). mTORC1 activity is finely regulated by a monomeric G-protein system. To be active, mTORC1 needs to colocalize on lysosomal membrane surface with the small G-protein Rheb loaded with GTP (Sengupta et al., 2010). Tuberous sclerosis complex (TSC) 1/TSC2 complex possesses GTPase activity for Rheb and inhibits mTORC1 function, mainly depending on amino acids availability via mechanisms that will be discussed in the "**Autophagy and metabolism crosstalk"** section. As already mentioned, mTORC1-ULK axis is the focal point of autophagy regulation and offers the

opportunity of feedback and feedforward mechanisms for the control of this process by different signaling pathways mediators: besides amino acids, insulin/ insulin growth factor -1 (IGF-1)-PI3KC1- v-akt murine thymoma viral oncogene homolog 1 (Akt) axis enhances mTOR activity via inhibitory phosphorylation of TSC2 and proline-rich Akt substrate of 40 kilodaltons (PRSA40) (Vander Haar et al., 2007), hence blocking autophagy. In the context of energetic stress, a pivotal role is played by adenosine monophosphate-activated protein kinase (AMPK), a sensor of adenosine monophophate (AMP)/ adenosine triphosphate (ATP) ratio and energetic stress (Hardie et al., 2012) necessary for starvation-induced autophagy (Egan et al., 2011).

AMPK-mediated induction of autophagy can be attributed to two different mechanisms: first, AMPK inactivates mTOR via phosphorylation of TSC2 (Inoki et al., 2003), (Li et al., 2004) and Raptor (Gwinn et al., 2008). Secondly, AMPK can directly control autophagy via ULK1 activation by phosphorylation promoting its dissociation from mTORC1 (Egan et al., 2011). Although it is clear that ULK complex is the major regulator of autophagy induction, it remains to be established how it can regulate the other mediators of autophagosome formation. ULK/ATG13/FIP200 can be considered as the pre-initiation complex necessary for the activation of the autophagic cascade.

Downstream of this complex is localized the initiation complex *ipso dicto*, which represents the scaffold for autophagosome nucleation (Mizushima, 2007). Indeed, autophagosome formation takes place around phosphatidylinositol-3-phosphate domains on the phagophore membrane. The initiation complex is propaedeutic for the allosteric activation of phosphatydilinositol-3 kinase class 3 (PI3KC3) Vps34, responsible for the phosphorylation of phosphatidylinositol on membranes for generating PI(3)-P domain (Kihara et al., 2001). This multiprotein complex thus consists of Vps34, a myristoylated Ser/Thr kinase Vps15, Atg14, activating molecule in Beclin-1 induced-autophagy 1 (AMBRA1) and Beclin-1, the latter representing the core of this structure.

The characterization of Beclin-1 interactome (He and Levine 2010) has permitted the identification of several proteins able to tune autophagic reaction and has highlighted Beclin-1 like another center of autophagy regulation, as confirmed by the fact that *Becn1*$^{-/-}$ mice die early in embryogenesis (Yue et al., 2003). Among its partners, Ambra1 (interacting with Beclin-1 via WD40 domain) is able to activate Beclin-1 dependent autophagic program and constitutes a central mediator of the process as confirmed by the fact that Ambra1$^{-/-}$ mice present severe impairment in central nervous system (CNS) development and signs of non-functional autophagy (Fimia et al., 2007)). Furthermore, Ambra1 plays a role in the relationship between autophagosome formation and cytoskeleton (Di Bartolomeo et al., 2010); indeed, the initiation complex interacts with Dinein light chain 1 and 2 via Ambra-1. Upon autophagy induction, Ambra1 is phosphorylated by ULK-1 (and counter-phosphorylated by mTORC1 in nutrient-rich conditions) thus allowing the release of the complex from cytoskeleton and its relocalization to endoplasmic reticulum (ER), a possible site of the autophagosome formation. (Di Bartolomeo et al., 2010)

Atg14, another mediator, essential for PI3KC3 function and autophagy induction, interacts with the coil-coiled domain of Beclin-1 and competes with the other autophagy regulator UV radiation resistance-associated gene (UVRAG) (Li et al., 2012). The main function of Atg14 in autophagy modulation consists of, but it is not limited to, the recruitment of PICKC3 complex to ER (Matsunaga et al., 2010). An Atg14 point mutant, unable to localize at the ER, fails to mount an effective starvation-induced autophagy (Matsunaga et al., 2010). Sequence analysis of Atg14 led to the identification of Barkor autophagosome targeting sequence (Bats) domain that is necessary for the direct binding to autophagosomes (Fan et al., 2011). Furthermore, Atg14 has been found to preferentially localizes at highly-curved and PI(3)P-enriched membranes, thus revealing a possible role of this protein in curvature sensing and maintenance of autophagosome structure. Moreover, in

nutrient deficient conditions, Atg14 also facilitate the autophagosome formation by releasing the constitutive inhibition mediated by the connexins, the main component of plasma protein GAP-Junction (Bejarano et al., 2014). Additionaly, it has been shown that ULK1 induces autophagy by directly phosphorylating Beclin-1 and Vps34 (Russell et al., 2013) in a sort of feed forward mechanism for achieving maximal autophagy induction; Beclin-1 phosphorylation depends on the presence of Atg14 in the complex (Fogel et al., 2013). At this stage, it is important to stress the concept that different Vps34 complexes exist, having pro- and anti-autophagic functions. In particular, upon nutrient starvation, AMPK inhibits non-autophagic Vps34 complexes and indirectly activate Vps34 pro-autophagic complex via Beclin-1 phosphorylation. Importantly, this event is strictly controlled by the presence of Atg14 in the Beclin-1 complex (Kim et al., 2013).

Another crucial point of regulation in the Beclin-1 interactome maze is represented by the UVRAG-Rubicon axis. UVRAG is an oncosuppressor gene found mutated in colon cancer (Kim et al., 2008b) and it behaves as a positive modulator of Beclin-1 dependent autophagosome maturation. UVRAG is found in the Beclin-1 complex in a mutually exclusive manner with respect to Atg14; similarly, the negative autophagy regulator Rubicon inhibits autophagy depending on the presence on UVRAG in the complex (Matsunaga et al., 2009). These notions underline that the distinct composition of Beclin-1 complexes at different stages of autophagosome maturation represents yet another level of modulation of the pathway. Moreover, it has been recently demonstrated that UVRAG undergoes inhibitory phosphorylation by mTORC1 (Kim et al., 2015). Importantly, UVRAG is also able to interact with VpsC/HOPS complex, thus ensuring a crosstalk between the endocytic and autophagic pathway (Kim et al., 2015). Besides being a central regulatory point of autophagic process, Beclin-1 is also implicated in the fine balance of life-or-death signals. In particular, it has been demonstrated that the anti-apoptotic member B-cell lymphoma 2 (Bcl-2)

(Pattingre et al., 2005) interacts-with and inhibits Beclin-1, thus maintaining autophagy at a baseline level in normal condition. In presence of pro-autophagic signals, such as hypoxia or nutrient deprivation, Beclin-1 is released by this inhibition; this occurs by means of increased expression of BH3 pro-apopototic members (Maiuri 2007) or by activation of c-Jun N-terminal kinase 1 (JNK1) (Pattingre et al., 2009). Beclin-1-PI3KC3 dependency in the autophagosome formation is one of the parameters used for classifying canonical or non-canonical forms of autophagy (Codogno et al., 2012).

Under particular circumstances or specific stimuli (i.e. etoposide, neurotoxins (Codogno et al., 2012)), the autophagosome formation step does not require Beclin-1-PI3KC3 complex. Furthermore, our group has recently found that unsaturated fatty acids such as oleic acid are able to stimulate a form of autophagy independent on both Beclin-1/PI3KC3 complexes and ULK-1/AMPK signaling. (Niso-Santano et al., 2015). Interestingly, this form of non-canonical autophagy relies on an intact Golgi apparatus, possibly indicating this organelle as the main source of autophagic membrane in this setting.

Upon pro-autophagic stimuli, the net result of this intricate regulatory network is the recruitment at PI(3)P scaffolding site of PI(3)P binding proteins necessary for autophagosome nucleation; the effectors are mainly constituted by DFCP1-domain containing proteins and Atg18/WIPI (and its interactor Atg2) (Axe et al., 2008).

Among the molecules recruited at the PI(3)P sites, a cardinal role in the autophagosome elongation and expansion steps is carried out by Atg12-Atg5-Atg16 and LC3-Phosphatidylethanolamine (PE) conjugation systems (Mizushima et al., 1998), in which Atg12 and LC3, like ubiquitin, undergo subsequent reactions in order to be attached to their substrates. In the

first pathway, Atg12 is covalently linked to Atg5 by the activity of the E1-Like activating enzyme Atg7 and the E2-like protein Atg10. The resulting Atg12-Atg5 conjugate interacts in a non-covalent manner with Atg16, which in turn organizes Atg12-Atg5 dimers around a multimeric structure linked to the autophagosome membrane via self-oligomerization. Importantly Atg12-Atg5-Atg16 tetramers serve as E3 enzyme in the LC3-PE conjugation system. In the second Ub-like conjugation system, LC3 first undergoes a proteolytic cleavage mediated by the cysteine protease Atg4, which leaves a Glycine residue exposed at LC3 C-terminus. Pre-processed LC3 is then activated by the E1 Atg7, associated to Atg3 and eventually linked to the membrane via amide bond between Gly and the membrane lipid PE. Although the Atg12-Atg5-Atg16 E3 is not strictly necessary for LC3-PE conjugation, it facilitates this step and it controls the positioning of the autophagosome synthesis site (Kaufmann et al., 2014).

Importantly, the cleavage of LC3 and the subsequent conjugation it is a widely used marker for monitoring autophagy induction; specifically, this event leads to the conversion of the cytosolic soluble form of LC3 to an unsoluble variant when LC3 is conjugated to the forming autophagosome (Klionsky et al., 2012). This process can be followed by tagging LC3 with a fluorescent marker such as green fluorescent protein (GFP) and by counting the so-called GFP-LC3 positive *puncta*. Conversely, autophagy induction can be monitored by evaluating the 2 kDa shift in the molecular weight of the cleaved form of LC3 (LC3-II). It is useful to highlight the fact that at the steady state, the autophagic level at a single-cell level is a consequence of a dynamic balance between the autophagosome formation and degradation. For this reason, autophagy must be evaluated in terms of autophagic flux, exploiting chemical inhibitors of the fusion of autophagosomes with lysosomes such as bafilomycinA1 or lysosomotropic agents like the anti-malaric chloroquine (Klionsky et al., 2012). Alternatively, the degradation of the LC3 interacting protein p62/ sequestosome 1 (SQSTM1) or the

degradation of radioactive-labeled long-lived proteins can be used as markers of *bona fide* autophagy induction.

The final step of autophagic reaction is represented by the fusion of the autophagosomal membrane with the lysosome; this occurs via a canonical pathway of cellular vescicle fusion; for autophagy, the system requires the lysosomal protein lysosome-associated membrane protein 2 (LAMP2) and the component of late-endosome/Trans-Golgi network Rab7 (Jager et al., 2004). After fusion, the degradation of the inner content of the autophagolysosome is mediated by different forms of Cathepsin (A, B and L in mammalian cells), which in turn are activated by the acidic lysosomal environement (Tanaka et al., 2000).

Although the molecular mechanisms and the complex interactions, among the different Atg proteins, orchestrating the autophagic process, have been (and are being) extensively characterized, it remains to be established the cellular origin of the autophagosomal membrane in mammalian cells. Different sites have been proposed as possible sources of the isolation membrane. In particular, through the detailed analysis of the double FYVE-containing protein 1 (DFCP1) protein, it has been shown (Axe et al., 2008) that, in condition of autophagy induction, isolation membranes emerged from PI(3)P- and DFCP1-enriched structures localized at the ER, named omegasomes for their characteristic shape. The translocation of DFCP1 from an intermediate Golgi-ER compartment to ER, upon nutrient depletion, relies on Vps34 and Beclin-1 function (Axe et al., 2008). Furthermore, Atg14l forms punctate structure at ER-level and it is necessary for the autophagosome biogenesis (Matsunaga et al., 2010). As further confirmation of this hypothesis, it should be noted that PI3-K inhibitors, such as 3-methyladenine or wortmannin, inhibit autophagy as well as omegasome formation (Axe et al., 2008).

Additionally, another line of investigation has instead proposed the mitochondrial membrane as the major source of autophagosomal membrane during starvation (Hailey et al., 2010), driven by the fact that an outer mitochondrial membrane protein colocalized with LC3 positive structures. The apparent divergence between the two sites of autophagosome biogenesis can be explained by a recent work (Hamasaki et al., 2013) in which the contact site between mitochondria and ER is described as the source of the isolation membrane. Indeed, the disruption of ER-mitochondria contact sites, by knocking out mitofusin-2, severely impaired the autophagosome formation. Moreover, mitochondrial associated ER-membranes are enriched of class III PI3-K components, such as Beclin-1, Vps34 and Atg14l, whose localization at mitochondria-associated ER membrane (MAM) is specifically controlled by syntaxin17.

Recently, other possible sites of membrane source have been proposed and include the plasma membrane (Ravikumar et al., 2010), the ER-Golgi intermediate compartment (ERGIC) (Ge et al., 2013) and the late endosome compartment. (Puri et al., 2013)

For concluding this section, it is important to underline the peculiar function of Atg9 in the autophagosome biogenesis. This protein is the only identified transmembrane Atg proteins and it is dynamically found associated to the isolation membrane and the autophagosome (JBC 2010 Reggiori). Importantly, Atg9 is able to cycle from trans-Golgi network to the autophagosome membrane in vescicles that have been suggested as a possible source of membrane (Mari et al., 2010).

C. HOUSEKEEPING FUNCTIONS OF AUTOPHAGY

Cells have adopted different processes for maintaining their own homeostasis and preserving their vital function upon basal conditions. In this setting, autophagy participates at cellular well being through different activities mainly represented by the elimination of damaged/long-lived proteins and organelles, the removal of aggregation-prone proteins and the elimination of intracellular pathogens. Failure of any of these functions constitutes the basis for the pathogenesis of autophagy-deficient diseases such as cancer, aging, neurodegenerative diseases and infections.

Whereas the so-called bulk or non-selective autophagy intervenes in response to general signals such as nutrient deprivation, the execution of these housekeeping functions relies on selective forms of autophagy, in turn depending on autophagy receptors and ubiquitin-like protein mediating these tasks. However, the boundaries between selective and not-selective autophagy are labile: selective organelle turnover occurs also during starvation-induced autophagy, as in the case of ribosomes (Cebollero et al., 2012) or peroxisomes (Kim and Klionsky, 2000), as well as the removal of aggregates (Lamark and Johansen, 2012) and the elimination of intracellular pathogens, likely for the redundancy in the pathways leading to autophagy activation. Similarly, the lack of *in vivo* models of selective-autophagy renders hard the dissociation of bulk *versus* selective phenotypes; as a caveat, it should be mentioned that the availability of tissue-specific Cre-controlled knockout models of autophagy essential genes *Atg5* and *Atg7* (*i.e* adipocytes, acinar cells, dendritic cells etc) presumably allows the investigation of the defective selective-autophagy phenotype related to the differentiated cell-type commitment.

The main forms of selective autophagy include (i) aggrephagy (removal of protein aggregates), (ii) mitophagy (elimination of aged/damaged mitochondria), (iii) pexophagy (dismissal of peroxisome), (iv)reticulophagy (elimination of parts of ER membranes) and (v) xenophagy

(elimination of intracellular pathogens). Forms of selective autophagy can also play an active role in the mobilization of energy stores as in the case of lipid droplets (lipophagy) or glycogen granules (glycophagy). (Green and Levine, 2014)

The direct consequence of 'doing-homework' is that autophagy itself may serve as a guardian of genome stability (Mathew et al., 2007) preventing cellular transformation as well as regulating the life-death balance (Maiuri et al., 2007).

As for the proteasomal system, autophagy participates in protein turnover and quality control via lysosomal degradation of long-lived, damaged and misfolded proteins. In spite of this apparent redundancy in the function, autophagy retains the unique capacity of sequestering and eliminating whole organelles and pathogens thus representing a 'Swiss-knife' for several cellular tasks, using ubiquitin as signal molecule (Kirkin et al., 2009b).

As previously mentioned, the basis for selective autophagy is the existence of autophagy receptor recognizing ubiquitinated substrates. p62/SQSTM1 has been the first identified autophagy-receptor (Pankiv et al., 2007) and actively participates in the clearance of ubiquitinated proteins and protein aggregates. Indeed, p62 presents a peculiar structure: a N-terminal domain necessary for self oligomerization, a central domain of interaction with different protein and a C-terminal domain which confers to this protein the ability to bind ubiquitin, with a marked preference for K63-polyUbiquitin chains chains (Pankiv et al., 2007). Importantly, p62 takes part into the autophagy-mediated Ub-protein and aggregates clearance via a LIR (LC3 interacting) domain, through which it binds non-covalently LC3 and GABARAPL isoforms.

Autophagy deficient cells are characterized by an accumulation of protein aggregates positive for p62 (Bjorkoy et al., 2005). Remarkably, p62 interacts with several E3 Ubiquitin-ligase proteins,

such as kelch-like ECH-associated protein 1 (Keap1), responsible for the degradation of the stress responsive transcription factor Nuclear Factor, Erythroid 2-Like 2 Nrf2 (Ichimura et al., 2013). Interestingly, p62 competes with Nrf2 for the binding to Keap1 and conditions of autophagy deficiency lead to the accumulation of p62 and the consequent activation of Nrf2 gene targets (Komatsu et al., 2010). Moreover, both p62 accumulation and Nrf2 activation have been linked to pathological phenotypes such as hepatocellular carcinoma and neurodegeneration (Levine and Kroemer, 2008). Hence, p62 plays a dual role in autophagy regulation: it represents itself an autophagic substrate and it is an adaptor for autophagic cargos.

Like p62, another autophagy receptor, neighbor of BRCA1 gene 1 (NBR1) retains the ability to bind both LC3 and ubiquitinated substrates independently on p62 (Kirkin et al., 2009a). NBR1 appears to play a key role in pexophagy (Deosaran et al., 2013). Ubiquitination is also determinant for the autophagic removal of damaged mitochondria; upon condition of mitochondrial depolarization and loss of inner membrane potential, the PTEN induced putative kinase 1 (PINK1) translocates to the outer mitochondrial membrane and in turn phosphorylates and recruits the U3 ligase Parkin (Geisler et al., 2010). Parkin promotes the ubiquitination of different targets on the outer mitochondrial membrane (including voltage-dependent anion channel 1 (VDAC1), Mitofusin) and favors their recognition via different autophagy receptor, such as p62 (Geisler et al., 2010), optineurin (Wong and Holzbaur, 2014) and NBR1 (Kirkin et al., 2009a). The requirement of adaptor receptors for mitophagy partially explains the complexity of this mechanism. Several components of the autophagic machinery are recruited on damaged mitochondria, independently of LC3 and p62, possibly suggesting an alternative model where mitochondria provide a *de novo* source of membrane for their own degradation (Itakura et al., 2012). Recently, it has emerged how BCL2/adenovirus E1B 19kDa interacting protein 3-like (BNIP3L, well known as NIX) and BNIP3 can also behave as

mitophagy specific receptor (Zhang and Ney, 2009). These proteins can promote the opening of BCL2-associated X protein (Bax)/ BCL2-antagonist/killer (Bak) permeability transition pore, thus causing loss of membrane potential, and recruit LC3 via their LIR domain (Novak et al., 2010); furthermore, both proteins share the capacity to dissociate Beclin-1 from Bcl-2 triggering mitophagy.

D. AUTOPHAGIC RESPONSE TO METABOLIC STRESS: THE CROSS-TALK BETWEEN AUTOPHAGY AND METABOLISM

Nutrient deprivation is the most physiological stimulus able to induce autophagy (Mizushima, 2007), both *in vitro* and *in vivo*. When cell lines are cultured in extracellular medium devoid of nutrients, the autophagic response is rapidly (within minutes) activated, hence allowing a prompt adaptation to starvation conditions. In particular, autophagy is activated as consequence of the concurrent absence of glucose (or low glucose concentrations, especially for highly glycolytic cancer cell lines) and amino acids or in response to serum (and consequently growth factors) deprivation (Mizushima and Komatsu, 2011). Similarly, when mice undergo a period of 24-48 hours starvation, autophagy is activated in the majority of mice tissues with some exceptions such as brain (Mizushima et al., 2004), likely due to Glucose-mediated protection at cerebral level.

Unlike selective autophagy, nutrient scarcity activates a bulk autophagic process in which large portions of cytoplasm are unselectively targeted to lysosomal degradation (Klionsky and Emr, 2000). It is probable that the basis of the phylogenetic conserved nature of autophagic process is the adaptation to nutrient deficient conditions and more generally to different types of metabolic perturbations. When cellular homeostasis is altered by metabolic stressors autophagy can supply nutrient and mobilize energy stores, thus providing energetic substrates (tricarboxylic acid (TCA) cycles intermediates) to be used for bioenergetics reactions (ATP production) (Rabinowitz and White, 2010) and for the synthesis of molecules that collaborate in mounting an efficient response to

stress (Galluzzi et al., 2014). As matter of fact, the crucial role of starvation-induced autophagy is corroborated by the experimental observation that *Atg5*$^{-/-}$ mice die few hours after birth as consequence of the incapacity to survive post-natal starvation in turn reflecting the inability of mobilizing energy stores (Kuma et al., 2004). To a similar extent, cells incompetent for autophagy activation are more sensitive than their competent counterpart to nutrient deprivation (Kroemer et al., 2010).

It appears evident how there is an intimate communication between metabolism and autophagy; in this section, we will analyze in detail the metabolic triggers and the sensors leading to autophagy induction.

On a cellular basis, autophagy is normally induced as result of a drop in the levels of essential nutrients such as glucose or amino acids, yet it can also be provoked by the accumulation of metabolic byproducts (i.e ammonia) or by exogenously providing fatty Acids or polyamines (i.e Spermidine). This topic has been extensively discussed in (Galluzzi et al., 2014).

1. Energy Charge/ Glucose deprivation

The energetic status of the cells can be resumed by the concept of 'energy charge' of the adenylate system (reflecting the intracellular concentrations of ATP, ADP and AMP), calculated according to the formula ([ATP] + 1/2 [ADP]) / [ATP + [ADP] + [AMP]) (Atkinson and Walton, 1967), (Galluzzi et al., 2014).When ATP synthesis is decreased, as consequence of a reduction in the glycolytic and in the oxidative phosphorylation (OXPHOS) pathways, energy charge absolute value diminishes as result of a drastic increase in AMP concentration. This event is able to trigger the activation of the main sensor of the cellular adenylate system: AMPK (Hardie et al., 2012).

AMPK presents a heterotrimeric structure composed of a catalytic α-subunit, a scaffolding β-subunit and a regulatory γ-subunit (Hawley et al., 2010) when 2 molecules of AMP (or, with lower

affinity ADP) bind to γ-subunit, T172 in the catalytic site can be phosphorylated by upstream kinases such as Liver kinase B1 (LKB1) (Hawley et al., 2003), Calcium/calmodulin-dependent protein kinase *2* (CAMMK2) and Transforming growth factor beta-activated kinase 1 (TAK1) leading to AMPK activation (Hawley et al., 2005). AMPK activation is essential for autophagy induction (Meley et al., 2006) mainly for its activity towards mTOR (Kim et al., 2011). As already discussed in the previous sections, AMPK-mediated inhibition of mTOR is multipronged: AMPK can phosphorylate and activate the tonic mTOR inhibitor TSC2 (Inoki et al., 2003) or its activator subunit Raptor (Gwinn et al., 2008). Furthermore, AMPK can directly activate autophagy via ULK-1 phosphorylation (Egan et al., 2011) or via Beclin-1 phosphorylation (Kim et al., 2013) in absence of glucose.

Being a protein kinase, AMPK needs ATP for its catalytic activity, underlying the notion that a minimal ATP concentration is required for starvation-induced autophagy (Galluzzi et al., 2014). Importantly, AMPK establishes a feed forward mechanism of autophagy activation linked to the phosphorylation of its activating kinase TAK1 (Lanna et al., 2014), which in turn can control autophagy via dissociation of Beclin-1 inhibitors TGF-beta activated kinase 1/MAP3K7 binding protein 1 (TAB1) and TAB2 (Criollo et al., 2011) or via inhibitor of kappa light polypeptide gene enhancer in B-cells, kinase beta (Ikkβ) activation (Comb et al., 2012).

As a caveat, it should be mentioned that, upon specific condition (and likely on a cell-line dependent basis), glucose availability could activate autophagy by promoting vacuolar ATPase activity (Sautin et al., 2005) or inhibiting mTOR (Ravikumar et al., 2003). Interestingly, Mizushima's lab has shown how glucose refeeding via a hyperinsulemic-euglycemic clamp was not as efficient as amino acids in inhibiting starvation-induced autophagy in liver and as insulin in muscle, thus suggesting a tissue-specific regulation of autophagy (Naito et al., 2013). A further level of complexity is represented by the observation that 2-DeoxyGlucose (2-DG), an analog of glucose

which is phosphorylated by HKs but that cannot be metabolized further to produce ATP, does not replicate the effects of Glucose deprivation in terms of autophag induction. This effect is due to the fact that HK-II interacts with and phosphorylates mTORC1 thus inhibiting its activity; importantly the binding is increased by glucose deprivation. For this reason, 2-DG administration in complete media does not efficiently trigger autophagy (Roberts et al., 2014).

2. Hypoxia and ROS

Like glucose deprivation, a decrease in $p[O_2]$ represents a condition of metabolic stress in which autophagy is activated (Bellot et al., 2009). This event is observed upon nutrient starvation and particularly in solid tumors (Maxwell et al., 1997); autophagy activation by hypoxia occurs via both transcription-dependent and –independent mechanisms (Pouyssegur et al., 2006); a drop in oxygen tension is primarily sensed by the hypoxia-responsive transcription factor hypoxia inducible factor 1, alpha subunit (HIF-1α), which both stimulates cells survival and orchestrates an anti-stress response thus promoting the expression of different factors. In particular, the HIF-1α dependent transcription of BNIP3 and BNIP3L causes Bcl2/Beclin-1 dissociation via the BH3 domain of these factors and activate the autophagic cascade (Bellot et al., 2009). Similarly, HIF1α favors the expression of the essential gene *Atg5* (Zhang et al., 2008).

Autophagic response to hypoxia can bypass HIF activity; in $Hif1^{-/-}$ MEF cells, autophagy is activated in an AMPK-dependent manner (Laderoute et al., 2006), highlighting the key function of this sensor in the response to hypoxia. Hypoxia and nutrient deprivation are accompanied by an increased production of reactive oxygen species (ROS), which can activate autophagy via multiple mechanisms, including HIF-1α transactivation (Scherz-Shouval and Elazar, 2011). Interestingly in ρ^0 cells, deficient in mitochondrial electron transport chain (mETC), the production of oxygen superoxide is diminished and correlates with an impaired autophagic reaction in response to nutrient

starvation, coming along with a reduced AMPK activation (Li et al., 2013). Moreover, ROS can negatively modulate mTOR pathway, hence promoting autophagy, via ataxia-telangiectasia mutated (ATM)-dependent activation of TSC2 (Alexander et al., 2010) and controlling TSC2 localization at peroxisomal level, where it inhibits Rheb (She et al., 2014). Eventually, a study from Elazar group has demonstrated how ROS can exert a direct control on autophagic machinery by favoring the oxidation of Cystein in the catalytic site of the protein (Scherz-Shouval et al., 2007).

3. NADH/NAD Ratio

Beyond a drop in ATP concentrations, nutrient starvation is characterized by a decrease in the concentrations of the major source of reducing power for bioenergetic reactions, namely nicotinamide adenine dinucleotide (NADH). As consequence of nutrient starvation, the two majors NADH-producing metabolic pathways, glycolysis and Krebs cycle, are downregulated. This event results in a reduction in NADH levels paralleled to an increase in NAD^+ levels (Houtkooper et al., 2010), both at mitochondrial and cytosolic level; the reduction in the NADH/NAD^+ ratio is an event *per se* able to trigger autophagy (Lee et al., 2008). The link between NADH/NAD and autophagy activation is represented by protein deacetylation reactions mediated by class III histone deacetylases (Sirtuins in mammalian cells) (Chalkiadaki and Guarente, 2012), that can be considered as the cellular NADH/NAD sensors. Sirtuin 1 (SIRT1, Sir2 in yeast), one of the major regulators of starvation response, requires NAD^+ as cofactor for its catalytic activity (Imai et al., 2000); the epigenetic control exerted by SIRT1 with regard to autophagy can be transcription dependent- or independent, as confirmed by the dual localization of SIRT1 both in the nucleus and in the cytoplasm. Upon nutrient starvation, cytoplasmic SIRT1 deacetylates the autophagic essential proteins ATG5, ATG7, ATG12 and LC3 (Lee et al., 2008) as well as Beclin-1 (Sun et al., 2015), hence releasing these proteins from inhibitory acetylation. Moreover, the overexpression of a SIRT1

mutant, confined to cytoplasm, triggers robust autophagy activation. Mice knockout for SIRT1 are perinatal lethal with signs of insufficient autophagy in various tissues (Lee et al., 2008), suggesting a pivotal role of SIRT1 in autophagy activation. Additionaly, outbred mice can reach 24 months of age, but present severe metabolic and developmental alterations (Madeo et al., 2014). Conversely, nuclear localized SIRT1 can transcriptionally control autophagy via deacetylation and activation of the pro-autophagic forkhead box O1 (FOXO1) and O3 (FOXO3a) transcription factors (Brunet et al., 2004); (Pirinen et al., 2014)), in turn regulating the transcription of several Atg genes (Pietrocola et al., 2013).

The exogenous supply of NAD precursor, such as nicotinamide riboside (Canto et al., 2012) or caloric restriction (Chen et al., 2008) activate SIRT1 functions which can be resumed, beyond the autophagy regulation, in the upregulation of mitochondrial functions mediated by peroxisome proliferator-activated receptor gamma coactivator 1-alpha (PGC-1α) expression. Importantly, there is a close yet-to-be fully elucidated interconnection between AMPK and SIRT1, which acts in concert for regulating autophagy, mitochondrial metabolism and energy expenditure (Canto et al., 2009). Noteworthy resveratrol, a natural compound found in wine, for decades considered as a direct SIRT1 activator (Lagouge et al., 2006), has been demonstrated to be a phosphodiesterase 4 (PDE4) inhibition (Park et al., 2012), in turn leading to an increase in [cAMP] concentration. Increase in cAMP levels results in the activation of the effector protein Epac-1 with consequent rise in Ca^{2+} levels and activation of CamKK-AMPK axis. (Park et al., 2012)

One of the proposed mechanisms, through which AMPK can controls SIRT1 activity, is an increase in NAD^+ cellular levels mediated by FOXO-1 transactivation, resulting in the expression of the NAD^+ producing enzyme nicotinamide phosphoribosyltransferase (NAMPT) (Canto et al., 2009). In line with these notions it is important to underline that the activation of NAD^+ consuming

enzymes, such as poly [ADP-ribose] polymerase 1 (PARP1), inhibits SIRT1 activation and autophagy (Bai et al., 2011). Conversely, pharmacological inhibition of PARP restores mitochondrial function in concomitance with SIRT-1 activation (Pirinen et al., 2014). Moreover, it has to be mentioned that all the events leading to SIRT1 activation correlates with an amelioration of metabolic syndrome (Guarente, 2006) and an increase in lifespan (Satoh et al., 2013).

4. Response to amino acids starvation

In eukaryotic cells the response to essential amino acids depletion is centered on two distinct systems that integrate the information about amino acids availability and convert it into the activation of protein synthesis, namely the eukaryotic translation initiation factor 2 alpha (eIF2α) and mTOR.

eIF2α represents the regulatory hub of the so-called General Amino acids Control (GAAC); in this system, a drop in amino acids levels results into the accumulation of uncharged tRNAs (Talloczy et al., 2002), in turn activating the eukaryotic translation initiation factor 2 alpha kinase 4 (known as GCN2) (Dong et al., 2000). Via inhibitory phosphorylation of eIF2α on Ser51, GCN2 both ensures a block of the translation (in absence of essential amino acids) and stimulates autophagy promoting the translation of the transcription factor activating transcription factor 4 (ATF4) (Harding et al., 2000). ATF4 controls the expression of several ATG genes, including ATG5, ULK1 and LC3 (Pietrocola et al., 2013). Cells expressing an eIF2α mutant (non-phosphorylatable by upstream kinases) are resistant to several autophagy-inducing conditions, demonstrating the important role of ATF4 in autophagic response. (Talloczy et al., 2002).

Importantly, the block of translation, following the inhibition of eIF2α activity, can be mediated by other types of cellular stress, each of them transduced by a specific eIF2α kinase; additionaly, the accumulation of unfolded protein in the ER activates the so-called unfolded protein

response (UPR), based on the activation of the eukaryotic translation initiation factor 2-alpha kinase 3 (EIF2AK3, also known as PERK) (Ron and Walter, 2007). Similarly, viral double strand DNA or the saturated fatty acids palmitate lead to eIF2α inactivation through activation of the EIFK2A2 kinase also known as PKR (Shen et al., 2012).

eIF2α phosphorylation can be hence considered as one of the key event of the 'integrated stress response', in which proteins synthesis is blocked and autophagy is coordinately activated in response to different stresses for maintaining cellular homeostasis (Kroemer et al., 2010). In the specific case of amino acids depletion, autophagy activation provides amino acids to be used for stress signal molecule synthesis and for energy production (Kroemer et al., 2010).

The Ser/Thr kinase mTOR responds to growth factors and amino acids (particulary Leucine) availability by phosphorylating and activating the eukaryotic translation initiation factor 4E binding protein 1 (4EBP1) (Efeyan et al., 2015) and the ribosomal S6 kinase (Efeyan et al., 2015), thus promoting protein synthesis (Laplante and Sabatini, 2012). The mechanisms through which aminocids activate mTOR are yet-to-be-fully characterized and they are interconnected with the complex small G-protein system controlling mTOR function.

mTOR is thought to sense the presence of amino acids availability within lysosomal lumen, since active mTORC1 is localized at the lysosomal membrane surface (Sancak et al., 2010). Furthermore, it has been established that amino acids sensing function of mTORC1 relies on the Rag GTPase proteins (Kim et al., 2008a); (Sancak et al., 2008). Four Rag proteins, associated as heterodimers control mTOR activity: when Leucine is available RagA/B are GTP-, whereas Rag C/D are GDP- loaded (Sancak et al., 2008)The GTP loading status of Rags GTPase depends both on the Ragulator complex (Bar-Peled et al., 2012) and on the lysosomal v-ATPase; according to this model,

when Leucine is present in the lysosomal lumen, v-ATPase undergoes conformational change that recruits ragulator complex at the lysosomal surface; in turn, ragulator exhibits GEF activity toward Rag A/B and anchors mTORC1 to the lysosmal membrane, where it is activated by Rheb.

Recently, Folliculin and the protein complex GATOR have been identifies as GAP towards Rag C/D and Rag A/B respectively (Baba et al., 2006); (Bar-Peled et al., 2013), thus behaving as negative regulator of mTORC1. Within one hour after birth wild-type mice undergo severe starvation, accompanied by mTOR signaling inhibition, resulting in hypoglicaemia and reduction in circulating aminoacids; interstingly, knock-in mice expressing a constitutive form of RagA succumb to post-natal fasting, as results of their inability to restore both glucose and aminoacids circulating levels, due to constitutive autophagy inhibition (Efeyan et al., 2013). Indeed, autophagy inhibition blocks aminoacids production necessary for gluconeogenesis. As recently shown, Rag proteins constitute a point of connection between the lysosomal sensing of amino acids availability, relying on vATPase, and the cytosolic sensing system, based on charged/uncharged tRNA. Indeed, when Leucine is present in the cellular milieu, Leucyl-tRNA synthtetase shows the ability to bind and activate activity Rag complex via its GAP activity, leading to mTORC1 activation (Han et al., 2012). These results underpin that two different mechanisms of amino acids sensing detect the availability of two separate pools of amino acids in the cytosol and in the lysosome (Meijer et al., 2014).

Highly proliferative cells, especially cancer cells, support their growth via Glutamine utilization coupled to mTOR activation (Galluzzi et al., 2013); indeed, a combination of Leucine plus Glutamine is more effective than Leucine alone in stimulating mTOR activity (Bauvy et al., 2009). In cancer cells, the major enzyme regulating Glutamine metabolism is glutamate dehydrogenase (GDH), one of the enzymes that, after hydrolysis of the Glutamine amine group, allows the conversion of Glutamate into 2-oxoglutarate, which entrers the TCA cycle for both energy production and

biosynthetic reactions. Glutamate dehydrogenase, likely through 2-oxoglutarate production, links Glutamine availability to mTOR activation and can be considered as a sensor of this key aminoacid; importantly, accumulation of 2-oxoglutarate can induce a pseudo-hypoxic status leading to prolyl hydroxylase inhibition and HIF-1 stabilization which does not explain mTOR activation by Glutamine (Duran et al., 2013); rather, this event appears to promote RagB-GTP binding (Duran et al., 2012).

Based on these findings, it appears clear that Leucine and Glutamine activate mTOR via distinct mechanisms. Recently, the basis of differential regulation has been unraveled following the observation that Glutamine-mediated mTOR activation occurs in RagA/B double knockout cells depending on lysosomal v-ATPase; interestingly, Glutamine control operated over mTOR depends on the Arf GTPase, trough a yet-to-be characterized mechanisms (Jewell et al., 2015).

As further level of complexity, it should be mentioned that Leucine vs Glutamine mTOR activation can be co-regulated; cancer cells that are not 'glutamine addicted' relies on Leucine for supporting their growth via mTOR activation; in this setting, cells promote Leucine uptake from the extracellular milieu via the SLC7A5/SLC3A2 system, in which efflux of L-glutamine is coordinated with the import of Leucine (Nicklin et al., 2009).

5. Lipids

The relationship between autophagy and lipid metabolism is multifacets; upon nutrient starvation, autophagy actively participates to lipolysis, a process in which triglycerides, stored in lipid droplets, are hydrolyzed to free fatty acid necessary for energy production. Activation of macrolipophagy is thus the mechanisms trough which cells can overcome nutrient scarcity; conversely, inhibition of autophagy, both in *vitro* and *in vivo* in liver of Cre-Alb-Atg7 mice, leads to

accumulation of lipid droplets. Upon starvation, mice hepatocytes activate autophagy for energy mobilization; interestingly, the efficacy of this process is impaired when the lipid balance is altered by feeding mice with high fat diet thus (i) confirming that exogenous supply of lipids can saturate the autophagy system and (ii) underlining a role of autophagy in obesity and metabolic syndrome. (Singh et al., 2009).

On the contrary, the exogenous supplementation of both saturated (*i.e.* palmitate) or unsaturated (oleate) fatty acids leads to autophagy induction, albeit via different mechanisms; palmitate-induced autophagy requires the ER-stress activated kinase PKR and JNK1 (Shen et al., 2012); (Holzer et al., 2011). Indeed, palmitate dissociates PKR from its inhibitory interaction with the transcription factor signal transducer and activator of transcription 3 (acute-phase response factor) (STAT3) that, in its cytosolic form, inhibits autophagy. As already discussed, oleate induced a form of non-canonical autophagy which bypasses its requirement of Beclin-1-PI3KC (Niso-Santano et al., 2015). Recently, it has been shown that the overexpression of stearoyl-CoA desaturase (delta-9-desaturase) (SCD1), responsible of the conversion of saturated to monounsaturated fatty acids, is able to trigger autophagy (Ogasawara et al., 2014). In line with this finding, chemical inhibition of SCD1 blocked starvation-induced autophagy in an mTOR independent manner, likely inhibiting the initial steps of the autophagosome formation;.interestingly, this block can be bypassed by oleate administration (Ogasawara et al., 2014). These results open the possibility that lipophagy or the exogenous supplementation of lipids play a role in the autophagosome biogenesis; patatin-like phospholipase domain containing 5 (PNPLA5), a lipase associated to lipid droplets, is necessary for the correct initiation of autophagic process (Dupont et al., 2014).

Considered the growing interest raised by this topic in the recent past, it is important to mention that the bacterially produced short-fatty acid butyrate represents the primary source of energy for

colonocytes. In conditions of microbiota depletion, autophagy is activated for supporting colonocytes metabolism; addiction of butyrate to germfree colonocytes inhibits autophagy, thus confirming the important role of this bacterial metabolite in autophagy regulation. (Donohoe et al., 2011).

6. Sensing of micronutrients: depletion of iron

Iron represents an essential cellular cofactor for several enzymes catalyzing Redox reaction. Cells store iron in large cytoplasmic ferritin oligomers, ready to be degraded in case of needs. Liberation of free iron from ferritin store required the engulfment and the lysosomal degradation of ferritin (ferritiophagy); drops in [Fe] or iron chelators activate ferritinophagy, in a process that requires the ferritin specific cargo receptor nuclear receptor coactivator 4 (NCOA4), which links light and heavy ferritin chains to LC3 (Mancias et al., 2014).

7. Metabolic byproducts: Ammonia

Ammonia, the major byproduct of amino acids transamination reactions, is a strong autophagy inducer. Particularly, the huge utilization of glutamine leads to accumulation of Ammonia in cultured cells following Glutaminolysis. Ammonia-induced autophagy does not require ULK1/2 and does not seem mTOR dependent; rather, ammonia activated UPR in the ER and stimulates AMPK activation. Importantly, ammonia-induced autophagy might represent one of the mechanisms through which glutamine-addicted cancers support their growth. (Cheong et al., 2011)

8. Transcription Factors, Metabolism and Autophagy

The crosstalk between autophagy and cellular metabolic requirements can occur at different levels; as previously shown, the rapid change in key energy-related metabolites can trigger an acute and nucleus-independent autophagic response, mainly relying on mTOR inhibition and AMPK activation or by epigenetic modifications directly affecting autophagic proteins (*i.e.* sirtuins).

In the recent past, it has been defined the existence of a gene regulatory network controlling autophagy, metabolic signals and lysosome biogenesis; the so called Coordinate Lysosome Expression and Regulation (CLEAR) gene network (Palmieri et al., 2011) has been built around the target genes of the Transcription Factor EB (TFEB), representing the center of this system (Sardiello et al., 2009). TFEB shuttles from the cytosol to the nucleus in condition of altered lysosomal storage and it activates target genes with the purpose of eliminating complex molecules, such as protein aggregates (Tsunemi et al., 2012). For this reason, TFEB acts by promoting both lysosome biogenesis and lysosomal activity, thus increasing lysosome number and function. Beyond conditions of lysosome saturation, nutrient deprivation was also found to influence TFEB activity; when nutrients and growth factors are deficient, TFEB retains the ability (i) to translocate in the nucleus, (ii) to provide phosphorylation by the mitogen-activated protein kinase (MAPK) family members ERK2, and (iii) to promote the expression of several pro-autophagic genes (Sardiello et al., 2009). TFEB thus represents the link between extracellular and intracellular nutrient availability and autophagy activation; further, among the genes found to be regulated by TFEB, several of them are related to the degradation of nutrient storage such as lipids and glycogen, emphasizing the correlation between autophagy activation and the mobilization of nutrients upon starvation. (Palmieri et al., 2011)

Moreover, in mice subjected to 24 hours starvation, TFEB levels are increased and are maintained high through an auto-regulatory loop, in which TFEB promotes its own transcription (Settembre et al., 2013). TFEB overexpression is linked to the up-regulation of genes involved in lipid metabolism; in particular, TFEB both directly controls PGC1-alpha expression, a gene operating control over mitochondrial β-oxidation and promotes lipid breakdown in mice liver, depending on autophagy (Settembre et al., 2013).

Importantly, TFEB activity stays under the repressive control of mTOR and the lysosomal amino acids sensing system; when amino acids are present inside the lysosomal lumen and the proton flux across the membrane is intact, mTORC1 phosphorylates and inhibits TFEB in a RagGTPase dependent manner (Settembre et al., 2012); phosphorylated TFEB is also sequestered by 14-3-3 chaperones family, which blocks its nuclear translocation. The cellular transcriptional function of TFEB is counteracted in cells by the activity of the transcription factor zinc finger with KRAB and SCAN domains 3 (ZKSCAN3) that, in condition of nutrient availability, represseses the transcription of several TFEB-activated genes (Chauhan et al., 2013).

It remains to be established if these transcription factors can directly sense the metabolic perturbations or whether their activation results from molecular pathways feedbacks culminating in a transcriptional response. Along the same line of principle, upon nutrient starvation, the sterol regulatory element binding protein 2 (SREBP2) is found associated to several autophagic genes promoter, opening the possibility that autophagy can be also activated in conditions of sterol depletion (Seo et al., 2011).

9. Metabolic Regulation of Autophagy in vivo

The rapid and intense autophagy response detected *in vitro* in cultured cells is not reproducible in time and size *in vivo*, due to the different homeostatic circuits activated in different organs and to the 'perturbation' represented by the humoral/neuroendocrine signals. In mice, despite the 24-48 hours of food deprivation (with free access to water) necessary to induce autophagy, glucose and circulating amino acids levels undergo only slight fluctuations, largely due to the utilization of hepatic and skeletal muscle energy stores (Mizushima et al., 2004).

The major determinant of autophagy induction upon fasting is a drop in insulin and insulin growth factor 1 (IGF-1); insulin signaling impinges on mTORC1 activation, which acts as a master controller of anabolic reactions. Consequently, a reduction of insulin, IGF-1 (and the consequent increase in the inhibitory insulin-like growth factor binding protein (IGFBP) results in mTOR inhibition and autophagy induction, necessary to preserve tissue homeostasis (Troncoso et al., 2012).

As previously mentioned, starvation induced autophagy cannot be inhibited *in vivo* by increased glucose levels; rather, increase in insulin levels is responsible for autophagy inhibition after refeeding in liver, whereas in muscle amino acids explain the reduction in autophagy. These observations underscore the central role played by mTOR in autophagy regulation *in vivo.*

Intriguingly, autophagy may serve as an unconventional form of secretion for different cytosolic proteins (Ponpuak et al., 2015) like interleukin (IL)-1B and IL-18. Upon fasting, pancreatic β-cells reduces insulin secretion, irrespective of autophagy induction. It has been recently uncovered that unlike most cells, β-cells do not activate autophagy upon starvation, thus maintaining low insulin levels (Goginashvili et al., 2015). Rather, starved β-cells activate PKD-mediated insulin granule degradation, in turn leading to mTORC1 activation and autophagy inhibition.

A major level of autophagy regulation *in vivo* is offered by neuroendocrine signals; epinephrine is secreted by adrenal gland in response to a drop in glucose concentration. The activation of β-adrenergic receptor in peripheral tissues activate lipophagy with a consequent rise of circulating fatty acids (Lizaso et al., 2013); knocking-out the gene coding for phenylethanolamine N-methyltransferase, indispensable for epinephrine production, leads to severe hepatic steatosis coupled to deficient autophagy and impaired triglyceride usage (Sharara-Chami et al., 2012).

Hormones regulating satiety/hunger status, such as leptin, adiponectin and ghrelin, can also modulate autophagy *in vivo*; it has been reported that different autophagy inducers, including rapamycin, spermidine and resveratrol, are able to reduce circulating levels of leptin *in vivo* (He et al., 2012a); surprisingly, administration of exogenous leptin both *in vitro* and *in vivo* is also found to activate autophagy, possibly underlying an unexpected feedback regulatory mechanism.

Adiponectin, secreted by adipose tissue and favoring both lipid mobilization and fat oxidation upon fasting conditions, is also able to activate autophagy. Knockout of this mediator leads to impaired autophag flux with high fat diet (HFD)-induced obesity (Guo et al., 2013b).

Upon fasting, growth hormone (GH) levels normally increase and stimulate hepatic autophagy, thus preventing hypoglycemia. Interestingly, mice knockout for a protein responsible for ghrelin acylation (an that cannot consequently secrete a functional form of this hormone) are lethal due to an impaired response to hypoglycemia (Zhang et al., 2015). Ghrelin, secreted by the gastrointestinal tract when stomach is empty, raises GH level and prevent excessive decrease in blood glucose; pro- and anti-autophagic activities are described for ghrelin, reflecting its function of balance between hunger signals and energy stores distribution (Zhang et al., 2015).

As previously discussed, the elucidation of the effect of autophagy *in vivo* is limited by the fact that mice deficient for autophagic essential genes (such as *Atg5* and *Atg7*) are not viable, whereas the availability of cell-type specific autophagy deficient mice has permitted to observe the metabolic perturbations linked to absence of autophagy.

Nevertheless, a ubiquitous Cre-Atg7 inducible knockout mouse has recently been developed. In this model, the consequence of autophagy inactivation depend on the time of tamoxifen administration; in particular, 8-10 weeks aged mice present signs of neurodegeneration, absence of

liver glycogen and white adipose tissue is replace by brown fat. These mice are susceptible to short-fasting period, as consequence of their inability to mobilize energy. Mice succumb for severe hypoglycemia that can be delayed by exogenously administering glucose. (Karsli-Uzunbas et al., 2014).

In mice deficient for autophagy in liver, the most relevant phenotype is the accumulation (also found in Beclin-1 heterozigous *(Becn1*$^{+/-}$*)* mice of lipid droplets in liver and the development of severe hepatic damage due to fat lipotoxicty and steatosis. (Marino et al., 2011a) Consequently, autophagy seems to play a pivotal role in mediating pancreatic β-cells fitness and its deficiency promotes pre metabolic syndrome, witnessed by reducing insulin tolerance. Intriguingly, *Atg7* deletion, in white adipose tissue, favors obesity resistance and promotes the replacement of white with brown adipose tissue (Singh et al., 2009). This effect appears to be linked to the fact that autophagy promotes adipocyte differentiation. In summary, the knowledge of the cell-specific autophagy deficient models could help to define an organ specific therapy for pre-pathological or pathological condition in which autophagy is implicated.

E. ROLE OF AUTOPHAGY IN THE PATHOGENESIS OF DISEASE

Considering the pleiotropic roles played by autophagy in cells, it appears clear that a dysfunction in this process could represent the basis for the development of a pathological phenotype; as consequence of its housekeeping function, autophagy has been implicated in cellular transformation and cancer (Galluzzi et al., 2015), neurodegeneration (Nixon, 2013), aging (Kroemer, 2015), metabolic disorders (Galluzzi et al., 2014), inflammation (Deretic et al., 2013) and infections (Deretic et al., 2013). For brevity, we will discuss in detail autophagy role in cancer, aging and metabolic disorders.

1. *Autophagy and Cancer*

The role of autophagy in tumorigenesis, tumor progression and response to chemotherapy has been object of a review published in 2015 in EMBO Journal (Galluzzi et al., 2015). Autophagy has been differentially implicated in various stages of tumor formation; in general, defective autophagy is thought to promote tumorigenesis and cellular transformation. Once the tumor is established, autophagy can instead promote tumor progression turning to be a self-protective mechanism for tumor cells, especially in late phases of tumor progression (Morselli et al., 2009).

In physiological conditions, autophagy helps to maintain metabolic homeostasis and to preserve genome stability, limiting ROS production (via elimination of dysfunctional mitochondria) (Kroemer et al., 2010), genotoxic stress (Mathew et al., 2007) and, as recently described, favoring the degradation of transformation-prone retrotransposing RNA (Guo et al., 2014)

Taken together, these findings underline how autophagy itself behaves as an oncosuppressor mechanism; this affirmation is corroborated not only by the fact that *Becn1*$^{+/-}$ mice spontaneously develop malignancies such as lymphomas and liver carcinomas (Liang et al., 1999); (Qu et al., 2003) but also by the higher rate of cancer development in Ambra1$^{+/-}$ mice. Moreover, mice bearing mosaic deletions of *Atg5* or carrying Alb-Cre-Atg7 transgene in the liver show high frequencies of benign neoplasia (Takamura et al., 2011). More generally, in both chemical-induced (Marino et al., 2007) and oncogene-driven (*i.e.* *KRAS*^{G12D} or *BRAF*^{V600E}) tumors, autophagy deficiency accelerates tumor establishment (Guo et al., 2013a).

The anti-tumor functions of autophagy are multiple and cellular transformation is accompanied by a remodeling in several metabolic pathways. The metabolic shift can be resumed into an increased glucose uptake and utilization coupled to high-rate mitochondrial respiration, with the purpose to

sustain the elevated metabolic requirement of cancer cells; furthermore, tumor cells develop a dependency on amino acids like Glutamine and Serine for anabolic and bioenergetics reactions. By removing dysfunctional mitochondria, autophagy avoids this metabolic rearrangement (Guo and White, 2013).

In hematopoietic malignancies, transformation is often linked to phenomena of aberrant differentiation potential of stem cells; autophagy copes for maintaining cell stem potential by preserving the structural integrity of bone marrow and cell stem niche (Mortensen et al., 2011), as observed in Hematopoietic Stem Cells (HSC) deficient for *Atg7*, in which a pre-neoplastic stem cell population is preferentially amplified. Similarly, HSC specific deletion of RB-1 inducible coiled-coil 1 (RB1CC1, well known as FIP200) impairs correct hematopoiesis and provokes severe anemia. The negative effect of autophagy ablation is not limited to HSC and FIP200 is effectively essential both for maintenance of CNS proliferative potential (Wang et al., 2013) and its deletion culminates in an increased rate of ROS generation and p53 checkpoint activation. (Wang et al., 2013).

Autophagy activation plays also a role in oncogene-induced senescence, a first-barrier mechanism against oncogene-induced transformation; in particular, the coordinated execution of cell cycle arrest and programmed cell death in healthy cells subjected to oncogenic stress prevents transformation. In $HRAS^{GV12}$ or $BRAF^{V600E}$ transformed cells, depletion of autophagic essential proteins impairs Oncogene Induced Senescence (OIS) (Elgendy et al., 2011) by increasing transformed-cell clonogenicity. Moreover, for its intrinsic nature, autophagy favors the elimination of oncogenic proteins, as in the case of a dominant negative p53 mutant, BCR-ABL1 gene and the autophagic target p62 whose accumulation has been directly associated to tumorigenesis (Mathew et al., 2009).

Another line of research hypothesized a positive role of autophagy in anti-tumor immune response, mainly because of its active role in ATP release from dying cells treated with specific chemotherapeutic agents (an event necessary for triggering immunogenic cell death (ICD) (Kroemer et al., 2013) and for its multipronged functions in mechanism of innate and adaptive immune response (Deretic et al., 2013). Autophagy is also able to limit inflammation by favoring lysosomal degradation of inflammasomes, activated both by pathogen-associated molecular patterns (PAMPs) and by damage-associated molecular pattern molecules (DAMPs) like depolarized mitochnodria and NF-kB pro-inflammatory pathways (Deretic et al., 2013). Eventually, autophagy may function as a mechanism of innate immunity against invading pathogens. Indeed, the activation of xenophagic response against potentially carcinogenic viruses (such as Hepatitis B virus (HBV), Human herpes virus 8 (HHV8) or bacteria (like *Helicobacter Pylori* or *Salmonella Enterica)* is yet-another mechanism for preventing transformation. Cells bearing genetic alterations in autophagic proteins, such as those correlated to Crohn's disease (Murthy et al., 2014) are more susceptible to infections by pathogens. Similarly, Beclin-1 mutations have been associated to human papilloma virus (HPV)-16 and HPV-18 infections in a cohort of cervical cancer carcinoma (Deretic et al., 2013).

Based on these considerations, it appears consequent that proteins that negatively modulate the autophagic process can be *bona fide* considered as oncoproteins whereas components of the autophagic machinery (or positive modulators of this process) can be enumerated among the oncosuppressor.

In the first category, it is important to mention that a wide variety of solid tumor present overexpression in the BECN1 sequestering proteins Bcl-2 and Bcl-$_{XL}$. Similarly, a common feature of human neoplasia is the overexpression of receptor tyrosine kinases (RTKs), which renders cell proliferation independent of external growth factor. (Hanahan and Weinberg, 2000). Of note, the

epithelial growth factor receptor (EGFR) hyperactivation promotes tumorigenesis due to the persistent activation of downstream targets, such as AKT1, in turn activating mTOR via TSC2 phosphorylation. Moreover, EGFR directly inhibits autophagy via BECN1 phosphorylation. (Fantin and Abraham, 2013)

The relation between Ras and autophagy appears to be context-dependent (Marino et al., 2011b): at least three members of RAS GTPase family (HRAS, KRAS, VRAS) are involved in malignant transformation (Shaw and Cantley, 2006). In response to mitogenic signals, Ras strongly activates PI3K/AKT axis and strongly inhibiting autophagy (Laplante and Sabatini, 2012); however, Ras can also promote p62 transactivation and NRF2 stabilization, in turn leading to compensatory autophagy (Duran et al., 2008). Another Ras member, the mTORC1 activator Rheb, is found overexpressed in human prostate carcinoma. (Nardella et al., 2008)

$BRAF^{V600E}$ is found mutated in cohorts of melanoma patients; hyperactivation of BRAF results in constitutive ERK (accompanied by TSC2 phosphorylation) and mTOR activation; ERK activation results also in persistent ER-stress activation that can activate autophagy. (Ma et al., 2005)

The same principle applies to the GF-activated transcription factor Myc, found rearranged in Burkitt's lymphoma; Myc can both inhibit, via eukaryotic translation initiation factor 4E binding protein 1 (Balakumaran et al., 2009) and induce (due to ER-stress dependent mechansims) autophagy (Hart et al., 2012).

In spite of these divergent mechanisms of action, it is important to highlight that Ras-dependent tumors presents metabolic alterations that render them particularly sensitive to nutrient depletion, underscoring the crucial role of autophagy in Ras-activated cancer. (Marino et al., 2011b)

Among the oncosuppressor genes, a pivotal role is played by the transcription factor p53; a germline mutations in this protein cause early-tumorigenesis (Li-Fraumeni), whereas somatic mutations are found in more than 50% human malignancies. Among the 'Guardian of the genome' functions, p53 transactivates several pro-autophagic genes (Pietrocola et al., 2013). Similarly, $p19^{ARF}$, an upstream p53 activator is found mutated in human cancers and promotes autophagy. (Reef et al., 2006).

By considering the autophagy machinery components, BECN1 and its interactors, AMBRA1 and UVRAG, have been found mutated in different cohorts of breast, brain, colorectal and various solid tumors (Liang et al., 2006); (Cianfanelli et al., 2015). As a caveat, it should be mentioned that several among these proteins take part in other processes than autophagy and this might explains the differential and context-dependent phenotype. Germline mutation in phosphatase and tensin homolog (PTEN) a phosphatase antagonizing PI3KI signals (and a positive autophagy modulator), have been associated to increased rate of tumorigenesis (Liaw et al., 1997); (Arico et al., 2001)

Once the tumor is established, autophagy generally supports its growth conferring resistance to environmental and nutritional stress and supporting its increased metabolic requirements (Galluzzi et al., 2015); in particular, autophagy favors dissemination and increases metastatic potential of malignant cells (Lazova et al., 2012). As already mentioned above, defects in autophagy promotes tumor establishment; most of the autophagy-deficient tumors represent form of benign neoplasia, with low proliferative potential (Guo and White, 2013), that can be further decreased by deletion of p62.

In the recent past, new established murine model have better clarified autophagic functions in tumor progression; the lung-specific deletion of *Atg7* in $BRAF^{V600E}$ driven carcinogenesis makes the

tumor evolve in benign oncocytomas, tumors characterized by lipid accumulation and dependence on exogenous glutamine, direct consequence of dysfunction in mitochondrial performance (Strohecker et al., 2013). This observation proves that autophagy supports tumor growth sustaining mitochondrial metabolism, glutamine utilization and energy production (Strohecker et al., 2013).

Similar phenotypes have been characterized in $KRAS^{G12D}$-driven lung and pancreatic carcinomas upon specific deletion of autophagy essential genes *Atg5* and *Atg7* (Rao et al., 2014), (Yang et al., 2014a), (Rosenfeldt et al., 2013) as well as in *BRCA2* knockout tumors coupled to monoallelic deletion of *BECN1* (Huo et al., 2013). The discordance in these models in represented by the mutational status of p53; in Pancreatic Ductal Adeno Carcinoma and KRAS induced lung cancers, the loss of p53 is epistatic to autophagy inhibition and renders tumor insensitive to autophagy inhibitory (genetic or pharmacological) intervention aimed to alter metabolism and to limit tumor growth (Rosenfeldt et al., 2013). Conversely, in a $KRAS^{G12D}$ –driven autochthonous adenocarcinoma, with stochastic loss of heterozigosity of p53, p53 status does not influence the response to autophagy inhibitory intervention (Yang et al., 2014a).

Thus, it appears evident that the impact of autophagy in tumor progression is oncogene- and context- dependent. It is well accepted that cancer cells, subjected to pharmacological inhibition of autophagy, are less resistant than their wild type counterpart to stress and chemotherapy (Boya et al., 2005). This effect is not always found in immunocompetent mice, where activation of autophagy is linked to recruitment of the immune system and immunogenic cell death response. Hence, in specific tumors responding to ICD-based therapy, autophagy induction may also represent a chemosensitizing strategy. Taken together, these observations suggest that inhibition of autophagy might represent a, yet-context- and oncogene-dependent, strategy for limiting tumor progression and sensitize tumor cells to death (Galluzzi et al., 2015). Until now, strategies based on lysomotropic agents as autophagy

inhibitors to be used in clinic are limited by the relative aspecificity of these compounds. It is thus interesting to develop autophagic specific inhibitor, possibly targeting upstream effectors of autophagic process.

2. Autophagy in metabolic disease

Linked to its metabolic regulatory functions in controlling lipid homeostasis, energy stores and amino acids recycling, autophagy is implicated in several metabolic-related pathologies such as atherosclerosis (Liao et al., 2012), diabetes or pre-diabetic syndromes (Gonzalez et al., 2011) and obesity (Yang et al., 2010). In particular, autophagy deficiency in liver has been associated with reduced ER-stress and autophagic response, linked to poor insulin sensitivity and glucose tolerance (Yang et al., 2010). In line with these notions, autophagy activation in liver prevents steatosis and minimizes ethanol intoxication. (Chen et al., 2012).

Among the metabolic-diseases, we can also enumerate all the pathologies known as lysosomal storage disorders (Parenti et al., 2015) and Mucopolysaccharidoses, in which, following to mutations in various genes, Glycogen and Glycosaminoglycans (GAG) breakdown are altered; this event leads either to the saturation of lysosomal degradation system or to impaired autophagosome-to-lysosome fusion mechanism (Parenti et al., 2015).

Pathologies, autophagy implication and therapeutic adaptation are listed in **Table 1** (Galluzzi et al., 2014)

Table 1. Examples of metabolic diseases characterized by perturbations in autophagy.

Disease	Perturbation(s)	Corrective intervention(s)	Ref.
A1AT deficiency	Mutations in *A1AT* render the protein prone to aggregate and accumulate in the ER of hepatocytes, resulting in chronic fibrotic liver injury.	Autophagy induction by carbamazepine as well as the adenoviral delivery of a TFEB-coding construct favors the clearance of mutant A1AT.	(Hidvegi et al., 2010) (Pastore et al., 2013)
Acute ethanol intoxicatio	Compensatory autophagic response to ethanol mediated by FOXO3.	Autophagy induction by rapamycin, resveratrol carbamazepine reduces steatosis and liver injury.	(Ni et al., 2013) (Lin et al., 2013)
Atherosclerosis	Compensatory autophagic response that limits ER stress-driven cell death in macrophages, favors the breakdown of lipid droplets and facilitates cholesterol efflux via ABCA1. Inhibition of autophagy impedes the removal of atherosclerotic material. In *Apoe*$^{-/-}$ mice, late atherosclerotic lesions exhibit autophagy defects. Moreover, the specific blockade of autophagy i macrophages correlates with inflammasome activation and disease progression.	Rapamycin and derivatives such as everolimus, which mediate immunosuppressive effects whil activating autophagy, are currently used in drug-eluting stents for the local treatment of coronary occlusion. *Ppm1d*$^{-/-}$ mice have increased autophagy levels, exhibit improved cholesterol clearance, and thei macrophages do not convert into foam cells	(Le Guezennec et al., 2012) (Liao et al., 2012) (Razani et al., 2012) (Jia and Hui, 2009) (Ouimet et al., 2011) (Mueller et al., 2008)
Cystic fibrosis (*CTFR*$^{\Delta F508}$ mutation)	Perturbed proteostasis with reduced expression BECN1, enhanced expression of SQST1 and poor stability of CTFR at the plasma membrane.	Cystamine, cysteamine and EGCG improve proteostasis in mice and patients, normalizing BECN1 and SQSTM1levels as well as CFTR stability.	(Villella et al., 2013) (Luciani et al., 2012)
Hepatic aging (in mice)	Autophagy defects correlating with the accumulation of lipofuscin, steatosis and fibrosi and with increases in circulating triglyceridesan transaminases.	Liver-specific knockout of *Igf1* promotes hepatic autophagy and increases mean lifespan.	(Xu et al., 2012)
Hepatosteatosis	High-fat diet-induced steatosis is accompanied b reduced autophagy and autophagic defects in the liver are sufficient to cause steatosis.	Induction of autophagy by the knockout of *Psme3* (which causes SIRT1activation), EGCG or caffeine reduces steatosis.	(Dong et al., 2013) (Zhou et al., 2014) (Sinha et al., 2014)
Lysosomal storage disorders (Pompe disease)	GAA deficiency impairs glycogen breakdown i lysosomes, resulting in the accumulation of glycogen granules and glycogen-loaded autophagosomes, which promote cause a severe myopathy.	The overexpression of TFEB favors the clearanc of glycogen granules by stimulating autophagy and by favoring the exocytosis of glycogen debris.	(Spampanato et al., 2013)
Mucopolysaccharidoses (Austin disease)	Mutations in *SUMF1* impair GAG catabolism, resulting in the accumulation of autophagosomes that fail to fuse with lysosomes. This favors the accumulation of toxic proteins and dysfunctional mitochondria in the brain.	Methyl-β-cyclodextrin reverts the autophagic block and ameliorates the symptomatology of these disease.	(Fraldi et al., 2010)

Obesity	Increases in white adipose tissue associated with chronic inflammation and systemic metabolic alterations.	Inhibition of autophagy by the knockout of *Atg7* or with NR3C2 agonists favors the conversion of the white adipose tissue into its brown counterpart. Induction of autophagy in the liver by TFEB expression prevents weight gain and metabolic syndrome. Similarly, the whole-body overexpression of ATG5 protec against diet-induced obesity.	(Karsli-Uzunbas et al., 2014) (Armani et al., 2014) (Settembre et al., 2013) (Pyo et al., 2013)
Obesity-related cardiomyopathy	High-fat diet impairs cardiac geometry and contractility while promoting MTOR hyperphosphorylation as well as IKBKB, AMPK and TSC2 dephosphorylation. Cardiac dysfunction is exacerbated by a dominant-negative mutant of the α2 isoform of AMPK.	Deletion of *Ptpn1* impedes the dephosphorylatio of AMPK, induces autophagy and reverts cardia defects. The transgenic expression of catalase restores autophagy and normalizes the activation of IKBKB, AMPK and mTOR.	(Turdi et al., 2011) (Kandadi et al., 2015) (Liang et al., 2015)
Obesity-related nephropathy	The damage to tubular epithelial cells provoked b proteinuria is exacerbated by the tissue-specific knockout of *Atg5* or by obesity, which suppresses proteinuria induced autophagy.	mTORC1 is activated in the proximal tubules of obese mice, and treatment with an mTOR inhibitor restores autophagy while limiting renal damage.	(Yamahara et al., 2013)
Sphingolipidoses (Gaucher disease)	Mutations in *NPC1* and *NPC2* coincide with the accumulation of SQSTM1 and autophagosomes in the brain, indicating a defective autophagic flux	The administration of hydroxypropyl-β-cyclodextrin reduces the accumulation of cholesterol and normalizes autophagic flux	(Pacheco et al., 2009) (Davidson et al., 2009)
Type I diabetes	Mutations in *CLEC16A* increases the susceptibility of developing diabetes while affecting the ability of CLEC16A to interact with PARK2 and RNF41, which compromises mitophagy in pancreatic β cells and ultimately impairs their ability to secrete insulin	The CLEC16A/PARK2/RNF41 complex and mitophagy stand out as promising targets for the treatment and prevention of type diabetes	(Soleimanpour et al., 2014)
Type II diabetes	High-fat diet induces insulin insensitivity in peripheral tissues.	Exercise induces autophagy in cardiac and skeletal muscle, adipose tissue, and pancreatic b cells. This improves insulin sensitivity in wild-type but not *Becn1*$^{+/-}$ mice and mice bearing a BCL2 mutant that constitutively inhibits BECN1. Whole-body expression of ATG5 protects against type 2 diabetes.	(He et al., 2012b) (He et al., 2012a) (Pyo et al., 2013)

Abbreviations. A1AT, alpha-1 antiproteinase, antitrypsin; ABCA1, ATP-binding cassette, sub-family A (ABC1), member 1; AMPK, 5' AMP-activated protein kinase; BCL2, B-cell CLL/lymphoma 2; BECN1, beclin 1; CFTR, cystic fibrosis transmembrane conductance regulator; CLEC16A, C-type lectin domain family 16, member A;

EGCG, epigallocatechin-3-gallate; ER, endoplasmic reticulum; FOXO3, forkhead box O3; GAA, glucosidase, alpha; acid; GAG, glycosaminoglycan; IGF1, insulin-like growth factor 1; IKBKB, inhibitor of kappa light polypeptide gene enhancer in B-cells, kinase beta; MTOR, mechanistic target of rapamycin; mTORC1, MTOR complex 1; NPC1, Niemann-Pick disease, type C1; NPC2, Niemann-Pick disease, type C2; NR3C2, nuclear receptor subfamily 3, group C, member 2; PARK2, parkin RBR E3 ubiquitin protein ligase; PSME3, proteasome (prosome, macropain) activator subunit 3; PTPN1, protein tyrosine phosphatase, non-receptor type 1; RNF41, ring finger protein 41, E3 ubiquitin protein ligase; IRT1, sirtuin 1; SQSTM1, sequestosome 1; SUMF1, sulfatase modifying factor 1; TFEB, transcription factor EB; TSC2, tuberous sclerosis 2.

3. AUTOPHAGY AND AGING

In 2014, Lopez-Otin and other published in *Cell* the so-called 'Hallmarks of Aging', describing the cellular processes leading to the time-dependent functional decline of organisms. Most of these signatures implicate, more or less directly, loss of proteostasis, mitochondria dysfunction, epigenetic alterations, genome instability and stem cells exhaustion. Due to its housekeeping function (see above) autophagy generally plays an anti-aging effect in differentiated cells (Rubinsztein et al., 2011), limiting their death by increasing mitochondrial fitness and eliminating cytotoxic proteins.

The key role of autophagy in aging is reinforced by the observation that ATG proteins or indirect modulators of autophagy have a reduced expression in aged tissues like brain. Of note, tissue-specific knockout of autophagic genes results in the accumulation of ubiquitinated proteins and protein aggregates. In aged-liver, overexpression of LAMP2A restores CMA and autophagy reducing aging-related cellular damage (Schneider and Cuervo, 2014). Similarly, HFD-fed aged mice present a severe downregulation of autophagy gene Atg7. Restauration of Atg7 levels in liver ameliorates the pre-diabetes syndrome (Yang et al., 2010)

Aging phenomena are intrinsically linked to nutrient sensing system in cells (Rubinsztein et al., 2011); in particular glucose-insuline and GH-IGF-1 pathways and their downstream substrates (Akt and mTOR) are highly conserved throughout the evolution; the downregulation of these pathways have been associated to longevity (Rubinsztein et al., 2011). Along the same line of principles, dietary restriction (DR) is the most physiological stimulus able to increase lifespan (Mattison et al., 2012); (Madeo et al., 2015). Interestingly, longevity related effects of DR are lost in *C.Elegans* strains deficient for autophagy (Melendez et al., 2003). DR mediates its effect via multiple pathways: a decreased mTOR signaling and the activation of AMPK and SIRT1, conditions intimately linked to autophagy induction (Rubinsztein et al., 2011). In all organisms, mTOR downregulation phenocopies the effect of DR; this is confirmed by the fact the rapamycin is able to extend lifespan in several organism including mammals (Bjedov et al., 2010); (Wilkinson et al., 2012). Again, rapamycin effect is lost when autophagy is inactive (Bjedov et al., 2010), even if off-target effects may also be related to the anti-aging effect of rapamycin itself.

Caloric restriction (CR) extends lifespan by up-regulating SIRT1 (Sir2 in *C.Elegans*), and SIRT1 silencing abrogates the anti-aging effect of CR (Rubinsztein et al., 2011). Particularly, resveratrol, a direct or indirect SIRT1 activator, shares with CR the ability to increase lifespan in model organism depending on autophagy (Morselli et al., 2011). Similarly, the administration of the autophagy inducer spermidine is able to extend lifespan in model organism and to reduce aging dependent memory impairment in flies (Gupta et al., 2013); (Eisenberg et al., 2009). As a caveat, it should be mentioned that autophagy-dependent anti-aging effect could be linked to non-cell autonomous function such as reduced inflammation or innate immunity (Alvers et al., 2009).

In summary, my thesis work encompasses different points treated in this introductive paragraph. In particular, we have investigated in detail a new level of metabolic regulation by

autophagy and characterized the molecular pathways linked to this modulation. Moreover, we have applied these findings to pathological settings in which autophagy modulation affects the outcome of disease.

III. AIM OF THE WORK

As mentioned at the end of the '**Introduction**'section, the natural compounds resveratrol, a polyphenol found in red wine grapes, and spermidine, the most bioactive polyamine in cells (found in healthy foods and beverage), are able to induce autophagy and to increase lifespan of model organism.

In 2011, Morselli *et al.* (Morselli et al., 2011) better characterized the molecular mechanism through which these molecules activate autophagy. Resveratrol-induced autophagy relies on SIRT1 activation, whereas SIRT1 activity is not required for spermidine-stimulated autophagy. In spite of the different phylogenetic pathways intercepted by resveratrol and spermidine, their mechanism of action impinges on common downstream effectors, which activate mTOR-independent autophagy and trigger similar modifications in the phosphoproteome. Importantly, both agents can provoke drastic modifications at the acetylproteome levels, as observed via SILAC mass spectometry approach after incubating HCT 116 colorectal carcinoma cells with these molecules that are able to induce massive modification on the acetylation of lysine-tails from various substrates.

Spermidine and resveratrol induce largely convergent change in protein acetylation patterns, confirming a significant overlap in their mechanism of action. Importantly, (de)acetylation reactions are predominant in cytosol and mitochondria, whereas in the nucleus acetylation is more prominent. As already discussed, resveratrol can provoke cytosolic protein (de)acetylation via its stimulatory

action toward SIRT1, whereas the anti-aging effect of spermidine, in different model organisms, is specifically linked to the inhibition of histone acetyltransferases (HAT).

Strikingly, both agents are able to stimulate autophagy in enucleated cells (cytoplasts), highlighting the fact that resveratrol- and spermidine-induced autophagy is a rapid and nucleus-independent response, possibly based on (de)acetylation reactions affecting autophagic machinery proteins. Indeed, among the differentially acetylated substrates identified by SILAC, more than 100 proteins were found to be part of the previously identified central/network of autophagy modulators (Behrends et al., 2010), underlying the importance of this epigenetic modulation in the regulation of the autophagic process. Particularly, upon incubation with these compounds, ATG5 and LC3 (already described as substrate of SIRT1 and EP300) were found deacetylated.

Based on these premises, it appears clear that the epigenetic modulation of autophagy in the cytoplasm via (de)acetylation reactions represents a further step of regulation of this process. Indeed, cells harbor multiple acetyltransferases and (de)acetylases, whose role on autophagy regulation has not been investigated in detail. Of note, acetylation rivals, with phosphorylation in the epigenetic regulation of several cellular processes and most of cellular proteins, are found acetylated.

The first aim of my thesis has been to determine if protein (de)acetylation reactions were a common feature of autophagy induction. By means of Stable Isotope Labeling with aminoacids in cell culture (SILAC) mass spectrometry approach, we decided to compare the short-term effects elicited by the most common autophagy inducers, such as nutrient starvation and rapamycin, on cytosolic acetylproteome. The analysis of the global patterns of acetylation allowed us (i) to define convergent and divergent pathways affected by these autophagy modulators, (ii) to identify the

substrates and (iii) to establish a new transcription-independent regulatory function of autophagy by acetylation.

In the context of starvation-induced autophagy and the crosstalk between autophagy and metabolism, **we aimed to determine whether acetylation could represent a further level of the 'metabolic regulation of autophagy' along with the already described AMP/AMPK- and amino acids/mTOR- axis.** The ideal link for this line of investigation is suggested by the property of the acetyltransferases to catalyze their reaction using AcetylCoA (AcCoA) as substrate. A review about Acetyl CoA metabolism has been published in (Pietrocola et al., 2015a)

AcCoa is a membrane-impermeant molecule constituted by an acetyl moiety (CH3CO) linked to coenzyme A (CoA), a derivative of vitamin B5 and cysteine, through a thioester bond (Shi and Tu, 2015). As thioester bonds are energy rich, the chemical structure of AcCoa facilitates the transfer of the acetyl moiety to a variety of acceptor molecules, including amino groups on proteins (Shi and Tu, 2015)

Nonetheless, acetylation is mostly studied as a post-translational modification that concerns the Nε amino group of lysine residues, eliminating their positive charge and increasing sterical hindrance (Choudhary et al., 2014). Thus, Nε acetylation can alter the functional profile of a specific protein by influencing its catalytic activity, its capacity to interact with other molecules (including other proteins), its subcellular localization, and/or its stability (Choudhary et al., 2014).

Nε acetylation can occur through a non-enzymatic mechanism, especially in alkaline environments like the mitochondrial matrix (Weinert et al., 2014), or, as already mentioned, it can be catalyzed by a diverse group of lysine acetyltransferases (KATs) (Choudhary et al., 2014) .The human genome encodes no less than 22 distinct KATs, which possess marked substrate specificity

(Roth et al., 2001) Many KATs have a relatively high Kd (low affinity) for AcCoA, meaning that, physiological fluctuations in the abundance of AcCoA within the cellular compartment, where such KATs are expressed, can affect their catalytic activity.

For this reason, **we decided to investigate whether during starvation-induced autophagy a drop in AcCoA levels could represent a new metabolic parameter able to influence autophagic response, *in vitro and in vivo*, though a reduction in KAT activity and consequently a decrease in protein levels, ultimately leading to autophagy induction.**

Furthermore, **we wanted to identify which KATs could behave as a 'sensor' of AcCoA levels and as regulator of autophagy**. Hence, we firstly decided to set up a method for the mass spectometry-based detection of AcCoA both *in vitro* and *in vivo*. Secondly, in order to prove that AcCoA could really affect protein acetylation levels, **we wanted to establish a rapid method for the Iimmunofluorescence-based detection of acetylated lysine tails of cytosolic protein.**

Then, **in order to reinforce the idea that AcCoA might impact on global acetylation levels, we focused our attention on the metabolic pathways leading to AcCoA generation and, through their genetic and pharmacological modulation, we evaluated how these modulations could affect autophagy, AcCoA levels and protein acetylation.**

In particular, we investigated the pathways leading to mitochondrial and cytosolic generation of AcCoA and its transport across different cellular compartment by focusing our attention on the cytosolic AcCoA and its crosstalk with cytosolic KATs and autophagic protein machinery. The crucial role of AcCoA in metabolism and signaling has been objet of a review (Pietrocola et al., 2015a).

In most mammalian cells, AcCoA is predominantly generated in the mitochondrial matrix by various metabolic circuitries, namely glycolytic Pyruvate, β-oxidation, and the catabolism of branched amino acids. (Figure 2) Glycolysis culminates in the generation of cytosolic pyruvate, which is imported into mitochondria by the mitochondrial pyruvate carrier (MPC), a heterodimer of MPC1 and MPC2 (Herzig et al., 2012). Mitochondrial pyruvate is decarboxylated to form AcCoA, CO2, and NADH by the so-called pyruvate dehydrogenase complex (PDC), a large multicomponent system that in humans is composed of (i) three proteins that are directly involved in CoA- and NAD^+-dependent pyruvate decarboxylation, *i.e.*, pyruvate dehydrogenase (lipoamide) (PDH, which exists in three isoforms), dihydrolipoamide S-acetyltransferase (DLAT), and dihydrolipoamide dehydrogenase (DLD); (ii) two regulatory components, *i.e.*, pyruvate dehydrogenase kinase (PDK, which also exists in four isoforms) and pyruvate dehydrogenase phosphatase (PDP, a heterodimer involving either of two catalytic subunits and either of two regulatory subunits); and (iii) one non-enzymatic subunit, *i.e.*, pyruvate dehydrogenase complex, component X (PDHX) (Patel et al., 2014). Importantly, Ac-CoA, NADH, and ATP, allosterically inhibit PDC as they activate PDK. Conversely, CoA, NAD+, and ADP promote pyruvate decarboxylation by inhibiting PDK.

These regulation circuitries ensure that the products of glycolysis are employed for ATP generation when cells are in energy-low conditions (characterized by elevated ADP, NAD+, and CoA levels), but diverted toward anabolic metabolism when the energy stores are depleted (characterized by elevated ATP, NADH, and AcCoA levels).

Alternatively, AcCoA can be generated as the end product of β-oxidation. In this case, one among several members of the acyl-CoA synthetase protein family catalyzes the CoA- and ATP-dependent conversion of cytosolic free fatty acids into acyl-CoA. Acyl-CoA is then condensed with L-carnitine to form acylcarnitine and free CoA, a cytosolic reaction catalyzed by carnitine

palmitoyltransferase 1 (CPT1). Acylcarnitine is imported into mitochondria, through the antiporter solute carrierfamily 25 (carnitine/acylcarnitine translocase), member 20 (SLC25A20), which exchanges it for free L-carnitine. Finally, mitochondrial acylcarnitine is reconverted by carnitine palmitoyltransferase2 (CPT2) into L-carnitine (which drives the so-called 'carnitine shuttle') and acyl-CoA, and the latter undergo β-oxidation to generate NADH and AcCoA for use as direct and indirect, respectively, respiratory substrates (Rufer et al., 2009).

Branched-chain amino acids (BCAA, *i.e.*, valine, leucine, and isoleucine) can also be employed to produce AcCoA (Harris et al., 2005) thanks to a molecular circuitry that may depend on the mitochondrial deacetylase sirtuin 3 (SIRT3), at least in some tissues (including brain, liver, kidney, and skeletal muscles) (Dittenhafer-Reed et al., 2015). To this aim, branched amino acids must be first transaminated to branched-chain α-ketoacids, a reaction that can be catalyzed by the cytosolic enzyme branched-chain amino acid transaminase 1 (BCAT1). Upon import into the mitochondrial matrix, via the carnitine shuttle (Violante et al., 2013), branched-chain α-ketoacids are processed via a multi-step reaction comparable to the decarboxylation of pyruvate. This irreversible reaction is catalyzed by the mitochondrial branched-chain α-ketoacid dehydrogenase (BCKD) complex, a large multicomponent enzymatic system yielding NADH, AcCoA, and other acyl-CoA thioesters (which can be processed by β-oxidation or the TCA) as end products (Harris et al., 2005). Of note, some mammalian cells express a mitochondrial variant of BCAT1 (*i.e.*, BCAT2), which is catalytically active (Yennawar et al., 2006). However, how branched chain amino acids enter the mitochondrial matrix has not been determined yet.

In addition to these nearly ubiquitous metabolic circuitries, there are organ-specific pathways for mitochondrial AcCoA generation. For instance, neurons can employ the ketonebody D-β-hydroxybutyrate to generate AcCoA (Cahill, 2006). This occurs via a three-step reaction involving

the NAD^+-dependent oxidation of D-β-hydroxybutyrate to acetoacetate (catalyzed by 3-hydroxybutyrate dehydrogenase, type1, BDH1), the transfer of CoA from succinyl-CoA to acetoacetate (catalyzed by 3-oxoacid CoA transferase 1, OXCT1, or OXCT2), and the CoA-dependent cleavage of acetoacetyl-CoA into two AcCoA molecules (catalyzed by an enzymatic complex with acetoacetyl-CoA thiolase activity) (Cahill, 2006)

In physiological and normoxic conditions, glycolysis- or β-oxidation-derived mitochondrial AcCoA represents the major source of cytosolic AcCoA upon transportation. That said, there are at least two relatively ubiquitous metabolic circuitries through which cells actually produce AcCoA in the cytosol. First, cytosolic AcCoA can originate from Glutamine reductive carboxylation, especially when glycolysis is blocked (Yang et al., 2014b), in hypoxic conditions (Metallo et al., 2012) or in the presence of mitochondrial defects (Mullen et al., 2012). Upon uptake from the extracellular milieu (which is mediated by various transporters, depending on cell type), cytosolic glutamine is metabolized by glutaminase (GLS) to generate glutamate, which enters mitochondria through the H^+-dependent glutamate/aspartate antiporter solute carrier family 25 (aspartate/glutamate carrier), member 13 (SLC25A13). Mitochondrial glutamate is converted into α-ketoglutarate (a reaction catalyzed by glutamate dehydrogenase 2, GLUD2, or glutamic-oxaloacetic transaminase 2, mitochondrial, GOT2), which undergoes reductive carboxylation within the TCA cycle to generate citrate. Finally, citrate can be exported back to the cytosol via the dicarboxylate antiporter solute carrier family 25 (mitochondrial carrier; citrate transporter), member 1 (SLC25A1), and converted into oxaloacetate and AcCoA by ATP citrate lyase (ACLY) (Zaidi et al., 2012).

Additionally, glutamate also can be converted into α-ketoglutarate by GLUD1, a cytosolic variant of GLUD2, at least in some settings (Grassian et al., 2014). Along similar lines, a cytosolic form of GOT2 (*i.e.*, GOT1) can catalyze the reversible interconversion of glutamate and oxaloacetate

into α-ketoglutarate and aspartate. Cytosolic α-ketoglutarate can be metabolized by isocitrate dehydrogenase 1 (IDH1) and aconitase 1 soluble (ACO1) to generate citrate for AcCoA synthesis by ACLY (Grassian et al., 2014) Second, a cytosolic counterpart of ACSS1, *i.e.*, acyl-CoA synthetase short-chain family, member 2 (ACSS2), employs acetate to produce AcCoA in an ATP-dependent manner (Schug et al., 2015).

Cytosolic acetate can derive from the extracellular milieu, upon uptake by various members of the monocarboxylate transporter protein family (Halestrap and Price, 1999), or it can be synthesized from ethanol-derived acetaldehyde by a cytosolic variant of aldehyde dehydrogenase 2 (ALDH2), namely aldehyde dehydrogenase 1 family, member A1 (ALDH1A1), at least in hepatocytes (Cederbaum, 2012). Although circulating acetate levels are relatively low in modern humans (as compared to their ancestors, owing to dietary changes) (Frost et al., 2014), the ACSS2-dependent conversion of acetate into AcCoA has been shown to be preponderant in primary and metastatic malignant cells of various origin (Mashimo et al., 2014), especially in hypoxic conditions (Kamphorst et al., 2014); (Schug et al., 2015).

Normally, mitochondrial AcCoA is metabolized within the TCA to yield NADH, the main substrate for ATP synthesis via oxidative phosphorylation (Boroughs and DeBerardinis, 2015). However, some cells, including hepatocytes, can employ mitochondrial AcCoA to synthesize ketone bodies, *i.e.*, acetoacetate and D-β-hydroxybutyrate.

Cytosolic AcCoA is the precursor of multiple anabolic reactions that underlie the synthesis of fatty acids and steroids, as well as specific amino acids including glutamate, proline, and arginine.

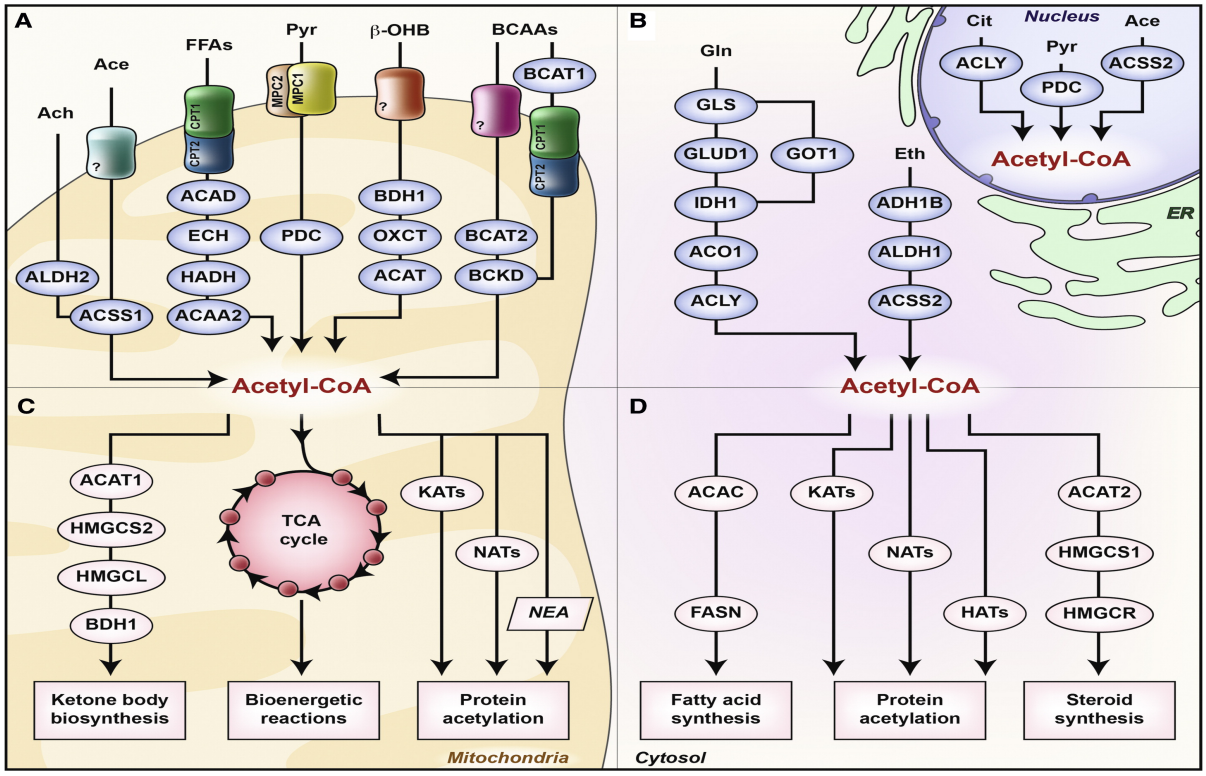

Figure 2. (Pietrocola et al., 2015a) Mitochondrial and cytosolic generation of Acetyl Coenzyme A. Abbreviations (ACAA2, acetyl-CoA acyltransferase 2;ACAC, acetyl-CoA carboxylase; ACAD, acyl-CoA dehydrogenase; ACAT1, acetyl-CoA carboxylase 1; ACAT2, acetyl-CoA acetyltransferase 2; Ace, acetate; Ach, acetaldehyde; ACO1, aconitase 1, soluble; ACSS1, acyl-CoA synthetase short-chain family, member 1; ADH1B, alcohol dehydrogenase IB (class I), beta polypeptide; ALDH1A1, aldehyde dehydrogenase 1 family, member A1; ALDH2, aldehyde dehydrogenase 2 family; BCAT1, branched chain amino-acid transaminase 1, cytosolic; BCAT2, branched chain amino-acid transaminase 2, mitochondrial; BCKD, branched-chain a-ketoacid dehydrogenase; BDH1,3-hydroxybutyrate dehydrogenase, type 1; b-OHB, D-b-hydroxybutyrate; Cit,

citrate; CPT1, carnitine palmitoyltransferase 1; CPT2, carnitine palmitoyltransferase 2; ECH, enoyl-CoA hydratase; ER, endoplasmic reticulum; Eth, ethanol; FASN, fatty acid synthase; Gln, glutamine; GLS, glutaminase; GLUD1, glutamate dehydrogenase 1; GOT1, glutamic-oxaloacetic transaminase 1, soluble; HADH, hydroxyacyl-CoA dehydrogenase; HAT, histone acetyltransferase;HMGCL, 3-hydroxymethyl-3-methylglutaryl-CoA lyase; HMGCR, 3-hydroxy-3-methyl-glutaryl-CoA reductase; HMGCS1, 3-hydroxy-3-methylglutaryl-CoA synthase 1, HMGCS2, 3-hydroxy-3-methylglutaryl-CoA synthase 2, IDH1, isocitrate dehydrogenase 1; KAT, lysine acetyltransferase; MPC1, mitochondrial pyruvate carrier 1; MPC2, mitochondrial pyruvate carrier 2; NAT, Na acetyltransferase; NEA, non-enzymatic acetylation; OXCT, 3-oxoacid CoA transferase.

From this dissertation, it is important to stress the notion that AcCoA exists in separate mitochondrial, peroxisomal, ER and nucleo-cytosolic compartments. Being a highly charged molecule, AcCoA cannot passively crosses cellular membranes, whereas it can freely shuttle from nucleus to cytosol via nuclear pores. This notion underlies that AcCoA compartmentalization relies on different transporters. (Figure 3)

The transport of AcCoA from the mitochondrial matrix to the cytosol heavily depends on the so-called ‘citrate-malate-pyruvate shuttle’. In this context, mitochondrial AcCoA is condensed with oxaloacetate by citrate synthase (CS), the first enzyme of the TCA cycle, thus generating citrate and free CoA. Citrate can be exported to the cytosol through SLC25A1 (also known as citrate carrier), followed by the regeneration of oxaloacetate and AcCoA upon the ATP- and CoA-dependent reaction catalyzed by ACLY (Zaidi et al., 2012). Cytosolic oxaloacetate is the substrate of malate dehydrogenase 1, NAD (soluble) (MDH1), catalyzing the NADH-dependent synthesis of malate, which can be transported back to the mitochondrial matrix via solute carrier family 25 (mitochondrial carrier; dicarboxylate transporter), member 10 (SLC25A10), an inorganic phosphate/dicarboxylate antiporter (Mizuarai et al., 2005), or solute carrier family 25 (mitochondrial carrier; oxoglutarate

carrier), member 11 (SLC25A11), an α-ketoglutarate/malate antiporter (Wallace, 2012). Alternatively, malic enzyme 1, NADP(+)-dependent, cytosolic (ME1) can convert malate into pyruvate, which can re-enter the mitochondrial matrix via the MPC (Bender et al., 2015).

AcCoA is also exported from mitochondria via the carnitine shuttle. As mentioned above, fatty acids enter mitochondria in the form of acylcarnitine via the antiporter SLC25A20, which generally exchanges them with free L-carnitine (Rebouche and Seim, 1998). Mitochondrial L-carnitine can also be converted by carnitine O-acetyltransferase (CRAT) into acetyl-L-carnitine, and the latter shares with free L-carnitine the ability to drive the SLC25A20 antiporter. Finally, cytosolic acetyl-L-carnitine can regenerate AcCoA and L-carnitine via the CoA-dependent reaction catalyzed by a cytosolic variant of CRAT (Madiraju et al., 2009).

The AcCoA concentration gradient across the inner mitochondrial membrane is influenced not only by the rate of AcCoA synthesis and consumption in the cytosol and within mitochondria, but also by the activity of: (i) the citrate carrier (SLC25A1), and (ii) ACLY, which is regulated by several signal transducers.

The export of citrate from mitochondria creates the need for the anaplerotic replenishment of TCA cycle intermediates that regenerate oxaloacetate, meaning that the extracellular availability of glutamine and the metabolic flux, through glutaminolysis, also influence the relative abundance of mitochondrial and cytosolic AcCoA. As direct consequence of this highly organized compartmentalization, different AcCoA pools have a major impact on protein acetylation on different cellular environments.

For instance, it has already been demonstrated that ACLY activity directly correlates with increase acetylation levels of histones (Wellen et al., 2009). For this reason, **we intended to**

demonstrate that genetic and pharmacological modulation of key enzymes, controlling synthesis or consumption of AcCoA, correlate with parallel fluctuations in cytosolic protein acetylation. Of note, we decided to perform an epistatic analysis of KATs, whose localization is not strictly limited to the nucleus, in order to identify new sensor of cytosolic AcCoA concentration able to convert the nutrient-stress signal into a pro-autophagic response.

The investigation of metabolic pathway controlling AcCoA in cells allowed us to identify new autophagic modulators to be potentially used for translational purpose. Particularly, caloric restriction has been demonstrated to play a pro-healthy role in different pathological context, including but not limited to cancer and aging (possibly depending on autophagy). *De facto*, nutrient deprivation still represents a hardly suitable strategy in clinics.

The study of the metabolic regulation of starvation-induced autophagy may thus help to identify compounds that, through autophagy induction, could mimic the metabolic alterations and the pro-healthy effects elicited by CR. To date, autophagy-based therapies have been inefficient due to side effects (*i.e.* sirolimus) or for the aspecificity of the compounds. Consequently, we aimed to validate the role of AcCoA-reducing agents into pathological settings in which autophagy is known to be involved in the pathogenic process.

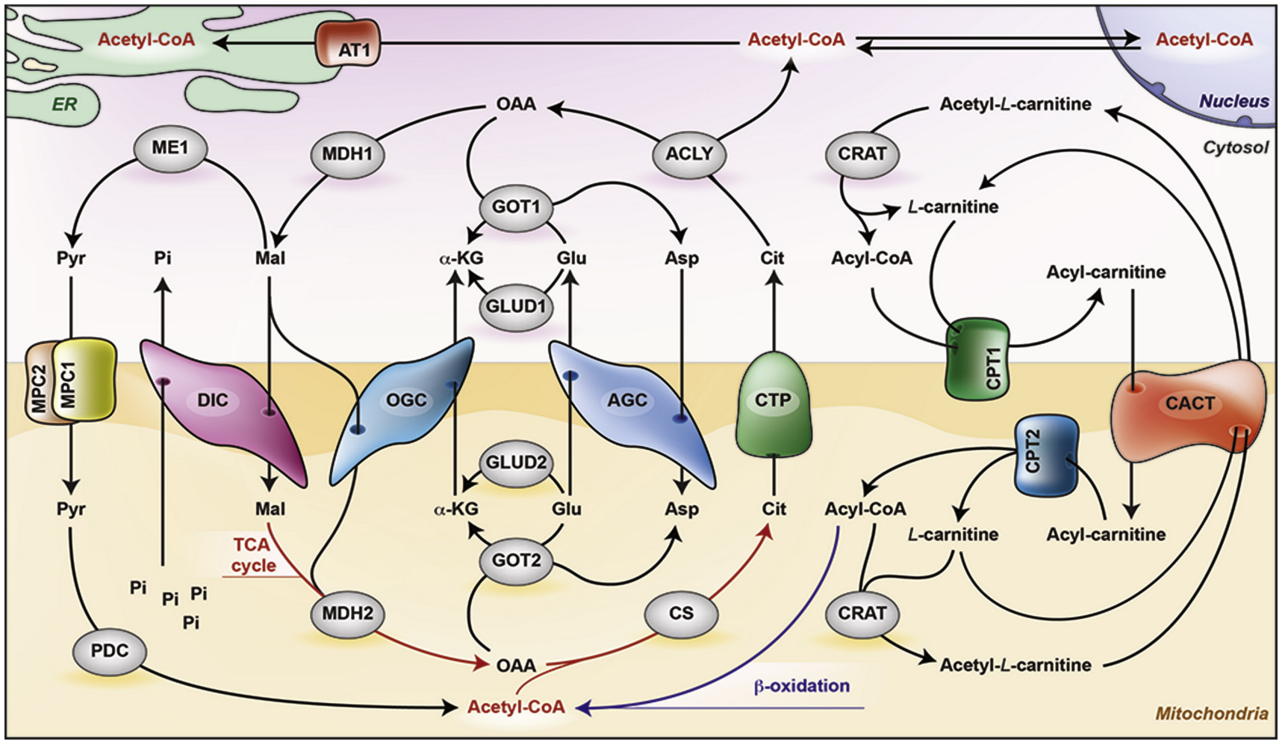

Figure 3. (Pietrocola et al., 2015a) Compartimentalization and transport of Acetyl CoA. Abbreviations a-KG, a-ketoglutarate; ACLY, ATP citrate lyase; AGC, aspartate/glutamate carrier (SLC25A13); Asp, aspartate; CACT, carnitine/acylcarnitine translocase (SLC25A20); Cit, citrate; CS, citrate synthase; CTP, citrate transporter (SLC25A1); DIC, dicarboxylate carrier (SLC25A10); Glu, glutamate; GLUD1, glutamate dehydrogenase 1; GLUD2, glutamate dehydrogenase 2; GOT1, glutamic-oxaloacetic transaminase 1, soluble; GOT2, glutamic-oxaloacetic transaminase 2, mitochondrial; Mal, malate; MDH1, malate dehydrogenase 1, NAD (soluble); MDH2, malate dehydrogenase 2, NAD(mitochondrial); ME1, malic enzyme 1, NADP(+)-dependent, cytosolic; MPC1, mitochondrial pyruvate carrier 1; MPC2, mitochondrial pyruvate carrier 2; OAA, oxaloacetate; OGC, oxoglutarate carrier (SLC25A11); PDC, pyruvate decarboxylase; Pi, inorganic phosphate; Pyr, pyruvate.

IV. RESULTS

During the first part of my thesis, we set up a method for the rapid detection of cytosolic protein acetylation via immunofluorescence staining of the acetylated-lysine tails. By means of this method, it is possible (**see Material and Methods Section**) to permeabilize cytosolic membrane without impairing nuclear membrane, hence allowing anti-acetylated lysine antibody to recognize only cytosolic proteins. Based on the finding that the polyphenol resveratrol triggered autophagy, via SIRT1 activation and (de)acetylation of cytosolic proteins, we investigated the pro-autophagic effects of phenolic-based compounds. Importantly, we established a correlation between cytosolic (but not nuclear) acetylation and autophagy induction. This work has been published in *Cell Cycle* in 2012 (Pietrocola et al., 2012). We indirectly confirmed these results *in vivo* by demonstrating that phenolic compounds contained in coffee were able to stimulate autophagy and to decrease protein acetylation in various murine organs (published in *Cell Cycle* on 2014 (Pietrocola et al., 2014). Driven by the fact that protein (de)acetylation could actually affect autophagic process regulation, we investigated if this epigenetic modulation could intervene upon physiological autophagy stimuli such as nutrient deprivation. Through metabolomics analysis, we observed that both short-term starvation *in vitro* and 48 hours starvation *in vivo* presented, as common feature, a drastic reduction in AcCoA levels, mirrored by a decrease in cytosolic protein acetylation and autophagy induction.

We thus explored whether pharmacological and genetic modulation of metabolic pathway, leading to AcCoA production, by various energy sources (namely glucose, acetate, branched chain amino acids, TCA cycle intermediates), could also modulate autophagy and protein acetylation. In this work, published in Molecular Cell (Marino et al., 2014), we demonstrated that a drop in cytosolic AcCoA correlated with a diminution in protein acetylation and with autophagy induction.

Consequently, we observed that AcCoA *per se* acts as a master repressor of starvation-induced autophagy, as confirmed by the finding that microinjection of AcCoA could inhibit autophagy induced by nutrient deprivation.

We exploited the discovery of AcCoA increasing agents as new autophagy inhibitors in a model of cardiovascular disease in which autophagy plays a detrimental role. Moreover, since AcCoA availability can directly control KATs activity, we screened a small interfering RNA (siRNA) library against human KATs, whose localization was not strictly confined to the nucleus, for their capacity to induce autophagy in response to an increase in AcCoA concentrations.

Importantly, we found that the KATs EP300 was the sensor of cytosolic AcCoA, transducing a signal of nutrient availability into the inhibition of autophagy. Indeed, in presence of nutrient, EP300 acetylates and inhibits key autophagic proteins such as ATG5, ATG7, LC3 and Beclin-1 thus limiting autophagy. Thus, AcCoA depletion directly impacts on EP300 activity, triggering short-term and nucleus independent autophagy, as confirmed by the fact that AcCoA lowering agents do work in cytoplasts. In summary, we demonstrated that nutrient deprivation is characterized by rapid drop in cytosolic AcCoA concentration, culminating into the inhibition of EP300 activity and autophagy activation.

Compounds able to reduce AcCoA concentration, as well as EP300 inhibitors or HDAC activators, can be *bona fine* considered as Caloric Restriction Mimetics 'CRMs'. According to this new definition, we screened among both the broad-range and the specific KATs inhibitors and we elucidated that, their inhibitory activity, towards KATs, correlated with autophagy induction. In particular, we found that spermidine could induce autophagy (also) via inhibition of EP300, (published in (Pietrocola et al., 2015b)

V. MATERIALS AND METHODS

Cell Culture

Human colon carcinoma HCT 116 cells were cultured in McCoy's 5A medium containing 10% fetal bovine serum, 100 mg/L sodium pyruvate, 10 mM HEPES buffer, 100 units/mL penicillin G sodium, and 100 mg/mL streptomycin sulfate (37_C, 5% CO2). Human osteosarcoma U2OS cells, their GFP-LC3-expressing derivatives, human neuroblastoma H4 GFP-LC3 cells (gift from Professor J. Yuan), and human GFP-LC3-expressing HeLa cells were cultured in DMEM medium containing 10% fetal bovine serum, 100 mg/L sodium pyruvate, 10mMHEPES buffer, 100 units/mL penicillin G sodium, and 100 mg/mL streptomycin sulfate (37_C,5%CO2). MEFs were cultured in the same DMEM with additional supplementation of nonessential amino-acids and β--mercaptoethanol. Cells were seeded in 6-well, 12-well plates or in 10, 15 cm dishes and grown for 24 hr before treatment with 10 μM rapamycin, 100 nM bafilomycin A1(Tocris Bioscience, Bristol), 5 mM dimethyl α-ketoglutarate, 20 mM HC, 10 mM a-ketoisocaproate, 50mML-leucine, 20mM sodium DCA, 20mM sodium butyrate, 5 mM 1,2,3-benzenetricarboxylic acid hydrate (BTC), 20 mM Potassium Hydorxycitrate, 10 mM PHX maleate salt, 5 mM (±)-a-LA, UK5099, 3 mg/mL puromycin (all from Sigma Aldrich), 100 mM curcumin, 3-methyl-butyrolactone, 50 mM anacardic acid, and 10 mM timosaponin A-III, PI-103, moperamide, amiodarone, nimodipine, nitrendipine, niguldipine,rotenone, rifluoperazine, sorafenib, tosylate, niclosamide, rottlerin,caffeine, metformin, clonidine, rilmenidine, 20,50-dideoxyadenosine, suramin, pimozide, STF-62247, spermidine, FK-866, tamoxifen citrate, glucosamine, HA 14-1, licochalcone A, vurcumin, Akt Inhibitor X, rockout, 2-deoxyglucose, etoposide, C2-dihydroceramide and temozolomide (all from Enzo Life Sciences, Villeurbanne). For serum and nutrient deprivation, cells were cultured in serum-free Hank's balanced salt solution

(HBSS). For *Cell cycle* paper, resveratrol, piceatannol, epicatechin, caffeic acid, gallic acid, quercetin and bafilomycin A1 were purchased from Sigma-Aldrich; oenin chloride, kuronamin chloride, peonidin-3-O-glucoside chloride and delphinidin-3-O-glucoside chloride from Extrasynthese, EX527 from Tocris Bioscience and myricetin from Indofine Chemical. For *Cell Death and Differentiation* paper (REF), Anacardic Acid, Garcinol, C646 were purchased from Sigma Aldrich.

Plasmid transfection and RNA interference in human cell cultures

Transient plasmid transfections were performed with the Attractene reagent (Qiagen, Hilden, Germany), and, unless otherwise indicated, cells were analyzed 24 h after transfection. siRNAs were reverse-transfected with the help ofthe RNAi MaxTM transfection reagent (Invitrogen, Eugene, USA).

Microinjection experiments

For microinjection, U2OS cells were cultured overnight on culture dishes before injection. The setup for the injection itself was as follows: 10mM CoA or AcCoA in PBS were injected for 0.2 s under a pressure of 150 hPa, using a microinjector (Eppendorf, Hamburg, Germany). Then cells were cultured for 3 h in the presence of 100 nM bafilomycin A1 (BafA1) and subsequently fixed and stained for fluorescence microscopy.

Immunofluorescence

Cells were fixed with 4% PFA for 15 min at room temperature, and permeabilized with 0.1% Triton X-100 for 10 min, except for staining of cytoplasmic acetyl-lysine-containing proteins, in which any permeabilization step further than PFA fixation was avoided. Non-specific binding sites were blocked with 5% bovine serum albumin in PBS, followed by incubation with primary antibodies overnight at 4 °C. Following the cells were incubated with appropriate Alexa FluorTM

conjugates (Molecular Probes-Invitrogen). In the case of cytoplasmic acetyl-lysine staining, an additional step of blocking using anti-acetylated-tubulin antibody (1:200) was applied. Ten μM Hoechst 33342 (Molecular Probes-Invitrogen, Eugene, USA) was employed for nuclear counterstaining. Fluorescence wide-field and confocal microscopy assessments were performed on an DM IRE2 microscope (Leica Microsystems, Wetzlar, Germany) equipped with a DC300F camera and with an LSM 510 microscope (Carl Zeiss, Jena, Germany), respectively or by means of BD Pathway Automated Videomicroscopy.

Immunohistochemical staining

Immunohistochemical staining of heart tissue sections was performed using the Novolink Kit (RE7140-K, Menarini Diagnostics, Florence, Italy), as previously described (Ladoire et al., 2012). Briefly, 4 mm-thick formalin fixed, paraffin embedded tissue sections were deparaffinized with 3 successive passages through xylene, and rehydrated through decreasing concentrations (100%, 95%, 80%, 70% and 50%) of ethanol. Antigen retrieval was performed by heating slides for 30 min in pH 6.0 citrate buffer at 95°C. Slides were then allowed to cool at room temperature for 45 min, mounted on Shandon Sequenza coverplates (72-199-50, Thermo Fisher Scientific, Waltham, USA) in distilled water, and then washed twice for 5 min with 0.1% Tween 20 (v/v in PBS). Thereafter, sections were incubated for 5 min with the Peroxidase Block reagent, and subsequently washed twice for 5 min with 0.1% Tween20 (v/v in PBS). Following incubation for 5 min at room temperature with the Protein Block reagent, tissue sections were washed twice for 5 min with 0.1% Tween 20 (v/v inPBS), and then incubated overnight at 4°C with a primary antibody specific for LC3B (clone 5F10, 0231-100 from Nanotools, Teningen, Germany), or with an isotypematched IgG1 (MAB002, R&D Systems, Minneapolis, USA), both dissolved in 1 % bovine serum albumin (w/v in TBS) at the final concentration of 25 mg/mL. The 5F10antibody recognizes both the soluble (LC3-I) and the

membrane-bound form (LC3-II) of LC3B. After two washes in 0.1% Tween 20 (v/v in PBS), sections were incubated for 30 min with the Post Primary Block reagent, washed again as before and incubated for 30 min with the horseradish peroxidase-coupled secondary antibodies. Upon two additional washes, secondary antibodies were revealed with the liquid DAB Substrate Chromogen system during 10 min of incubation. Finally, slides were washed in distilled water, and counterstained with hematoxylin.

Automated microscopy

U2OS, HeLa or H4 cells stably expressing GFP-LC3 were seeded in 96-well imaging plates (BD Falcon, Sparks, USA) 24 h before stimulation. Cells were treated with the indicated agents for 4 h. Subsequently, cells were fixed with 4% PFA and counterstained with 10 μM Hoechst 33342. Images were acquired using a BD pathway 855 automated microscope (BD Imaging Systems, San Jose, USA) equipped with a 40X objective (Olympus, Center Valley, USA) coupled to a robotized Twister II plate handler (Caliper Life Sciences, Hopkinton, USA). Images were analyzed for the presence of GFP-LC3 puncta in the cytoplasm by means of the BD Attovision software (BD Imaging Systems). Cell surfaces were segmented and divided into cytoplasmic and nuclear regions according to standard proceedings. RB 2x2 andMarr-Hildreth algorithms were used to detect cytoplasmic GFP-LC3 positive dots. Statistical analyses were conducted using the R software (http://www.r-project.org/). For quantitative analyses of protein acetylation, cell surfaces were segmented into cytoplasmic and nucleic regions, and staining intensity of each individual cell was measured for statistical analysis.

Immunoblotting

For immunoblotting, 25 µg of proteins were separated on 4-12% Bis-Tris acrylamide (Invitrogen) or 12% Tris-Glycine SDS-PAGE precast gels (Biorad, Hercules, USA) and electrotransferred to Immobilon™ membranes (Millipore Corporation, Billerica, USA). Membranes were then sliced in different parts according to the molecular weight of the protein of interest to allow simultaneous detection of different antigens within the same experiment. Unspecific binding sites were saturated by incubating membranes for 1 h in 0.05% Tween 20 (v:v in TBS) supplemented with 5% non-fat powdered milk (w:v in TBS), followed by an overnight incubation with primary antibodies specific for acetylated-lysine, LC3, phospho-AMPK (Thr172), AMPK, phospho-ribosomal protein S6 kinase (Thr421/Ser424), ribosomal protein S6 kinase, or STQM/p62 (Santa Cruz Biotechnology). Development was performed withappropriate horseradish peroxidase (HRP)-labeled secondary antibodies (Southern Biotech, Birmingham, USA) plus the SuperSignal West Pico chemoluminescent substrate (Thermo Scientific-Pierce). An anti-glyceraldehyde-3-phosphate dehydrogenase antibody (Chemicon International, Temecula, USA) was used to controlequal loading of lanes.

Cell fractionation

Cells were trypsinized, pelleted at 1000 rpm for 4 min, washed withPBS and then pelleted again at 1000 rpm for 4 min. Cells were then resuspended in 5 mlof ice-cold hyposmotic buffer and kept on ice for 5 min. Following the cells were broken to release nuclei using a pre-chilled dounce homogenizer (20 strokes with a tight pestle) and were then centrifuged at 10000 g for 20 min at 4ºC to pellet nuclei and mitochondria. The supernatant was the cytosolic fraction.

Mouse experiments and tissue processing

C57BL/6 mice (Charles River Laboratory, Lentilly, France) were bred and maintained according to both the FELASA and the Animal Experimental Inserm Ethics Committee Guidelines (project: 2012-69). Mice were housed in a temperature-controlled environment with 12 h light/dark cycles and received food and water *ad libitum*. For HC-related experiments, mice were injected intraperitoneally with a single 100 mg/kg dose and 6 h later were sacrificed and tissues were immediately frozen in liquid nitrogen. For autophagy inducing agents, mice were intraperitoneally injected once with a dose of 100 mg/kg (Hydroxycitrate) or c646 (30 mg/kg). 6 hours after injection, mice were sacrificed and tissues were immediately frozen in liquid nitrogen for further processing (see below). For DCA- and DMKG related experiments, mice were subjected to 24 h starvation and injected intraperitoneally each 8 h with a 100 mg/kg of either DCA or DMKG solution prepared in PBS. After 24 h of starvation, mice were sacrificed and tissues were immediately frozen in liquid nitrogen after extraction and homogenized two cycles for 20 s at 5,500 rpm using Precellys 24 tissue homogenator (Bertin Technologies, Montigny-le-Bretonneux, France) in a 20 mM Tris buffer (pH 7.4) containing 150 mM NaCl, 1% Triton X-100, 10 mM EDTA and Complete® protease inhibitor cocktail (Roche Applied Science, Penzberg, Germany). Tissue extracts were then centrifuged at 12,000 g at 4 ºC and supernatants were collected. Protein concentration in the supernatants was evaluated by the bicinchoninic acid technique (BCA protein assay kit, Pierce Biotechnology, Rockford, USA). For hydroxycitrate-related weight-loss experiments, autophagy-deficient *Atg4b*-/- mice were used. *Atg4b*-/- mice have been previously described (Mariño et al., 2010). For Cell Cycle paper on coffee (Pietrocola et al., 2014), six weeks aged female C57BL/6 mice (Charles River Laboratory, Lentilly, France) and transgenic C57BL/6 mice expressing the fusion protein GFP-LC3 under the control of CAG (cytomegalovirus immediate-early (CMVie) enhancer and chicken β-actin

promoter) promoter, were bred and maintained according to both the FELASA and the European Community regulations for animal use in research (2010/63UE) as well as the local Ethics Committee for Animal Welfare (project number: 2012-065, 2012-067). For long-term coffee experiments, mice were first administered with 1%, 3% and 10 % w/v of regular and decaffeinated coffee in drinking water *ad libitum* in order to select a dose not affecting body weight; mice were then administrated with 3% w/v of coffee for two weeks. Mice were sacrificed and tissues were recovered and immediately frozen in liquid nitrogen 24, 48 or 72 h, one week and two weeks after treatment. For short-term coffee experiments, mice were administered with 3% w/v dose of regular and decaffeinated coffee by gavage and sacrificed after 1, 2, 4 and 6 h, when tissues were immediately frozen in liquid nitrogen. After extraction, tissues were homogenized during two cycles for 20 s at 5.500 rpm using a Precellys 24 tissue homogenator (Bertin Technologies, Montigny-le-Bretonneux, France) in a 20 mM Tris buffer (pH 7.4) containing 150 mM NaCl, 1% Triton X-100, 10 mM EDTA and Complete protease inhibitor cocktail (Roche Applied Science, Penzberg, Germany). Tissue extracts were then centrifuged at 12.000 g at 4 ºC and supernatants were collected. Protein concentration in the supernatants was evaluated by the bicinchoninic acid technique (BCA protein assay kit, Pierce Biotechnology, Rockford, USA).

In vivo model of pressure overload

Male WT mice (8–10 wk old) were subjected to pressure overload by surgical thoracic aortic constriction (TAC) or sham surgery as described. Animals were injected IP with either vehicle (PBS) or DMKG (300mg/kg) on the morning of the surgery and daily thereafter. Two-dimensional echocardiography was performed prior to surgery and 1 week post-surgery in non-sedated mice to quantify functional parameters using a Vevo 2100 high-resolution imaging system (VisualSonics). Mice were sacrificed 1 week post-surgery and hearts isolated for morphological and biochemical

analysis. Histological analysis was performed on formalin-perfused, paraffin-embedded sections with H&E and trichrome staining for analysis of fibrosis. Measurement of myocyte cross-sectional area was obtained from atransverse section of LV stained with wheat germ agglutinin. Quantitative analysis was obtained through measurement of an average of 900 cells in each section from two (sham) or three (TAC) animals.

Quantitative analysis of GFP-LC3 dots in mouse tissue sections

To avoid *postmortem* autophagy induction, dead mice were immediately perfused with 4% paraformaldehyde (w:v in PBS, pH 7.4). Tissues were then harvested and further fixed with the same solution for at least 4 h, followed by treatment with 15% sucrose (w:v in PBS) for 4 h and with 30% sucrose (w:v in PBS) overnight. Tissue samples were embedded in Tissue-Tek OCT compound (Sakura Finetechnical Co. Ltd., Tokyo, Japan) and stored at -70 °C. Five μm-thick tissue sections were prepared with a CM3050 S cryostat (Leica Microsystems), air-dried for 1 h, washed in PBS for 5 min, dried at RT for 30 min, and mounted with VECTASHIELD anti-fading medium. In each organ, the number of GFP-LC3 dots was counted in five independent visual fields from at least five mice using a TCS SP2 confocal fluorescence microscope (Leica Microsystems GmbH).

Preparation of cytoplasts

U2OS cells stably expressing GFP-LC3 were trypsinized and incubated in 3 ml of complete medium supplemented with 7.5 mg/mL cytochalasin B for 45 min at 37°C. This cell suspension was layered onto a discontinuous Ficoll density gradient (3 mL of 55%, 1 mL of 90%, and 3 mL of 100% Ficoll-Paques; GE Healthcare) in complete medium containing 7.5 mg/mL cytochalasin B. Gradients were prepared in ultracentrifuge tubes and pre-equilibrated at 37°C in a CO2 incubator overnight. Gradients containing cell suspensions were centrifuged in a prewarmed rotor (SW41; Beckman

Coulter) at 30,000 g for 30 min at 32°C. The cytoplast-enriched fraction was collected from the interface between 55 and 90% Ficoll layers, washed in complete medium, and incubated for 4 h at 37°C before treatments.

ATP measurement

Intracellular ATP was measured by means of a kit (Calbiochem, Darmstadt, Germany) based on an energy-dependent luciferase-driven luciferin conversion following the manufacturer's instructions. In short, cells were treated with lysis buffer containing 1% trichloroacetic acid for 1 min. The luciferin solution was added, and the luciferase activity was measured as an indicator of ATP content. For assessment of the chemoluminescent signal, the plates were read in a Fluostar luminometer (BMG Labtech, Ortenberg, Germany).

Quantitation of NADH/NADPH

The levels of reduced nicotinamide adenine dinucleotide (NADH) were measured by means of a FACS Vantage SE (Becton Dickinson), taking advantage of the autofluorescence of NADH and NAPDH (excitation at 340 nm and emission at 450 nm) (Mayevsky and Rogatsky, 2007). Treatment with 60 μM of the poly (ADP-ribose) polymerase (PARP) inhibitor PJ34 was used as positive control to measure the increase of cellular NADH, whereas membrane permeabilization with 0.5% saponin resulted in aloss of autofluorescence.

Sample preparation for metabolomic analysis

Cells were cultured in 6-well dishes being at an approximate 80% of confluence the day of the experiment. After the corresponding treatment, cells were detached with trypsin, transferred into 1.5 mL microcentrifuge tubes, centrifuged 2 min at 1000 x G (4ºC) and then washed with icecold PBS after carefully removing the trypsin-containing solution. Cells were centrifuged again and PBS was

carefully removed. Cell pellets were then resuspended in 150 µL of ice-cold hyposmotic buffer (water with HEPES and EDTA, pH 7.4) at 1 mM containing internal standard AcCoA (13C2) at 1 mg/L, vortexed and heated at 100 °C for 5 min. Samples were incubated in liquid nitrogen for 5 min and thawed at 4ºC temperature. This cycle was repeated twice. The samples were then kept for 1 h at -20°C and centrifuged at 4°C during 15 min at 13,000 g. Supernatants were transferred in HPLC vials and injected into HPLC/MS or kept at -80 °C until injection. For metabolite analysis in cytosolic fractions, cells were processed as previously described in this section, with the difference that cells were fractionated after adding the internal standard AcCoA ($^{13}C_2$) at 1 mg/L. Cells were broken using a pre-chilled dounce homogenizer (20 strokes with a tight pestle) and were then centrifuged at 10000 g for 20 min at 4ºC to pellet nuclei and mitochondria. The supernatant (i.e. the cytosolic fraction) was heated at 100 °C for 5 min. Fractions were then incubated in liquid nitrogen for 5 min and thawed at 4ºC two times. This cycle was performed two times. The samples were then were kept for 1 h at -20°C and centrifuged at 4°C during 15 min at 13,000 g. Supernatants were transferred in HPLC vials and injected into HPLC/MS or kept at -80 °C until injection. For animal tissues, flash-frozen tissue fragments of 60 to 80 mg were placed into dry ice pre-cooled homogenization tubes containing ceramic beads (Precellys lysis tubes soft tissue homogenizing CK14-KT03961-1-003.2 2mL). Five µl of lysis buffer (Methanol/water (80/20,v/v, -20°C, supplemented with the internal standard AcCoA 13C2, 1mg/L) was added to the tubes for each mg of tissue. Tissues were homogenized twice for 20 s at 5500 rpm using the Precellys 24 tissue homogenator (Bertin Technologies). Once homogenized, tissue extracts were centrifuged 10 min at 12,000 x G (4°C), and supernatants were collected and transferred to 1.5ml Eppendorf tubes.

Tubes containing supernatants were lyophilized in a SpeedVac concentrator (Thermo Scientific) for 2h at 35ºC. Dried samples were stored at -80 until analysis, when they were

resuspended in 100 µL of analytical-grade water, transferred to HPLC vials and injected into the HPLC-MS system.

Untargeted analysis of intracellular metabolites by high performance liquid chromatography (HPLC) coupled to a quadrupole- time of flight (QTOF) mass spectrometer.

Profiling of intracellular metabolites was performed on a RRLC 1260 system (Agilent Technologies, Waldbronn, Germany) coupled to a QTOF 6520 (Agilent) equipped with an electrospray source operating in positive ion and full scan mode from 100 to 1000 Da. The gas temperature was set at 350°C with a gas flow of 10 l/min. The capillary voltage was set at 4.0 kV, and the fragmentor at 150 V. Two reference masses were used to maintain the mass accuracy during analysis: 121.050873 (C5H4N4) and 922.009798 (C18H18O6N3P3F24).Five µL of sample were injected on a SB Aq column (150 mm Å~ 2.1 mm particle size3.5 µm) protected by a pre-column Eclipse plus (30 mm Å~ 2.1 mm particle size 3.5µm) from Agilent technologies.The gradient mobile phase consisted of water with 10 mmol/L of ammonium acetate and 0.01% of acetic acid (A) and acetonitrile (B). Initial condition is 98% phase A and 2% phase B. Molecules are then eluted using a gradient from 2% to 95% phase B in 10 min .The column was washed using 95% mobile phase B for 1 minute and equilibrated using 2% mobile phase B for 8 min. The flow rate was set to 0.3 ml/min.

Targeted analysis of AcCoA by HPLC coupled to a triple quadruple (QQQ) mass spectrometer.

Targeted analyses were performed on Rapid Resolution Liquid Chromatography (RRLC) 1200SL system (Agilent Technologies) coupled to a Triple Quadruple QQQ 6410 mass spectrometer (Agilent Technologies). RRLC analysis was done on 150 × 2.1 mm, 3.5 µm Eclipse Plus SB-Aq column with a pre-column 30 mm × 2.1 mm 3.5 µm Eclipse plus (Agilent Technologies) with water

containing 10 mmol/L of ammonium acetate and 0.01% of acetic acid in channel A and acetonitrile in channel B in gradient mode at a flow rate of 0.3 ml/min: t=0 min 2% B; t=9 min 95% B; t=11 min 95% B; re-equilibration time of 3 min. Mass spectrometer analysis was done in positive electrospray ionization mode at +4 kV on the QQQ system operating in MRM mode. MRM transitions were optimized with standard of AcCoA and AcCoA A 2-C^{13} with direct infusion. Two transitions were recorded for each compound;

AcCoA 810.1> 428 (collision energy: 20V)

AcCoA 810.1>303.1 (collision energy : 28V)

Internal standard AcCoA $^{13}C_2$ 812>428 (collision energy : 24V)

Internal standard AcCoA $^{13}C_2$ 812>305.1 (collision energy : 36V)

SILAC cell culture and sample processing

HCT 116 cells were cultured for two weeks in three different SILAC media (Invitrogen) containing either (i) light isotopes of L-arginine and L-lysine (Arg0/Lys0), (ii) L-arginine-13C6 HCl (Euroisotop) and LLysine 2HCl 4,4,5,5-D4 (Euroisotop) (Arg6/Lys4), and (iii) L-arginine-13C615N4 HCl and L-Lysine 13C6 15N4 HCl (Invitrogen) (Arg10/Lys8) and complemented as previously described (Blagoev and Mann, 2006). Cells were treated for 4 h with 10 µM rapamycin (Arg10/Lys8) or incubated in Hank´s Balanced Salt Solution (NF) (Arg6/Lys4) andthen lysed. The lysates were precipitated using ice-cold (- 20 °C) acetone (4 volumes of the sample extract), vortexed and placed for 2 h at -20°C. The resulting solution was centrifuged for 10 min at 16,000 g and the supernatant was removed. The pellet was subsequently washed twice with ice-cold 4:1 acetone/water. The final pellet was dried using a SpeedVac (Thermo-Scientific) for 10-15 min. Pellets were dissolved indenaturant 6M/2M urea/thiourea (both from Merck, Darmstadt, Germany) andbenzonase (Merck)

was added to the nuclear fraction. All steps were performed at RT to avoid carbamoylation of amines. Reduction of cysteines was performed with 5 mM DTT (Sigma-Aldrich) for 30 min followed by alkylation with 11 mM iodoacetamide for 20 min in the dark. The proteins were digested with 1:100 protease LysC (Wako, Neuss, Germany) for 3.5 h, diluted 4 times with 50 mM ammonium bicarbonate and the digested with 1:100 trypsin (Promega, Madison, USA) overnight. The nuclear fraction mixture was centrifuged at 10,000 g for 10 min and the supernatant was filtered througha 0.45 μm MillexHV filter (Millipore). From each fraction ~100 μg digested protein were collected for isoelectric focusing, a step required for subsequent normalization. The acetyl lysine peptide enrichment was performed as previously described (Choudhary et al., 2009). After peptide enrichment and isoelectric focusing, samples were subjected to mass spectrometry analysis and data were processed as described below.

SILAC sample processing and analysis

Upon digestion, peptides were concentrated and desalted on SepPak C18 (Waters, Milford, USA) purification cartridges and eluted using a highly organic buffer (80% acetonitrile, 0.5% acetic acid). Eluates were lyophilized in a vacuum centrifuge, dissolved in immunoprecipitation buffer (50 mM MOPS pH 7.2, 10 mM sodium phosphate, 50 mM sodium chloride) and mixed with anti-acetyl lysine antibodies conjugated to agarose beads. The mixture was left for 12 h at 4 ^{o}C on a rotation wheel. The flow-through (containing non-bound peptides) was removed and beads were washed 4 times with the immunoprecipitation buffer and twice with deionized water. Bead-bound peptides were eluted with 0.1% trifluoroacetic acid. Eluates and 3 separately collected digested protein samples were desalted using SepPak C18 cartridges and 5% of each acetyl lysine-enriched eluate was used for separate mass spectrometric (MS) analysis. Peptides were fractionated according to pI on a strong cation exchange chromatography (SCX) column using a pH step elution gradient as described

(Tsonev and Hirsh, 2008). The resulting fractions were then desalted on a C18 Stage-tip as described (Rappsilber and Mann, 2007) prior to MS analysis, which was performed on either an LTQ-Orbitrap-XL (Thermo Sceintific-Pierce, Whaltam, USA) connected to an Agilent 1200 nanoflow HPLC system (Agilent) or an LTQ-Orbitrap-Velos (Thermo Scientific-Pierce) connected to an Agilent 1100 nanoflow HPLC system (Agilent), using a nanoelectrospray ion source (Thermo Scientific-Pierce). Peptides were separated by reversed phase chromatography using an in-house made fused silica emitter (75 μm ID) packed with Reprosil-Pur C18-AQ 3 μm reversed phase material (Dr. Maisch GmbH, Ammerbuch-Entringen Germany). Peptides were loaded in 98% solvent A (0.5% acetic acid) followed by 100 min linear gradient to 50% solvent B (80% acetonitrile, 0.5% acetic acid). Survey full scan MS spectra (m/z range 300-200, resolution 60.000 @m/z 400) were acquired followed by fragmentation of the 10 (in case of using the LTQ-Orbitrap-XL) or the 20 (in case of using the LTQ-Orbitrap-Velos) most intense multiply charged ions. Ions selected for MS/MS were placed on a dynamic exclusion list for 45 sec. Real-time internal lock mass recalibration was used during data acquisition (Rappsilber and Mann, 2007). For unfractionated acetyl lysine-enriched eluates an additional MS analysis was performed on the LTQ-Orbitrap Velos using HCD fragmentation (normalized collision energy of 40) of the 10 most intense ions from each MS spectrum creating MS/MS spectra at resolution 7500. All samples used for protein normalization were analyzed on an LTQ FT ULTRA mass spectrometer (Thermo Finnigan, Ringoes, USA) where the 5 most intense ions from each precursor scan were selected for fragmentation in the LTQ. In this case, no real-time lock mass recalibration was used. Reverse phase chromatography settings were the same as described for the analysis done on the Orbitrap spectrometers.

SILAC data processing

Raw files were processed with MaxQuant v. 1.1.1.14 (Cox and Mann, 2008) into centroided data and submitted to database searching using the Andromeda search algorithm (Cox et al., 2011). Pre-processing by MaxQuant was performed to determine charge states, miscleavages and SILAC states and to filter the MS/MS spectra keeping the 6 most intense peaks within a 100 Da bin. Cysteine carbamidomethyl was chosen as fixed modification while N-termini acetylation and methionine oxidation were chosen as variable modifications. Furthermore, acetylation of light, medium and heavy isotope lysines (Lys0/Lys4/Lys8) was chosen as variable modification. Processed MS/MS spectra were searched against a concatenated targetdecoy database of forward and reversed sequences from the IPI database (152616 sequences, FASTA file created 20080506). For the search trypsin/P+DP was used forthe *in silico* protein digestion allowing 4 miscleavages. The mass tolerance for the MS spectra acquired in the Orbitrap was set to 7 ppm whereas the MS/MS tolerance was set to 0.6 Da for the CID MS/MS spectra from the LTQ and to 0.04 Da for the HCD MS/MS spectra. Upon peptide search, protein and peptide identification was performed given an estimated maximal false discovery rate (FDR) of 1% at both the protein and peptide level. For FDR calculation, posterior error probabilities were calculated based on peptides of at least 6 amino acids having an Andromeda score of at least 30. For protein quantification only unmodified peptides and peptides modified by N-termini acetylation (N-term) and methionine oxidation (M). If a counterpart to a given lysine acetylated peptide was identified, this counterpeptide was also excluded by protein quantitation. According to the protein group assignment performed by MaxQuant, both razor and unique peptides are used for protein quantification. A minimum of two ratio counts was required for protein quantification. For quantification of lysine-acetylated sites the least modified peptides were used. The ratios for the sites were normalized by the corresponding protein ratios to account for eventual

changes in protein abundance. In case a protein ratio was not determined, normalization was based on a logarithm transformation algorithm as previously described (Cox et al., 2011).

Statistical analysis

Unless otherwise mentioned, experiments were performed in triplicate and repeated at least twice. Data were analyzed using the GraphPad Prism 5 software and statistical significance was assessed by means of two-tailed Student's *t or* ANOVA tests, as appropriate. Tumor growth modeling was carried by linear mixed effect modeling on log pre-processed tumor surfaces. Reported p-values are obtained from testing jointly that both tumor growth slopes and intercepts (on log scale) are the same between treatment groups of interests. For sake of clarity, the outcome of the test is only given for comparisons found significant at $p < 0.05$. *Post-hoc* pairwise testing at single sampling time point confirmed the effects reported on the graphs.

Measurement of the Degradation of Long-lived Proteins

As described in (Bauvy et al., 2009), cells were incubated for 18 h at 37 °C with 0.2 μCi/mL-[^{14}C] valine. Unincorporated radioisotope was removed by three rinses with phosphate-buffered saline (pH 7.4). Cells were then incubated in nutrient- and serum-free medium (without amino acids and in the absence of fetal calf serum) plus 0.1% bovine serum albumin and 10 mM unlabeled valine. When required, 200 nM wortmannin, a potent inhibitor of the formation of autophagic vacuoles, or 4 × AA were added throughout the chase period. After the first hour of incubation, at which time short-lived proteins were being degraded, the medium was replaced with the appropriate fresh medium, and the incubation was continued for an additional 4 h period. Cells and radiolabeled proteins from the 4 h chase medium were precipitated in 10% (v/v) trichloroacetic acid at 4 °C. The precipitated proteins were separated from soluble radioactivity by centrifugation at 600 × g for 10 min and then

dissolved in 250 µl Soluene 350. The rate of protein degradation was calculated as acid-soluble radioactivity recovered from both cells and the medium.

Cytofluorometric assessment of mitochondrial outer membrane permeabilization

Live cells were co-stained with 20 nM 3,3'dihexiloxalocarbo- cyanine iodide (DiOC6(3), from Molecular Probes-Invitrogen), which measures mitochondrial transmembrane potential ($\Delta\psi m$), and 1 µg/mL propidium iodide (PI), which identifies cells with ruptured plasma membrane. Cytofluorometric acquisitions were performed on a FACSCalibur or a FACScan cytofluorometer (BD Biosciences) equipped with a 70 µm nozzle. Analysis was performed by means of the CellQuestTM or DIVA 6.1 software (BD Biosciences) upon gating on the events characterized by normal forward scatter and side scatter parameters.

EP300 gene deletion in MEFs

EP300 conditional KO MEFs (EP300flox/flox) were infected with pre-packaged viral particles expressing recombinant Cre (Vector Biolabs, Philadelphia, USA) according to the manufacturer's instructions to obtain EP300Δ/Δ MEFs. Successful deletion of EP300 was assessed by means of immunoblotting against EP300 protein.

In vitro acetylation assay

Recombinant GST-EP300 fusion protein, corresponding to the amino acids 1066-1707(14-418, Millipore), was assessed for its acetyltransferase activity on the EP300 natural substrates recombinant histone H3 protein (M2503S, New England Biolabs) and recombinant human p53 GST-fusion protein (14-865, Millipore).Briefly, 1 µg of EP300 HAT domain was incubated in presence of an HAT assay buffer (250mM Tris-HCl, pH 8.0, 50% glycerol, 0.5 mM EDTA and 5 mM

dithiothreitol), 1 µg of substrate protein and growing concentrations of AcCoA (A2056, Sigma Aldrich) for 1 hour at 30 ° C. The reaction was stopped by adding 4x SDS buffer and boiling the samples. Acetylation of substrate proteins was measured by immunoblotting using specific antibodies against H3K56 (Cell Signaling, Danvers, USA), p53 K373 (Millipore) and EP300 K1499 (Cell Signaling).

VI. DISCUSSION

My thesis project has consisted into the definition of AcCoA as a key metabolite regulating starvation-induced autophagy. AcCoA occupies a central position in cellular dynamics, as it controls the balance between anabolic and catabolic reactions, both as a central metabolic intermediate and as a signal transducer. We have been able to demonstrate that acute nutrient depletion in cultured human cells and starvation of rodents share as common metabolic feature a rapid decrease in the levels of AcCoA, which leads to the deacetylation of cellular proteins.

We found that multiple distinct manipulations designed to increase or reduce intracellular AcCoA lead to the suppression or induction of autophagy, respectively, in mice or in cultured human cells. Thus, the inhibition of AcCoA synthesis by interventions on pyruvate, acetate, BCAAs, and fatty acid metabolism induces autophagy, while stimulation of AcCoA synthesis inhibits autophagy induced by multiple distinct stimuli. As for the well-established AMP/ATP-AMPK, amino acids/mTOR, and NADH/NAD-SIRT1 systems, we identified the acetyltransferase EP300 as the sensor of cytosolic AcCoA levels. Following the increase in AcCoA concentration, EP300 allows the rapid adaptation to a nutrient-rich condition by inhibiting, in a transcription independent manner, key proteins of the autophagic pathway, such as ATG5, ATG7 and as recently discovered, Beclin-1.

Moreover, EP300 retains the capacity of auto-acetylation, thus boosting its activity in a feedforward manner. The rational between AcCoA-levels and EP300 activity relies on the fact that at variance with kinases, which operate close to independently from ATP concentrations (due to their high Kd for ATP), acetyltransferases are profoundly influenced in their catalytic activity by the availability of acetyl groups, provided by AcCoA. Thus, subtle differences in AcCoA levels may

impact on the level of overall protein acetylation, which reflects the compounded activity of acetyltransferases and deacetylases (Wellen et al., 2009).

Accordingly, AcCoA depletion was accompanied by a reduction of the acetylation of most proteins, as indicated by immunofluorescence detection of acetylated proteins or mass spectrometry. Notwithstanding this prominent (de)acetylation effect elicited by starvation, SILAC approach has revealed that a few proteins are hyperacetylated. Similarly, the hyperacetylation of specific proteins contrasting with this general pattern, the hyperacetylation of specific proteins has been linked to autophagy induction by starvation. This is exemplified by the proautophagic Esa1p/ TIP60-mediated hyperacetylation of Atg3p in yeast (Lin et al., 2012) or the hyperacetylaton of tubulin (Geeraert et al., 2010) and ULK1 in human cells (Lin et al., 2012), although the metabolic basis of these events remain to be elucidated.

As previously discussed, the depletion of energy-rich metabolites strongly induces autophagy. Upon starvation, reduction in ATP/AMP ratio results in AMPK activation and consequently mTOR inhibition; similarly, decrease in NADH/NAD^+ ratio leads to SIRT1 activation and deacetylation of autophagic genes. Notwithstanding the importance of ATP/AMPK and NADH/sirtuin-1, our results point to the existence of an additional control instance, cytosolic AcCoA. Indeed, at early time points of starvation, intracellular AcCoA was found to be reduced well before ATP depletion or NADH oxidation became detectable.

At the same time, manipulations designed to reduce AcCoA levels and to induce autophagy also result into the activation of AMPK and the inhibition of mTOR. However AMPK was dispensable for autophagy induction by these agents, as confirmed by the fact that MEFs, lacking the

AMPK subunits PRKAA1 and PRKAA2, still responded to starvation and AcCoA depletion/increase by an increase/reduction in autophagic flux.

It is possible that ATP-, NADH-, and AcCoA-regulated processes are closely interconnected, based on multiple pathways that link energy homeostasis among these molecules, as well as on the fact that AMPK phosphorylates the acetyltransferase EP300.

Moreover, our results add a further level of complexity into the intricate landscape of the 'mTOR-centric' sensing of amino acids levels. Indeed, we observed that the BCAA leucine could signal to the autophagic machinery (also) via an increase in AcCoA levels, depending on its oxidative decarboxylation catalyzed by branched chain alpha-ketoacid dehydrogenase BCKDH. Whether Leucine can inhibit autophagy independently of mTOR it remains to be characterized. Similarly, it would be interesting to explore whether a crosstalk between EP300 and mTOR exists.

As abovementioned, AcCoA metabolism is highly compartmentalized. In this study, we demonstrated that the nucleo-cytosolic pool of AcCoA is responsible for autophagy inhibition. Indeed, blocking the mitochondrial export of citrate, via inhibition of SLC25A1 or inhibiting the activity of ACLY, prevents the AcCoA-elevating agents mediated inhibition of autophagy.

Conversely, replenishing the nucleo-cytosolic pool of AcCoA by the microinjection of AcCoA into cultured human cells or by the systemic administration of dimethlyl-α-ketoglutarate *in vivo* and *in vitro* suppresses starvation-induced autophagy. Based on these findings, it appears clear that AcCoA compartmentalization impacts on protein acetylation. Of note, specific acetyltransferases and deacetylases are also subjected to subcellular compartmentalization. This applies, for instance, to EP300 as well as to the deacetylase SIRT1, both of which shuttle between the nucleus and the cytosol (Chang and Guarente, 2014).

The notion that nucleo-cytosolic pool of AcCoA could influence histone acetylation has already been investigated by other groups (Wellen et al., 2009). In this work, histone acetylation correlated with cytosolic AcCoA levels generated through ACLY activity. Furthermore, it has been recently shown that in cancer cells overexpressing the oncogene Akt, an increment in AcCoA/CoA ratio drives the metabolic reprogramming of tumor cells affecting histone acetylation (Lee et al., 2014). Again, this increase in AcCoA levels relies on ACLY activation by Akt, which phosphorylates ACLY on Ser455 hence boosting its catalytic activity. ATP-Citrate Lyase is thus the major determinant of protein acetylation at nucleo-cytosolic level via AcCoA production. Chemical (via the competitive inhibitor Hydroxycitrate) or genetic inhibition of ACLY rapidly triggers autophagy and protein (de)acetylation both *in vitro* and *in vivo* and possibly represents a new identified target in pathological settings.

In my thesis work, we have not analyzed in detail the consequences that manipulations of AcCoA metabolism have at nuclear level. Nonetheless, in yeast and flies, it has been observed that histone deacetylation, caused by AcCoA shortage favors the expression of pro-autophagic genes (Eisenberg et al., 2014) Similarly, it has been shown that down-regulation of the HAT MYST1 allows the activation of a pro-autophagic nuclear program trough deacetylation of H4K16 in yeast (Fullgrabe et al., 2013). Moreover LC3 is deacetylated by SIRT1 in the nucleus, allowing it to shuttle back to the cytoplasm (in complex with tumor protein p53 inducible nuclear protein 2, TP53INP2) and participate in the assembly of autophagosomes (Huang et al., 2015). These results indicate that (de) acetylation reactions can also be important for transcription-dependent autophagy.

Related to this, it has been recently shown that PDC exists in the nucleus, generating a specific pool of AcCoA necessary for histone acetylation and it would be interesting to define how nuclear PDC can modulate autophagy at nuclear level (Sutendra et al., 2014).

As extensively argumented, different fuels and metabolic pathways can lead to AcCoA generation; in our experimental settings, we observed that glucose and amino acids deprivation are responsible for the observed decrease in AcCoA and protein acetylation upon starvation. Nonetheless, it is important to underline that the source of AcCoA can be cell line or model-organism dependent; in yeast, nucleo-cytosolic AcCoA metabolism mainly relies on acetate (Eisenberg et al., 2014). Indeed, yeast cells overexpressing the ortholog of mammalian ACSS2 (i.e., Acs2p) have increased levels of AcCoA, resulting into elevated histone acetylation and autophagy inhibition. Moreover, the brain-specific knockout of AcCoAS (the sole ortholog of mammalian ACSS1 and ACSS2 in Drosophila) suffices to induces autophagy and extend lifespan. Recently, has emerged how tumors rely on acetate catabolism for their proliferation (Comerford et al., 2014) and several human cancers (including brain metastatic tumors) overexpress Acss2 in order to maximize acetate utilization to sustain their growth (Mashimo et al., 2014).

Hence, AcCoA production can also depend on the cellular type and on the metabolic reprogramming elicited by a pathologic process like cellular transformation. In line with this latter notion, the expression levels of proteins involved in AcCoA metabolism and transport, as well as in (de)acetylation reactions, exhibit remarkable variations in cells of different histological origin . Thus, the cellular differentiation and activation state might also affect the relative abundance of multiple AcCoA-relevant enzymes, adding yet another layer of complexity to this regulatory network. However, in our setting, the administration of any Acetyl CoA source or the stimulation of any AcCoA metabolic route it is sufficient for inhibiting starvation-induced autophagy.

Mice deprived of food (but with access to water *ad libitum*) for 24 hr exhibit a significant reduction in total AcCoA levels in several organs, including the heart and muscles, corresponding to a decrease in protein acetylation levels However, the same experimental conditions have no major

effects on AcCoA concentrations in the brain and actually increase hepatic AcCoA and protein acetylation levels (Chow et al., 2014). This latter phenomenon has been causally linked to the mobilization of subcutaneous fat stores, one of the first effects of short-term fasting (Browning et al., 2012).

In fasting conditions, indeed, fatty acids are released by adipocytes and employed (at least in part) as substrate for β-oxidation (which produces AcCoA) within hepatocytes (which are particularly rich in mitochondria) (Browning et al., 2012).Repeated intraperitoneal injections of dimethyl-α-ketoglutarate or dichloroacetate (DCA) efficiently prevent the drop of AcCoA levels provoked by starvation in the heart and muscle of mice.

Along similar lines, the provision of excess acetate has been shown to increase AcCoA levels in the hypothalamus upon the activation of ACAC, eventually resulting in the synthesis of anorectic neuropeptides and appetite suppression (Frost et al., 2014) Finally, ethanol intake augments AcCoA levels in hepatic mitochondria (Fritz et al., 2013).

The aforementioned findings indicate that alterations in food and alcohol intake have a direct impact on intracellular AcCoA levels. However, it appears unlikely that the starvation induced decrease of AcCoA in the heart and muscles solely and directly results from reduced glucose availability.

Indeed, intracellular AcCoA concentrations drop well before glycemia decreases, at the same time as circulating triglycerides increase. This phenomenon may therefore reflect the ability of starvation to cause a diminution in the plasma levels of various cytokines and growth factors, including INS and IGF1, coupled to an increase in the circulating amounts of the IGF1 antagonist insulin-like growth factor binding protein 1 (IGFBP1) (Cheng et al., 2014).

Limited growth factor signaling results indeed in reduced AKT1 activation, which has (at least) two negative consequences for AcCoA metabolism. First, AKT1 signaling is required for normal glucose uptake through plasma membrane glucose transporters (at least in muscle and adipose tissue) (Wieman et al., 2007). Second, AKT1 normally phosphorylates ACLY on S473, hence stimulating AcCoA production (Lee et al., 2014). Although this hypothetical pathway linking starvation to dwindling AcCoA levels has not been formally explored *in vivo*, signs of AKT1 activation (*i.e.*, AKT1 phosphorylation on S473) positively correlate with histone acetylation levels in human gliomas and prostate cancers (Lee et al., 2014).

Another major pathway that may link starvation to dropping AcCoA levels in some cells involves SIRT1, which is activated in energy-low conditions (high NAD^+ levels) (Morselli et al., 2010) and inhibits ACSS2 (Sahar et al., 2014). This latter effect may explain the circadian rhythmicity of hepatic AcCoA levels in mice (Sahar et al., 2014).

Obviously, metabolic disorders also affect AcCoA concentrations. For example, type-1 diabetes causes a major increase in hepatic AcCoA concentrations (Perry et al., 2014). Interestingly, this effect can be mimicked by a 3-day HFD regimen combined with an artificial elevation of circulating corticosterone levels (which occur spontaneously in animal models of type 1 diabetes) and can be reverted by the administration of mifepristone, an antagonist of glucocorticoid receptors (Perry et al., 2014). Thus, the increased turnover of fatty acids and acetate associated with type I diabetes may elevate mitochondrial AcCoA levels, ultimately promoting hepatic gluconeogenesis by virtue of its capacity to allosterically activate PC and inhibit the PDC. Further supporting this notion, mice genetically endowed with a muscle-specific defect in β-oxidation are significantly less prone to develop diet-induced INS resistance than their wild-type counterparts.

Based on these observations, it appears clear as AcCoA is a metabolic and signaling molecule able to influence several cellular process and its levels affect the propensity of cells to grow, progress along the cell cycle, mount autophagic responses to stress, and succumb to regulated cell death. (Figure 4).

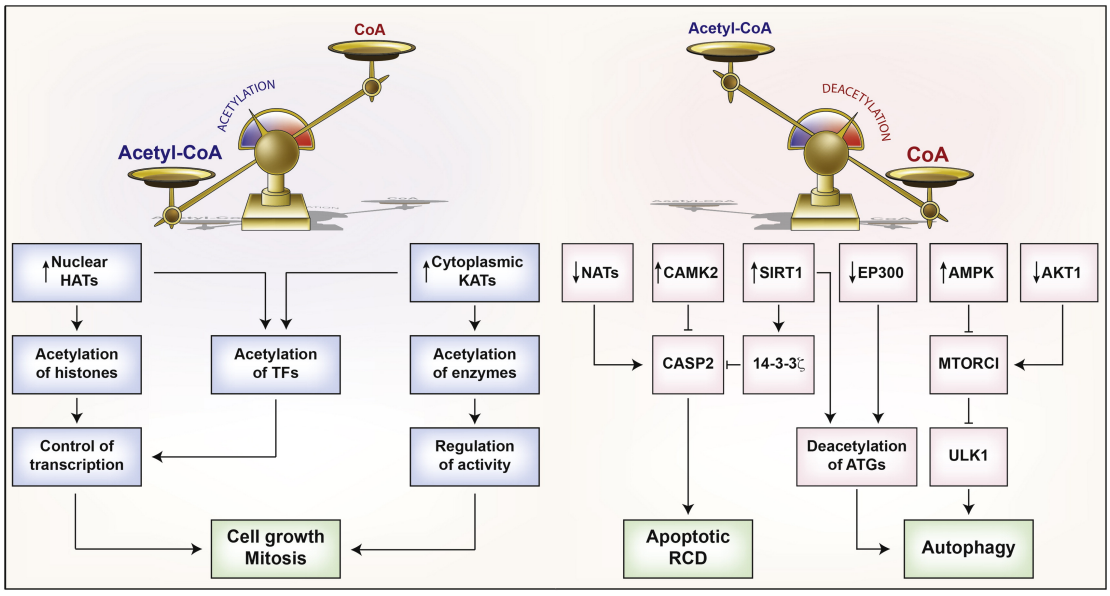

Figure 4. (Pietrocola et al., 2015a). Impact of Acetyl CoA on various Cellular functions. Abbreviations HAT, histone acetyltransferase; KAT, lysine acetyltransferase; MTORCI, mechanistic target of rapamycin complex I; NAT, Na acetyltransferase; ULK1, unc-51-like autophagy activating kinase 1.

In this work, we defined the fall of AcCoA levels and protein (de) acetylation as new hallmarks of nutrient starvation. We thus hypothesized that compounds able to induce similar cellular modifications could also replicate the preclinical positive effects linked to nutrient deprivation. Indeed, long-term caloric restriction (that is, reduced calorie intake without malnutrition) or intermittent short-term starvation (fasting) has been shown to prolong the mean and the maximum lifespan of yeast, plants, worms, flies and rodents. (Rubinsztein et al., 2011) Caloric restriction may also have beneficial effects on longevity in primates and it may improve healthspan, particularly by reducing the incidence of highly penetrant pathologies such as metabolic diseases, cancer, arteriosclerosis and neurodegeneration. More recently, strategies of long-term starvation have been adopted, even if in preclinical studies, for improving the effect of chemotherapy in different cancer models (Lee et al., 2012). Unlike alternate day fasting, long-term starvation is accompanied by a significant weigh-loss, which in non-obese patiens or in the context of chemotherapy can represent an undesirable effect; for this reason, intermittent fasting regimens can mediate the positive effects of starvation avoiding weigh-loss. Nonetheless, even in context of metabolic disorders and more particularly obesity, long-term starvation has turned to be a poorly suitable strategy for the amelioration of the metabolic syndrome. Similarly, most normal-weighted, apparently healthy individuals with pre-diabetes, dyslipidaemia or other signs of imminent severe disease are refractory to harsh diets, vigorous exercise, alternate-day fasting or similar strategies to improve their health (Madeo et al., 2014). For this reason, the administration of compounds able to mimic the metabolic and molecular changes triggered by fasting can be adopted to induce the positive effects of starvation limiting its side effects. Although the use of Caloric Restriction Mimetics has already been proposed, there is no consensus for the biochemical definition and their classification. Following our study, we define CRMs as compounds that, as starvation, reduce

protein acetylation levels. There are three biochemical ways to achieve this effect: first, the nucleocytosolic pool of AcCoA can be reduced by preventing the synthesis of AcCoA in mitochondria and in the cytosol or, alternatively, by preventing its export from mitochondria into the cytosol. Second the direct inhibition of KATs, whose activity directly depends on AcCoA concentration. Third, the activation of protein Deacetylases such as Sirtuins that deacetylate key substrate acetylated by KATs. The net result of these different manipulations is the modulation of different molecular pathways (i.e AMPK activation, mTOR inhibition) as well as the establishment of an epigenetic nuclear program, which ultimately lead to pro-healthy effects, including autophagy (Figure 5). A series of hypothetical CRMs is listed on table 2. (Madeo et al., 2014).

Table 2. Biochemical and functional characteristics of CRMs

Category	Target	Agent (source)	Preclinical and clinical effects possibly linked to autophagy induction
AcCoA depleting agents	Mitochondrial pyruvate carrier	UK5099 (synthetic)	Unknown
	Carnitine palmitoyl transferase 1	Perhexiline maleate (synthetic)	Anti-angina pectoris agent. Improvement of hypertrophic cardiomyopathy.
	Mitochondrial citrate carrier	1,2,3-benzene-tricarboxylate (synthetic)	Reduction of insulin secretion in rat islets.
	ATP citrate lyase	Hydroxycitrate (from *Garcinia cambogia* and *Hibiscus subdariffa*)	Autophagy-dependent reduction in weight-loss in mice. Reduction of body weight, insulin resistance and oxidative stress in obese Zucker rats. Antitumor effects on transplantable mouse cancers if combine with lipoic acid. Weight loss in controlled clinical trials.
		Radicicol (*Diheterospora chlamydosporia)*	Anti-inflammatory action in sepsis in mice. Improved muscle regeneration in mice. Protection against renal and myocardial ischemia-reperfusion damage in rodents.
		SB-204990	Decrease in chlolesterol and tryglicerydes in rats. Tumor growth suppression in mice.
	Pyruvate dehydrogenase	CPI-613	Anti-tumor effects in mice.
Acetyl transferase inhibitors	Histone acetyl transferase	Curcumin (from *Curcuma longa)*	Improves heart function in rat model of myocardial infarction Heart failure prevention and cardiac hypertrophy reversion Tumor growth inhibition in an rthotopic model of pancreatic cancer in mice. Inhibition of forestomach, duodenal, and colon

			carcinogenesis in mice. Lifespan extension in *C. elegans* and *D. melanogaster*. Improvement of Glucose Tolerane and Insulin resistant phenotype in db/db mice. Prevenzion of Azt-induced colon cancer in db/db mice.
		Epigallocatechin-3-gallate (EGCG) (from green tea)	Lifespan extension in CElegans and rats. Neuroprotection in Alzheimer's mouse model, ischemic stroke and ALS mouse model. Inhibition of hepatosteatosis and increase of lipolysis in high-fat diet fed mice. Suppression of dextran-sulfate induced cholitis. Reduced weight gain and insulin resistance in mice receiving obesogenic diet.

Category	**Target**	**Agent (source)**	**Preclinical and clinical effects possibly linked to autophagy induction**
		Spermidine	Autophagy dependent lifespan extension in yeast, nematodes, flies. Lifespan extension in mice. Prevention of colon cancer development in mice. Reduction in arterial aging and ROS-mediated oxidative stress. Reduction in skin inflammation in mice. Reversion of age-mediated memory impairment in flies.
		Anacardic Acid (*Anacardium occidentale)*	Tumor growth and angiogenesis inhibition in human cancers xenografted to mice.
		Garcinol (*Garcinia indica)*	Antitumoral effects in squamous cell carcinoma of head and neck. Xenograft model. Anti-carcinogenesis effect via 5-lipooxygenase inhibition.
		MB-3	Unknown
		CPTH2	Unknown
		C646	Immunostimulation by inhibition of Treg in mice.
		Gallic Acid (different plants)	Anti-proliferative effects on xenografted mouse tumors in mice Reduces infiltration of tumor by T reg cells in mice. Reduced weight gain in rats under high-fat diet. Suppression of β-amyloid neurotoxicity.
Deacetylase activators	Sirtuin 1	Resveratrol (different plants, red wine)	Extends lifespan of mice on high-fat diet. SIRT-1 dependent autophagy induction in mammalian and nematodes. Amelioration of metabolic syndrome and inflammation in Rhesus Monkey fed an obesogenic diet. Chemopreventive effect on colon cancer in the $Apc^{Min/+}$ mouse model. Prevents β-cell dedifferentiation under high-fat/high-sugar conditions in nonhuman primates and isolated human islets Improvement of insulin sensitivity and glucose control in diabetic patients.
		Nicotinamide riboside Nicotinamide mononucleotide	Protection against high-fat diet induced abnormalities. Lifespan extension in *S. cerevisiae*. Amelioration of diet and age-dependent diabetic pathophysiology.
		SRT1720 (synthetic)	Amelioration of metabolic syndrome in obese Zucker rats Lifespan extension and amelioration of metabolic syndrome in HFD-fed mice. Life span extension and improved insulin sensitvity in mice fed a standard diet.

		Quercetin (different plants, red wine, green tea)	Increased mitochondrial biogenesis in brain and muscle with augmented exercise tolerance. Reduction in inflammation, weight gain and metabolic syndrome in mice. Tumor growth reduction in orthotopic model of pancreatic cancer.
		Piceatannol (*Picea abies*, red wine)	Improvement of metabolic syndrome in db/db obese mice.

In my work, we observed that the inhibition of both pyruvate entry into the mitochondria via MPC and the block of intra-mitochondrial generation of Acetyl CoA via PDH are able to induce the triad of Acetyl CoA reduction, protein (de) acetylation and autophagy induction. Similarly, the inhibition of citrate export in the cytosol and its consequent conversion into Acetyl CoA and oxaloacetate by ACLY provoke the same effects. Along the same notions, reducing Acetyl CoA production from Acetate by inhibiting ACSS1 and from FFA blocking CPT can also stimulate the CRMs triad. For this reason, ACLY inhibitors (such as HC and SB204990), UK-5009 (MPC-inihibtiors) or perhexiline (CPT1 inhibitors) can be enumerated into CRMs.

KATs inhibitors include a variety of natural compounds known for pro-healthy as well as pro-autophagic effects. For a series of broad-range KATs inhibitors such as Curcumin, Anacardic Acid and Garcinol, we established a direct correlation between the (de) acetylation, mTOR inhibition and autophagy induction. On the contrary, the EP300 specific inhibitor C646 showed a dose-dependent effect in term of protein (de) acetylation, whereas it maintained the ability to induce autophagy even at concentrations to which we do not observe (de) acetylation. Importantly, we observed that Spermidine, known for its lifespan extension and pro-autophagic effects, behave as a competitive inhibitor of EP300.

Resveratrol is considered to be the first example of a SIRT1 activator, although it has been disputed whether this effect is achieved by direct molecular interactions with the SIRT1 protein

causing its allosteric activation or whether it involves indirect mechanisms — for example, an increase in cellular cyclic AMP levels (as a result of the resveratrol-mediated inhibition of phosphodiesterase) leading to activation of AMPK. Irrespective of these unknown factors, resveratrol potently stimulates autophagy via SIRT1 in nematodes and mammalian cell, as already discussed. Importantly, Resveratrol-based compounds have been shown to induce general (de) acetylation and to induce autophagy in cultured cell line (Pietrocola et al., 2012).

The net effect of protein deacetylation is detectable only upon a general inhibition of KATs, as in the case of AcCoA drop or via administration of non-specific KATs inhibitors but it cannot be reproduced by knocking-down or via chemical inhibition of individual KATs. Another major caveat concerns the specificity of several natural CRMs. For example, EGCG (a polyphenol found in green tea) and curcumin have multiple molecular targets and may have pleiotropic effects as a result of their suboptimal specificity. Therefore, genetic studies are of particular importance to identify the health-promoting targets of CRMs. Notwithstanding these aspects, it is important to underline that genetic modulation of CRMs targets confirmed their pivotal role in the regulation of healthy-related phenomena; Knocking down the gene encoding ACLY was shown to induce cytoprotective autophagy that delayed the toxicity caused by the expression of a mutant form of Huntingtin in cultured human cells, and knocking down the gene encoding AcCoA synthetase extended the lifespan of *D. melanogaster*. (Eisenberg et al., 2014) Moreover, SIRT1-transgenic mice share features with mice that have been subjected to a calorically restricted diet, including improved metabolic parameters and motor capabilities, reduced DNA damage during ageing — which has oncosuppressive effects — and ameliorated angiotensin II-induced vascular pathology. The knockout of genes encoding acetyl transferases (particularly HATs) is often embryonically lethal, which reflects the crucial role of these enzymes in several cellular processes and in early

development (Yao et al., 1998). Nevertheless, there is some genetic evidence that modulating acetyl transferase activity can be an efficient way to mimic dietary restriction. The KAT3 family of acetyl transferases (including CREB-binding protein (CBP) and EP300) is a particularly crucial hub that translates nutrient availability into transient or epigenetic modifications of effector proteins. Interestingly, genetic ablation of the cysteine histidine-rich 1 (CH1) domain of EP300 or of CBP, which is responsible for insulin responsiveness, mimicked the beneficial effect of caloric restriction as it increased insulin sensitivity and glucose tolerance, and also reduced body weight and white adipose tissue when these mice were fed either normal or high-fat diets (Bedford et al., 2011). EP300 consequently seems to be a reasonable target for mimicking caloric restriction, and the putative health-promoting effects of nonspecific acetyl transferase inhibitors (such as curcumin, gallic acid or EGCG) could indeed be linked to their ability to block EP300 activity (Mielgo-Ayuso et al., 2014). On the basis of these considerations, it is particularly important to evaluate the therapeutic and toxicological profiles of more selective EP300 inhibitors (such as C646) in preclinical studies. It is reasonable to expect — but remains to be shown — that truly specific EP300 inhibitors might combine maximum efficacy with minimum toxicity. In favour of this possibility, small-molecule inhibitors of EP300 lack the toxicity of their natural template garcinol when added to T cells *in vitro* (Mantelingu et al., 2007). Similarly, analogues of anarcadic acid have been developed with the aim of generating agents that kill malignant cells but that spare normal cells (Eliseeva et al., 2007). These findings highlight the potential therapeutic value of more specific EP300 inhibitors.

The hypothesis that optimal CRMs are pharmacological agents that induce autophagy via protein deacetylation has several practical implications that warrant further investigation.

First, autophagy-regulatory deacetylation reactions might be used as biomarkers to measure the *in vitro* and *in vivo* effects of CRMs (for example, in blood cells). As an example, antibodies recognizing proteins carrying acetylated lysine residues (irrespective of the context) or — more specifically — antibodies recognizing EP300 only when it is acetylated on Lys1499 (Delvecchio et al., 2013) can be used to detect the effect of starvation or CRMs on distinct tissues and cell types *in vivo* and *in vitro*. Similarly, the deacetylation of specific sirtuin substrates can be determined as a proxy of sirtuin activity. It remains to be determined which deacetylation reactions would be optimally suitable as caloric restriction- or CRM-relevant biomarkers.

Second, if the detection of deacetylation and the induction of autophagy constituted accurate biomarkers for predicting the efficacy of CRMs, such biomarkers might in turn facilitate pharmacological screens for the identification of new CRMs. In such screens, cultured cells would be exposed to candidate CRMs and autophagy would be detected (for example, by monitoring the redistribution of green fluorescent protein (GFP)–LC3 to autophagosomes). General protein deacetylation or deacetylation of specific proteins could also be measured.

Third, if deacetylation constituted the point at which autophagy is regulated by AcCoA, acetyl transferases and deacetylases, it seems obvious that particular combinations of autophagy inducers should interact in a synergistic manner. In the same way as a kinase inhibitor may be expected to synergize with an activator of a phosphatase acting on the same substrate, acetyl transferase inhibitors should synergize with deacetylase activators. As a proof of principle, spermidine was shown to synergize with resveratrol to induce autophagy (Morselli et al., 2011). It will be important to investigate such interactions in more detail to gain insights into their putative beneficial and collateral effects *in vivo*.

Fourth, it will be important to evaluate novel combination regimens in addition to CRMs. As cytosolic AcCoA and EP300 repress mTORC1 activity and several CRMs extend lifespan by inhibiting the TOR pathway, it seems that the CRM-modulated and IGF1-, AKT-, and TORC1-dependent pathways functionally intersect. Thus, it will be interesting to investigate whether the combination of CRMs with inhibitors of IGF1, AKT or TORC1 is more effective than these agents alone.

Finally, the evaluation of current and future CRMs in clinical trials for the treatment of diabetes, metabolic syndrome and other diseases should benefit from the monitoring of suitable biomarkers. In particular, setting up a consistent method for LC3-detection and protein acetylation in blood peripheral cells may represent a novel approach for rapid evaluation of autophagy in clinical settings.

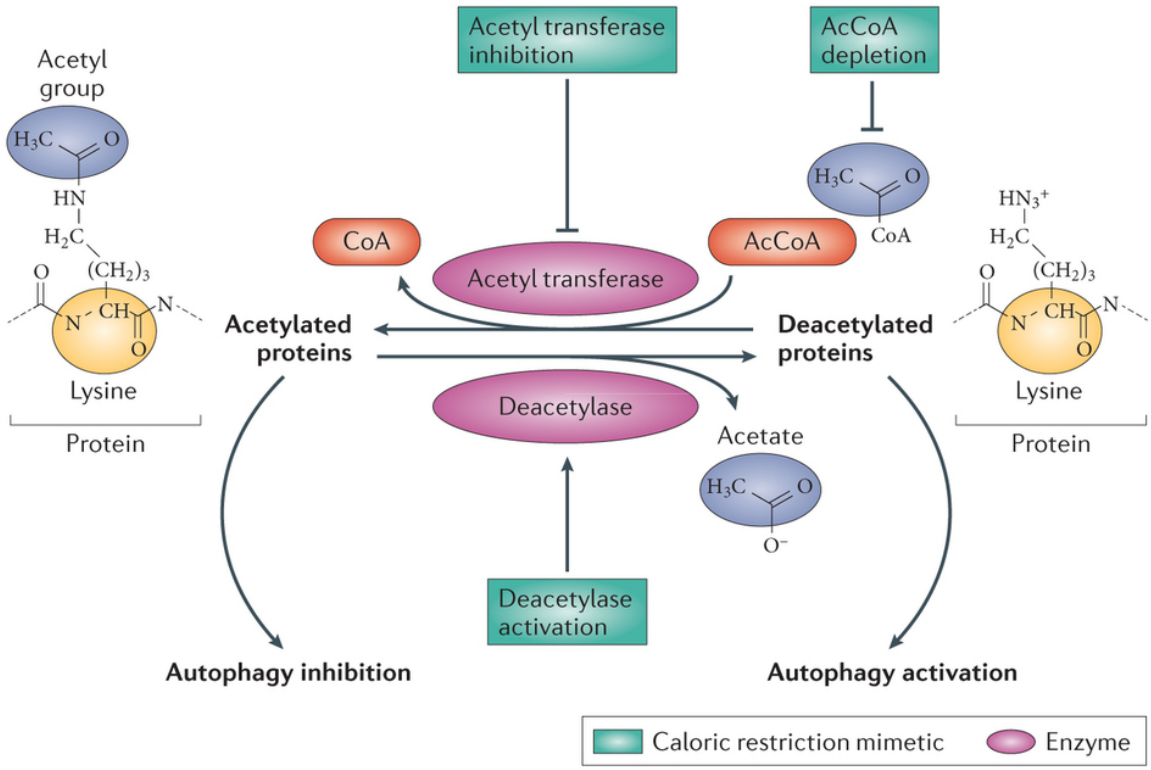

Figure 5. General properties of CRMs. (Madeo et al., 2014)

VII. REFERENCES

Alers, S., Loffler, A.S., Wesselborg, S., and Stork, B. (2012). Role of AMPK-mTOR-Ulk1/2 in the regulation of autophagy: cross talk, shortcuts, and feedbacks. Mol Cell Biol *32*, 2-11.

Alexander, A., Cai, S.L., Kim, J., Nanez, A., Sahin, M., MacLean, K.H., Inoki, K., Guan, K.L., Shen, J., Person, M.D.*, et al.* (2010). ATM signals to TSC2 in the cytoplasm to regulate mTORC1 in response to ROS. Proc Natl Acad Sci U S A *107*, 4153-4158.

Alvers, A.L., Fishwick, L.K., Wood, M.S., Hu, D., Chung, H.S., Dunn, W.A., Jr., and Aris, J.P. (2009). Autophagy and amino acid homeostasis are required for chronological longevity in Saccharomyces cerevisiae. Aging Cell *8*, 353-369.

Arico, S., Petiot, A., Bauvy, C., Dubbelhuis, P.F., Meijer, A.J., Codogno, P., and Ogier-Denis, E. (2001). The tumor suppressor PTEN positively regulates macroautophagy by inhibiting the phosphatidylinositol 3-kinase/protein kinase B pathway. J Biol Chem *276*, 35243-35246.

Armani, A., Cinti, F., Marzolla, V., Morgan, J., Cranston, G.A., Antelmi, A., Carpinelli, G., Canese, R., Pagotto, U., Quarta, C.*, et al.* (2014). Mineralocorticoid receptor antagonism induces browning of white adipose tissue through impairment of autophagy and prevents adipocyte dysfunction in high-fat-diet-fed mice. FASEB J *28*, 3745-3757.

Atkinson, D.E., and Walton, G.M. (1967). Adenosine triphosphate conservation in metabolic regulation. Rat liver citrate cleavage enzyme. J Biol Chem *242*, 3239-3241.

Axe, E.L., Walker, S.A., Manifava, M., Chandra, P., Roderick, H.L., Habermann, A., Griffiths, G., and Ktistakis, N.T. (2008). Autophagosome formation from membrane compartments enriched in phosphatidylinositol 3-phosphate and dynamically connected to the endoplasmic reticulum. J Cell Biol *182*, 685-701.

Baba, M., Hong, S.B., Sharma, N., Warren, M.B., Nickerson, M.L., Iwamatsu, A., Esposito, D., Gillette, W.K., Hopkins, R.F., 3rd, Hartley, J.L.*, et al.* (2006). Folliculin encoded by the BHD gene interacts with a binding protein, FNIP1, and AMPK, and is involved in AMPK and mTOR signaling. Proc Natl Acad Sci U S A *103*, 15552-15557.

Baehrecke, E.H. (2005). Autophagy: dual roles in life and death? Nat Rev Mol Cell Biol *6*, 505-510.

Bai, P., Canto, C., Oudart, H., Brunyanszki, A., Cen, Y., Thomas, C., Yamamoto, H., Huber, A., Kiss, B., Houtkooper, R.H.*, et al.* (2011). PARP-1 inhibition increases mitochondrial metabolism through SIRT1 activation. Cell metabolism *13*, 461-468.

Balakumaran, B.S., Porrello, A., Hsu, D.S., Glover, W., Foye, A., Leung, J.Y., Sullivan, B.A., Hahn, W.C., Loda, M., and Febbo, P.G. (2009). MYC activity mitigates response to

rapamycin in prostate cancer through eukaryotic initiation factor 4E-binding protein 1-mediated inhibition of autophagy. Cancer Res *69*, 7803-7810.

Bar-Peled, L., Chantranupong, L., Cherniack, A.D., Chen, W.W., Ottina, K.A., Grabiner, B.C., Spear, E.D., Carter, S.L., Meyerson, M., and Sabatini, D.M. (2013). A Tumor suppressor complex with GAP activity for the Rag GTPases that signal amino acid sufficiency to mTORC1. Science *340*, 1100-1106.

Bar-Peled, L., Schweitzer, L.D., Zoncu, R., and Sabatini, D.M. (2012). Ragulator is a GEF for the rag GTPases that signal amino acid levels to mTORC1. Cell *150*, 1196-1208.
Bauvy, C., Meijer, A.J., and Codogno, P. (2009). Assaying of autophagic protein degradation. Methods Enzymol *452*, 47-61.

Bedford, D.C., Kasper, L.H., Wang, R., Chang, Y., Green, D.R., and Brindle, P.K. (2011). Disrupting the CH1 domain structure in the acetyltransferases CBP and p300 results in lean mice with increased metabolic control. Cell metabolism *14*, 219-230.

Behrends, C., Sowa, M.E., Gygi, S.P., and Harper, J.W. (2010). Network organization of the human autophagy system. Nature *466*, 68-76.

Bejarano, E., Yuste, A., Patel, B., Stout, R.F., Jr., Spray, D.C., and Cuervo, A.M. (2014). Connexins modulate autophagosome biogenesis. Nat Cell Biol *16*, 401-414.

Bellot, G., Garcia-Medina, R., Gounon, P., Chiche, J., Roux, D., Pouyssegur, J., and Mazure, N.M. (2009). Hypoxia-induced autophagy is mediated through hypoxia-inducible factor induction of BNIP3 and BNIP3L via their BH3 domains. Mol Cell Biol *29*, 2570-2581.

Bender, T., Pena, G., and Martinou, J.C. (2015). Regulation of mitochondrial pyruvate uptake by alternative pyruvate carrier complexes. EMBO J *34*, 911-924.

Bjedov, I., Toivonen, J.M., Kerr, F., Slack, C., Jacobson, J., Foley, A., and Partridge, L. (2010). Mechanisms of life span extension by rapamycin in the fruit fly Drosophila melanogaster. Cell metabolism *11*, 35-46.

Bjorkoy, G., Lamark, T., Brech, A., Outzen, H., Perander, M., Overvatn, A., Stenmark, H., and Johansen, T. (2005). p62/SQSTM1 forms protein aggregates degraded by autophagy and has a protective effect on huntingtin-induced cell death. J Cell Biol *171*, 603-614.

Boroughs, L.K., and DeBerardinis, R.J. (2015). Metabolic pathways promoting cancer cell survival and growth. Nat Cell Biol *17*, 351-359.

Boya, P., Gonzalez-Polo, R.A., Casares, N., Perfettini, J.L., Dessen, P., Larochette, N., Metivier, D., Meley, D., Souquere, S., Yoshimori, T.*, et al.* (2005). Inhibition of macroautophagy triggers apoptosis. Mol Cell Biol *25*, 1025-1040.

Boya, P., Reggiori, F., and Codogno, P. (2013). Emerging regulation and functions of autophagy. Nat Cell Biol *15*, 713-720.

Browning, J.D., Baxter, J., Satapati, S., and Burgess, S.C. (2012). The effect of short-term fasting on liver and skeletal muscle lipid, glucose, and energy metabolism in healthy women and men. J Lipid Res *53*, 577-586.

Brunet, A., Sweeney, L.B., Sturgill, J.F., Chua, K.F., Greer, P.L., Lin, Y., Tran, H., Ross, S.E., Mostoslavsky, R., Cohen, H.Y.*, et al.* (2004). Stress-dependent regulation of FOXO transcription factors by the SIRT1 deacetylase. Science *303*, 2011-2015.

Cahill, G.F., Jr. (2006). Fuel metabolism in starvation. Annu Rev Nutr *26*, 1-22.

Canto, C., Gerhart-Hines, Z., Feige, J.N., Lagouge, M., Noriega, L., Milne, J.C., Elliott, P.J., Puigserver, P., and Auwerx, J. (2009). AMPK regulates energy expenditure by modulating NAD+ metabolism and SIRT1 activity. Nature *458*, 1056-1060.

Canto, C., Houtkooper, R.H., Pirinen, E., Youn, D.Y., Oosterveer, M.H., Cen, Y., Fernandez-Marcos, P.J., Yamamoto, H., Andreux, P.A., Cettour-Rose, P.*, et al.* (2012). The NAD(+) precursor nicotinamide riboside enhances oxidative metabolism and protects against high-fat diet-induced obesity. Cell metabolism *15*, 838-847.

Cebollero, E., Reggiori, F., and Kraft, C. (2012). Reticulophagy and ribophagy: regulated degradation of protein production factories. Int J Cell Biol *2012*, 182834.

Cederbaum, A.I. (2012). Alcohol metabolism. Clin Liver Dis *16*, 667-685.

Chalkiadaki, A., and Guarente, L. (2012). Sirtuins mediate mammalian metabolic responses to nutrient availability. Nat Rev Endocrinol *8*, 287-296.

Chan, E.Y. (2009). mTORC1 phosphorylates the ULK1-mAtg13-FIP200 autophagy regulatory complex. Sci Signal *2*, pe51.

Chang, H.C., and Guarente, L. (2014). SIRT1 and other sirtuins in metabolism. Trends Endocrinol Metab *25*, 138-145.

Chauhan, S., Goodwin, J.G., Chauhan, S., Manyam, G., Wang, J., Kamat, A.M., and Boyd, D.D. (2013). ZKSCAN3 is a master transcriptional repressor of autophagy. Molecular cell *50*, 16-28.

Chen, D., Bruno, J., Easlon, E., Lin, S.J., Cheng, H.L., Alt, F.W., and Guarente, L. (2008). Tissue-specific regulation of SIRT1 by calorie restriction. Genes Dev *22*, 1753-1757.

Chen, G., Ke, Z., Xu, M., Liao, M., Wang, X., Qi, Y., Zhang, T., Frank, J.A., Bower, K.A., Shi, X.*, et al.* (2012). Autophagy is a protective response to ethanol neurotoxicity. Autophagy *8*, 1577-1589.

Cheng, C.W., Adams, G.B., Perin, L., Wei, M., Zhou, X., Lam, B.S., Da Sacco, S., Mirisola, M., Quinn, D.I., Dorff, T.B*., et al.* (2014). Prolonged fasting reduces IGF-1/PKA to promote hematopoietic-stem-cell-based regeneration and reverse immunosuppression. Cell Stem Cell *14*, 810-823.

Cheong, H., Lindsten, T., Wu, J., Lu, C., and Thompson, C.B. (2011). Ammonia-induced autophagy is independent of ULK1/ULK2 kinases. Proc Natl Acad Sci U S A *108*, 11121-11126.

Choudhary, C., Weinert, B.T., Nishida, Y., Verdin, E., and Mann, M. (2014). The growing landscape of lysine acetylation links metabolism and cell signalling. Nat Rev Mol Cell Biol *15*, 536-550.

Chow, J.D., Lawrence, R.T., Healy, M.E., Dominy, J.E., Liao, J.A., Breen, D.S., Byrne, F.L., Kenwood, B.M., Lackner, C., Okutsu, S*., et al.* (2014). Genetic inhibition of hepatic acetyl-CoA carboxylase activity increases liver fat and alters global protein acetylation. Mol Metab *3*, 419-431.

Cianfanelli, V., Fuoco, C., Lorente, M., Salazar, M., Quondamatteo, F., Gherardini, P.F., De Zio, D., Nazio, F., Antonioli, M., D'Orazio, M*., et al.* (2015). AMBRA1 links autophagy to cell proliferation and tumorigenesis by promoting c-Myc dephosphorylation and degradation. Nat Cell Biol *17*, 20-30.

Codogno, P., Mehrpour, M., and Proikas-Cezanne, T. (2012). Canonical and non-canonical autophagy: variations on a common theme of self-eating? Nat Rev Mol Cell Biol *13*, 7-12.

Comb, W.C., Hutti, J.E., Cogswell, P., Cantley, L.C., and Baldwin, A.S. (2012). p85alpha SH2 domain phosphorylation by IKK promotes feedback inhibition of PI3K and Akt in response to cellular starvation. Molecular cell *45*, 719-730.

Comerford, S.A., Huang, Z., Du, X., Wang, Y., Cai, L., Witkiewicz, A.K., Walters, H., Tantawy, M.N., Fu, A., Manning, H.C*., et al.* (2014). Acetate dependence of tumors. Cell *159*, 1591-1602.

Criollo, A., Niso-Santano, M., Malik, S.A., Michaud, M., Morselli, E., Marino, G., Lachkar, S., Arkhipenko, A.V., Harper, F., Pierron, G*., et al.* (2011). Inhibition of autophagy by TAB2 and TAB3. EMBO J *30*, 4908-4920.

Davidson, C.D., Ali, N.F., Micsenyi, M.C., Stephney, G., Renault, S., Dobrenis, K., Ory, D.S., Vanier, M.T., and Walkley, S.U. (2009). Chronic cyclodextrin treatment of murine Niemann-Pick C disease ameliorates neuronal cholesterol and glycosphingolipid storage and disease progression. PLoS One *4*, e6951.

Delvecchio, M., Gaucher, J., Aguilar-Gurrieri, C., Ortega, E., and Panne, D. (2013). Structure of the p300 catalytic core and implications for chromatin targeting and HAT regulation. Nat Struct Mol Biol *20*, 1040-1046.

Deosaran, E., Larsen, K.B., Hua, R., Sargent, G., Wang, Y., Kim, S., Lamark, T., Jauregui, M., Law, K., Lippincott-Schwartz, J.*, et al.* (2013). NBR1 acts as an autophagy receptor for peroxisomes. J Cell Sci *126*, 939-952.

Deretic, V., Saitoh, T., and Akira, S. (2013). Autophagy in infection, inflammation and immunity. Nat Rev Immunol *13*, 722-737.

Di Bartolomeo, S., Corazzari, M., Nazio, F., Oliverio, S., Lisi, G., Antonioli, M., Pagliarini, V., Matteoni, S., Fuoco, C., Giunta, L.*, et al.* (2010). The dynamic interaction of AMBRA1 with the dynein motor complex regulates mammalian autophagy. J Cell Biol *191*, 155-168.

Dittenhafer-Reed, K.E., Richards, A.L., Fan, J., Smallegan, M.J., Fotuhi Siahpirani, A., Kemmerer, Z.A., Prolla, T.A., Roy, S., Coon, J.J., and Denu, J.M. (2015). SIRT3 mediates multi-tissue coupling for metabolic fuel switching. Cell metabolism *21*, 637-646.

Dong, J., Qiu, H., Garcia-Barrio, M., Anderson, J., and Hinnebusch, A.G. (2000). Uncharged tRNA activates GCN2 by displacing the protein kinase moiety from a bipartite tRNA-binding domain. Molecular cell *6*, 269-279.

Dong, S., Jia, C., Zhang, S., Fan, G., Li, Y., Shan, P., Sun, L., Xiao, W., Li, L., Zheng, Y.*, et al.* (2013). The REGgamma proteasome regulates hepatic lipid metabolism through inhibition of autophagy. Cell metabolism *18*, 380-391.

Donohoe, D.R., Garge, N., Zhang, X., Sun, W., O'Connell, T.M., Bunger, M.K., and Bultman, S.J. (2011). The microbiome and butyrate regulate energy metabolism and autophagy in the mammalian colon. Cell metabolism *13*, 517-526.

Dupont, N., Chauhan, S., Arko-Mensah, J., Castillo, E.F., Masedunskas, A., Weigert, R., Robenek, H., Proikas-Cezanne, T., and Deretic, V. (2014). Neutral lipid stores and lipase PNPLA5 contribute to autophagosome biogenesis. Curr Biol *24*, 609-620.

Duran, A., Linares, J.F., Galvez, A.S., Wikenheiser, K., Flores, J.M., Diaz-Meco, M.T., and Moscat, J. (2008). The signaling adaptor p62 is an important NF-kappaB mediator in tumorigenesis. Cancer Cell *13*, 343-354.

Duran, R.V., MacKenzie, E.D., Boulahbel, H., Frezza, C., Heiserich, L., Tardito, S., Bussolati, O., Rocha, S., Hall, M.N., and Gottlieb, E. (2013). HIF-independent role of prolyl hydroxylases in the cellular response to amino acids. Oncogene *32*, 4549-4556.
Duran, R.V., Oppliger, W., Robitaille, A.M., Heiserich, L., Skendaj, R., Gottlieb, E., and Hall, M.N. (2012). Glutaminolysis activates Rag-mTORC1 signaling. Molecular cell *47*, 349-358.

Efeyan, A., Comb, W.C., and Sabatini, D.M. (2015). Nutrient-sensing mechanisms and pathways. Nature *517*, 302-310.

Efeyan, A., Zoncu, R., Chang, S., Gumper, I., Snitkin, H., Wolfson, R.L., Kirak, O., Sabatini, D.D., and Sabatini, D.M. (2013). Regulation of mTORC1 by the Rag GTPases is necessary for neonatal autophagy and survival. Nature *493*, 679-683.

Egan, D.F., Shackelford, D.B., Mihaylova, M.M., Gelino, S., Kohnz, R.A., Mair, W., Vasquez, D.S., Joshi, A., Gwinn, D.M., Taylor, R.*, et al.* (2011). Phosphorylation of ULK1 (hATG1) by AMP-activated protein kinase connects energy sensing to mitophagy. Science *331*, 456-461.

Eisenberg, T., Knauer, H., Schauer, A., Buttner, S., Ruckenstuhl, C., Carmona-Gutierrez, D., Ring, J., Schroeder, S., Magnes, C., Antonacci, L.*, et al.* (2009). Induction of autophagy by spermidine promotes longevity. Nat Cell Biol *11*, 1305-1314.

Eisenberg, T., Schroeder, S., Andryushkova, A., Pendl, T., Kuttner, V., Bhukel, A., Marino, G., Pietrocola, F., Harger, A., Zimmermann, A.*, et al.* (2014). Nucleocytosolic depletion of the energy metabolite acetyl-coenzyme a stimulates autophagy and prolongs lifespan. Cell metabolism *19*, 431-444.

Elgendy, M., Sheridan, C., Brumatti, G., and Martin, S.J. (2011). Oncogenic Ras-induced expression of Noxa and Beclin-1 promotes autophagic cell death and limits clonogenic survival. Molecular cell *42*, 23-35.

Eliseeva, E.D., Valkov, V., Jung, M., and Jung, M.O. (2007). Characterization of novel inhibitors of histone acetyltransferases. Mol Cancer Ther *6*, 2391-2398.

Fan, W., Nassiri, A., and Zhong, Q. (2011). Autophagosome targeting and membrane curvature sensing by Barkor/Atg14(L). Proc Natl Acad Sci U S A *108*, 7769-7774.

Fantin, V.R., and Abraham, R.T. (2013). Self-eating limits EGFR-dependent tumor growth. Cell *154*, 1184-1186.

Fimia, G.M., Stoykova, A., Romagnoli, A., Giunta, L., Di Bartolomeo, S., Nardacci, R., Corazzari, M., Fuoco, C., Ucar, A., Schwartz, P.*, et al.* (2007). Ambra1 regulates autophagy and development of the nervous system. Nature *447*, 1121-1125.

Fogel, A.I., Dlouhy, B.J., Wang, C., Ryu, S.W., Neutzner, A., Hasson, S.A., Sideris, D.P., Abeliovich, H., and Youle, R.J. (2013). Role of membrane association and Atg14-dependent phosphorylation in beclin-1-mediated autophagy. Mol Cell Biol *33*, 3675-3688.
Fraldi, A., Annunziata, F., Lombardi, A., Kaiser, H.J., Medina, D.L., Spampanato, C., Fedele, A.O., Polishchuk, R., Sorrentino, N.C., Simons, K.*, et al.* (2010). Lysosomal fusion and SNARE function are impaired by cholesterol accumulation in lysosomal storage disorders. EMBO J *29*, 3607-3620.

Fritz, K.S., Green, M.F., Petersen, D.R., and Hirschey, M.D. (2013). Ethanol metabolism modifies hepatic protein acylation in mice. PLoS One *8*, e75868.

Frost, G., Sleeth, M.L., Sahuri-Arisoylu, M., Lizarbe, B., Cerdan, S., Brody, L., Anastasovska, J., Ghourab, S., Hankir, M., Zhang, S*., et al.* (2014). The short-chain fatty acid acetate reduces appetite via a central homeostatic mechanism. Nat Commun *5*, 3611.

Fullgrabe, J., Lynch-Day, M.A., Heldring, N., Li, W., Struijk, R.B., Ma, Q., Hermanson, O., Rosenfeld, M.G., Klionsky, D.J., and Joseph, B. (2013). The histone H4 lysine 16 acetyltransferase hMOF regulates the outcome of autophagy. Nature *500*, 468-471.

Galluzzi, L., Kepp, O., Vander Heiden, M.G., and Kroemer, G. (2013). Metabolic targets for cancer therapy. Nat Rev Drug Discov *12*, 829-846.

Galluzzi, L., Pietrocola, F., Bravo-San Pedro, J.M., Amaravadi, R.K., Baehrecke, E.H., Cecconi, F., Codogno, P., Debnath, J., Gewirtz, D.A., Karantza, V*., et al.* (2015). Autophagy in malignant transformation and cancer progression. EMBO J *34*, 856-880.

Galluzzi, L., Pietrocola, F., Levine, B., and Kroemer, G. (2014). Metabolic control of autophagy. Cell *159*, 1263-1276.

Ge, L., Melville, D., Zhang, M., and Schekman, R. (2013). The ER-Golgi intermediate compartment is a key membrane source for the LC3 lipidation step of autophagosome biogenesis. Elife *2*, e00947.

Geeraert, C., Ratier, A., Pfisterer, S.G., Perdiz, D., Cantaloube, I., Rouault, A., Pattingre, S., Proikas-Cezanne, T., Codogno, P., and Pous, C. (2010). Starvation-induced hyperacetylation of tubulin is required for the stimulation of autophagy by nutrient deprivation. J Biol Chem *285*, 24184-24194.

Geisler, S., Holmstrom, K.M., Skujat, D., Fiesel, F.C., Rothfuss, O.C., Kahle, P.J., and Springer, W. (2010). PINK1/Parkin-mediated mitophagy is dependent on VDAC1 and p62/SQSTM1. Nat Cell Biol *12*, 119-131.

Goginashvili, A., Zhang, Z., Erbs, E., Spiegelhalter, C., Kessler, P., Mihlan, M., Pasquier, A., Krupina, K., Schieber, N., Cinque, L*., et al.* (2015). Insulin granules. Insulin secretory granules control autophagy in pancreatic beta cells. Science *347*, 878-882.

Gonzalez, C.D., Lee, M.S., Marchetti, P., Pietropaolo, M., Towns, R., Vaccaro, M.I., Watada, H., and Wiley, J.W. (2011). The emerging role of autophagy in the pathophysiology of diabetes mellitus. Autophagy *7*, 2-11.

Grassian, A.R., Parker, S.J., Davidson, S.M., Divakaruni, A.S., Green, C.R., Zhang, X., Slocum, K.L., Pu, M., Lin, F., Vickers, C*., et al.* (2014). IDH1 mutations alter citric acid cycle metabolism and increase dependence on oxidative mitochondrial metabolism. Cancer Res *74*, 3317-3331.

Green, D.R., and Levine, B. (2014). To be or not to be? How selective autophagy and cell death govern cell fate. Cell *157*, 65-75.

Guarente, L. (2006). Sirtuins as potential targets for metabolic syndrome. Nature *444*, 868-874.

Guo, H., Chitiprolu, M., Gagnon, D., Meng, L., Perez-Iratxeta, C., Lagace, D., and Gibbings, D. (2014). Autophagy supports genomic stability by degrading retrotransposon RNA. Nat Commun *5*, 5276.

Guo, J.Y., and White, E. (2013). Autophagy is required for mitochondrial function, lipid metabolism, growth, and fate of KRAS(G12D)-driven lung tumors. Autophagy *9*, 1636-1638.

Guo, J.Y., Xia, B., and White, E. (2013a). Autophagy-mediated tumor promotion. Cell *155*, 1216-1219.

Guo, R., Zhang, Y., Turdi, S., and Ren, J. (2013b). Adiponectin knockout accentuates high fat diet-induced obesity and cardiac dysfunction: role of autophagy. Biochim Biophys Acta *1832*, 1136-1148.

Gupta, V.K., Scheunemann, L., Eisenberg, T., Mertel, S., Bhukel, A., Koemans, T.S., Kramer, J.M., Liu, K.S., Schroeder, S., Stunnenberg, H.G.*, et al.* (2013). Restoring polyamines protects from age-induced memory impairment in an autophagy-dependent manner. Nat Neurosci *16*, 1453-1460.

Gwinn, D.M., Shackelford, D.B., Egan, D.F., Mihaylova, M.M., Mery, A., Vasquez, D.S., Turk, B.E., and Shaw, R.J. (2008). AMPK phosphorylation of raptor mediates a metabolic checkpoint. Molecular cell *30*, 214-226.

Hailey, D.W., Rambold, A.S., Satpute-Krishnan, P., Mitra, K., Sougrat, R., Kim, P.K., and Lippincott-Schwartz, J. (2010). Mitochondria supply membranes for autophagosome biogenesis during starvation. Cell *141*, 656-667.

Halestrap, A.P., and Price, N.T. (1999). The proton-linked monocarboxylate transporter (MCT) family: structure, function and regulation. Biochem J *343 Pt 2*, 281-299.
Hamasaki, M., Furuta, N., Matsuda, A., Nezu, A., Yamamoto, A., Fujita, N., Oomori, H., Noda, T., Haraguchi, T., Hiraoka, Y.*, et al.* (2013). Autophagosomes form at ER-mitochondria contact sites. Nature *495*, 389-393.

Han, J.M., Jeong, S.J., Park, M.C., Kim, G., Kwon, N.H., Kim, H.K., Ha, S.H., Ryu, S.H., and Kim, S. (2012). Leucyl-tRNA synthetase is an intracellular leucine sensor for the mTORC1-signaling pathway. Cell *149*, 410-424.

Hanahan, D., and Weinberg, R.A. (2000). The hallmarks of cancer. Cell *100*, 57-70.

Hardie, D.G., Ross, F.A., and Hawley, S.A. (2012). AMPK: a nutrient and energy sensor that maintains energy homeostasis. Nat Rev Mol Cell Biol *13*, 251-262.

Harding, H.P., Novoa, I., Zhang, Y., Zeng, H., Wek, R., Schapira, M., and Ron, D. (2000). Regulated translation initiation controls stress-induced gene expression in mammalian cells. Molecular cell *6*, 1099-1108.

Harris, R.A., Joshi, M., Jeoung, N.H., and Obayashi, M. (2005). Overview of the molecular and biochemical basis of branched-chain amino acid catabolism. J Nutr *135*, 1527S-1530S.

Hart, L.S., Cunningham, J.T., Datta, T., Dey, S., Tameire, F., Lehman, S.L., Qiu, B., Zhang, H., Cerniglia, G., Bi, M.*, et al.* (2012). ER stress-mediated autophagy promotes Myc-dependent transformation and tumor growth. J Clin Invest *122*, 4621-4634.

Hawley, S.A., Boudeau, J., Reid, J.L., Mustard, K.J., Udd, L., Makela, T.P., Alessi, D.R., and Hardie, D.G. (2003). Complexes between the LKB1 tumor suppressor, STRAD alpha/beta and MO25 alpha/beta are upstream kinases in the AMP-activated protein kinase cascade. J Biol *2*, 28.

Hawley, S.A., Pan, D.A., Mustard, K.J., Ross, L., Bain, J., Edelman, A.M., Frenguelli, B.G., and Hardie, D.G. (2005). Calmodulin-dependent protein kinase kinase-beta is an alternative upstream kinase for AMP-activated protein kinase. Cell metabolism *2*, 9-19.

Hawley, S.A., Ross, F.A., Chevtzoff, C., Green, K.A., Evans, A., Fogarty, S., Towler, M.C., Brown, L.J., Ogunbayo, O.A., Evans, A.M.*, et al.* (2010). Use of cells expressing gamma subunit variants to identify diverse mechanisms of AMPK activation. Cell metabolism *11*, 554-565.

He, C., Bassik, M.C., Moresi, V., Sun, K., Wei, Y., Zou, Z., An, Z., Loh, J., Fisher, J., Sun, Q.*, et al.* (2012a). Exercise-induced BCL2-regulated autophagy is required for muscle glucose homeostasis. Nature *481*, 511-515.

He, C., and Klionsky, D.J. (2009). Regulation mechanisms and signaling pathways of autophagy. Annu Rev Genet *43*, 67-93.
He, C., Sumpter, R., Jr., and Levine, B. (2012b). Exercise induces autophagy in peripheral tissues and in the brain. Autophagy *8*, 1548-1551.

Herzig, S., Raemy, E., Montessuit, S., Veuthey, J.L., Zamboni, N., Westermann, B., Kunji, E.R., and Martinou, J.C. (2012). Identification and functional expression of the mitochondrial pyruvate carrier. Science *337*, 93-96.

Hidvegi, T., Ewing, M., Hale, P., Dippold, C., Beckett, C., Kemp, C., Maurice, N., Mukherjee, A., Goldbach, C., Watkins, S.*, et al.* (2010). An autophagy-enhancing drug promotes degradation of mutant alpha1-antitrypsin Z and reduces hepatic fibrosis. Science *329*, 229-232.

Holzer, R.G., Park, E.J., Li, N., Tran, H., Chen, M., Choi, C., Solinas, G., and Karin, M. (2011). Saturated fatty acids induce c-Src clustering within membrane subdomains, leading to JNK activation. Cell *147*, 173-184.

Hosokawa, N., Hara, T., Kaizuka, T., Kishi, C., Takamura, A., Miura, Y., Iemura, S., Natsume, T., Takehana, K., Yamada, N.*, et al.* (2009). Nutrient-dependent mTORC1 association with the ULK1-Atg13-FIP200 complex required for autophagy. Mol Biol Cell *20*, 1981-1991.

Houtkooper, R.H., Williams, R.W., and Auwerx, J. (2010). Metabolic networks of longevity. Cell *142*, 9-14.

Huang, R., Xu, Y., Wan, W., Shou, X., Qian, J., You, Z., Liu, B., Chang, C., Zhou, T., Lippincott-Schwartz, J.*, et al.* (2015). Deacetylation of nuclear LC3 drives autophagy initiation under starvation. Molecular cell *57*, 456-466.

Huo, Y., Cai, H., Teplova, I., Bowman-Colin, C., Chen, G., Price, S., Barnard, N., Ganesan, S., Karantza, V., White, E.*, et al.* (2013). Autophagy opposes p53-mediated tumor barrier to facilitate tumorigenesis in a model of PALB2-associated hereditary breast cancer. Cancer Discov *3*, 894-907.

Ichimura, Y., Waguri, S., Sou, Y.S., Kageyama, S., Hasegawa, J., Ishimura, R., Saito, T., Yang, Y., Kouno, T., Fukutomi, T.*, et al.* (2013). Phosphorylation of p62 activates the Keap1-Nrf2 pathway during selective autophagy. Molecular cell *51*, 618-631.

Imai, S., Armstrong, C.M., Kaeberlein, M., and Guarente, L. (2000). Transcriptional silencing and longevity protein Sir2 is an NAD-dependent histone deacetylase. Nature *403*, 795-800.

Inoki, K., Zhu, T., and Guan, K.L. (2003). TSC2 mediates cellular energy response to control cell growth and survival. Cell *115*, 577-590.

Itakura, E., Kishi-Itakura, C., Koyama-Honda, I., and Mizushima, N. (2012). Structures containing Atg9A and the ULK1 complex independently target depolarized mitochondria at initial stages of Parkin-mediated mitophagy. J Cell Sci *125*, 1488-1499.

Jager, S., Bucci, C., Tanida, I., Ueno, T., Kominami, E., Saftig, P., and Eskelinen, E.L. (2004). Role for Rab7 in maturation of late autophagic vacuoles. J Cell Sci *117*, 4837-4848.

Jewell, J.L., Kim, Y.C., Russell, R.C., Yu, F.X., Park, H.W., Plouffe, S.W., Tagliabracci, V.S., and Guan, K.L. (2015). Metabolism. Differential regulation of mTORC1 by leucine and glutamine. Science *347*, 194-198.

Jewell, J.L., Russell, R.C., and Guan, K.L. (2013). Amino acid signalling upstream of mTOR. Nat Rev Mol Cell Biol *14*, 133-139.

Jia, L., and Hui, R.T. (2009). Everolimus, a promising medical therapy for coronary heart disease? Med Hypotheses *73*, 153-155.

Jung, C.H., Jun, C.B., Ro, S.H., Kim, Y.M., Otto, N.M., Cao, J., Kundu, M., and Kim, D.H. (2009). ULK-Atg13-FIP200 complexes mediate mTOR signaling to the autophagy machinery. Mol Biol Cell *20*, 1992-2003.

Kamphorst, J.J., Chung, M.K., Fan, J., and Rabinowitz, J.D. (2014). Quantitative analysis of acetyl-CoA production in hypoxic cancer cells reveals substantial contribution from acetate. Cancer Metab *2*, 23.

Kandadi, M.R., Panzhinskiy, E., Roe, N.D., Nair, S., Hu, D., and Sun, A. (2015). Deletion of protein tyrosine phosphatase 1B rescues against myocardial anomalies in high fat diet-induced obesity: Role of AMPK-dependent autophagy. Biochim Biophys Acta *1852*, 299-309.

Karsli-Uzunbas, G., Guo, J.Y., Price, S., Teng, X., Laddha, S.V., Khor, S., Kalaany, N.Y., Jacks, T., Chan, C.S., Rabinowitz, J.D*., et al.* (2014). Autophagy is required for glucose homeostasis and lung tumor maintenance. Cancer Discov *4*, 914-927.

Kaufmann, A., Beier, V., Franquelim, H.G., and Wollert, T. (2014). Molecular mechanism of autophagic membrane-scaffold assembly and disassembly. Cell *156*, 469-481.

Kaushik, S., and Cuervo, A.M. (2012). Chaperone-mediated autophagy: a unique way to enter the lysosome world. Trends Cell Biol *22*, 407-417.

Kihara, A., Noda, T., Ishihara, N., and Ohsumi, Y. (2001). Two distinct Vps34 phosphatidylinositol 3-kinase complexes function in autophagy and carboxypeptidase Y sorting in Saccharomyces cerevisiae. J Cell Biol *152*, 519-530.

Kim, E., Goraksha-Hicks, P., Li, L., Neufeld, T.P., and Guan, K.L. (2008a). Regulation of TORC1 by Rag GTPases in nutrient response. Nat Cell Biol *10*, 935-945.
Kim, J., Kim, Y.C., Fang, C., Russell, R.C., Kim, J.H., Fan, W., Liu, R., Zhong, Q., and Guan, K.L. (2013). Differential regulation of distinct Vps34 complexes by AMPK in nutrient stress and autophagy. Cell *152*, 290-303.

Kim, J., and Klionsky, D.J. (2000). Autophagy, cytoplasm-to-vacuole targeting pathway, and pexophagy in yeast and mammalian cells. Annual review of biochemistry *69*, 303-342.

Kim, J., Kundu, M., Viollet, B., and Guan, K.L. (2011). AMPK and mTOR regulate autophagy through direct phosphorylation of Ulk1. Nat Cell Biol *13*, 132-141.

Kim, M.S., Jeong, E.G., Ahn, C.H., Kim, S.S., Lee, S.H., and Yoo, N.J. (2008b). Frameshift mutation of UVRAG, an autophagy-related gene, in gastric carcinomas with microsatellite instability. Hum Pathol *39*, 1059-1063.

Kim, Y.M., Jung, C.H., Seo, M., Kim, E.K., Park, J.M., Bae, S.S., and Kim, D.H. (2015). mTORC1 phosphorylates UVRAG to negatively regulate autophagosome and endosome maturation. Molecular cell *57*, 207-218.

Kirkin, V., Lamark, T., Sou, Y.S., Bjorkoy, G., Nunn, J.L., Bruun, J.A., Shvets, E., McEwan, D.G., Clausen, T.H., Wild, P.*, et al.* (2009a). A role for NBR1 in autophagosomal degradation of ubiquitinated substrates. Molecular cell *33*, 505-516.

Kirkin, V., McEwan, D.G., Novak, I., and Dikic, I. (2009b). A role for ubiquitin in selective autophagy. Molecular cell *34*, 259-269.

Klionsky, D.J., Abdalla, F.C., Abeliovich, H., Abraham, R.T., Acevedo-Arozena, A., Adeli, K., Agholme, L., Agnello, M., Agostinis, P., Aguirre-Ghiso, J.A.*, et al.* (2012). Guidelines for the use and interpretation of assays for monitoring autophagy. Autophagy *8*, 445-544.

Klionsky, D.J., and Emr, S.D. (2000). Autophagy as a regulated pathway of cellular degradation. Science *290*, 1717-1721.

Komatsu, M., Kurokawa, H., Waguri, S., Taguchi, K., Kobayashi, A., Ichimura, Y., Sou, Y.S., Ueno, I., Sakamoto, A., Tong, K.I.*, et al.* (2010). The selective autophagy substrate p62 activates the stress responsive transcription factor Nrf2 through inactivation of Keap1. Nat Cell Biol *12*, 213-223.

Kroemer, G. (2015). Autophagy: a druggable process that is deregulated in aging and human disease. J Clin Invest *125*, 1-4.

Kroemer, G., Galluzzi, L., Kepp, O., and Zitvogel, L. (2013). Immunogenic cell death in cancer therapy. Annu Rev Immunol *31*, 51-72.

Kroemer, G., Marino, G., and Levine, B. (2010). Autophagy and the integrated stress response. Molecular cell *40*, 280-293.
Kuma, A., Hatano, M., Matsui, M., Yamamoto, A., Nakaya, H., Yoshimori, T., Ohsumi, Y., Tokuhisa, T., and Mizushima, N. (2004). The role of autophagy during the early neonatal starvation period. Nature *432*, 1032-1036.

Laderoute, K.R., Amin, K., Calaoagan, J.M., Knapp, M., Le, T., Orduna, J., Foretz, M., and Viollet, B. (2006). 5'-AMP-activated protein kinase (AMPK) is induced by low-oxygen and glucose deprivation conditions found in solid-tumor microenvironments. Mol Cell Biol *26*, 5336-5347.

Lagouge, M., Argmann, C., Gerhart-Hines, Z., Meziane, H., Lerin, C., Daussin, F., Messadeq, N., Milne, J., Lambert, P., Elliott, P.*, et al.* (2006). Resveratrol improves mitochondrial function and protects against metabolic disease by activating SIRT1 and PGC-1alpha. Cell *127*, 1109-1122.

Lamark, T., and Johansen, T. (2012). Aggrephagy: selective disposal of protein aggregates by macroautophagy. Int J Cell Biol *2012*, 736905.

Lanna, A., Henson, S.M., Escors, D., and Akbar, A.N. (2014). The kinase p38 activated by the metabolic regulator AMPK and scaffold TAB1 drives the senescence of human T cells. Nat Immunol *15*, 965-972.

Laplante, M., and Sabatini, D.M. (2012). mTOR signaling in growth control and disease. Cell *149*, 274-293.

Lazova, R., Camp, R.L., Klump, V., Siddiqui, S.F., Amaravadi, R.K., and Pawelek, J.M. (2012). Punctate LC3B expression is a common feature of solid tumors and associated with proliferation, metastasis, and poor outcome. Clinical cancer research : an official journal of the American Association for Cancer Research *18*, 370-379.

Le Guezennec, X., Brichkina, A., Huang, Y.F., Kostromina, E., Han, W., and Bulavin, D.V. (2012). Wip1-dependent regulation of autophagy, obesity, and atherosclerosis. Cell metabolism *16*, 68-80.

Lebovitz, C.B., Bortnik, S.B., and Gorski, S.M. (2012). Here, there be dragons: charting autophagy-related alterations in human tumors. Clinical cancer research : an official journal of the American Association for Cancer Research *18*, 1214-1226.

Lee, C., Raffaghello, L., Brandhorst, S., Safdie, F.M., Bianchi, G., Martin-Montalvo, A., Pistoia, V., Wei, M., Hwang, S., Merlino, A.*, et al.* (2012). Fasting cycles retard growth of tumors and sensitize a range of cancer cell types to chemotherapy. Sci Transl Med *4*, 124ra127.

Lee, I.H., Cao, L., Mostoslavsky, R., Lombard, D.B., Liu, J., Bruns, N.E., Tsokos, M., Alt, F.W., and Finkel, T. (2008). A role for the NAD-dependent deacetylase Sirt1 in the regulation of autophagy. Proc Natl Acad Sci U S A *105*, 3374-3379.
Lee, J.V., Carrer, A., Shah, S., Snyder, N.W., Wei, S., Venneti, S., Worth, A.J., Yuan, Z.F., Lim, H.W., Liu, S.*, et al.* (2014). Akt-dependent metabolic reprogramming regulates tumor cell histone acetylation. Cell metabolism *20*, 306-319.

Levine, B., and Deretic, V. (2007). Unveiling the roles of autophagy in innate and adaptive immunity. Nat Rev Immunol *7*, 767-777.

Levine, B., and Kroemer, G. (2008). Autophagy in the pathogenesis of disease. Cell *132*, 27-42.

Li, L., Chen, Y., and Gibson, S.B. (2013). Starvation-induced autophagy is regulated by mitochondrial reactive oxygen species leading to AMPK activation. Cell Signal *25*, 50-65.

Li, X., He, L., Che, K.H., Funderburk, S.F., Pan, L., Pan, N., Zhang, M., Yue, Z., and Zhao, Y. (2012). Imperfect interface of Beclin1 coiled-coil domain regulates homodimer and heterodimer formation with Atg14L and UVRAG. Nat Commun *3*, 662.

Li, Y., Corradetti, M.N., Inoki, K., and Guan, K.L. (2004). TSC2: filling the GAP in the mTOR signaling pathway. Trends Biochem Sci *29*, 32-38.

Liang, C., Feng, P., Ku, B., Dotan, I., Canaani, D., Oh, B.H., and Jung, J.U. (2006). Autophagic and tumour suppressor activity of a novel Beclin1-binding protein UVRAG. Nat Cell Biol *8*, 688-699.

Liang, L., Shou, X.L., Zhao, H.K., Ren, G.Q., Wang, J.B., Wang, X.H., Ai, W.T., Maris, J.R., Hueckstaedt, L.K., Ma, A.Q.*, et al.* (2015). Antioxidant catalase rescues against high fat diet-induced cardiac dysfunction via an IKKbeta-AMPK-dependent regulation of autophagy. Biochim Biophys Acta *1852*, 343-352.

Liang, X.H., Jackson, S., Seaman, M., Brown, K., Kempkes, B., Hibshoosh, H., and Levine, B. (1999). Induction of autophagy and inhibition of tumorigenesis by beclin 1. Nature *402*, 672-676.

Liao, X., Sluimer, J.C., Wang, Y., Subramanian, M., Brown, K., Pattison, J.S., Robbins, J., Martinez, J., and Tabas, I. (2012). Macrophage autophagy plays a protective role in advanced atherosclerosis. Cell metabolism *15*, 545-553.

Liaw, D., Marsh, D.J., Li, J., Dahia, P.L., Wang, S.I., Zheng, Z., Bose, S., Call, K.M., Tsou, H.C., Peacocke, M.*, et al.* (1997). Germline mutations of the PTEN gene in Cowden disease, an inherited breast and thyroid cancer syndrome. Nat Genet *16*, 64-67.

Lin, C.W., Zhang, H., Li, M., Xiong, X., Chen, X., Chen, X., Dong, X.C., and Yin, X.M. (2013). Pharmacological promotion of autophagy alleviates steatosis and injury in alcoholic and non-alcoholic fatty liver conditions in mice. J Hepatol *58*, 993-999.
Lin, S.Y., Li, T.Y., Liu, Q., Zhang, C., Li, X., Chen, Y., Zhang, S.M., Lian, G., Liu, Q., Ruan, K.*, et al.* (2012). GSK3-TIP60-ULK1 signaling pathway links growth factor deprivation to autophagy. Science *336*, 477-481.

Liu, Y., Shoji-Kawata, S., Sumpter, R.M., Jr., Wei, Y., Ginet, V., Zhang, L., Posner, B., Tran, K.A., Green, D.R., Xavier, R.J.*, et al.* (2013). Autosis is a Na+,K+-ATPase-regulated form of cell death triggered by autophagy-inducing peptides, starvation, and hypoxia-ischemia. Proc Natl Acad Sci U S A *110*, 20364-20371.

Lizaso, A., Tan, K.T., and Lee, Y.H. (2013). beta-adrenergic receptor-stimulated lipolysis requires the RAB7-mediated autolysosomal lipid degradation. Autophagy *9*, 1228-1243.

Luciani, A., Villella, V.R., Esposito, S., Gavina, M., Russo, I., Silano, M., Guido, S., Pettoello-Mantovani, M., Carnuccio, R., Scholte, B.*, et al.* (2012). Targeting autophagy as a

novel strategy for facilitating the therapeutic action of potentiators on DeltaF508 cystic fibrosis transmembrane conductance regulator. Autophagy *8*, 1657-1672.

Ma, L., Chen, Z., Erdjument-Bromage, H., Tempst, P., and Pandolfi, P.P. (2005). Phosphorylation and functional inactivation of TSC2 by Erk implications for tuberous sclerosis and cancer pathogenesis. Cell *121*, 179-193.

Madeo, F., Pietrocola, F., Eisenberg, T., and Kroemer, G. (2014). Caloric restriction mimetics: towards a molecular definition. Nat Rev Drug Discov *13*, 727-740.

Madeo, F., Zimmermann, A., Maiuri, M.C., and Kroemer, G. (2015). Essential role for autophagy in life span extension. J Clin Invest *125*, 85-93.

Madiraju, P., Pande, S.V., Prentki, M., and Madiraju, S.R. (2009). Mitochondrial acetylcarnitine provides acetyl groups for nuclear histone acetylation. Epigenetics *4*, 399-403.

Maiuri, M.C., Zalckvar, E., Kimchi, A., and Kroemer, G. (2007). Self-eating and self-killing: crosstalk between autophagy and apoptosis. Nat Rev Mol Cell Biol *8*, 741-752.

Mancias, J.D., Wang, X., Gygi, S.P., Harper, J.W., and Kimmelman, A.C. (2014). Quantitative proteomics identifies NCOA4 as the cargo receptor mediating ferritinophagy. Nature *509*, 105-109.

Mantelingu, K., Reddy, B.A., Swaminathan, V., Kishore, A.H., Siddappa, N.B., Kumar, G.V., Nagashankar, G., Natesh, N., Roy, S., Sadhale, P.P*., et al.* (2007). Specific inhibition of p300-HAT alters global gene expression and represses HIV replication. Chem Biol *14*, 645-657.

Mari, M., Griffith, J., Rieter, E., Krishnappa, L., Klionsky, D.J., and Reggiori, F. (2010). An Atg9-containing compartment that functions in the early steps of autophagosome biogenesis. J Cell Biol *190*, 1005-1022.
Marino, G., Madeo, F., and Kroemer, G. (2011a). Autophagy for tissue homeostasis and neuroprotection. Curr Opin Cell Biol *23*, 198-206.

Marino, G., Martins, I., and Kroemer, G. (2011b). Autophagy in Ras-induced malignant transformation: fatal or vital? Molecular cell *42*, 1-3.

Marino, G., Pietrocola, F., Eisenberg, T., Kong, Y., Malik, S.A., Andryushkova, A., Schroeder, S., Pendl, T., Harger, A., Niso-Santano, M*., et al.* (2014). Regulation of autophagy by cytosolic acetyl-coenzyme A. Molecular cell *53*, 710-725.

Marino, G., Salvador-Montoliu, N., Fueyo, A., Knecht, E., Mizushima, N., and Lopez-Otin, C. (2007). Tissue-specific autophagy alterations and increased tumorigenesis in mice deficient in Atg4C/autophagin-3. J Biol Chem *282*, 18573-18583.

Mashimo, T., Pichumani, K., Vemireddy, V., Hatanpaa, K.J., Singh, D.K., Sirasanagandla, S., Nannepaga, S., Piccirillo, S.G., Kovacs, Z., Foong, C.*, et al.* (2014). Acetate is a bioenergetic substrate for human glioblastoma and brain metastases. Cell *159*, 1603-1614.

Mathew, R., Karp, C.M., Beaudoin, B., Vuong, N., Chen, G., Chen, H.Y., Bray, K., Reddy, A., Bhanot, G., Gelinas, C.*, et al.* (2009). Autophagy suppresses tumorigenesis through elimination of p62. Cell *137*, 1062-1075.

Mathew, R., Kongara, S., Beaudoin, B., Karp, C.M., Bray, K., Degenhardt, K., Chen, G., Jin, S., and White, E. (2007). Autophagy suppresses tumor progression by limiting chromosomal instability. Genes Dev *21*, 1367-1381.

Matsunaga, K., Morita, E., Saitoh, T., Akira, S., Ktistakis, N.T., Izumi, T., Noda, T., and Yoshimori, T. (2010). Autophagy requires endoplasmic reticulum targeting of the PI3-kinase complex via Atg14L. J Cell Biol *190*, 511-521.

Matsunaga, K., Saitoh, T., Tabata, K., Omori, H., Satoh, T., Kurotori, N., Maejima, I., Shirahama-Noda, K., Ichimura, T., Isobe, T.*, et al.* (2009). Two Beclin 1-binding proteins, Atg14L and Rubicon, reciprocally regulate autophagy at different stages. Nat Cell Biol *11*, 385-396.

Mattison, J.A., Roth, G.S., Beasley, T.M., Tilmont, E.M., Handy, A.M., Herbert, R.L., Longo, D.L., Allison, D.B., Young, J.E., Bryant, M.*, et al.* (2012). Impact of caloric restriction on health and survival in rhesus monkeys from the NIA study. Nature *489*, 318-321.

Maxwell, P.H., Dachs, G.U., Gleadle, J.M., Nicholls, L.G., Harris, A.L., Stratford, I.J., Hankinson, O., Pugh, C.W., and Ratcliffe, P.J. (1997). Hypoxia-inducible factor-1 modulates gene expression in solid tumors and influences both angiogenesis and tumor growth. Proc Natl Acad Sci U S A *94*, 8104-8109.

Meijer, A.J., Lorin, S., Blommaart, E.F., and Codogno, P. (2014). Regulation of autophagy by amino acids and MTOR-dependent signal transduction. Amino Acids.

Melendez, A., Talloczy, Z., Seaman, M., Eskelinen, E.L., Hall, D.H., and Levine, B. (2003). Autophagy genes are essential for dauer development and life-span extension in C. elegans. Science *301*, 1387-1391.

Meley, D., Bauvy, C., Houben-Weerts, J.H., Dubbelhuis, P.F., Helmond, M.T., Codogno, P., and Meijer, A.J. (2006). AMP-activated protein kinase and the regulation of autophagic proteolysis. J Biol Chem *281*, 34870-34879.

Metallo, C.M., Gameiro, P.A., Bell, E.L., Mattaini, K.R., Yang, J., Hiller, K., Jewell, C.M., Johnson, Z.R., Irvine, D.J., Guarente, L.*, et al.* (2012). Reductive glutamine metabolism by IDH1 mediates lipogenesis under hypoxia. Nature *481*, 380-384.

Mielgo-Ayuso, J., Barrenechea, L., Alcorta, P., Larrarte, E., Margareto, J., and Labayen, I. (2014). Effects of dietary supplementation with epigallocatechin-3-gallate on weight loss, energy homeostasis, cardiometabolic risk factors and liver function in obese women: randomised, double-blind, placebo-controlled clinical trial. Br J Nutr *111*, 1263-1271.

Mizuarai, S., Miki, S., Araki, H., Takahashi, K., and Kotani, H. (2005). Identification of dicarboxylate carrier Slc25a10 as malate transporter in de novo fatty acid synthesis. J Biol Chem *280*, 32434-32441.
Mizushima, N. (2007). Autophagy: process and function. Genes Dev *21*, 2861-2873.
Mizushima, N., and Komatsu, M. (2011). Autophagy: renovation of cells and tissues. Cell *147*, 728-741.
Mizushima, N., Levine, B., Cuervo, A.M., and Klionsky, D.J. (2008). Autophagy fights disease through cellular self-digestion. Nature *451*, 1069-1075.

Mizushima, N., Noda, T., Yoshimori, T., Tanaka, Y., Ishii, T., George, M.D., Klionsky, D.J., Ohsumi, M., and Ohsumi, Y. (1998). A protein conjugation system essential for autophagy. Nature *395*, 395-398.

Mizushima, N., Yamamoto, A., Matsui, M., Yoshimori, T., and Ohsumi, Y. (2004). In vivo analysis of autophagy in response to nutrient starvation using transgenic mice expressing a fluorescent autophagosome marker. Mol Biol Cell *15*, 1101-1111.
Mizushima, N., Yoshimori, T., and Levine, B. (2010). Methods in mammalian autophagy research. Cell *140*, 313-326.

Mizushima, N., Yoshimori, T., and Ohsumi, Y. (2011). The role of Atg proteins in autophagosome formation. Annu Rev Cell Dev Biol *27*, 107-132.

Mohseni, N., McMillan, S.C., Chaudhary, R., Mok, J., and Reed, B.H. (2009). Autophagy promotes caspase-dependent cell death during Drosophila development. Autophagy *5*, 329-338.
Morselli, E., Galluzzi, L., Kepp, O., Vicencio, J.M., Criollo, A., Maiuri, M.C., and Kroemer, G. (2009). Anti- and pro-tumor functions of autophagy. Biochim Biophys Acta *1793*, 1524-1532.

Morselli, E., Maiuri, M.C., Markaki, M., Megalou, E., Pasparaki, A., Palikaras, K., Criollo, A., Galluzzi, L., Malik, S.A., Vitale, I.*, et al.* (2010). Caloric restriction and resveratrol promote longevity through the Sirtuin-1-dependent induction of autophagy. Cell Death Dis *1*, e10.

Morselli, E., Marino, G., Bennetzen, M.V., Eisenberg, T., Megalou, E., Schroeder, S., Cabrera, S., Benit, P., Rustin, P., Criollo, A.*, et al.* (2011). Spermidine and resveratrol induce autophagy by distinct pathways converging on the acetylproteome. J Cell Biol *192*, 615-629.

Mortensen, M., Soilleux, E.J., Djordjevic, G., Tripp, R., Lutteropp, M., Sadighi-Akha, E., Stranks, A.J., Glanville, J., Knight, S., Jacobsen, S.E.*, et al.* (2011). The autophagy protein Atg7 is essential for hematopoietic stem cell maintenance. J Exp Med *208*, 455-467.

Mueller, M.A., Beutner, F., Teupser, D., Ceglarek, U., and Thiery, J. (2008). Prevention of atherosclerosis by the mTOR inhibitor everolimus in LDLR-/- mice despite severe hypercholesterolemia. Atherosclerosis *198*, 39-48.

Mullen, A.R., Wheaton, W.W., Jin, E.S., Chen, P.H., Sullivan, L.B., Cheng, T., Yang, Y., Linehan, W.M., Chandel, N.S., and DeBerardinis, R.J. (2012). Reductive carboxylation supports growth in tumour cells with defective mitochondria. Nature *481*, 385-388.

Murthy, A., Li, Y., Peng, I., Reichelt, M., Katakam, A.K., Noubade, R., Roose-Girma, M., DeVoss, J., Diehl, L., Graham, R.R.*, et al.* (2014). A Crohn's disease variant in Atg16l1 enhances its degradation by caspase 3. Nature *506*, 456-462.

Naito, T., Kuma, A., and Mizushima, N. (2013). Differential contribution of insulin and amino acids to the mTORC1-autophagy pathway in the liver and muscle. J Biol Chem *288*, 21074-21081.

Nardella, C., Chen, Z., Salmena, L., Carracedo, A., Alimonti, A., Egia, A., Carver, B., Gerald, W., Cordon-Cardo, C., and Pandolfi, P.P. (2008). Aberrant Rheb-mediated mTORC1 activation and Pten haploinsufficiency are cooperative oncogenic events. Genes Dev *22*, 2172-2177.

Nezis, I.P., Lamark, T., Velentzas, A.D., Rusten, T.E., Bjorkoy, G., Johansen, T., Papassideri, I.S., Stravopodis, D.J., Margaritis, L.H., Stenmark, H.*, et al.* (2009). Cell death during Drosophila melanogaster early oogenesis is mediated through autophagy. Autophagy *5*, 298-302.

Ni, H.M., Du, K., You, M., and Ding, W.X. (2013). Critical role of FoxO3a in alcohol-induced autophagy and hepatotoxicity. Am J Pathol *183*, 1815-1825.
Nicklin, P., Bergman, P., Zhang, B., Triantafellow, E., Wang, H., Nyfeler, B., Yang, H., Hild, M., Kung, C., Wilson, C.*, et al.* (2009). Bidirectional transport of amino acids regulates mTOR and autophagy. Cell *136*, 521-534.

Niso-Santano, M., Malik, S.A., Pietrocola, F., Bravo-San Pedro, J.M., Marino, G., Cianfanelli, V., Ben-Younes, A., Troncoso, R., Markaki, M., Sica, V.*, et al.* (2015). Unsaturated fatty acids induce non-canonical autophagy. EMBO J *34*, 1025-1041.

Nixon, R.A. (2013). The role of autophagy in neurodegenerative disease. Nat Med *19*, 983-997.

Novak, I., Kirkin, V., McEwan, D.G., Zhang, J., Wild, P., Rozenknop, A., Rogov, V., Lohr, F., Popovic, D., Occhipinti, A.*, et al.* (2010). Nix is a selective autophagy receptor for mitochondrial clearance. EMBO Rep *11*, 45-51.

Ogasawara, Y., Itakura, E., Kono, N., Mizushima, N., Arai, H., Nara, A., Mizukami, T., and Yamamoto, A. (2014). Stearoyl-CoA desaturase 1 activity is required for autophagosome formation. J Biol Chem *289*, 23938-23950.

Ouimet, M., Franklin, V., Mak, E., Liao, X., Tabas, I., and Marcel, Y.L. (2011). Autophagy regulates cholesterol efflux from macrophage foam cells via lysosomal acid lipase. Cell metabolism *13*, 655-667.

Pacheco, C.D., Elrick, M.J., and Lieberman, A.P. (2009). Tau deletion exacerbates the phenotype of Niemann-Pick type C mice and implicates autophagy in pathogenesis. Hum Mol Genet *18*, 956-965.

Palmieri, M., Impey, S., Kang, H., di Ronza, A., Pelz, C., Sardiello, M., and Ballabio, A. (2011). Characterization of the CLEAR network reveals an integrated control of cellular clearance pathways. Hum Mol Genet *20*, 3852-3866.

Pankiv, S., Clausen, T.H., Lamark, T., Brech, A., Bruun, J.A., Outzen, H., Overvatn, A., Bjorkoy, G., and Johansen, T. (2007). p62/SQSTM1 binds directly to Atg8/LC3 to facilitate degradation of ubiquitinated protein aggregates by autophagy. J Biol Chem *282*, 24131-24145.

Parenti, G., Andria, G., and Ballabio, A. (2015). Lysosomal storage diseases: from pathophysiology to therapy. Annu Rev Med *66*, 471-486.

Park, S.J., Ahmad, F., Philp, A., Baar, K., Williams, T., Luo, H., Ke, H., Rehmann, H., Taussig, R., Brown, A.L.*, et al.* (2012). Resveratrol ameliorates aging-related metabolic phenotypes by inhibiting cAMP phosphodiesterases. Cell *148*, 421-433.

Pastore, N., Blomenkamp, K., Annunziata, F., Piccolo, P., Mithbaokar, P., Maria Sepe, R., Vetrini, F., Palmer, D., Ng, P., Polishchuk, E.*, et al.* (2013). Gene transfer of master autophagy regulator TFEB results in clearance of toxic protein and correction of hepatic disease in alpha-1-anti-trypsin deficiency. EMBO Mol Med *5*, 397-412.

Patel, M.S., Nemeria, N.S., Furey, W., and Jordan, F. (2014). The pyruvate dehydrogenase complexes: structure-based function and regulation. J Biol Chem *289*, 16615-16623.
Pattingre, S., Bauvy, C., Levade, T., Levine, B., and Codogno, P. (2009). Ceramide-induced autophagy: to junk or to protect cells? Autophagy *5*, 558-560.

Pattingre, S., Tassa, A., Qu, X., Garuti, R., Liang, X.H., Mizushima, N., Packer, M., Schneider, M.D., and Levine, B. (2005). Bcl-2 antiapoptotic proteins inhibit Beclin 1-dependent autophagy. Cell *122*, 927-939.

Perry, R.J., Zhang, X.M., Zhang, D., Kumashiro, N., Camporez, J.P., Cline, G.W., Rothman, D.L., and Shulman, G.I. (2014). Leptin reverses diabetes by suppression of the hypothalamic-pituitary-adrenal axis. Nat Med *20*, 759-763.

Pietrocola, F., Galluzzi, L., Bravo-San Pedro, J.M., Madeo, F., and Kroemer, G. (2015a). Acetyl Coenzyme A: A Central Metabolite and Second Messenger. Cell metabolism *21*, 805-821.

Pietrocola, F., Izzo, V., Niso-Santano, M., Vacchelli, E., Galluzzi, L., Maiuri, M.C., and Kroemer, G. (2013). Regulation of autophagy by stress-responsive transcription factors. Semin Cancer Biol *23*, 310-322.

Pietrocola, F., Lachkar, S., Enot, D.P., Niso-Santano, M., Bravo-San Pedro, J.M., Sica, V., Izzo, V., Maiuri, M.C., Madeo, F., Marino, G.*, et al.* (2015b). Spermidine induces autophagy by inhibiting the acetyltransferase EP300. Cell Death Differ *22*, 509-516.

Pietrocola, F., Malik, S.A., Marino, G., Vacchelli, E., Senovilla, L., Chaba, K., Niso-Santano, M., Maiuri, M.C., Madeo, F., and Kroemer, G. (2014). Coffee induces autophagy in vivo. Cell Cycle *13*, 1987-1994.

Pietrocola, F., Marino, G., Lissa, D., Vacchelli, E., Malik, S.A., Niso-Santano, M., Zamzami, N., Galluzzi, L., Maiuri, M.C., and Kroemer, G. (2012). Pro-autophagic polyphenols reduce the acetylation of cytoplasmic proteins. Cell Cycle *11*, 3851-3860.

Pirinen, E., Canto, C., Jo, Y.S., Morato, L., Zhang, H., Menzies, K.J., Williams, E.G., Mouchiroud, L., Moullan, N., Hagberg, C.*, et al.* (2014). Pharmacological Inhibition of poly(ADP-ribose) polymerases improves fitness and mitochondrial function in skeletal muscle. Cell metabolism *19*, 1034-1041.

Ponpuak, M., Mandell, M.A., Kimura, T., Chauhan, S., Cleyrat, C., and Deretic, V. (2015). Secretory autophagy. Curr Opin Cell Biol *35*, 106-116.

Pouyssegur, J., Dayan, F., and Mazure, N.M. (2006). Hypoxia signalling in cancer and approaches to enforce tumour regression. Nature *441*, 437-443.

Puri, C., Renna, M., Bento, C.F., Moreau, K., and Rubinsztein, D.C. (2013). Diverse autophagosome membrane sources coalesce in recycling endosomes. Cell *154*, 1285-1299.

Pyo, J.O., Yoo, S.M., Ahn, H.H., Nah, J., Hong, S.H., Kam, T.I., Jung, S., and Jung, Y.K. (2013). Overexpression of Atg5 in mice activates autophagy and extends lifespan. Nat Commun *4*, 2300.

Qu, X., Yu, J., Bhagat, G., Furuya, N., Hibshoosh, H., Troxel, A., Rosen, J., Eskelinen, E.L., Mizushima, N., Ohsumi, Y.*, et al.* (2003). Promotion of tumorigenesis by heterozygous disruption of the beclin 1 autophagy gene. J Clin Invest *112*, 1809-1820.

Rabinowitz, J.D., and White, E. (2010). Autophagy and metabolism. Science *330*, 1344-1348.

Rao, S., Tortola, L., Perlot, T., Wirnsberger, G., Novatchkova, M., Nitsch, R., Sykacek, P., Frank, L., Schramek, D., Komnenovic, V.*, et al.* (2014). A dual role for autophagy in a murine model of lung cancer. Nat Commun *5*, 3056.

Ravikumar, B., Moreau, K., Jahreiss, L., Puri, C., and Rubinsztein, D.C. (2010). Plasma membrane contributes to the formation of pre-autophagosomal structures. Nat Cell Biol *12*, 747-757.

Ravikumar, B., Stewart, A., Kita, H., Kato, K., Duden, R., and Rubinsztein, D.C. (2003). Raised intracellular glucose concentrations reduce aggregation and cell death caused by mutant huntingtin exon 1 by decreasing mTOR phosphorylation and inducing autophagy. Hum Mol Genet *12*, 985-994.

Razani, B., Feng, C., Coleman, T., Emanuel, R., Wen, H., Hwang, S., Ting, J.P., Virgin, H.W., Kastan, M.B., and Semenkovich, C.F. (2012). Autophagy links inflammasomes to atherosclerotic progression. Cell metabolism *15*, 534-544.

Rebouche, C.J., and Seim, H. (1998). Carnitine metabolism and its regulation in microorganisms and mammals. Annu Rev Nutr *18*, 39-61.

Reef, S., Zalckvar, E., Shifman, O., Bialik, S., Sabanay, H., Oren, M., and Kimchi, A. (2006). A short mitochondrial form of p19ARF induces autophagy and caspase-independent cell death. Molecular cell *22*, 463-475.

Roberts, D.J., Tan-Sah, V.P., Ding, E.Y., Smith, J.M., and Miyamoto, S. (2014). Hexokinase-II positively regulates glucose starvation-induced autophagy through TORC1 inhibition. Molecular cell *53*, 521-533.

Ron, D., and Walter, P. (2007). Signal integration in the endoplasmic reticulum unfolded protein response. Nat Rev Mol Cell Biol *8*, 519-529.
Rosenfeldt, M.T., O'Prey, J., Morton, J.P., Nixon, C., MacKay, G., Mrowinska, A., Au, A., Rai, T.S., Zheng, L., Ridgway, R.*, et al.* (2013). p53 status determines the role of autophagy in pancreatic tumour development. Nature *504*, 296-300.

Roth, S.Y., Denu, J.M., and Allis, C.D. (2001). Histone acetyltransferases. Annual review of biochemistry *70*, 81-120.

Rubinsztein, D.C., Marino, G., and Kroemer, G. (2011). Autophagy and aging. Cell *146*, 682-695.

Rufer, A.C., Thoma, R., and Hennig, M. (2009). Structural insight into function and regulation of carnitine palmitoyltransferase. Cell Mol Life Sci *66*, 2489-2501.

Russell, R.C., Tian, Y., Yuan, H., Park, H.W., Chang, Y.Y., Kim, J., Kim, H., Neufeld, T.P., Dillin, A., and Guan, K.L. (2013). ULK1 induces autophagy by phosphorylating Beclin-1 and activating VPS34 lipid kinase. Nat Cell Biol *15*, 741-750.

Sahar, S., Masubuchi, S., Eckel-Mahan, K., Vollmer, S., Galla, L., Ceglia, N., Masri, S., Barth, T.K., Grimaldi, B., Oluyemi, O.*, et al.* (2014). Circadian control of fatty acid

elongation by SIRT1 protein-mediated deacetylation of acetyl-coenzyme A synthetase 1. J Biol Chem *289*, 6091-6097.

Sahu, R., Kaushik, S., Clement, C.C., Cannizzo, E.S., Scharf, B., Follenzi, A., Potolicchio, I., Nieves, E., Cuervo, A.M., and Santambrogio, L. (2011). Microautophagy of cytosolic proteins by late endosomes. Dev Cell *20*, 131-139.

Sancak, Y., Bar-Peled, L., Zoncu, R., Markhard, A.L., Nada, S., and Sabatini, D.M. (2010). Ragulator-Rag complex targets mTORC1 to the lysosomal surface and is necessary for its activation by amino acids. Cell *141*, 290-303.

Sancak, Y., Peterson, T.R., Shaul, Y.D., Lindquist, R.A., Thoreen, C.C., Bar-Peled, L., and Sabatini, D.M. (2008). The Rag GTPases bind raptor and mediate amino acid signaling to mTORC1. Science *320*, 1496-1501.

Sardiello, M., Palmieri, M., di Ronza, A., Medina, D.L., Valenza, M., Gennarino, V.A., Di Malta, C., Donaudy, F., Embrione, V., Polishchuk, R.S.*, et al.* (2009). A gene network regulating lysosomal biogenesis and function. Science *325*, 473-477.

Satoh, A., Brace, C.S., Rensing, N., Cliften, P., Wozniak, D.F., Herzog, E.D., Yamada, K.A., and Imai, S. (2013). Sirt1 extends life span and delays aging in mice through the regulation of Nk2 homeobox 1 in the DMH and LH. Cell metabolism *18*, 416-430.

Sautin, Y.Y., Lu, M., Gaugler, A., Zhang, L., and Gluck, S.L. (2005). Phosphatidylinositol 3-kinase-mediated effects of glucose on vacuolar H+-ATPase assembly, translocation, and acidification of intracellular compartments in renal epithelial cells. Mol Cell Biol *25*, 575-589.

Scherz-Shouval, R., and Elazar, Z. (2011). Regulation of autophagy by ROS: physiology and pathology. Trends Biochem Sci *36*, 30-38.

Scherz-Shouval, R., Shvets, E., Fass, E., Shorer, H., Gil, L., and Elazar, Z. (2007). Reactive oxygen species are essential for autophagy and specifically regulate the activity of Atg4. EMBO J *26*, 1749-1760.

Schneider, J.L., and Cuervo, A.M. (2014). Liver autophagy: much more than just taking out the trash. Nat Rev Gastroenterol Hepatol *11*, 187-200.

Schug, Z.T., Peck, B., Jones, D.T., Zhang, Q., Grosskurth, S., Alam, I.S., Goodwin, L.M., Smethurst, E., Mason, S., Blyth, K.*, et al.* (2015). Acetyl-CoA synthetase 2 promotes acetate utilization and maintains cancer cell growth under metabolic stress. Cancer Cell *27*, 57-71.

Sengupta, S., Peterson, T.R., and Sabatini, D.M. (2010). Regulation of the mTOR complex 1 pathway by nutrients, growth factors, and stress. Molecular cell *40*, 310-322.

Seo, Y.K., Jeon, T.I., Chong, H.K., Biesinger, J., Xie, X., and Osborne, T.F. (2011). Genome-wide localization of SREBP-2 in hepatic chromatin predicts a role in autophagy. Cell metabolism *13*, 367-375.

Settembre, C., De Cegli, R., Mansueto, G., Saha, P.K., Vetrini, F., Visvikis, O., Huynh, T., Carissimo, A., Palmer, D., Klisch, T.J., *et al.* (2013). TFEB controls cellular lipid metabolism through a starvation-induced autoregulatory loop. Nat Cell Biol *15*, 647-658.

Settembre, C., Zoncu, R., Medina, D.L., Vetrini, F., Erdin, S., Erdin, S., Huynh, T., Ferron, M., Karsenty, G., Vellard, M.C., *et al.* (2012). A lysosome-to-nucleus signalling mechanism senses and regulates the lysosome via mTOR and TFEB. EMBO J *31*, 1095-1108.

Shaw, R.J., and Cantley, L.C. (2006). Ras, PI(3)K and mTOR signalling controls tumour cell growth. Nature *441*, 424-430.

She, C., Zhu, L.Q., Zhen, Y.F., Wang, X.D., and Dong, Q.R. (2014). Activation of AMPK protects against hydrogen peroxide-induced osteoblast apoptosis through autophagy induction and NADPH maintenance: new implications for osteonecrosis treatment? Cell Signal *26*, 1-8.

Shen, S., Niso-Santano, M., Adjemian, S., Takehara, T., Malik, S.A., Minoux, H., Souquere, S., Marino, G., Lachkar, S., Senovilla, L., *et al.* (2012). Cytoplasmic STAT3 represses autophagy by inhibiting PKR activity. Molecular cell *48*, 667-680.

Shi, L., and Tu, B.P. (2015). Acetyl-CoA and the regulation of metabolism: mechanisms and consequences. Curr Opin Cell Biol *33*, 125-131.
Singh, R., Kaushik, S., Wang, Y., Xiang, Y., Novak, I., Komatsu, M., Tanaka, K., Cuervo, A.M., and Czaja, M.J. (2009). Autophagy regulates lipid metabolism. Nature *458*, 1131-1135.

Sinha, R.A., Farah, B.L., Singh, B.K., Siddique, M.M., Li, Y., Wu, Y., Ilkayeva, O.R., Gooding, J., Ching, J., Zhou, J., *et al.* (2014). Caffeine stimulates hepatic lipid metabolism by the autophagy-lysosomal pathway in mice. Hepatology *59*, 1366-1380.

Soleimanpour, S.A., Gupta, A., Bakay, M., Ferrari, A.M., Groff, D.N., Fadista, J., Spruce, L.A., Kushner, J.A., Groop, L., Seeholzer, S.H., *et al.* (2014). The diabetes susceptibility gene Clec16a regulates mitophagy. Cell *157*, 1577-1590.

Spampanato, C., Feeney, E., Li, L., Cardone, M., Lim, J.A., Annunziata, F., Zare, H., Polishchuk, R., Puertollano, R., Parenti, G., *et al.* (2013). Transcription factor EB (TFEB) is a new therapeutic target for Pompe disease. EMBO Mol Med *5*, 691-706.

Strohecker, A.M., Guo, J.Y., Karsli-Uzunbas, G., Price, S.M., Chen, G.J., Mathew, R., McMahon, M., and White, E. (2013). Autophagy sustains mitochondrial glutamine metabolism and growth of BrafV600E-driven lung tumors. Cancer Discov *3*, 1272-1285.

Sun, T., Li, X., Zhang, P., Chen, W.D., Zhang, H.L., Li, D.D., Deng, R., Qian, X.J., Jiao, L., Ji, J., *et al.* (2015). Acetylation of Beclin 1 inhibits autophagosome maturation and promotes tumour growth. Nat Commun *6*, 7215.

Sutendra, G., Kinnaird, A., Dromparis, P., Paulin, R., Stenson, T.H., Haromy, A., Hashimoto, K., Zhang, N., Flaim, E., and Michelakis, E.D. (2014). A nuclear pyruvate dehydrogenase complex is important for the generation of acetyl-CoA and histone acetylation. Cell *158*, 84-97.

Takamura, A., Komatsu, M., Hara, T., Sakamoto, A., Kishi, C., Waguri, S., Eishi, Y., Hino, O., Tanaka, K., and Mizushima, N. (2011). Autophagy-deficient mice develop multiple liver tumors. Genes Dev *25*, 795-800.

Talloczy, Z., Jiang, W., Virgin, H.W.t., Leib, D.A., Scheuner, D., Kaufman, R.J., Eskelinen, E.L., and Levine, B. (2002). Regulation of starvation- and virus-induced autophagy by the eIF2alpha kinase signaling pathway. Proc Natl Acad Sci U S A *99*, 190-195.

Tanaka, Y., Guhde, G., Suter, A., Eskelinen, E.L., Hartmann, D., Lullmann-Rauch, R., Janssen, P.M., Blanz, J., von Figura, K., and Saftig, P. (2000). Accumulation of autophagic vacuoles and cardiomyopathy in LAMP-2-deficient mice. Nature *406*, 902-906.

Troncoso, R., Vicencio, J.M., Parra, V., Nemchenko, A., Kawashima, Y., Del Campo, A., Toro, B., Battiprolu, P.K., Aranguiz, P., Chiong, M.*, et al.* (2012). Energy-preserving effects of IGF-1 antagonize starvation-induced cardiac autophagy. Cardiovasc Res *93*, 320-329.

Tsunemi, T., Ashe, T.D., Morrison, B.E., Soriano, K.R., Au, J., Roque, R.A., Lazarowski, E.R., Damian, V.A., Masliah, E., and La Spada, A.R. (2012). PGC-1alpha rescues Huntington's disease proteotoxicity by preventing oxidative stress and promoting TFEB function. Sci Transl Med *4*, 142ra197.

Turdi, S., Kandadi, M.R., Zhao, J., Huff, A.F., Du, M., and Ren, J. (2011). Deficiency in AMP-activated protein kinase exaggerates high fat diet-induced cardiac hypertrophy and contractile dysfunction. J Mol Cell Cardiol *50*, 712-722.

Vander Haar, E., Lee, S.I., Bandhakavi, S., Griffin, T.J., and Kim, D.H. (2007). Insulin signalling to mTOR mediated by the Akt/PKB substrate PRAS40. Nat Cell Biol *9*, 316-323.

Villella, V.R., Esposito, S., Bruscia, E.M., Vicinanza, M., Cenci, S., Guido, S., Pettoello-Mantovani, M., Carnuccio, R., De Matteis, M.A., Luini, A.*, et al.* (2013). Disease-relevant proteostasis regulation of cystic fibrosis transmembrane conductance regulator. Cell Death Differ *20*, 1101-1115.

Violante, S., Ijlst, L., Ruiter, J., Koster, J., van Lenthe, H., Duran, M., de Almeida, I.T., Wanders, R.J., Houten, S.M., and Ventura, F.V. (2013). Substrate specificity of human carnitine acetyltransferase: Implications for fatty acid and branched-chain amino acid metabolism. Biochim Biophys Acta *1832*, 773-779.

Wallace, D.C. (2012). Mitochondria and cancer. Nat Rev Cancer *12*, 685-698.

Wang, C., Liang, C.C., Bian, Z.C., Zhu, Y., and Guan, J.L. (2013). FIP200 is required for maintenance and differentiation of postnatal neural stem cells. Nat Neurosci *16*, 532-542.

Weinert, B.T., Iesmantavicius, V., Moustafa, T., Scholz, C., Wagner, S.A., Magnes, C., Zechner, R., and Choudhary, C. (2014). Acetylation dynamics and stoichiometry in Saccharomyces cerevisiae. Mol Syst Biol *10*, 716.

Wellen, K.E., Hatzivassiliou, G., Sachdeva, U.M., Bui, T.V., Cross, J.R., and Thompson, C.B. (2009). ATP-citrate lyase links cellular metabolism to histone acetylation. Science *324*, 1076-1080.

Wieman, H.L., Wofford, J.A., and Rathmell, J.C. (2007). Cytokine stimulation promotes glucose uptake via phosphatidylinositol-3 kinase/Akt regulation of Glut1 activity and trafficking. Mol Biol Cell *18*, 1437-1446.

Wilkinson, J.E., Burmeister, L., Brooks, S.V., Chan, C.C., Friedline, S., Harrison, D.E., Hejtmancik, J.F., Nadon, N., Strong, R., Wood, L.K.*, et al.* (2012). Rapamycin slows aging in mice. Aging Cell *11*, 675-682.
Wong, Y.C., and Holzbaur, E.L. (2014). Optineurin is an autophagy receptor for damaged mitochondria in parkin-mediated mitophagy that is disrupted by an ALS-linked mutation. Proc Natl Acad Sci U S A *111*, E4439-4448.

Xu, L., Ma, H., Miao, M., and Li, Y. (2012). Impact of subclinical hypothyroidism on the development of non-alcoholic fatty liver disease: a prospective case-control study. J Hepatol *57*, 1153-1154.

Yamahara, K., Kume, S., Koya, D., Tanaka, Y., Morita, Y., Chin-Kanasaki, M., Araki, H., Isshiki, K., Araki, S., Haneda, M.*, et al.* (2013). Obesity-mediated autophagy insufficiency exacerbates proteinuria-induced tubulointerstitial lesions. J Am Soc Nephrol *24*, 1769-1781.

Yang, A., Rajeshkumar, N.V., Wang, X., Yabuuchi, S., Alexander, B.M., Chu, G.C., Von Hoff, D.D., Maitra, A., and Kimmelman, A.C. (2014a). Autophagy is critical for pancreatic tumor growth and progression in tumors with p53 alterations. Cancer Discov *4*, 905-913.

Yang, C., Ko, B., Hensley, C.T., Jiang, L., Wasti, A.T., Kim, J., Sudderth, J., Calvaruso, M.A., Lumata, L., Mitsche, M.*, et al.* (2014b). Glutamine oxidation maintains the TCA cycle and cell survival during impaired mitochondrial pyruvate transport. Molecular cell *56*, 414-424.

Yang, L., Li, P., Fu, S., Calay, E.S., and Hotamisligil, G.S. (2010). Defective hepatic autophagy in obesity promotes ER stress and causes insulin resistance. Cell metabolism *11*, 467-478.

Yao, T.P., Oh, S.P., Fuchs, M., Zhou, N.D., Ch'ng, L.E., Newsome, D., Bronson, R.T., Li, E., Livingston, D.M., and Eckner, R. (1998). Gene dosage-dependent embryonic

development and proliferation defects in mice lacking the transcriptional integrator p300. Cell *93*, 361-372.

Yennawar, N.H., Islam, M.M., Conway, M., Wallin, R., and Hutson, S.M. (2006). Human mitochondrial branched chain aminotransferase isozyme: structural role of the CXXC center in catalysis. J Biol Chem *281*, 39660-39671.

Yue, Z., Jin, S., Yang, C., Levine, A.J., and Heintz, N. (2003). Beclin 1, an autophagy gene essential for early embryonic development, is a haploinsufficient tumor suppressor. Proc Natl Acad Sci U S A *100*, 15077-15082.

Zaidi, N., Swinnen, J.V., and Smans, K. (2012). ATP-citrate lyase: a key player in cancer metabolism. Cancer Res *72*, 3709-3714.

Zhang, H., Bosch-Marce, M., Shimoda, L.A., Tan, Y.S., Baek, J.H., Wesley, J.B., Gonzalez, F.J., and Semenza, G.L. (2008). Mitochondrial autophagy is an HIF-1-dependent adaptive metabolic response to hypoxia. J Biol Chem *283*, 10892-10903.
Zhang, J., and Ney, P.A. (2009). Role of BNIP3 and NIX in cell death, autophagy, and mitophagy. Cell Death Differ *16*, 939-946.

Zhang, Y., Fang, F., Goldstein, J.L., Brown, M.S., and Zhao, T.J. (2015). Reduced autophagy in livers of fasted, fat-depleted, ghrelin-deficient mice: reversal by growth hormone. Proc Natl Acad Sci U S A *112*, 1226-1231.

Zhou, J., Farah, B.L., Sinha, R.A., Wu, Y., Singh, B.K., Bay, B.H., Yang, C.S., and Yen, P.M. (2014). Epigallocatechin-3-gallate (EGCG), a green tea polyphenol, stimulates hepatic autophagy and lipid clearance. PLoS One *9*, e87161.

Molecular Cell
Article

Regulation of Autophagy by Cytosolic Acetyl-Coenzyme A

Guillermo Mariño,[1,2,3,12] Federico Pietrocola,[1,2,3,12] Tobias Eisenberg,[4,12] Yongli Kong,[5] Shoaib Ahmad Malik,[1,2,3] Aleksandra Andryushkova,[4] Sabrina Schroeder,[4] Tobias Pendl,[4] Alexandra Harger,[6] Mireia Niso-Santano,[1,2,3] Naoufal Zamzami,[1,2,3] Marie Scoazec,[1,2] Silvère Durand,[1,2] David P. Enot,[1,2] Álvaro F. Fernández,[7] Isabelle Martins,[1,2,3] Oliver Kepp,[1,2,3] Laura Senovilla,[1,2,3] Chantal Bauvy,[3,8] Eugenia Morselli,[1,2,3] Erika Vacchelli,[1,2,3] Martin Bennetzen,[9] Christoph Magnes,[6] Frank Sinner,[6] Thomas Pieber,[6,10] Carlos López-Otín,[7] Maria Chiara Maiuri,[1,2,3] Patrice Codogno,[3,8] Jens S. Andersen,[9] Joseph A. Hill,[5] Frank Madeo,[4,13,*] and Guido Kroemer[1,2,3,11,13,*]

[1]Equipe 11 Labelisée par la Ligue Nationale Contre le Cancer, INSERM U1138, Centre de Recherche des Cordeliers, 75006 Paris, France
[2]Metabolomics and Molecular Cell Biology Platforms, Gustave Roussy, 94805 Villejuif, France
[3]Université Paris Descartes/Paris 5, Sorbonne Paris Cité, 75006 Paris, France
[4]Institute of Molecular Biosciences, University of Graz, 8036 Graz, Austria
[5]Department of Internal Medicine (Cardiology), University of Texas Southwestern Medical Center, Dallas, TX 75390, USA
[6]Institute of Medical Technologies and Health Management, Joanneum Research, 8036 Graz, Austria
[7]Departamento de Bioquímica y Biología Molecular, Instituto Universitario de Oncología, Universidad de Oviedo, Oviedo 33006, Spain
[8]INSERM U845, 75014 Paris, France
[9]Department of Biochemistry and Molecular Biology, University of Southern Denmark, 5230 Odense, Denmark
[10]Medical University of Graz, Division of Endocrinology and Metabolism, Department of Internal Medicine, 8036 Graz, Austria
[11]Pôle de Biologie, Hôpital Européen Georges Pompidou, AP-HP, 75015 Paris, France
[12]These authors contributed equally to this work
[13]Co-senior authors
*Correspondence: frank.madeo@uni-graz.at (F.M.), kroemer@orange.fr (G.K.)
http://dx.doi.org/10.1016/j.molcel.2014.01.016

SUMMARY

Acetyl-coenzyme A (AcCoA) is a major integrator of the nutritional status at the crossroads of fat, sugar, and protein catabolism. Here we show that nutrient starvation causes rapid depletion of AcCoA. AcCoA depletion entailed the commensurate reduction in the overall acetylation of cytoplasmic proteins, as well as the induction of autophagy, a homeostatic process of self-digestion. Multiple distinct manipulations designed to increase or reduce cytosolic AcCoA led to the suppression or induction of autophagy, respectively, both in cultured human cells and in mice. Moreover, maintenance of high AcCoA levels inhibited maladaptive autophagy in a model of cardiac pressure overload. Depletion of AcCoA reduced the activity of the acetyltransferase EP300, and EP300 was required for the suppression of autophagy by high AcCoA levels. Altogether, our results indicate that cytosolic AcCoA functions as a central metabolic regulator of autophagy, thus delineating AcCoA-centered pharmacological strategies that allow for the therapeutic manipulation of autophagy.

INTRODUCTION

Macroautophagy ("autophagy") involves the highly regulated sequestration of cytoplasmic organelles or portions of the cytosol in double-membrane vesicles, called autophagosomes, which later fuse with lysosomes, resulting in the degradation of the inner autophagosomal membrane and luminal content (Mizushima and Komatsu, 2011). Autophagy plays an essential role in cellular adaptation to multiple types of stress, recycling of superfluous or damaged cellular material, quality control of organelles, removal of protein aggregates, and destruction of intracellular pathogens (Kroemer et al., 2010). Although autophagy plays a major role in antagonizing degenerative processes and avoiding unwarranted cell death, its excessive induction may result in maladaptive tissue remodeling (Levine and Kroemer, 2008; López-Otín et al., 2013; Zhu et al., 2007).

Autophagy can be induced by a plethora of cell-extrinsic and cell-intrinsic stressors, in a biphasic process. The rapid phase of autophagy induction, which occurs on a timescale of minutes to hours, does not require de novo synthesis of macromolecules and relies on posttranscriptional regulators (Morselli et al., 2011; Tasdemir et al., 2008), contrasting with more protracted autophagic responses that rely on the execution of transcriptional programs (Settembre et al., 2011; Warr et al., 2013). At the posttranscriptional level, the autophagic pathway is regulated by multiple (de)phosphorylation reactions. Multiple components of the "core machinery" of autophagy are either kinases (such as the protein kinases autophagy-related gene 1 [ATG1] and mammalian target of rapamycin [mTOR] or the lipid kinase Vps34) or kinase substrates (Behrends et al., 2010). Another posttranslational modification that participates in the regulation of autophagy is acetylation. Multiple components of the core machinery of autophagy have been shown to undergo changes in their acetylation status (Bánréti et al., 2013; Lee et al., 2008; Lee and Finkel, 2009; Morselli et al., 2011; Yi et al., 2012), and

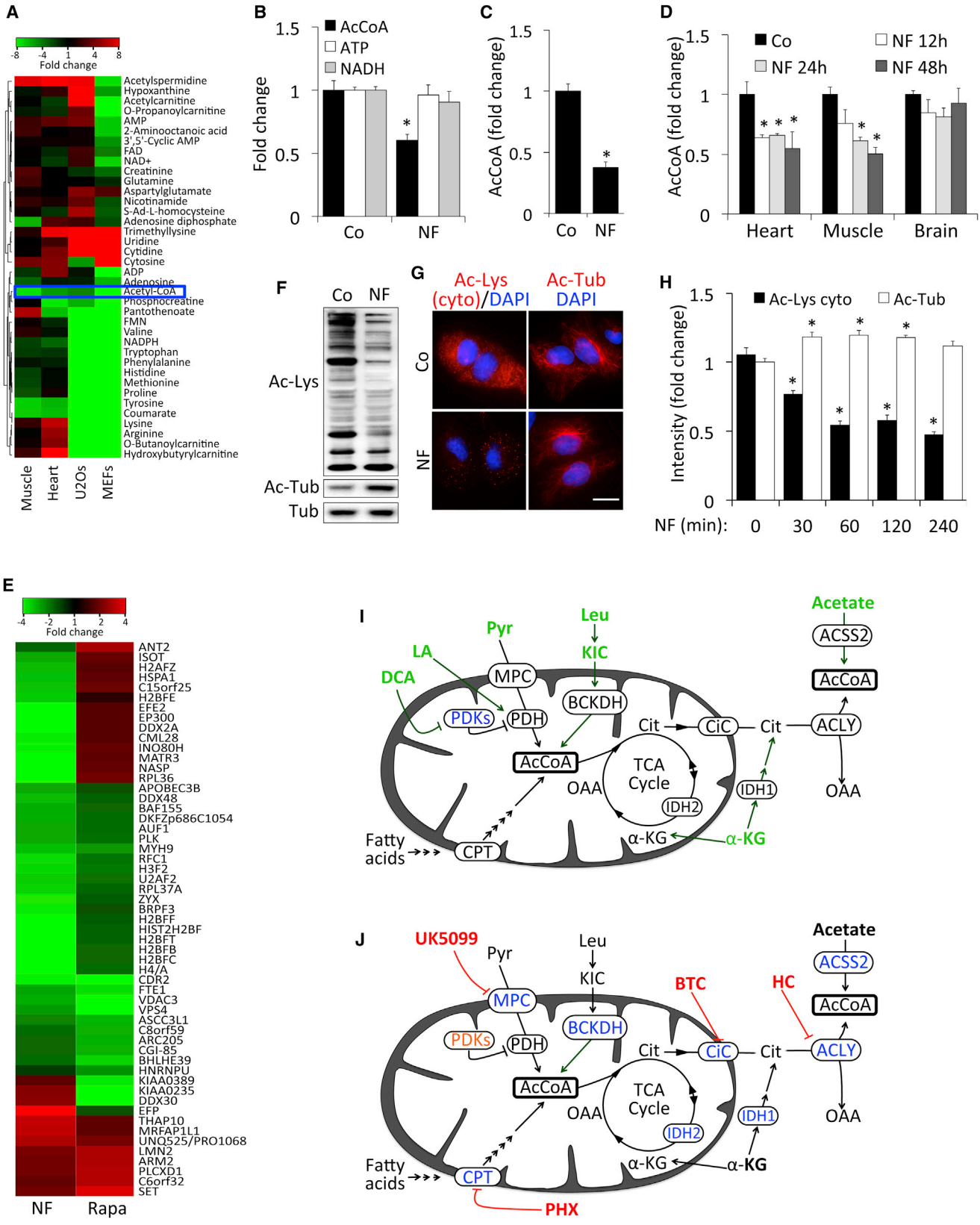

(legend on next page)

similarly core regulators of autophagy such as the transcription factors p53 and forkhead box P3 (FOXP3) can be regulated by acetylation (Contreras et al., 2013).

Metabolic perturbation, in particular amino acid, serum, or glucose deprivation, can induce autophagy, and potent energy sensors including AMP-dependent protein kinase (AMPK), the mammalian target of rapamycin complex 1 (mTORC1), and the NADH-dependent deacetylases of the sirtuin family control autophagy (Kroemer et al., 2010). Thus, decreases in intracellular amino acids, ATP, and NADH give rise to mTORC1 inhibition, AMPK stimulation, and sirtuin-1 activation, respectively, thereby stimulating the induction of autophagy via intersecting pathways (Kroemer et al., 2010).

Here, we report the unexpected finding that acetyl-CoA (AcCoA) is yet another metabolite that plays a cardinal role in the regulation of starvation-induced autophagy. Inhibition of enzymes required for the maintenance of cytosolic AcCoA induces autophagy through a transcription-independent process related to the reduced activity of the acetyltransferase EP300. Moreover, manipulations designed to increase cytosolic AcCoA prevent autophagy in vitro and in vivo.

RESULTS

Starvation Induces Depletion of Acetyl-CoA and Protein Deacetylation

Autophagy can be potently induced by exposing cells to nutrient-free media or by subjecting mice to starvation (Mizushima and Komatsu, 2011). Mass spectrometric metabolomic profiling of starved cells (in vitro) or organs (in vivo) revealed the intracellular depletion of very few common metabolites, one of which was AcCoA (Figure 1A). Starvation-induced AcCoA depletion could be confirmed in murine and human cell lines, both in total cellular homogenates (Figure 1B) and in cytosolic fractions (Figure 1C). At the analyzed short (<6 hr) incubation times, the starvation-induced decrease of AcCoA was not accompanied by the depletion of ATP or NADH (Figure 1B and Figures S1A–S1C available online). In mice, heart and muscle tissues responded to nutrient depletion by mounting a strong autophagic response (Mizushima et al., 2004), which we found to be commensurate with a reduction in AcCoA levels (Figures 1A and 1D) and a decrease in cytoplasmic protein acetylation (Figures S1E and S1F). In contrast, brain tissue, in which autophagy induction is not observed after fasting (Mizushima et al., 2004), presented no alterations in AcCoA levels or protein acetylation even after prolonged (48 hr) starvation (Figures 1D and S1G).

Starved cells exhibited a preponderant deacetylation of their proteins, as determined by SILAC technology (Figure 1E; Table S1). Global deacetylation of the majority of cellular proteins was confirmed by immunoblot analyses (Figure 1F), although some proteins like tubulin were hyperacetylated after starvation (Geeraert et al., 2010; Lee et al., 2010) (Figure 1F and 1G). For the rapid evaluation of the global acetylation status of cytoplasmic proteins, we developed a protocol in which plasma membranes but not nuclear envelopes were permeabilized (Pietrocola et al., 2012), acetylated tubulin was blocked with a specific antibody, and antibody staining of proteins with acetylated lysines was revealed by immunofluorescence. Using this method, we could detect starvation-induced deacetylation of cytoplasmic proteins (Figures 1G and 1H). These results suggest that AcCoA depletion is linked to the deacetylation of cytoplasmic proteins.

Maintaining AcCoA Levels during Starvation Inhibits Autophagy Induction

AcCoA is produced in mitochondria by three major pathways (Figures 1I and 1J), namely pyruvate decarboxylation, fatty acid oxidation, and the catabolism of branched-chain amino acids (BCAAs) (Wellen et al., 2009).

Pyruvate decarboxylation is catalyzed by pyruvate dehydrogenase (PDH), which is negatively regulated by pyruvate dehydrogenase kinase (PDK) isoenzymes (PDK1, PDK2, PDK3, and PDK4) (Roche and Hiromasa, 2007). Knockdown of PDK2 or PDK4 inhibited both starvation-induced AcCoA depletion and autophagy, as measured by two assays (GFP-LC3 distribution to cytoplasmic puncta and LC3 lipidation detectable by immunoblot, both in the presence/absence of the lysosomal inhibitor

Figure 1. Nutrient Starvation Leads to a Reduction of Both AcCoA Levels and Cytoplasmic Protein Acetylation

(A) Clustering of metabolites, the concentration of which significantly changed in MEFs and human U2OS cells after 4 hr of nutrient-free (NF) culture and in skeletal muscle and heart tissues from C57Bl/6 mice after 48 hr of fasting. The results are presented as fold-change values in relation to appropriate nonstarved controls.

(B and C) Targeted mass spectrometric analyses confirmed a reduction of total AcCoA, but not of NADH or ATP (B) or cytosolic AcCoA (C) in human U2OS cell line and MEFs after 4 hr of nutrient starvation.

(D) Targeted analyses also confirmed a reduction of AcCoA in vivo.

(E) Clustering of proteins found to be differentially acetylated in response to nutrient starvation or rapamycin treatment, as detected by SILAC technology. Only sites regulated >2-fold were included in statistical analyses.

(F) Representative immunoblots of total cell lysates showing a reduction of protein acetylation and an increase of tubulin acetylation after 4 hr of nutrient starvation.

(G) Representative immunofluorescence microphotographs reflecting detection of cytoplasmic lysine-acetylated proteins (left panels) or acetylated tubulin (right panels), after 4 hr of nutrient starvation. Scale bar, 10 μm.

(H) Quantification of data depicted in (G) at different time points during nutrient starvation. Results are reported as means ± SEM of at least six replicates per condition. *$p < 0.05$ (unpaired Student's t test) compared to the corresponding controls.

(I and J) Schematic representation of the main cellular pathways involved in the generation of mitochondrial and cytoplasmic AcCoA pools. Strategies to elevate or deplete AcCoA are shown in (I) and (J), respectively. Blue, knockdown of genes. Orange, overexpression of genes. Green, compounds causing AcCoA elevation. Red, compounds causing AcCoA depletion. ACLY, ATP-citrate lyase; ACSS2 (acetyl-Coenzyme A synthetase-2); α-KG (α-ketoglutarate); BCKDH (branched-chain ketoacid dehydrogenase); BTC (benzenetricarboxylate); CiC (citrate carrier); Cit (citrate); CPT (carnitine palmitoyltransferase); DCA (dichloroacetate); DMKG (dimethyl α-ketoglutarate); HC (hydroxycitrate); KIC (α-ketoisocaproic acid); IDH (isocitrate dehydrogenase); LA (lipoic acid); Leu (leucine); MPC (mitochondrial pyruvate carrier); OAA (oxalacetate); PDH (pyruvate dehydrogenase); PDKs (pyruvate dehydrogenase kinases); PHX (perhexiline); Pyr (pyruvate); TCA, tricarboxylic acid; UK5099 (α-cyano-β-(1-phenylindol-3-yl)acrylate). See also Figure S1.

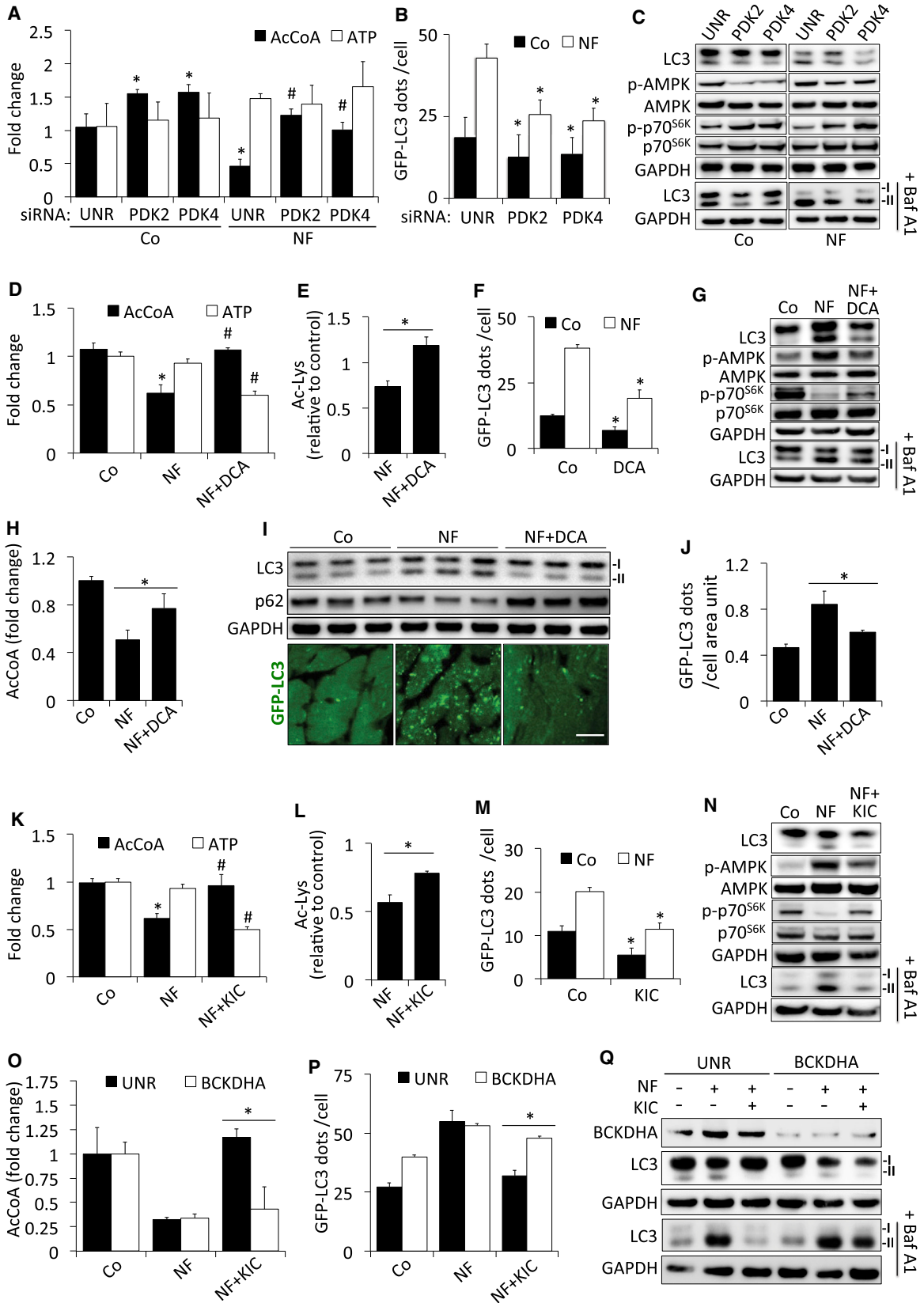

(legend on next page)

bafilomycin A1, BafA1, to measure autophagic flux) but had no significant effect on cellular ATP content (Figures 2A–2C and S2A). Starvation-induced autophagy inhibition by PDK2/4 knockdown was accompanied by a reversion of starvation-associated mTORC1 inhibition and AMPK activation (Figure 2C). Similarly, pharmacological inhibition of PDKs with dichloroacetate (DCA) resulted in the suppression of starvation-induced AcCoA depletion (but not in an increase of ATP levels), protein deacetylation, mTORC1 inhibition, AMPK activation, turnover of long-lived proteins, and autophagic flux, both in vitro, in starved human cells (Figures 2D–2G and S4L), and in vivo, in the heart (Figure 2H–2J and S2B), skeletal muscle, and liver (data not shown) from starved mice. Direct stimulation of PDH activity by its cofactor lipoic acid (LA) (Zachar et al., 2011) also allowed starved cells to maintain high AcCoA and cytoplasmic acetylation levels, as it blunted starvation-induced mTORC1 inhibition, AMPK activation, turnover of long-lived proteins, and autophagic flux (Figures S2C–S2F and S4L).

BCAAs (such as leucine) are transaminated to branched-chain α-ketoacids (such as, in the case of leucine, α-ketoisocaproic acid, KIC), which subsequently undergo oxidative decarboxylation, yielding AcCoA as the end product. This irreversible reaction is catalyzed by the mitochondrial branched-chain α-ketoacid dehydrogenase complex (BCKDH) (Chuang, 2013). Supplementation of leucine, the most bioactive BCAA, was sufficient to maintain high AcCoA levels and cytoplasmic protein acetylation during nutrient deprivation, correlating with the suppression of autophagy (Figures S2G–S2J). Addition of KIC was sufficient to avoid AcCoA depletion and protein deacetylation in starved cells, as it prevented starvation-associated mTORC1 inhibition and AMPK activation. Concomitantly, KIC inhibited the starvation-induced increase in autophagic flux and turnover of long-lived proteins (Figures 2K–2N and S4L). On a molar basis, KIC (which barely increased intracellular leucine levels, as determined my mass spectrometry) was more efficient than leucine in suppressing autophagy (Figures S2K and S2L). Depletion of BCKDH E1α subunit (BCKDHA) inhibited the conversion of KIC into AcCoA (Figure 2O) as it abolished the KIC-mediated suppression of starvation-induced autophagy (Figures 2P and 2Q). In contrast, BCKDHA depletion did not abolish the slight increase in intracellular leucine concentrations induced by KIC supplementation (Figure S2M). Altogether, these findings support the contention that KIC inhibits autophagy through its conversion into AcCoA rather than by replenishing amino acids.

When supplemented to starved cells, the short-chain fatty acid butyrate, which can be catabolized to AcCoA (Donohoe et al., 2012), maintained high cytosolic AcCoA, increased protein acetylation, and inhibited autophagic flux (Figures S3A–S3D). Supplementation of dimethyl-α-ketoglutarate (DMKG), a cell-permeant precursor of α-ketoglutarate (Willenborg et al., 2009), also maintained high AcCoA and cytoplasmic acetylation levels and low autophagy (linked to a coordinated modulation of mTORC1 and AMPK pathways activity) under starvation conditions in vitro (Figures 3A–3D). DMKG supplementation failed to enhance intracellular amino acid levels in starved cells (Figure S3H). Simultaneous depletion of both isocitrate dehydrogenase isoforms (IDH1 and IDH2) abolished the ability of DMKG to replenish cytosolic AcCoA levels (Figure 3E) as well as its antiautophagic function (Figures 3F and 3G). These results suggest that DMKG-derived α-ketoglutarate undergoes reductive carboxylation to isocitrate, followed by IDH1/2-mediated isomerization to the AcCoA precursor citrate (Figures 1I and 1J).

Beyond these in vitro effects, DMKG efficiently reduced autophagy in vivo. Parenteral administration of DMKG to starved mice avoided the depletion of AcCoA (Figure 3H) and the deacetylation of cytoplasmic proteins (Figure S3E), as well as fasting-induced autophagy in heart (Figures 3I and 3J) and skeletal muscles (data not shown). Moreover, DMKG inhibited the maladaptive accumulation of autophagosomes induced by surgical thoracic aortic constriction (TAC) (Figures 3K, 3L, S3F, and S3G). Repeated DMKG injections suppressed multiple features of TAC-induced heart failure, namely cardiomyocyte hypertrophy (Figure 3M), left ventricular dilatation (Figure 3N), cardiac muscle fibrosis (Figure 3O), and reduced contractile performance (Figure 3P). Thus, suppression of maladaptive autophagy by increasing AcCoA levels can blunt pressure overload-induced cardiomyopathy, confirming the beneficial effects of genetic autophagy inhibition in this pathology (Zhu et al., 2007).

It should be noted that none of the AcCoA-replenishing agents (DCA, LA, KIC, butyrate, or DMKG) were capable of increasing

Figure 2. Starvation-Induced Autophagy Is Inhibited by AcCoA Replenishment

(A–C) Effects of the knockdown of pyruvate dehydrogenase kinase 2 or 4 (PDK2 or PKD4). Depletion of PDK2 or PDK4 from U2OS cells kept in nutrient-free (NF) conditions led to an increase in AcCoA levels but not in ATP (A). In addition, PDK2 or PDK4 knockdown inhibited NF-induced autophagy, as measured by GFP-LC3 puncta formation (B) or by LC3 lipidation (C). This inhibition of NF-induced autophagy was accompanied by a reduction in AMPK phosphorylation as well as by an increase in mTORC1 activity (C).

(D–G) In vitro effects of dichloroacetate (DCA). Inhibition of PDKs by DCA resulted in an increase in both AcCoA levels (D) and cytoplasmic protein acetylation (E), together with the inhibition of NF-induced autophagy, as measured by GFP-LC3 puncta formation (F) and LC3 lipidation. This effect of DCA was associated with a reduction in NF-induced AMPK phosphorylation, as well as with an increase in mTORC1 activity (G).

(H–J) In vivo effects of DCA. Intraperitoneal injection of DCA (but not vehicle alone) resulted in increased AcCoA levels after 24 hr of starvation (NF) in mouse tissues (H). (I) DCA treatment inhibited starvation-induced autophagy in vivo, as measured by assessing LC3 lipidation (upper panel) of heart tissues from C57Bl/6 mice or by fluorescence microscopic analyses of hearts from GFP-LC3 transgenic mice (lower panel), quantified in (J).

(K–Q) Reversion of starvation-induced autophagy by ketoisocaproic acid (KIC). Supplementation of KIC to cells cultured in NF conditions resulted in an increase in AcCoA levels, ATP decrease (K), and cytoplasmic protein acetylation (L), together with an inhibition of autophagy (M), inhibition of AMPK phosphorylation, and reversion of 70^{s6k} dephosphorylation (N). Branched-chain ketoacid dehydrogenase (BCKDH) knockdown prevented the AcCoA increase (O) and autophagy inhibition (P and Q) mediated by KIC supplementation.

*$p < 0.05$ (unpaired Student's t test) compared to control conditions; #$p < 0.05$ (unpaired Student's t test) compared to cells kept in nutrient-free (NF) conditions. See also Figure S2.

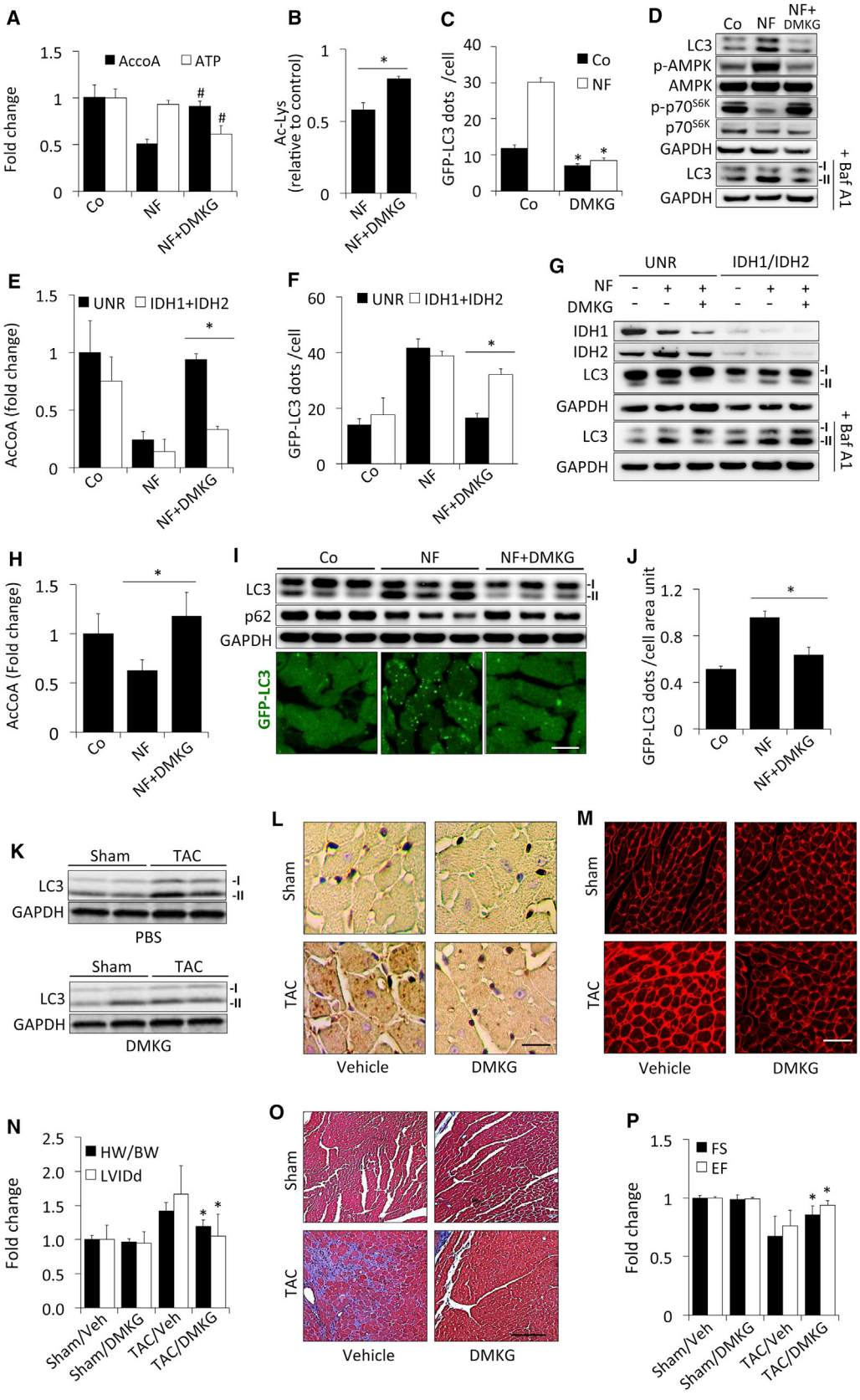

(legend on next page)

cellular ATP levels in starved cells. Rather, when combined with starvation, such agents induced a decrease in cellular ATP (Figures 2A, 2D, 2K, 3A, S2C, and S3A), which may be attributed to autophagy inhibition, as treatment with the autophagy inhibitor 3-methyladenine (3-MA) similarly reduced ATP content (Figure S4J) and autophagy-deficient *Atg5*$^{-/-}$ or *Atg7*$^{-/-}$ mouse embryonic fibroblasts (MEFs) contained lower cellular ATP levels than WT MEFs (Lin et al., 2012b). These results suggest that an increase in cellular AcCoA levels is sufficient to counteract autophagy induction by nutrient deprivation. Moreover, pharmacological and metabolic manipulations designed to increase AcCoA were capable of suppressing autophagy induced by clinically relevant compounds, including metformin, rotenone, Akt inhibitors, and rapamycin (Figure S3I; Table S2). Thus, AcCoA acts as a broad-spectrum autophagy repressor, well beyond its capacity to inhibit starvation-induced autophagy.

AcCoA Depletion Is Sufficient to Induce Autophagy

Next, we addressed the question as to whether a reduction in AcCoA levels would be sufficient to increase autophagic activity, even in cells that are kept in rich medium. Before it can be converted to AcCoA, pyruvate has to be transported across the inner mitochondrial membrane by the mitochondrial pyruvate carrier (MPC) complex (Herzig et al., 2012). Knockdown of MPC or its inhibition by UK5099 led to the depletion of intracellular AcCoA without reducing ATP (Figures 4A and 4E). AcCoA depletion was coupled to deacetylation of cytoplasmic proteins (Figures 4B and 4F), induction of GFP-LC3 puncta (Figures 4C and 4G), and lipidation of endogenous LC3-I to LC3-II, both in the presence and absence of BafA1, confirming an increase of autophagic flux (Figures 4D and 4H). UK5099 also increased the autophagy-dependent turnover of long-lived proteins (Figure S4L). Moreover, transfection-enforced overexpression of several PDK isoforms, which catalyze the inhibitory phosphorylation of PDH, led to a reduction in both AcCoA levels (without significantly altering ATP concentration) and cytoplasmic protein acetylation, together with an increase in autophagic flux and autophagy-dependent protein degradation (Figures 4I–4L, S4A, and S4B).

In addition to pyruvate decarboxylation, fatty acid oxidation may generate AcCoA. Inhibition of mitochondrial carnitine palmitoyltransferase-1 (CPT1), the rate-limiting enzyme in fatty acid-oxidation, by perhexiline (PHX) (Foster, 2004), reduced AcCoA cellular levels, and induced signs of autophagy (Figures S4C–S4E). Similarly, knockdown of CPT1c, a CPT1 isoform highly expressed in human cancer cells (Zaugg et al., 2011), stimulated autophagic flux in U2OS osteosarcoma cells (Figures S4F and S4G).

Importantly, all the interventions designed to deplete AcCoA also resulted in mTORC1 inhibition (as indicated by reduced phosphorylation of its substrate p70^{s6k}) and AMPK stimulation (Figures 4D, 4H, 4L, and S4E) yet failed to reduce intracellular ATP levels (Figure S4J) or to reduce the mitochondrial transmembrane potential (Figure S4K). Depletion of AcCoA was not cytotoxic and actually prevented cell death induced by transgenic Q74 huntingtin (Williams et al., 2008) (Figures S4H and S4I), consistent with the reported cytoprotective action of autophagy (Rubinsztein et al., 2007). Thus, the interruption of glycolytic and lipolytic AcCoA generation in mitochondria, via inhibition of MCP or CPT1, respectively, can induce cytoprotective autophagy.

Cytosolic, Not Mitochondrial nor Nuclear, AcCoA Regulates Autophagy

AcCoA-dependent acetylation affects the function of proteins in mitochondria, as well as in other organelles including nuclei (Hebert et al., 2013; Masri et al., 2013; Wellen et al., 2009). Cytosolic AcCoA is mostly generated from citrate, which is transported from mitochondria to the cytosol by the mitochondrial citrate carrier (CiC). Once in the cytosol, citrate is converted back to oxaloacetate and AcCoA by ATP-citrate lyase (ACLY) (Wellen et al., 2009). Based on these premises, we analyzed whether cytosolic AcCoA reduction would be sufficient to stimulate autophagic flux. Inhibition of CiC by the substrate analog 1,2,3-benzenetricarboxylate (BTC) induced the triad of AcCoA depletion (measured specifically in the cytosolic fraction), protein deacetylation, and autophagy (Figures 5A–5D). Similarly, either knockdown of ACLY or addition of hydroxycitrate (HC), its competitive inhibitor (Lowenstein and Brunengraber, 1981), also reduced cytoplasmic AcCoA levels (Figures 5E and 5I), induced cytoplasmic protein deacetylation (Figures 5F and 5J), and strongly stimulated autophagy in vitro (Figures 5G, 5H, 5K, and 5L).

Oral administration of HC to WT mice for 2 days triggered a systemic autophagic response (Figures 5M and 5N) comparable to that induced by starvation (Figure S5A). Prolonged treatment

Figure 3. Inhibition of Autophagy by Dimethy-α-Ketoglutarate

(A–G) Inhibition of autophagy by DMKG in vitro. Addition of DMKG to cell cultured in nutrient-free (NF) conditions increased cellular AcCoA levels and decreased ATP levels (A) and cytoplasmic protein acetylation (B). DMKG treatment also abolished NF-induced GFP-LC3 puncta (C) and LC3 lipidation (D). (E–G) Knockdown of isocitrate dehydrogenase-1 and dehydrogenase-2 (IDH1/2) prevented AcCoA increase (E) and autophagy inhibition (F and G) after DMKG supplementation. (H–J) Inhibition of starvation-induced autophagy by DMKG in vivo. Intraperitoneal injection of DMKG increased cardiac AcCoA levels (H) after 24 hr of starvation (NF), as compared with vehicle-treated mice. DMKG treatment inhibited starvation-induced autophagy in vivo, as measured by LC3 lipidation (upper panel in I) or by microscopic analysis of hearts from GFP-LC3 transgenic mice (lower panel in I, quantified in J). Scale bar, 10 μm.

(K–P) Effects of DMKG treatment on pressure overload-induced maladaptive autophagy in the heart. Daily intraperitoneal injections of DMKG (300 mg/kg) decreased cardiac autophagy induced by thoracic aortic constriction (TAC), as measured by immunoblotting (K) or immunohistochemistry (L). DMKG administration also suppressed TAC-induced cardiomyocyte hypertrophy (measured by staining with wheat germ agglutinin in transverse sections of the left ventricle) (M), ventricular hypertrophy expressed as the heart weight/body weight ratio (HW/BW) or left ventricle internal diameter (LVID) (N), cardiac muscle fibrosis measured by trichrome staining (O), and reduction in contractile performance quantified as ejection fraction or fractional shortening (P). Scale bars, 15 μm in (D), 40 μm in (F), and 100 μm in (I).

All values are shown as means ± SEM of at least three experiments. *$p < 0.05$ (unpaired Student's t test) compared to the corresponding control conditions; $^{\#}p < 0.05$ (unpaired Student's t test) compared to values from starved cells. See also Figure S3.

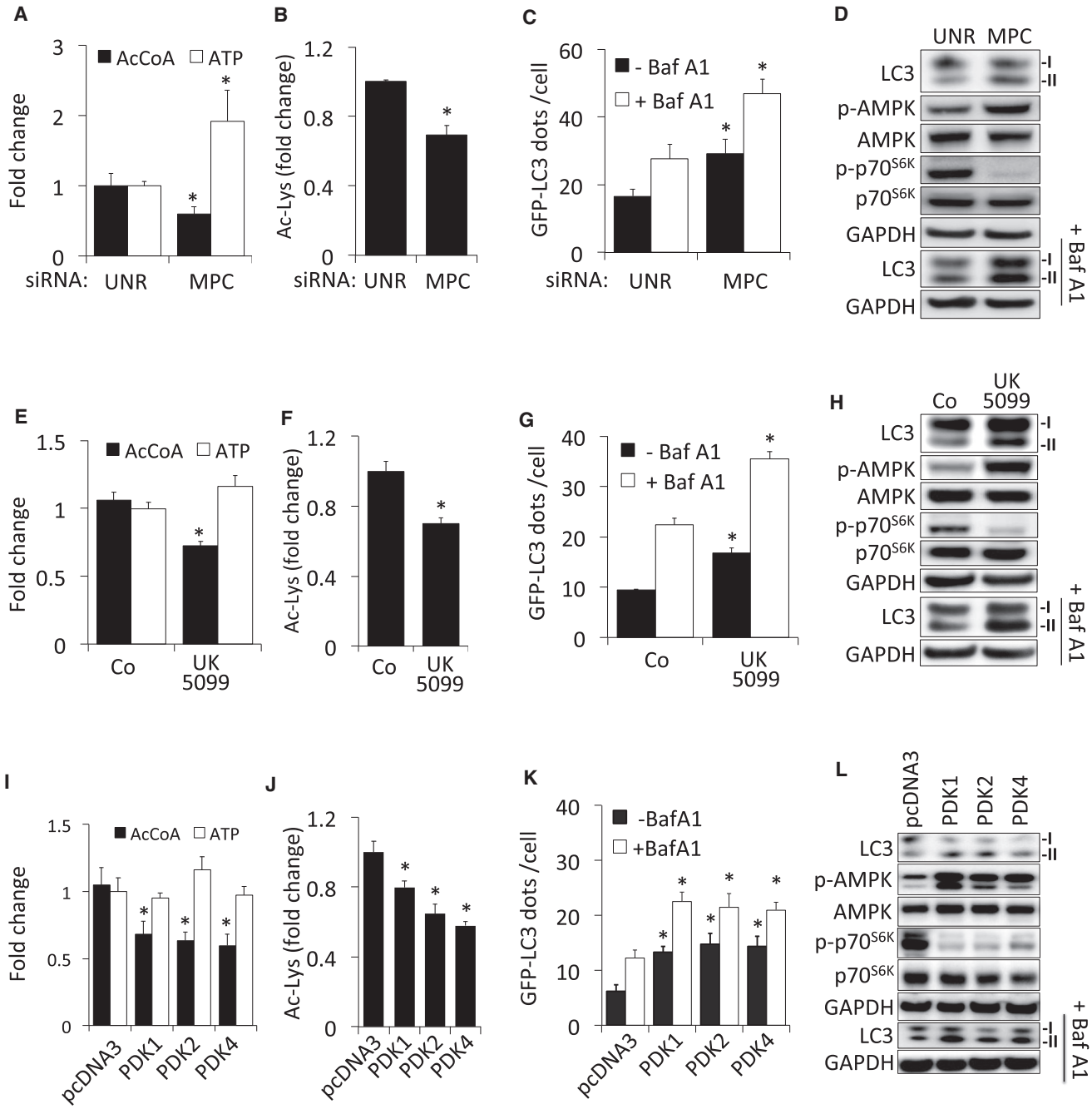

Figure 4. Inhibition of Pyruvate Decarboxylation Stimulates Autophagic Flux

(A–H) Inhibition of the mitochondrial pyruvate carrier (MPC). Knockdown of MPC or its pharmacological inhibition by UK5099 reduced AcCoA but not ATP levels (A and E) and cytoplasmic protein acetylation (B and F), while it increased GFP-LC3 puncta (C and G) and LC3 lipidation (D and H).

(I–L) Inhibition of pyruvate decarboxylation by overexpression of pyruvate dehydrogenase kinase (PDK) isoforms. Overexpression of PDK1, PDK2, or PDK4 in U2OS cells led to a decrease in AcCoA (but not ATP) levels (I); deacetylation of cytoplasmic proteins (J); increased GFP-LC3 puncta (K), lipidation of LC3, and AMPK phosphorylation; and decreased $p70^{s6k}$ phosphorylation by mTORC1 (L).

All values are shown as means ± SEM of at least three experiments. *$p < 0.05$ (unpaired Student's t test) as compared to the corresponding condition in untreated controls (or pcDNA3 transfected cells). See also Figure S4.

(2 weeks) with HC is known to cause significant weight loss (Onakpoya et al., 2011), and this effect was not accompanied by reduced food intake (Figure S5B). Surprisingly, weight reduction by HC was only observed in autophagy-competent wild-type mice, not in autophagy-deficient *Atg4b*$^{-/-}$ mice (Mariño et al., 2010) (Figure 5O).

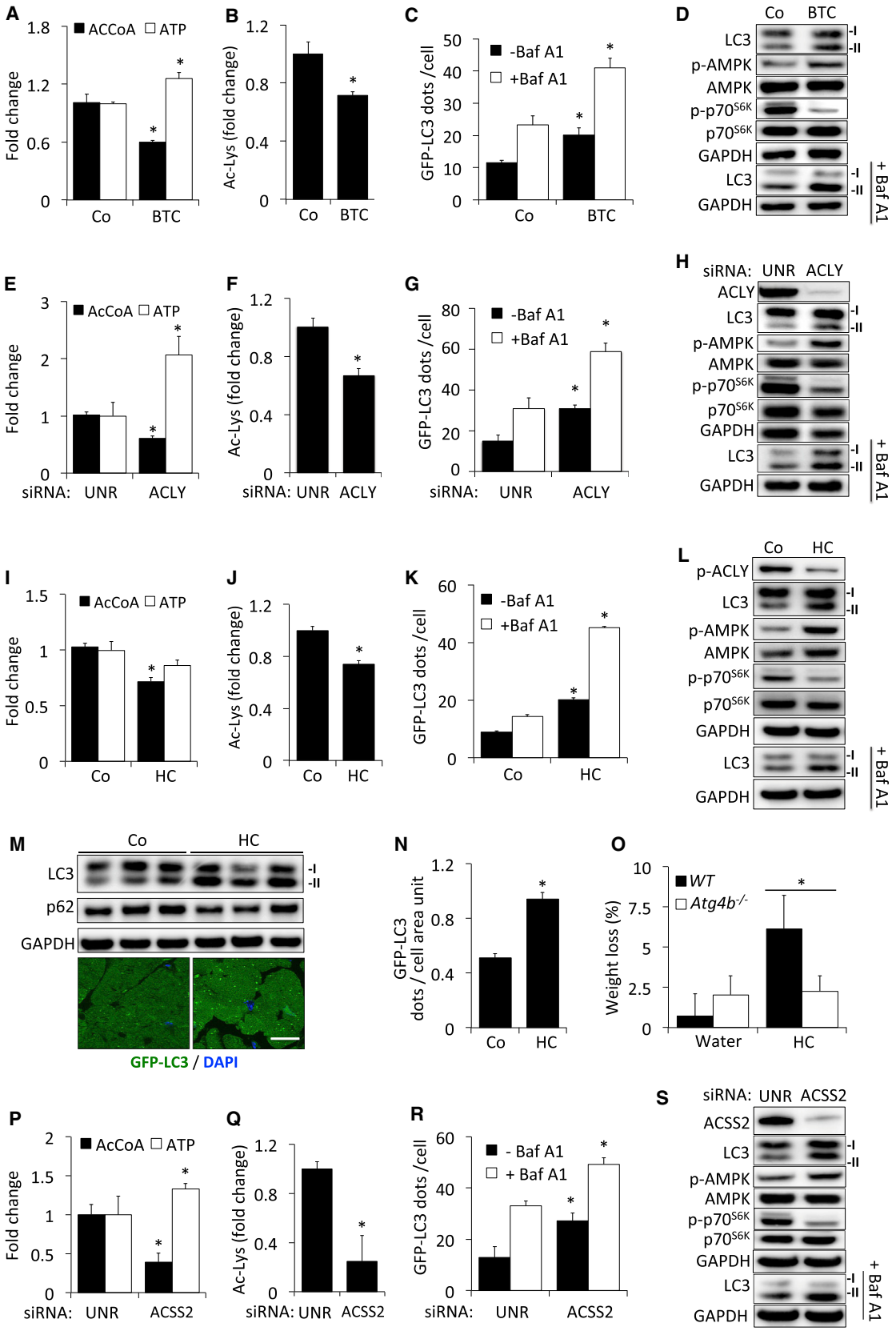

(legend on next page)

Although cytosolic AcCoA is mostly generated from citrate via ACLY, it can also be generated from acetate by the acyl-CoA synthetase short-chain family member 2 (ACSS2) (Wellen and Thompson, 2012). Knockdown of ACSS2 induced the triad of cytosolic AcCoA depletion, protein deacetylation, and autophagy induction (Figures 5P–5S).

Depletion of cytosolic AcCoA by the aforementioned experimental approaches was accompanied by an increase in AMPK phosphorylation and a decrease in mTORC1-mediated $p70^{s6k}$ phosphorylation (Figures 5D, 5H, 5L, and 5S). Importantly, interventions designed to deplete cytosolic AcCoA (i.e., blockade of the mitochondrial citrate carrier by BTC or inhibition of ACLY by HC) abolished both the protein hyperacetylation and autophagy suppression by manipulations designed to elevate mitochondrial AcCoA levels in starved cells (i.e., addition of the PDH activator DCA, the α-ketoglutarate precursor DMKG, or the leucine derivate KIC) (Figures 6A and 6B). This supports the idea that the cytosolic (rather than the mitochondrial) pool of AcCoA modulates autophagic flux. Consistent with this notion, all treatments that increased total cellular AcCoA levels (DCA, LA, DMKG, KIC, and UK5099) also raised the cytosolic concentration of AcCoA (Figures S5C and S5D). To directly assess the impact of cytosolic AcCoA on autophagy, starved U2OS cells stably expressing GFP-LC3 were microinjected with AcCoA. The introduction of AcCoA (but not that of CoA) into the cytosol of starved cells increased cytoplasmic protein acetylation and simultaneously reduced starvation-induced autophagic flux (Figures 6C and 6D). This experiment provides direct evidence in favor of the idea that cytosolic AcCoA represses autophagy.

Through nuclear pores, cytosolic AcCoA can freely diffuse into the nucleus, modulate the acetylation of histone and other chromatin binding factors, and hence affect gene transcription programs (Wellen and Thompson, 2012), which in turn might impinge on autophagy. To evaluate this possibility, we experimentally enucleated GFP-LC3-expressing cells and exposed the resulting cytoplasts to AcCoA-modulating conditions in the presence of BafA1. AcCoA-depleting agents (BTC, HC, UK5099) stimulated autophagic flux in cytoplasts as efficiently as in nucleated control cells (Figures 6E and 6F). Moreover, starvation-induced autophagy was fully induced in cytoplasts and was indistinguishably repressed by AcCoA replenishing agents in cytoplasts and cells (Figures 6G and 6H). Thus, short-term alterations in cytosolic AcCoA concentrations can regulate autophagy through purely cytoplasmic (nonnuclear) effects.

The Acetyltransferase EP300 Is Required for AcCoA-Mediated Autophagy Inhibition

Cells harbor multiple acetyltransferases and deacetylases that control the acetylation of nuclear and cytoplasmic proteins (Nakamura et al., 2010). Among the 78 acetyltransferases annotated in the human genome, we chose 43 whose localization is not strictly restricted to the nucleus. We evaluated the effects of the knockdown of these 43 acetyltransferases on the modulation of autophagic flux by AcCoA-elevating agents, as measured by the accumulation of GFP-LC3 dots in the presence of BafA1 and p62 degradation (Figures 7A, S7A, and S7B; Table S3). Although the knockdown of several acetyltransferases increased autophagic flux (Figure 7A; Table S4), only that of EP300 reverted the autophagy-inhibitory effects of butyrate, DCA, KIC, LA, and DMKG (Figure 7A). These results were confirmed by quantifying GFP-LC3 dots in the presence of BafA1 (Figures 7B and 7D) or by assessing LC3 lipidation in U2OS cells (Figures 7C and 7E). Moreover, knockdown of EP300 decreased mTORC1 activity and abolished the activation of mTORC1 by AcCoA donors (Figures 7E, S7A, and S7B). Pharmacological inhibition of EP300 protein by c646, which competes for AcCoA binding to EP300 (Bowers et al., 2010), also induced autophagy both in vitro, in cultured cells, and in vivo, in mice (Figures 7F, 7I, and 7J). Consistently, either EP300 inhibition by c646 (in human cells) or *EP300* gene deletion (in MEFs) precluded the inhibitory effect of AcCoA-replenishing agents on starvation-induced autophagy (Figures 7G and S7E–S7H).

The activity of EP300 was highly sensitive to variations in AcCoA concentrations that are close to those observed in the cytosol of mammalian cells (Yeh and Kim, 1980). In fact, the autoacetylation of recombinant EP300 protein on K1499 (which reflects its acetyltransferase activity) (Thompson et al., 2004), as well as its capacity to acetylate other substrates (such as recombinant tumor suppressor p53 or histone H3 proteins), was influenced by AcCoA concentration in a cell-free system (Figure 7H). Acetylation of EP300 was also reduced after the culture of cells in nutrient-free conditions, as determined by SILAC technology (Figure 1E) and confirmed by immunobloting (Figures S7C and S7D). Starvation-induced deacetylation of the K1499 residue in EP300 could be avoided when AcCoA was replenished by addition of DCA, KIC, DMKG, or LA (Figures S7C and S7E).

Taken together, these results indicate that EP300 is responsible for AcCoA-mediated autophagy repression and underscore the link between AcCoA concentration, EP300 activity, and autophagy regulation.

Figure 5. Depletion of Cytosolic AcCoA Increases Autophagic Flux

(A–D) Inhibition of citrate transport from mitochondria to cytoplasm by benzenetricarboxylate (BTC). Short-term (4 hr) incubation with BTC reduced AcCoA but not ATP levels (A), reduced cytoplasmic protein acetylation (B), and increased GFP-LC3 puncta (C) and LC3 lipidation (D).

(E–L) Inhibition of ATP citrate lyase (ACLY) in vitro. Depletion of ACLY by siRNAs or addition of its competitive inhibitor, hydroxycitrate (HC), reduced AcCoA but not ATP levels (E and I) and reduced cytoplasmic protein acetylation (F and J), while it increased autophagic flux (G, H, K, and L). Hydroxycitrate specifically inhibits ACLY catalytic activity, reducing its phosphorylation on Ser455 (L).

(M–O) Inhibition of ACLY in vivo. Intraperitoneal injection of HC (100 mg/kg) induced a rapid (6 hr) increase in LC3 lipidation and p62 depletion (upper panel in M), in hearts from C57Bl/6 mice, or stimulated the formation of GFP-LC3 puncta in transgenic mice (bottom panels in M, quantified in N). Effects of 1 week of HC treatment (900 mg/kg per day, orally) with standard chow ad libitum on the body weight of *WT* and *Atg4b*$^{-/-}$ mice. Averages ± SD of weight loss are depicted.

(P–S) Effects of the knockdown of cytoplasmic AcCoA synthetase (ACSS2). ACSS2 depletion reduced AcCoA but not ATP levels (P) and reduced cytoplasmic protein acetylation (Q), while it increased autophagic flux (R and S). Scale bar, 10 μm.

All values are shown as means ± SEM of at least three experiments. *$p < 0.05$ (unpaired Student's t test) as compared to the corresponding condition in controls (or UNR siRNA-transfected cells). See also Figure S5.

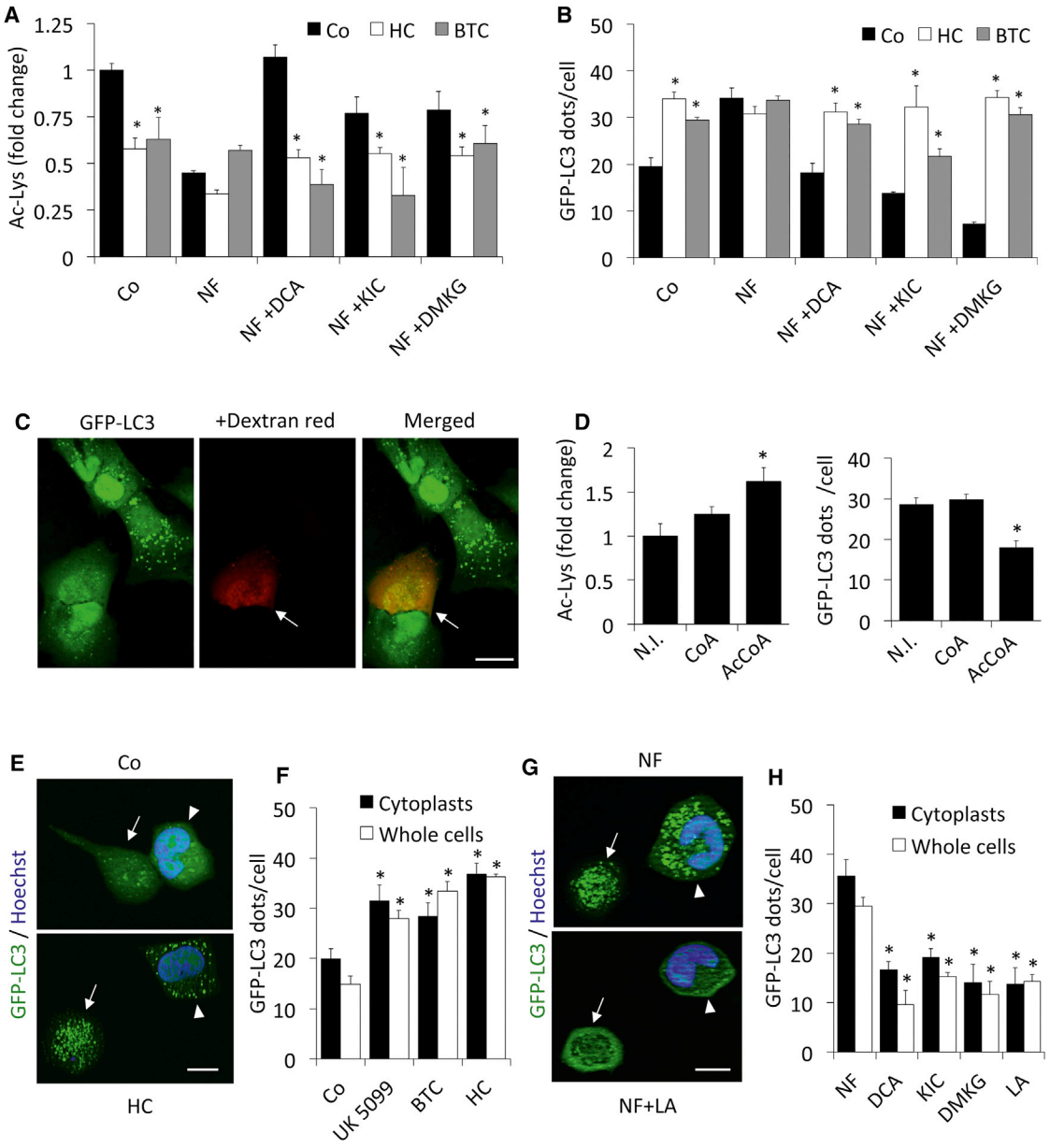

Figure 6. Modulation of Autophagy by Cytosolic AcCoA

(A and B) Inhibition of mitochondria-to-cytoplasm transport of AcCoA reverts autophagic flux inhibition and cytoplasmic protein hyperacetylation elicited by dichloroacetate (DCA), α-ketoisocaproic acid (KIC), or dimethyl α-ketoglutarate (DMKG). Quantification of cytoplasmic protein acetylation and GFP-LC3 puncta (in the presence of BafA1), treated with DCA, KIC, or DMKG in the absence or presence of the tricarboxylate carrier inhibitor benzenetricarboxylate (BTC) or hydroxycitrate (HC) (A and B).

(C and D) Effects of AcCoA microinjection. Representative pictures of AcCoA-injected U2OS cells (C) showing reduced accumulation of GFP-LC3 puncta compared with noninjected (N.I.) cells. Dextran red was added to the AcCoA- or CoA-containing solutions to monitor injection. Scale bar, 10 μm. After injection, cells were incubated in nutrient-free conditions in the presence of 100 nM BafA1 and fixed after 3 hr. (D) Statistical analysis of cytoplasmic protein acetylation and GFP-LC3 puncta. *$p < 0.05$ (unpaired Student's t test) as compared to untreated controls (or CoA-microinjected cells).

(E–H) Effects of enucleation on autophagy. U2OS cells stably expressing GFP-LC3 were enucleated to obtain cytoplasts. Cytoplasts were treated for 5 hr with AcCoA reducing agents in the presence of Baf A1. Shown are representative images of cells and cytoplasts for untreated (Co) and hydroxycitrate (HC)-treated samples (E), as well as quantitative data (F). Representative images (G) of cells and cytoplasts subjected to 5 hr of starvation (NF) or to starvation in the presence of lipoic acid (LA). GFP-LC3 dots per cell or cytoplast in nutrient-free (NF) conditions, alone or with supplementation of the indicated agents (H). Arrows indicate cytoplasts, whereas arrowheads mark nonenucleated cells. Scale bars, 10 μm. All values are shown as means ± SEM of at least three experiments. *$p < 0.05$ (unpaired Student's t test) compared to the corresponding condition in controls (or UNR siRNA-transfected cells). See also Figure S6.

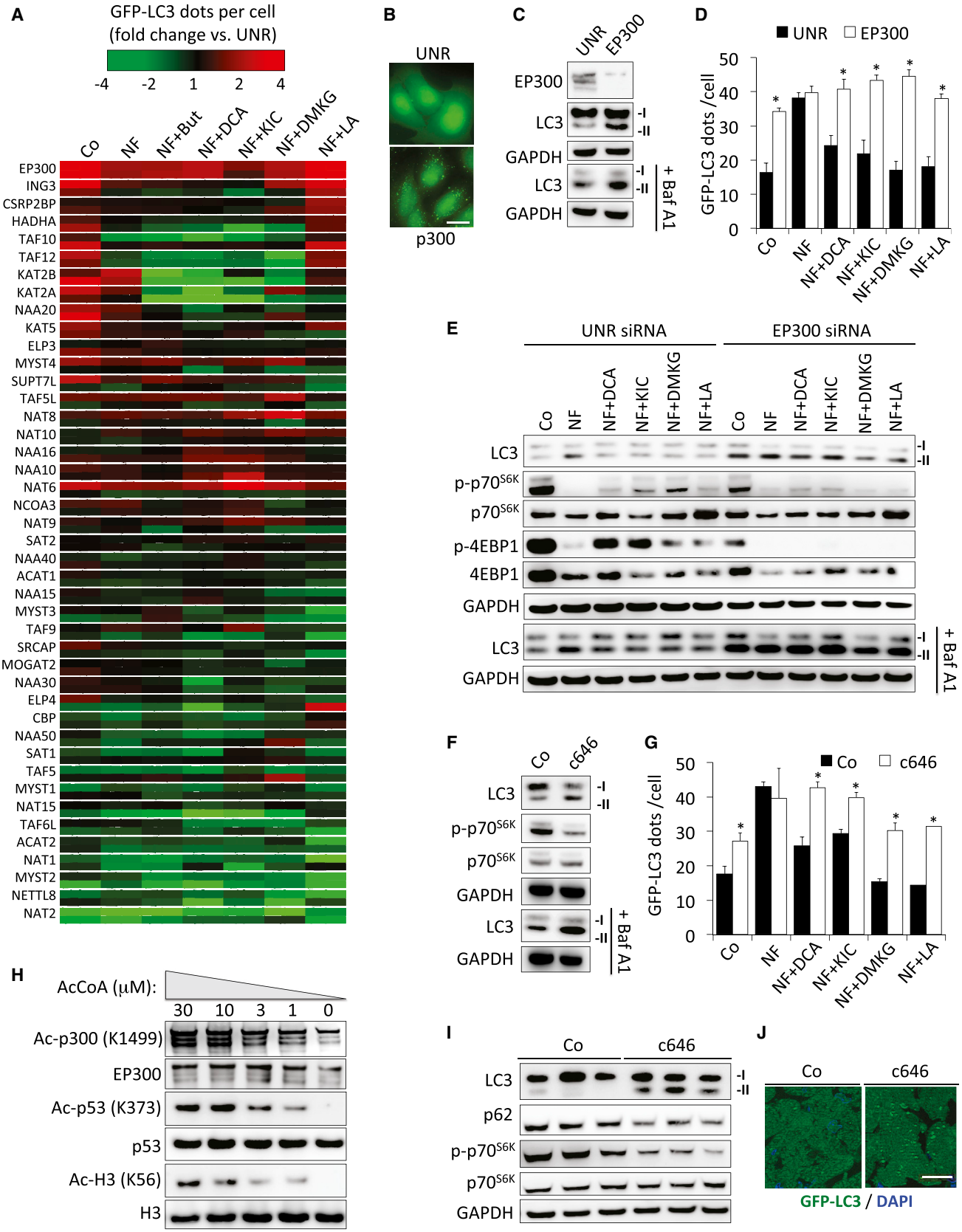

(legend on next page)

DISCUSSION

Here we report that multiple distinct manipulations designed to increase or reduce intracellular AcCoA lead to the suppression or induction of autophagy, respectively, in mice or in cultured human cells. Thus, the inhibition of AcCoA synthesis by interventions on pyruvate, acetate, BCAAs, and fatty acid metabolism induces autophagy, while stimulation of AcCoA synthesis inhibits autophagy induced by multiple distinct stimuli.

At variance with kinases, which operate close to independently from ATP concentrations (due to their high K_d for ATP), acetyltransferases are profoundly influenced in their catalytic activity by the availability of acetyl groups, provided by AcCoA. Thus, subtle differences in AcCoA levels may impact on the level of overall protein acetylation, which reflects the compounded activity of acetyltransferases and deacetylases (Wellen and Thompson, 2012). Accordingly, AcCoA depletion was accompanied by a reduction of the acetylation of most proteins, as indicated by immunofluorescence detection of acetylated proteins or mass spectrometry. This finding is in accord with multiple reports showing that deacetylation favors autophagy. Starvation can induce the sirtuin-1-induced deacetylation of essential autophagy proteins including ATG5, ATG7, ATG12, and LC3 (Lee et al., 2008; Lee and Finkel, 2009); the HDAC6-mediated deacetylation of cortactin (Lee et al., 2010); and the HDAC6-mediated deacetylation and activation of salt-inducible kinase 2 (SIK2), a member of the AMPK family, which is counteracted by the acetyltransferase EP300 (Yang et al., 2013). Moreover, the direct activation of deacetylases and inhibition of acetyltransferases can stimulate the induction of autophagy (Eisenberg et al., 2009; Morselli et al., 2011). Contrasting with this general pattern, the hyperacetylation of some specific proteins has been linked to autophagy induction by starvation. This is exemplified by the proautophagic Esa1p/TIP60-mediated hyperacetylation of Atg3p in yeast (Yi et al., 2012) or the hyperacetylaton of tubulin (Geeraert et al., 2010; Lee et al., 2010) and ULK1 in human cells (Lin et al., 2012a). Accordingly, we found that starvation led to the hyperacetylation of a few proteins, as determined by SILAC technology. Future studies must determine through which mechanisms starvation may stimulate the hyperacetylation of a few exceptional substrates in spite of a context of reduced AcCoA levels.

The depletion of energy-rich metabolites is a strong inducer of autophagy. As an example, an unfavorable shift in the ratio between ATP and AMP causes activation of AMPK, which phosphorylates multiple substrates in the cardinal autophagy regulators, including the ULK1, mTORC1, and Beclin 1 complexes (Kim et al., 2013). Moreover, depletion of NADH causes the activation of sirtuin-1 and other sirtuins with autophagy-stimulatory consequences (Jang et al., 2012). AMPK and sirtuin-1 can cooperate in autophagy induction, forming a cooperative switch for the rapid adaptation of cells to dwindling energy sources (Cantó et al., 2009; Lan et al., 2008). Notwithstanding the importance of ATP/AMPK and NADH/sirtuin-1, our results point to the existence of an additional control instance, cytosolic AcCoA. Indeed, at early time points of starvation, intracellular AcCoA was found to be reduced well before ATP depletion or NADH oxidation became detectable.

It is possible that ATP-, NADH-, and AcCoA-regulated processes are closely interconnected, based on multiple pathways that link energy homeostasis among these molecules, as well as on the fact that AMPK phosphorylates the acetyltransferase EP300 (Yang et al., 2001) and closely cooperates with the deacetylase sirtuin-1 (Kroemer et al., 2010). Moreover, sirtuin-1 deacetylates liver kinase B1 (LKB1), increasing its capacity to phosphorylate and activate AMPK (Lan et al., 2008). In accord with this postulated interconnectivity, artificial depletion or replenishment of AcCoA was accompanied by the activation or inhibition of AMPK, as well as the mirror-like inhibition or activation of mTORC1. MEFs lacking the AMPK subunits PRKAA1 and PRKAA2 still responded to starvation and AcCoA depletion/increase by an increase/reduction in autophagic flux (Figures S6A and S6B), supporting the idea that acetylation-dependent control of autophagy can occur independently from AMPK. In contrast, our data are fully compatible with the possibility that cytosolic AcCoA depletion stimulates autophagy via the repression of mTORC1 activity. Indeed, in all experiments, cytosolic AcCoA levels negatively correlated with the phosphorylation of the mTORC1 substrate $p70^{S6K}$.

Interestingly, inhibition of EP300 acetyltransferase counteracted the autophagy-suppressive action of high AcCoA. In fact, none of the AcCoA-elevating agents used in this study were able to inhibit starvation-induced autophagy in the absence of EP300 expression. Moreover, genetic or pharmacological inhibition of EP300 consistently induced autophagy in several model systems. Notwithstanding the caveat that EP300 inhibition might induce autophagy via toxic side effects, these results,

Figure 7. Identification of EP300 as the Acetyltransferase Responsible for AcCoA-Mediated Autophagy Inhibition

(A) Systematic analysis of acetyltransferases. Results are clustered as fold change values in the number of GFP-LC3 dots (after a 3 hr period incubation with BafA1), obtained by comparing USOS cells transfected with two distinct acetyltransferase-specific siRNAs (both shown) to cells transfected with unrelated control siRNAs, in the indicated cultured conditions. NF refers to nutrient-free.

(B–E) Effects of EP300 depletion on autophagic flux and mTORC1 activity. Autophagy was assessed by GFP-LC3 puncta in the presence of BafA1 (B and D) or by immunoblotting (C and E).

(F and G) Effects of EP300 inhibition by c646 on autophagic flux and mTORC1 activity, as determined by immunoblotting (F) or quantitation of GFP-LC3 dots in the presence of BafA1 (G).

(H) Effects of AcCoA concentrations on the enzymatic activity of recombinant EP300 protein in vitro, in a chemically defined system. The autoacetylation of EP300 and the acetylation of p53 or histone H3 by EP300 were determined by immunobloting with antibodies recognizing Ac-K1499 EP300, Ac-K373 p53, or Ac-K56 Histone3.

(I and J) In vivo induction of autophagy by the EP300 inhibitor c646. After intraperitoneal injection of c646, hearts from WT mice were subjected to immunoblot analyses (I), or hearts from GFP-LC3-transgenic mice were analyzed by fluorescence microscopy (J). Scale bar, 10 μm.

Values are shown as means ± SEM ($n \geq 3$). *$p < 0.05$, Student's t test with respect to cells transfected with unrelated (UNR) siRNAs or cultured with vehicle only (Co) in otherwise identical culture conditions. See also Figure S7.

together with the fact that EP300 activity is regulated by AcCoA levels, suggest that EP300 may function as an AcCoA sensor that translates elevations in intracellular AcCoA into autophagy inhibition. EP300 is known to acetylate ATG proteins, thereby interfering with their proautophagic function (Lee and Finkel, 2009). Although this seems a plausible mechanism by which high AcCoA may inhibit autophagy in an EP300-dependent fashion, additional EP300 targets may be involved in this process. Thus, EP300 inhibition prevented mTORC1 activation upon AcCoA replenishment, suggesting that EP300 inhibition might stimulate autophagy indirectly, via the suppression of mTORC1 activity. The molecular links between EP300 and mTORC1 require further in-depth investigation.

Chronic elevation of AcCoA by excessive caloric intake may suppress autophagy, thereby accelerating the manifestation of age-associated pathologies. On the other hand, dietary and pharmacological manipulations causing a decrease in AcCoA might ameliorate our health by stimulating autophagy. In this context, it appears intriguing that HC, an antiobesity agent (Onakpoya et al., 2011), enhances autophagic flux, which in turn is required for body weight reduction. In contrast, several components used to experimentally stimulate weight gain, such as DMKG or KIC (Campbell et al., 2006; Zanchi et al., 2011), were found to suppress autophagy.

Altogether, the present data unravel a whole range of metabolic and pharmacological manipulations that, by targeting AcCoA, allow for the induction or suppression of autophagy irrespective of the nutritional status.

EXPERIMENTAL PROCEDURES

Chemicals, Cell Lines, and Culture Conditions

Unless otherwise specified, chemicals were purchased from Sigma-Aldrich (St. Louis), culture media and supplements for cell culture from GIBCO-Invitrogen (Carlsbad), and plasticware from Corning (Corning). Human colon carcinoma HCT 116 cells were cultured in McCoy's 5A medium containing 10% fetal bovine serum, 100 mg/L sodium pyruvate, 10 mM HEPES buffer, 100 units/mL penicillin G sodium, and 100 μg/mL streptomycin sulfate (37°C, 5% CO_2). Human osteosarcoma U2OS cells, their GFP-LC3-expressing derivatives, human neuroblastoma H4 GFP-LC3 cells (gift from Professor J. Yuan), and human GFP-LC3-expressing HeLa cells were cultured in DMEM medium containing 10% fetal bovine serum, 100 mg/L sodium pyruvate, 10 mM HEPES buffer, 100 units/mL penicillin G sodium, and 100 μg/mL streptomycin sulfate (37°C, 5% CO_2). MEFs were cultured in the same DMEM with additional supplementation of nonessential amino-acids and β-mercaptoethanol. Cells were seeded in 6-well, 12-well plates or in 10, 15 cm dishes and grown for 24 hr before treatment with 10 μM rapamycin, 100 nM bafilomycin A1 (BafA1), (Tocris Bioscience, Bristol), 5 mM dimethyl α-ketoglutarate, 20 mM HC, 10 mM α-ketoisocaproate, 50 mM L-leucine, 20 mM sodium DCA, 20 mM sodium butyrate, 5 mM 1,2,3-benzenetricarboxylic acid hydrate (BTC), 10 μM PHX maleate salt, 5 mM (±)-α-LA, UK5099, 3 μg/mL puromycin (all from Sigma Aldrich), 100 μM curcumin, 3-methyl-butyrolactone, 50 μM anacardic acid, and 10 μM timosaponin A-III, PI-103, moperamide, amiodarone, nimodipine, nitrendipine, niguldipine, rotenone, rifluoperazine, sorafenib tosylate, niclosamide, rottlerin, caffeine, metformin, clonidine, rilmenidine, 2′,5′-dideoxyadenosine, suramin, pimozide, STF-62247, spermidine, FK-866, tamoxifen citrate, glucosamine, HA 14-1, licochalcone A, vurcumin, Akt Inhibitor X, rockout, 2-deoxyglucose, etoposide, C2-dihydroceramide and temozolomide (all from Enzo Life Sciences, Villeurbanne). For serum and nutrient deprivation, cells were cultured in serum-free Hank's balanced salt solution (HBSS).

The complete set of experimental procedures is available online in the Supplemental Information.

SUPPLEMENTAL INFORMATION

Supplemental Information includes seven figures, five tables, and Supplemental Experimental Procedures and can be found with this article at http://dx.doi.org/10.1016/j.molcel.2014.01.016.

AUTHOR CONTRIBUTIONS

G.M., F.P., S.A.M., Y.K., M.N.-S., N.Z., I.M., L.S., E.M., E.V., M.B., S.S., A.F.F., A.A., C.B., C.M., M.C.M., T.E., T.P., and A.H. performed the experiments. M.S., S.D., D.P.E., M.B., C.M., F.S., and J.S.A. performed mass spectrometry and data analysis. C.L.-O., P.C., J.S.A., O.K., and J.A.H. helped to design the study. G.M., F.M., F.P., P.C., T.E., and G.K. designed the study, analyzed the data, and wrote the paper.

ACKNOWLEDGMENTS

We thank Drs. Paul K. Brindle (St. Jude Hospital), Dr. David Rubinsztein (Cambridge University), Dr. Benoit Viollet (Cochin Institute), Junyin Yuan (Harvard University), and Noboru Mizushima (The University of Tokyo) for transgenic cell lines and mice. This work is supported by grants to G.K. from the Ligue Nationale contre le Cancer (Equipe labellisée), Agence Nationale pour la Recherche (ANR), Association pour la Recherche sur le Cancer, European Research Council (Advanced Investigator Award), Fondation pour la Recherche Médicale (FRM), Institut National du Cancer, Cancéropôle Ile-de-France, Fondation Bettencourt-Schueller, the LabEx Onco-Immunology, and the Paris Alliance of Cancer Research Institutes. M.N.-S. is supported by FRM; S.A.M. by the Higher Education Commission (HEC) of Pakistan; T.E. by an APART fellowship of the Austrian Academy of Sciences; C.L-O. by grants from Ministerio de Economía y Competitividad (MINECO), Instituto de Salud Carlos III (RTICC), and the Botín Foundation; and F.M. by FWF grants LIPOTOX, P23490-B12, and P24381-B20.

Received: July 10, 2013
Revised: November 17, 2013
Accepted: January 17, 2014
Published: February 20, 2014

REFERENCES

Bánréti, A., Sass, M., and Graba, Y. (2013). The emerging role of acetylation in the regulation of autophagy. Autophagy *9*, 819–829.

Behrends, C., Sowa, M.E., Gygi, S.P., and Harper, J.W. (2010). Network organization of the human autophagy system. Nature *466*, 68–76.

Bowers, E.M., Yan, G., Mukherjee, C., Orry, A., Wang, L., Holbert, M.A., Crump, N.T., Hazzalin, C.A., Liszczak, G., Yuan, H., et al. (2010). Virtual ligand screening of the p300/CBP histone acetyltransferase: identification of a selective small molecule inhibitor. Chem. Biol. *17*, 471–482.

Campbell, B., Roberts, M., Kerksick, C., Wilborn, C., Marcello, B., Taylor, L., Nassar, E., Leutholtz, B., Bowden, R., Rasmussen, C., et al. (2006). Pharmacokinetics, safety, and effects on exercise performance of L-arginine alpha-ketoglutarate in trained adult men. Nutrition *22*, 872–881.

Cantó, C., Gerhart-Hines, Z., Feige, J.N., Lagouge, M., Noriega, L., Milne, J.C., Elliott, P.J., Puigserver, P., and Auwerx, J. (2009). AMPK regulates energy expenditure by modulating NAD+ metabolism and SIRT1 activity. Nature *458*, 1056–1060.

Chuang, D. (2013). Branched-chain amino acids. In Encyclopedia of Biological Chemistry, Second Edition, W. Lennarz and M. Lane, eds. (Waltham, MA: Academic Press), pp. 244–249.

Contreras, G.A., Bell, C.S., Del Bianco, G.P., Pérez, N., Kleinosky, M.T., Murphy, J.R., and Heresi, G.P. (2013). Prevalence and risk factors associated with resistance-associated mutations to etravirine in a cohort of perinatally HIV-infected children. J. Antimicrob. Chemother. *68*, 2344–2348.

Donohoe, D.R., Collins, L.B., Wali, A., Bigler, R., Sun, W., and Bultman, S.J. (2012). The Warburg effect dictates the mechanism of butyrate-mediated histone acetylation and cell proliferation. Mol. Cell *48*, 612–626.

Eisenberg, T., Knauer, H., Schauer, A., Büttner, S., Ruckenstuhl, C., Carmona-Gutierrez, D., Ring, J., Schroeder, S., Magnes, C., Antonacci, L., et al. (2009). Induction of autophagy by spermidine promotes longevity. Nat. Cell Biol. *11*, 1305–1314.

Foster, D.W. (2004). The role of the carnitine system in human metabolism. Ann. N Y Acad. Sci. *1033*, 1–16.

Geeraert, C., Ratier, A., Pfisterer, S.G., Perdiz, D., Cantaloube, I., Rouault, A., Pattingre, S., Proikas-Cezanne, T., Codogno, P., and Poüs, C. (2010). Starvation-induced hyperacetylation of tubulin is required for the stimulation of autophagy by nutrient deprivation. J. Biol. Chem. *285*, 24184–24194.

Hebert, A.S., Dittenhafer-Reed, K.E., Yu, W., Bailey, D.J., Selen, E.S., Boersma, M.D., Carson, J.J., Tonelli, M., Balloon, A.J., Higbee, A.J., et al. (2013). Calorie restriction and SIRT3 trigger global reprogramming of the mitochondrial protein acetylome. Mol. Cell *49*, 186–199.

Herzig, S., Raemy, E., Montessuit, S., Veuthey, J.L., Zamboni, N., Westermann, B., Kunji, E.R., and Martinou, J.C. (2012). Identification and functional expression of the mitochondrial pyruvate carrier. Science *337*, 93–96.

Jang, S.Y., Kang, H.T., and Hwang, E.S. (2012). Nicotinamide-induced mitophagy: event mediated by high NAD+/NADH ratio and SIRT1 protein activation. J. Biol. Chem. *287*, 19304–19314.

Kim, J., Kim, Y.C., Fang, C., Russell, R.C., Kim, J.H., Fan, W., Liu, R., Zhong, Q., and Guan, K.L. (2013). Differential regulation of distinct Vps34 complexes by AMPK in nutrient stress and autophagy. Cell *152*, 290–303.

Kroemer, G., Mariño, G., and Levine, B. (2010). Autophagy and the integrated stress response. Mol. Cell *40*, 280–293.

Lan, F., Cacicedo, J.M., Ruderman, N., and Ido, Y. (2008). SIRT1 modulation of the acetylation status, cytosolic localization, and activity of LKB1. Possible role in AMP-activated protein kinase activation. J. Biol. Chem. *283*, 27628–27635.

Lee, I.H., and Finkel, T. (2009). Regulation of autophagy by the p300 acetyltransferase. J. Biol. Chem. *284*, 6322–6328.

Lee, I.H., Cao, L., Mostoslavsky, R., Lombard, D.B., Liu, J., Bruns, N.E., Tsokos, M., Alt, F.W., and Finkel, T. (2008). A role for the NAD-dependent deacetylase Sirt1 in the regulation of autophagy. Proc. Natl. Acad. Sci. USA *105*, 3374–3379.

Lee, J.Y., Koga, H., Kawaguchi, Y., Tang, W., Wong, E., Gao, Y.S., Pandey, U.B., Kaushik, S., Tresse, E., Lu, J., et al. (2010). HDAC6 controls autophagosome maturation essential for ubiquitin-selective quality-control autophagy. EMBO J. *29*, 969–980.

Levine, B., and Kroemer, G. (2008). Autophagy in the pathogenesis of disease. Cell *132*, 27–42.

Lin, S.Y., Li, T.Y., Liu, Q., Zhang, C., Li, X., Chen, Y., Zhang, S.M., Lian, G., Liu, Q., Ruan, K., et al. (2012a). GSK3-TIP60-ULK1 signaling pathway links growth factor deprivation to autophagy. Science *336*, 477–481.

Lin, T.C., Chen, Y.R., Kensicki, E., Li, A.Y., Kong, M., Li, Y., Mohney, R.P., Shen, H.M., Stiles, B., Mizushima, N., et al. (2012b). Autophagy: resetting glutamine-dependent metabolism and oxygen consumption. Autophagy *8*, 1477–1493.

López-Otín, C., Blasco, M.A., Partridge, L., Serrano, M., and Kroemer, G. (2013). The hallmarks of aging. Cell *153*, 1194–1217.

Lowenstein, J.M., and Brunengraber, H. (1981). Hydroxycitrate. Methods Enzymol. *72*, 486–497.

Mariño, G., Fernández, A.F., Cabrera, S., Lundberg, Y.W., Cabanillas, R., Rodríguez, F., Salvador-Montoliu, N., Vega, J.A., Germanà, A., Fueyo, A., et al. (2010). Autophagy is essential for mouse sense of balance. J. Clin. Invest. *120*, 2331–2344.

Masri, S., Patel, V.R., Eckel-Mahan, K.L., Peleg, S., Forne, I., Ladurner, A.G., Baldi, P., Imhof, A., and Sassone-Corsi, P. (2013). Circadian acetylome reveals regulation of mitochondrial metabolic pathways. Proc. Natl. Acad. Sci. USA *110*, 3339–3344.

Mizushima, N., and Komatsu, M. (2011). Autophagy: renovation of cells and tissues. Cell *147*, 728–741.

Mizushima, N., Yamamoto, A., Matsui, M., Yoshimori, T., and Ohsumi, Y. (2004). *In vivo* analysis of autophagy in response to nutrient starvation using transgenic mice expressing a fluorescent autophagosome marker. Mol. Biol. Cell *15*, 1101–1111.

Morselli, E., Mariño, G., Bennetzen, M.V., Eisenberg, T., Megalou, E., Schroeder, S., Cabrera, S., Bénit, P., Rustin, P., Criollo, A., et al. (2011). Spermidine and resveratrol induce autophagy by distinct pathways converging on the acetylproteome. J. Cell Biol. *192*, 615–629.

Nakamura, A., Kawakami, K., Kametani, F., Nakamoto, H., and Goto, S. (2010). Biological significance of protein modifications in aging and calorie restriction. Ann. N Y Acad. Sci. *1197*, 33–39.

Onakpoya, I., Hung, S.K., Perry, R., Wider, B., and Ernst, E. (2011). The use of garcinia extract (hydroxycitric acid) as a weight loss supplement: a systematic review and meta-analysis of randomised clinical trials. J. Obes. *2011*, 509038.

Pietrocola, F., Mariño, G., Lissa, D., Vacchelli, E., Malik, S.A., Niso-Santano, M., Zamzami, N., Galluzzi, L., Maiuri, M.C., and Kroemer, G. (2012). Pro-autophagic polyphenols reduce the acetylation of cytoplasmic proteins. Cell Cycle *11*, 3851–3860.

Roche, T.E., and Hiromasa, Y. (2007). Pyruvate dehydrogenase kinase regulatory mechanisms and inhibition in treating diabetes, heart ischemia, and cancer. Cell. Mol. Life Sci. *64*, 830–849.

Rubinsztein, D.C., Gestwicki, J.E., Murphy, L.O., and Klionsky, D.J. (2007). Potential therapeutic applications of autophagy. Nat. Rev. Drug Discov. *6*, 304–312.

Settembre, C., Di Malta, C., Polito, V.A., Garcia Arencibia, M., Vetrini, F., Erdin, S., Erdin, S.U., Huynh, T., Medina, D., Colella, P., et al. (2011). TFEB links autophagy to lysosomal biogenesis. Science *332*, 1429–1433.

Tasdemir, E., Maiuri, M.C., Galluzzi, L., Vitale, I., Djavaheri-Mergny, M., D'Amelio, M., Criollo, A., Morselli, E., Zhu, C., Harper, F., et al. (2008). Regulation of autophagy by cytoplasmic p53. Nat. Cell Biol. *10*, 676–687.

Thompson, P.R., Wang, D., Wang, L., Fulco, M., Pediconi, N., Zhang, D., An, W., Ge, Q., Roeder, R.G., Wong, J., et al. (2004). Regulation of the p300 HAT domain via a novel activation loop. Nat. Struct. Mol. Biol. *11*, 308–315.

Warr, M.R., Binnewies, M., Flach, J., Reynaud, D., Garg, T., Malhotra, R., Debnath, J., and Passegué, E. (2013). FOXO3A directs a protective autophagy program in haematopoietic stem cells. Nature *494*, 323–327.

Wellen, K.E., and Thompson, C.B. (2012). A two-way street: reciprocal regulation of metabolism and signalling. Nat. Rev. Mol. Cell Biol. *13*, 270–276.

Wellen, K.E., Hatzivassiliou, G., Sachdeva, U.M., Bui, T.V., Cross, J.R., and Thompson, C.B. (2009). ATP-citrate lyase links cellular metabolism to histone acetylation. Science *324*, 1076–1080.

Willenborg, M., Panten, U., and Rustenbeck, I. (2009). Triggering and amplification of insulin secretion by dimethyl alpha-ketoglutarate, a membrane permeable alpha-ketoglutarate analogue. Eur. J. Pharmacol. *607*, 41–46.

Williams, A., Sarkar, S., Cuddon, P., Ttofi, E.K., Saiki, S., Siddiqi, F.H., Jahreiss, L., Fleming, A., Pask, D., Goldsmith, P., et al. (2008). Novel targets for Huntington's disease in an mTOR-independent autophagy pathway. Nat. Chem. Biol. *4*, 295–305.

Yang, W., Hong, Y.H., Shen, X.Q., Frankowski, C., Camp, H.S., and Leff, T. (2001). Regulation of transcription by AMP-activated protein kinase: phosphorylation of p300 blocks its interaction with nuclear receptors. J. Biol. Chem. *276*, 38341–38344.

Yang, F.C., Tan, B.C., Chen, W.H., Lin, Y.H., Huang, J.Y., Chang, H.Y., Sun, H.Y., Hsu, P.H., Liou, G.G., Shen, J., et al. (2013). Reversible acetylation regulates salt-inducible kinase (SIK2) and its function in autophagy. J. Biol. Chem. *288*, 6227–6237.

Yeh, L.A., and Kim, K.H. (1980). Regulation of acetyl-coA carboxylase: properties of coA activation of acetyl-coA carboxylase. Proc. Natl. Acad. Sci. USA *77*, 3351–3355.

Yi, C., Ma, M., Ran, L., Zheng, J., Tong, J., Zhu, J., Ma, C., Sun, Y., Zhang, S., Feng, W., et al. (2012). Function and molecular mechanism of acetylation in autophagy regulation. Science *336*, 474–477.

Zachar, Z., Marecek, J., Maturo, C., Gupta, S., Stuart, S.D., Howell, K., Schauble, A., Lem, J., Piramzadian, A., Karnik, S., et al. (2011). Non-redox-active lipoate derivates disrupt cancer cell mitochondrial metabolism and are potent anticancer agents *in vivo*. J. Mol. Med. *89*, 1137–1148.

Zanchi, N.E., Gerlinger-Romero, F., Guimarães-Ferreira, L., de Siqueira Filho, M.A., Felitti, V., Lira, F.S., Seelaender, M., and Lancha, A.H., Jr. (2011). HMB supplementation: clinical and athletic performance-related effects and mechanisms of action. Amino Acids *40*, 1015–1025.

Zaugg, K., Yao, Y., Reilly, P.T., Kannan, K., Kiarash, R., Mason, J., Huang, P., Sawyer, S.K., Fuerth, B., Faubert, B., et al. (2011). Carnitine palmitoyltransferase 1C promotes cell survival and tumor growth under conditions of metabolic stress. Genes Dev. *25*, 1041–1051.

Zhu, H., Tannous, P., Johnstone, J.L., Kong, Y., Shelton, J.M., Richardson, J.A., Le, V., Levine, B., Rothermel, B.A., and Hill, J.A. (2007). Cardiac autophagy is a maladaptive response to hemodynamic stress. J. Clin. Invest. *117*, 1782–1793.

Cell Cycle
Publication details, including instructions for authors and subscription information:
http://www.tandfonline.com/loi/kccy20

Pro-autophagic polyphenols reduce the acetylation of cytoplasmic proteins

Federico Pietrocola[abc], Guillermo Mariño[abc], Delphine Lissa[abc], Erika Vacchelli[abc], Shoaib Ahmad Malik[abc], Mireia Niso-Santano[abc], Naoufal Zamzami[abc], Lorenzo Galluzzi[cd], Maria Chiara Maiuri[abc] & Guido Kroemer[adefg]

[a] INSERM; U848; Villejuif, France

[b] Université Paris Sud/Paris XI; Le Kremlin-Bicêtre, France

[c] Institut Gustave Roussy; Villejuif, France

[d] Université Paris Descartes/Paris V; Sorbonne Paris Cité; Paris, France

[e] Metabolomics Platform; Institut Gustave Roussy; Villejuif, France

[f] Pôle de Biologie; Hôpital Européen Georges Pompidou; AP-HP; Paris, France

[g] Centre de Recherche des Cordeliers; Paris, France

Published online: 27 Sep 2012.

Cell Cycle 11:20, 3851–3860; October 15, 2012; © 2012 Landes Bioscience

Pro-autophagic polyphenols reduce the acetylation of cytoplasmic proteins

Federico Pietrocola,[1-3] Guillermo Mariño,[1-3] Delphine Lissa,[1-3] Erika Vacchelli,[1-3] Shoaib Ahmad Malik,[1-3] Mireia Niso-Santano,[1-3] Naoufal Zamzami,[1-3] Lorenzo Galluzzi,[3,4] Maria Chiara Maiuri[1-3] and Guido Kroemer[1,4-7,*]

[1]INSERM; U848; Villejuif, France; [2]Université Paris Sud/Paris XI; Le Kremlin-Bicêtre, France; [3]Institut Gustave Roussy; Villejuif, France; [4]Université Paris Descartes/Paris V; Sorbonne Paris Cité; Paris, France; [5]Metabolomics Platform; Institut Gustave Roussy; Villejuif, France; [6]Pôle de Biologie; Hôpital Européen Georges Pompidou; AP-HP; Paris, France; [7]Centre de Recherche des Cordeliers; Paris, France

Keywords: Beclin 1, LC3, longevity, p62/SQSTM1, trichostatin A, U2OS

Resveratrol is a polyphenol contained in red wine that has been amply investigated for its beneficial effects on organismal metabolism, in particular in the context of the so-called "French paradox," i.e., the relatively low incidence of coronary heart disease exhibited by a population with a high dietary intake of cholesterol and saturated fats. At least part of the beneficial effect of resveratrol on human health stems from its capacity to promote autophagy by activating the NAD-dependent deacetylase sirtuin 1. However, the concentration of resveratrol found in red wine is excessively low to account alone for the French paradox. Here, we investigated the possibility that other mono- and polyphenols contained in red wine might induce autophagy while affecting the acetylation levels of cellular proteins. Phenolic compounds found in red wine, including anthocyanins (oenin), stilbenoids (piceatannol), monophenols (caffeic acid, gallic acid) glucosides (delphinidin, kuronamin, peonidin) and flavonoids (catechin, epicatechin, quercetin, myricetin), were all capable of stimulating autophagy, although with dissimilar potencies. Importantly, a robust negative correlation could be established between autophagy induction and the acetylation levels of cytoplasmic proteins, as determined by a novel immunofluorescence staining protocol that allows for the exclusion of nuclear components from the analysis. Inhibition of sirtuin 1 by both pharmacological and genetic means abolished protein deacetylation and autophagy as stimulated by resveratrol, but not by piceatannol, indicating that these compounds act through distinct molecular pathways. In support of this notion, resveratrol and piceatannol synergized in inducing autophagy as well as in promoting cytoplasmic protein deacetylation. Our results highlight a cause-effect relationship between the deacetylation of cytoplasmic proteins and autophagy induction by red wine components.

Introduction

Autophagy is a catabolic pathway leading to the lysosomal degradation of intracellular material, including organelles and portions of the cytoplasm. Baseline levels of autophagy play a prominent homeostatic role and contribute to organismal development.[1] Moreover, the autophagic flow is significantly upregulated as an adaptive response to distinct adverse conditions such as metabolic stress (nutrient deprivation and hypoxia) and infection by intracellular pathogens.[2,3] In line with this notion, autophagic defects underlie a panel of clinically relevant pathologies encompassing heart failure, hereditary myopathies, neurodegenerative diseases, chronic inflammatory states, steatosis/steatohepatitis and cancer.[2,3] Conversely, the pharmacological or genetic stimulation of autophagy increases the capacity of cells to withstand metabolic stress, as it facilitates the maintenance of high ATP levels,[4,5] sustains genomic stability[6] and reduces the abundance of potentially toxic cellular components, such as permeabilized mitochondria as well as protein aggregates that may promote neurodegeneration.[7,8]

Rapamycin, the best characterized pharmacological inducer of autophagy, acts by inhibiting the mammalian target of rapamycin complex 1 (mTORC1)[9] and has been shown to prolong the lifespan of all organisms studied so far, including mice.[10-14] In *Saccharomyces cerevisiae*, *Caenorhabditis elegans* and *Drosophila melanogaster*, the lifespan-extending activity of rapamycin is lost in conditions in which autophagy cannot be induced.[10,15,16] Of note, rapamycin and the so-called rapalogs are the most effective inducers of autophagy currently used in the clinics, yet have severe immunosuppressive effects.[17] Thus, the pharmacological profile of alternative, non-toxic pro-autophagic compounds (such as rilmenidine and carbamazepine) is being characterized in suitable preclinical models of chronic degenerative diseases.[18,19]

Non-toxic compounds such as resveratrol and spermidine are also being evaluated for their potential to induce autophagy in vivo and to improve healthy aging.[20-23] Resveratrol is a natural polyphenol found in grapes, red wine, berries, knotweed, peanuts and other plants. This molecule first attracted interest as it was believed to explain the so-called "French paradox," that is, the

*Correspondence to: Guido Kroemer; Email: kroemer@orange.fr
Submitted: 08/25/12; Revised: 08/30/12; Accepted: 08/30/12
http://dx.doi.org/10.4161/cc.22027

relatively low incidence of coronary heart disease manifested by a population with a high dietary intake of cholesterol and saturated fats.[24,25] However, the concentrations of resveratrol found in red wine are excessively low to entirely account for this phenomenon.[24] Besides operating as an antioxidant, resveratrol is a potent inducer of autophagy,[26] an effect that stems from the activation of the NAD^+-dependent deacetylase sirtuin 1 (SIRT1).[21,27,28] Resveratrol was initially proposed to directly activate SIRT1,[24,25] although less direct mechanisms may actually be preponderant.[29,30] SIRT1 was originally characterized for its activity of histone deacetylase.[31] However, at least two lines of evidence indicate that SIRT1 operates on cytoplasmic, rather than nuclear, substrates to mediate resveratrol-induced autophagy. First, the pro-autophagic activity of resveratrol is fully preserved in enucleated cells (i.e., cytoplasts). Second, a SIRT1 variant that cannot be imported into the nucleus (owing to the deletion of its nuclear localization signal) is as proficient at inducing autophagy as its wild-type counterpart.[21]

Recent proteomic studies revealed that 5–10% of mammalian and bacterial proteins undergo reversible lysine acetylation, a post-translational modification consisting of the addition of an acetyl group to the ε amino group of lysine residues.[32,33] (De)acetylation reactions de facto rival (de)phosphorylation for importance as post-translational mechanisms for the regulation of protein function.[33] Indeed, the (de)acetylation of multiple distinct proteins affects transcriptional programs (in particular when histones and transcription factors are involved) as well as multiple transcription-independent processes, including chromosome separation during mitosis [following the (de)acetylation of cohesin],[34] cytoskeletal dynamics,[35] DNA repair,[36] RNA processing,[37] receptor signaling,[38] metabolic circuitries[39] and cell death.[40,41]

In mammals, (de)acetylation reactions are catalyzed by at least 30 acetyltransferases and approximately 18 deacetylases,[42,43] several of which have been involved in the control of autophagy: SIRT1,[44] SIRT2,[45] histone deacetylase 6 (HDAC6)[46] and p300.[47] However, attempts to identify one or a few critical substrates whose (de)acetylation would entirely account for the regulation of autophagy by these enzymes have failed. For instance, p300 can acetylate several autophagy-relevant proteins, including ATG5, ATG7, ATG12 and LC3B,[47] while SIRT1 can catalyze the deacetylation of ATG5, ATG7, LC3B,[48] as well as of the transcription factor forkhead box O3 (FOXO3), which, in turn, controls the expression of several pro-autophagic proteins.[49] Moreover, resveratrol as well as spermidine (a natural polyamine found in citrus fruits and soybeans) provoke the (de)acetylation of several dozens of autophagy-relevant proteins,[21,50] suggesting that (de)acetylation reactions regulate autophagy by a multipronged effect.

Based on these premises, we wondered whether chemical compounds contained in red wine other than resveratrol might induce autophagy and stimulate protein deacetylation. Driven by the published literature,[51-53] we focused our attention on a series of polyphenols and monophenols found in red wine that are suspected to mediate beneficial effects on health. Here, we report that several of these compounds indeed operate as autophagy inducers, correlating with their capacity to reduce the acetylation of cytoplasmic proteins.

Results and Discussion

Autophagy induction by mono- and polyphenols. For the purpose of this study, we chose a series of natural phenols contained in red wine or other plant products that have been suggested to mediate beneficial effects on human health. These compounds includd one anthocyanin (oenin), one stilbenoid (piceatannol), two monophenols (caffeic acid, gallic acid), three glucosides (delphinidin, kuronamin, peonidin) and four flavonoids (catechin, epicatechin, quercetin, myricetin). As a positive control for autophagy induction, we selected rapamycin, a natural macrolide produced by *Streptomyces hygroscopicus* that potently inhibits mTORC1.[9] Thus, human osteosarcoma U2OS cells stably expressing a GFP-LC3 chimera were exposed for a short time (6 h) to the abovementioned phenols (final concentration = 30 μM) or to 1 μM rapamycin, and then the number of cytoplasmic GFP-$LC3^+$ puncta per cell was assessed by quantitative fluorescence microscopy (**Fig. 1A and B**).[54,55] As an alternative readout, we employed immunoblotting to monitor the lipidation of LC3 (resulting in the generation of a variant with increased electrophorectic mobility, i.e., LC3-II) as well as the degradation of the autophagic substrate p62 (**Fig. 1C**). As recommended by widely accepted guidelines,[54,56] these analyses were performed in the absence as well as in the presence of bafilomycin A1, a selective inhibitor of the vacuolar ATPase that prevents the fusion between autophagosomes and lysosomes, hence blocking the turnover of GFP-$LC3^+$ vesicles (and the degradation of autophagic substrates).[57] Beyond resveratrol, which is a well-established inducer of autophagy,[24] all tested components of red wine provoked the accumulation of cytoplasmic GFP-$LC3^+$ puncta, although to a variable extent (**Fig. 1A and B**). Along similar lines, all phenolic compounds mentioned above were capable of increasing the abundance of LC3-II relative to that of its slowly migrating counterpart LC3-I and of stimulating the degradation of p62, which is indicative of a functional autophagic flux (**Fig. 1C**). In support of this notion, both the accumulation of GFP-$LC3^+$ dots and LC3 lipidation following the administration of phenolic compounds were exacerbated by bafilomycin A1 (**Fig. 1B and C**). Of note, piceatannol, which is structurally very similar to resveratrol (it just contains one additional hydroxyl group on the second benzyl ring), turned out to be as efficient as resveratrol in triggering autophagy. Altogether, these results demonstrate that phenolic compounds contained in red wine other than resveratrol induce bona fide autophagy.

Deacetylation of cytoplasmic proteins in response to mono- and polyphenols. Since the regulation of autophagy by natural compounds including resveratrol and spermidine has been related to the modulation of acetyltransferase and deacetylases,[50] we explored whether the aforementioned phenolic compounds would be able to alter the acetylation of cellular proteins, focusing on the nuclear vs. the cytoplasmic cell compartment. Under standard permeabilization conditions, the immunofluorescence microscopy-based quantification of acetylated lysines virtually

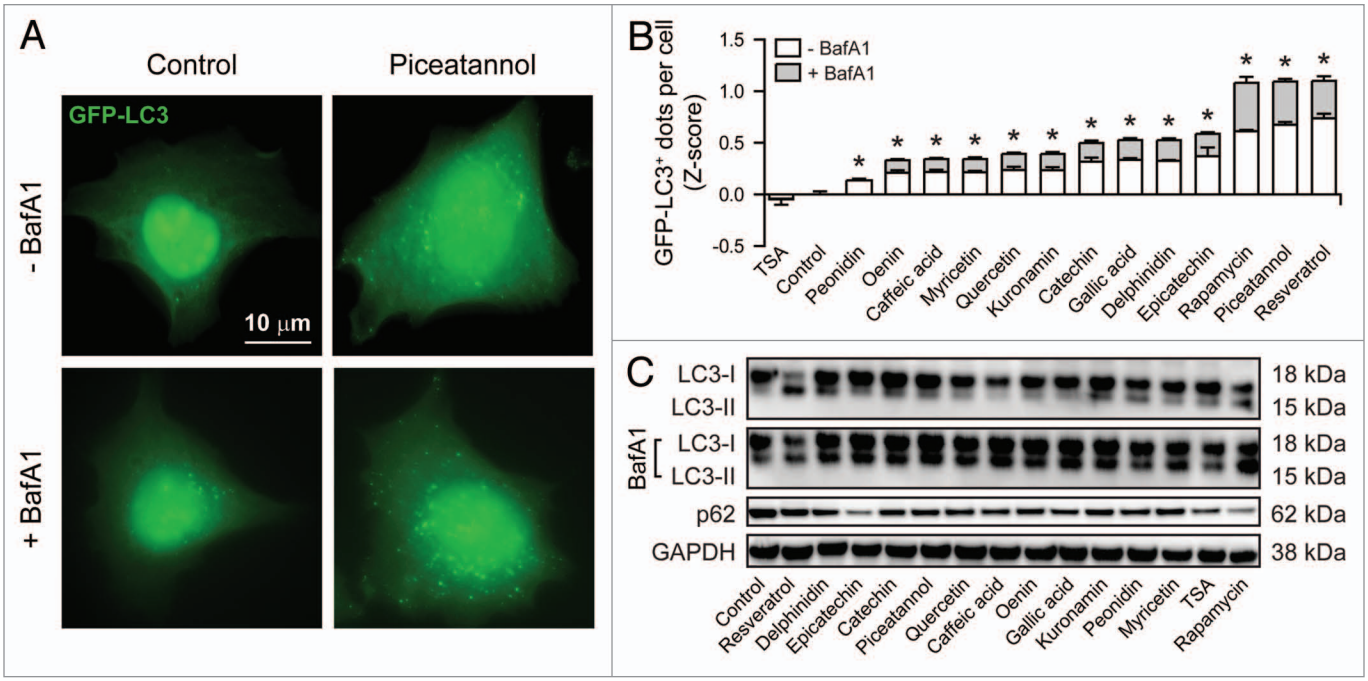

Figure 1. Autophagy induction by mono- and polyphenols. GFP-LC3-expressing human osteosarcoma U2OS cells (A and B) or their wild-type counterparts (C) were either left untreated or treated with 1 μM rapamycin, 10 μM trichostatin A (TSA) or 30 μM of the indicated phenolic compounds, alone or in combination with 50 nM bafilomycin A1 (BafA1) for 6 h. Thereafter, cells were either processed for the immunofluorescence microscopy-assisted quantification of cytoplasmic GFP-LC3$^+$ dots (A and B) or for the immunoblotting-based detection of LC3 lipidation and p62 degradation (C). Representative images are reported in (A) (scale bar = 10 μm) and (C) (GAPDH levels were monitored to ensure equal loading of lanes). In (B), quantitative data are reported. White and light gray columns represent the Z-score of the number of GFP-LC3$^+$ dots detected per cell in the absence and in the presence of BafA1, respectively. Results from one representative experiments are presented as means ± SEM (n = 500 cells/condition). *$p < 0.05$ (unpaired, two-tailed Student's t-test), as compared with untreated cells.

generates results for the nuclear compartment only due to the sky-scraping abundance of (normally hyperacetylated) histones, which de facto covers any cytoplasmic signal. In this setting, trichostatin A, an inhibitor of class I and II histone deacetylases that we employed as positive control, robustly increased the fluorescent signal obtained with a monoclonal antibody specific for acetylated lysines. Conversely, we failed to detect any significant effect of red wine components and rapamycin on the acetylation of nuclear proteins (**Fig. 2A and B**). To further investigate the impact of pro-autophagic phenols on protein acetylation, we developed a protocol in which plasma membranes but not nuclear envelopes get permeabilized, allowing for the selective staining of cytoplasmic components. By this method, we observed that both trichostatin A and rapamycin increase the levels of protein acetylation in the cytoplasm. Conversely, cytoplasmic protein acetylation was reduced by a large array of mono- and polyphenols (**Fig. 3A and B**).

To validate these results by means of alternative techniques, U2OS whole-cell extracts were subjected to immunoblotting procedures based on antibodies specific for acetylated lysine residues (**Fig. 4A**), α tubulin acetylated on lysine 40, as a representative of the cytoplasmic compartment (**Fig. 4B**), and histone 3 (H3) acetylated on lysine 9, as a representative of the nuclear compartment (**Fig. 4C**). Confirming the results obtained by immunofluorescence microscopy, TSA increased the acetylation of all proteins, including α tubulin and H3. Conversely, resveratrol and piceatannol reduced the global levels of protein acetylation, yet affected cytoplasmic (α tubulin), but not nuclear (H3) proteins (**Fig. 4A–F**). Of note, all phenols included in this study were able to reduce the global levels of protein acetylation (**Fig. 4G**).

Correlation between autophagy induction and deacetylation. Based on the observations that mono- and polyphenols contained in red wine induce autophagy and reduce the acetylation of cellular proteins, we determined to which extent these two phenomena would correlate. While there was no statistically significant relationship between the number of GFP-LC3$^+$ puncta and the levels of nuclear protein acetylation resulting from the administration to U2OS cells of the phenolic compounds used in this study (**Fig. 5A**), a highly significant negative correlation between the number of GFP-LC3$^+$ puncta and the levels of cytosolic protein acetylation could be detected (**Fig. 5B**). Thus, on a cell population level, we could measure a decrease in cytoplasmic acetylation in response to resveratrol that was proportional to the accumulation of GFP-LC3$^+$ dots (**Fig. 5B**). Conversely, there was no correlation between the levels of cytoplasmic protein acetylation and autophagy induction at the single-cell level, neither in untreated cells nor in cells receiving resveratrol (**Fig. 5C and D**).[24,25]

Resveratrol is known to induce autophagy by activating sirtuin 1,[24,25] which can be inhibited by the metabolically stable indolic compound EX527.[58,59] Importantly, both the

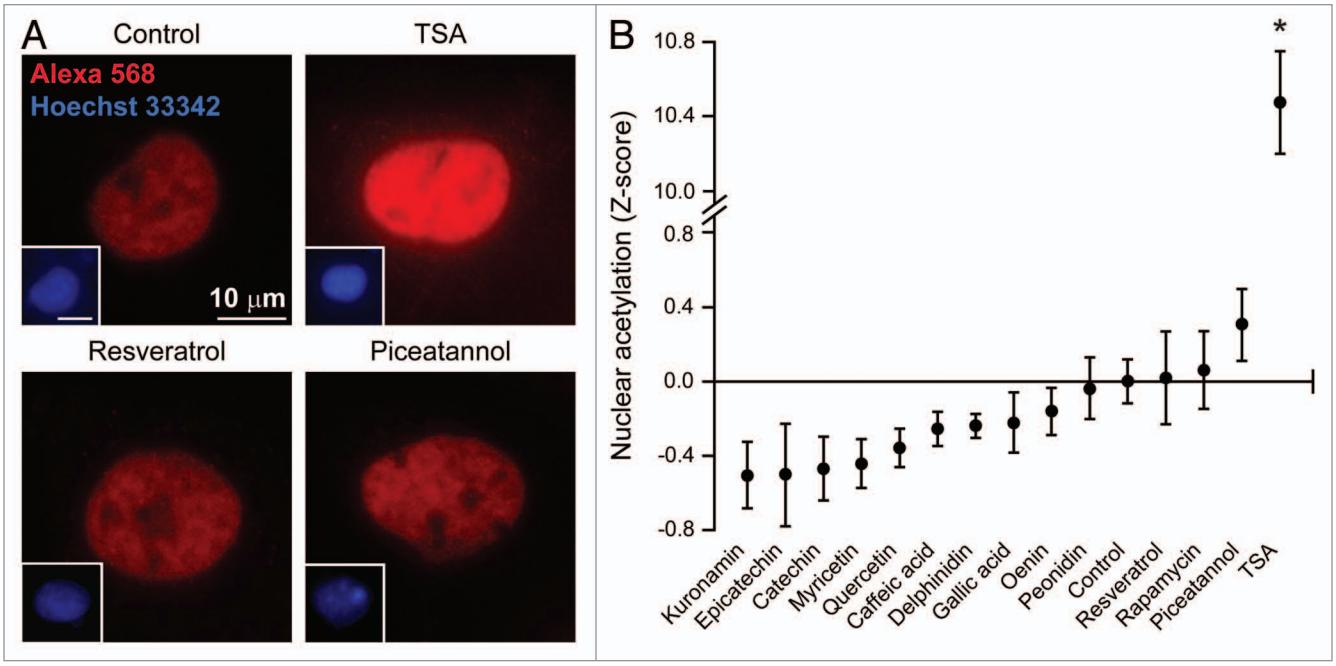

Figure 2. Effect of phenolic compounds on the acetylation of nuclear proteins. Wild-type human osteosarcoma U2OS cells were either left untreated or treated with 1 μM rapamycin, 10 μM trichostatin A (TSA) or 30 μM of the indicated phenolic compounds for 6h, and then processed according to standard procedures for the immunofluorescence-assisted detection of acetylated lysine residues (red signal from the Alexa 568 fluorochrome). This protocol mostly yields a nuclear staining, as confirmed by the counterstaining of chromatin with Hoechst 33342 (blue signal). Representative images are reported in (A) (scale bars = 10 μm) and quantitative data in (B). Results from one representative experiments are presented as Z-score means ± SEM (n = 500 cells/condition). *p < 0.05 (unpaired, two-tailed Student's t-test), as compared with untreated cells.

accumulation of GFP-LC3$^+$ puncta and the deacetylation of cytoplasmic proteins as stimulated in U2OS cells by resveratrol could be inhibited by EX527. Conversely, EX527 failed to affect autophagy induction as well as cytoplasmic deacetylation reactions as stimulated by piceatannol (**Fig. 6A and B**). Results obtained upon the depletion of SIRT1 by means of a previously validated siRNA[60] confirm that, contrary to piceatannol, resveratrol stimulates autophagy and the deacetylation of cytoplasmic proteins by a SIRT1-dependent mechanism (**Fig. 6C and D**). This notion is further strenghtened by the observations that resveratrol and piceatannol combined in growing concentrations were more efficient at inducing the accumulation of GFP-LC3$^+$ puncta as well as the deacetylation of cytoplasmic proteins in U2OS cells than either compound alone (**Fig. 6E and F**). Altogether, our findings suggest a cause-effect relationship between autophagy induction and the deacetylation of cytoplasmic proteins.

Concluding remarks. The results presented in this work point to a strong negative correlation between the capacity of different mono- and polyphenols to trigger autophagy and their potential to cause the deacetylation of cytoplasmic proteins. Spermidine-induced autophagy correlates with its inhibitory effects on histone acetylases and resveratrol-induced autophagy has been linked to its capacity to activate the protein deacetylase sirtuin 1.[25,50] In accord with previous reports,[50] the pharmacological or genetic inhibition of sirtuin 1 reduced both autophagy induction and cytoplasmic protein deacetylation as triggered by resveratrol, hence establishing a bona fide cause-effect relationship between these two phenomena. Surprisingly, a large panel of mono- and polyphenols contained in red wine and many other food preparations that are suggested to have beneficial effects on human health was able to coordinately promote the deacetylation of cytoplasmic proteins and the autophagic flux. These observations are in line with the speculation that chemical compounds that extend the lifespan (or at least the healthy lifespan), including natural polyphenols,[61,62] do so (at least in part) by inducing autophagy.[63] Interestingly, the phenolic compounds found in red wine may induce autophagy through heterogeneous, yet-to-be elucidated mechanisms. Of note, piceatannol, the metabolic product resulting from the oxidation of resveratrol by human cytochrome P450 enzyme CYP1B1,[64] induced autophagy (while promoting the deacetylation of cytoplasmic proteins) through a yet elusive mechanism that appears to be virtually independent from SIRT1. Accordingly, piceatannol (as quercetin) has been reported to bind and activate SIRT1 with a K_M much higher than that of resveratrol.[62] Intriguingly, we found that resveratrol and piceatannol combined in growing concentrations induce autophagy and stimulate the deacetylation of cytoplasmic proteins more efficiently than either compound separately, suggesting that distinct polyphenols may synergize in the activation of autophagy. Whether such a synergistic effect would account for the French paradox remains an open conundrum.[65,66]

In this work, we developed a simple assay to measure the acetylation of cytoplasmic (as opposed to nuclear) proteins. This protocol is based on a relatively mild fixation/permeabilization step (which allows antibodies to access the cytoplasmic, but not

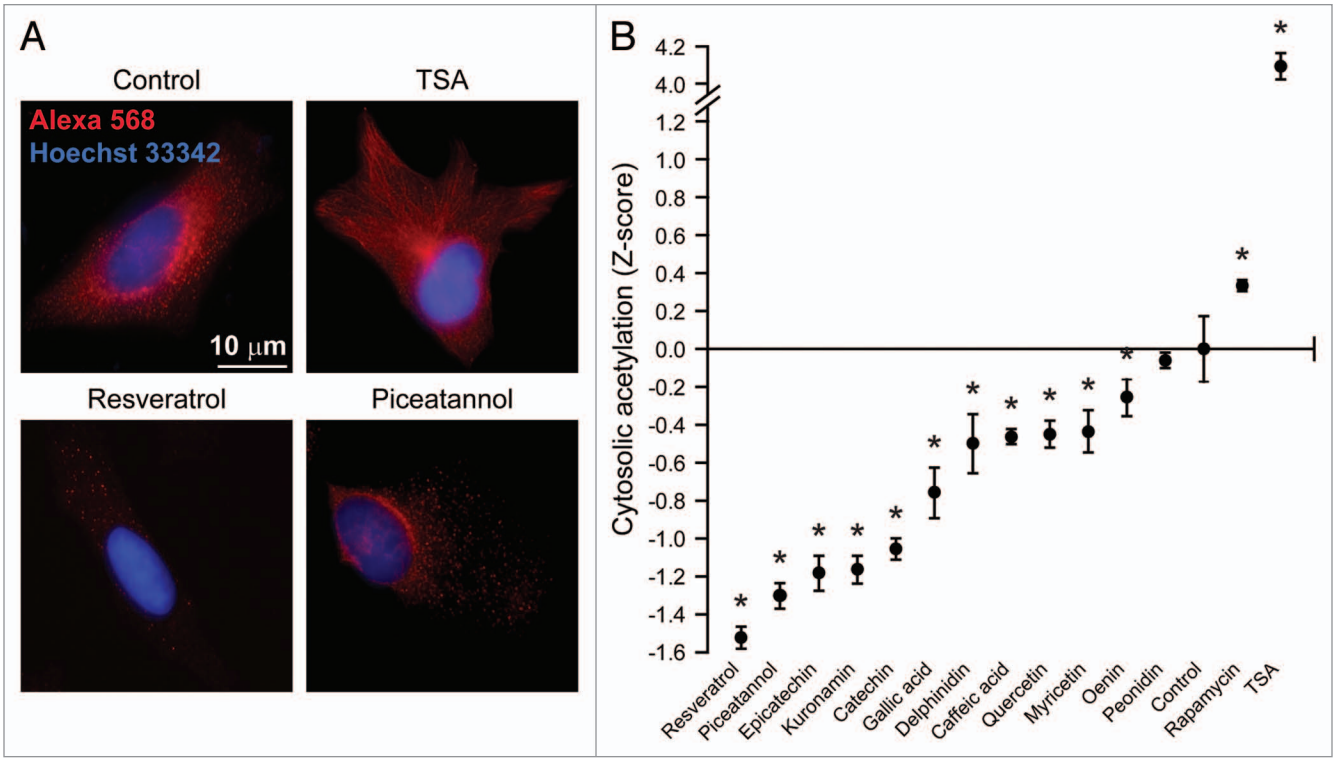

Figure 3. Effect of phenolic compounds on the acetylation of cytoplasmic proteins. Wild-type human osteosarcoma U2OS cells were either left untreated or treated with 1 μM rapamycin, 10 μM trichostatin A (TSA) or 30 μM of the indicated phenolic compounds for 6 h. Thereafter, cells were fixed with paraformaldehyde, but not permeabilized, and immunostained with an antibody that specifically recognizes acetylated lysine residues (red signal from the Alexa 568 fluorochrome). This protocol yields a near-to-completely cytoplasmic staining, as confirmed by the counterstaining of chromatin with Hoechst 33342 (blue signal). Representative images are reported in (A) (scale bars = 10 μm) and quantitative data in (B). Results from one representative experiments are presented as Z-score means ± SEM (n = 500 cells/condition). *p < 0.05 (unpaired, two-tailed Student's t-test), as compared with untreated cells.

the nuclear, compartment) in combination with immunofluorescence microscopy based on an antibody that specifically recognizes proteins containing acetylated lysine residues. When this method is coupled to quantitative imaging (to define cytoplasmic regions of interest and to exclude false-positive nuclei, as resulting, for instance, from mitosis or apoptosis-associated nuclear breakdown),[67-69] it accurately reflects the level of cytoplasmic protein acetylation as measured with other, more laborious techniques. We surmise that this method can be adapted to distinct cell types, including primary leukocytes and epithelial cells, thus offering a cost-effective alternative to measure the metabolic (and pro-autophagic) status of cells. Irrespective of these speculative considerations, our data establish a strong correlation and cause-effect relationship between cytoplasmic deacetylation reactions and autophagy induction.

Materials and Methods

Chemical, cell lines and culture conditions. Resveratrol, piceatannol, epicatechin, caffeic acid, gallic acid, quercetin and bafilomycin A1 were purchased from Sigma-Aldrich; oenin chloride, kuronamin chloride, peonidin-3-O-glucoside chloride and delphinidin-3-O-glucoside chloride from Extrasynthese, rapamycin and EX527 from Tocris Bioscience and myricetin from Indofine Chemical. Culture media and supplements for cell culture were obtained from Gibco-Invitrogen and conventional plasticware from Corning. 96-well black/clear imaging plates were purchased from BD Falcon. Wild-type human osteosarcoma U2OS cells and their GFP-LC3-expressing derivatives were cultured in Dulbecco's modified essential medium (DMEM) supplemented with 10% fetal bovine serum (FBS), 100 mg/L sodium pyruvate, 10 mM HEPES buffer, 100 units/mL penicillin G sodium and 100 μg/mL streptomycin sulfate (37°C, 5% CO_2). Cells were seeded in 6- or 96-well plates and let adapt to the culture substrate for 12–24 h prior to experimental assessments.

RNA interference in human cell cultures. U2OS cells stably expressing GFP-LC3 were grown in 96-well imaging plates until ~50% confluence and then subjected to siRNA transfection by means of the Oligofectamine transfection reagent (Invitrogen), following the manufacturer's recommendations. The following siRNA duplexes were employed, both purchased from Sigma-Aldrich: the SIRT1 targeting siRNA siSIRT1 (sense 5'-ACU UUG CUG UAA CCC UGU A-3')[60] and the irrelevant, non-targeting siRNA siUNR (sense 5'-GCC GGU AUG CCG GUU AAG U-3'),[70,71] employed as a negative control. Cells were subjected to experimental procedures no earlier than 24 h after transfection.

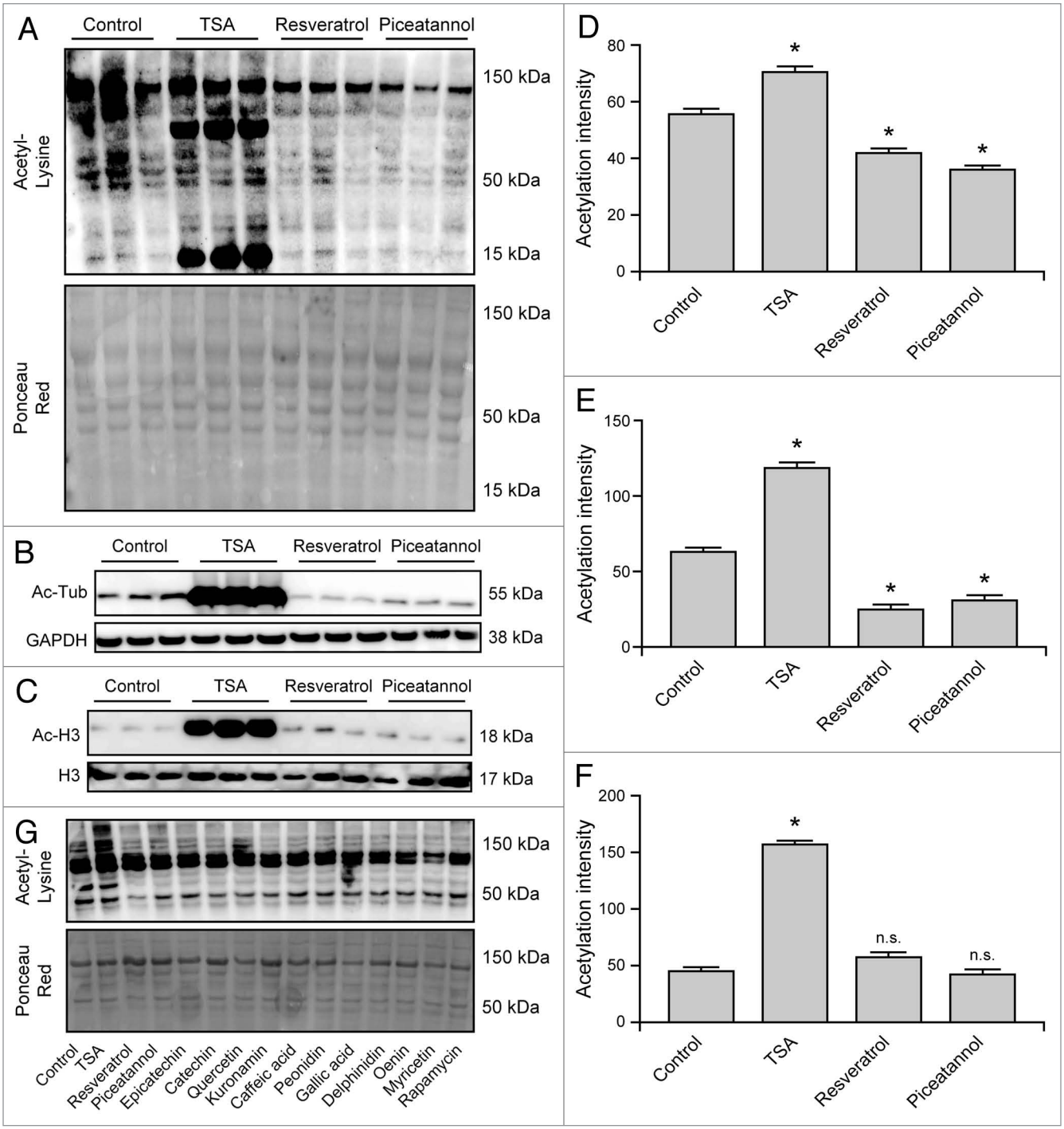

Figure 4. Immunoblotting-assisted detection of protein acetylation in cells responding to mono- and polyphenols. Wild-type human osteosarcoma U2OS cells were either left untreated or treated with 1 μM rapamycin, 10 μM trichostatin A (TSA) or 30 μM of the indicated phenolic compounds, encompassing resveratrol and piceatannol, for 6 h (A–G). Thereafter, cells were subjected to the immunoblotting-assisted quantification of global protein acetylation (A, D and G), α tubulin (Tub) acetylation (as a representative of cytoplasmic proteins) (B and E) and histone 3 (H3) acetylation (as a representative of nuclear proteins) (C and F). Images from one representative experiment are depicted in (A–C and G) (Ponceau Red staining or the levels of GAPDH and H3 were used to monitor equal loading of lanes), while quantitative results are reported in (D–F). Results from n = 3 independent experiments are reported as means ± SEM *$p < 0.05$, n.s. = non-significant (unpaired, two-tailed Student's t-test), as compared with untreated cells.

Immunofluorescence microscopy. In all cases but for the specific detection of acetylated lysines in the cytoplasm, cells were fixed with 4% paraformaldeyde (PFA, w:v in PBS) for 15 min at room temperature and then permeabilized with 0.1% TritonX-100 (v:v in PBS) for 10 min, as previously reported.[72] Conversely, for the cytoplasm-restricted detection of acetylated lysines, fixation in PFA was not followed by any type of permeabilization. In both experimental settings, non-specific

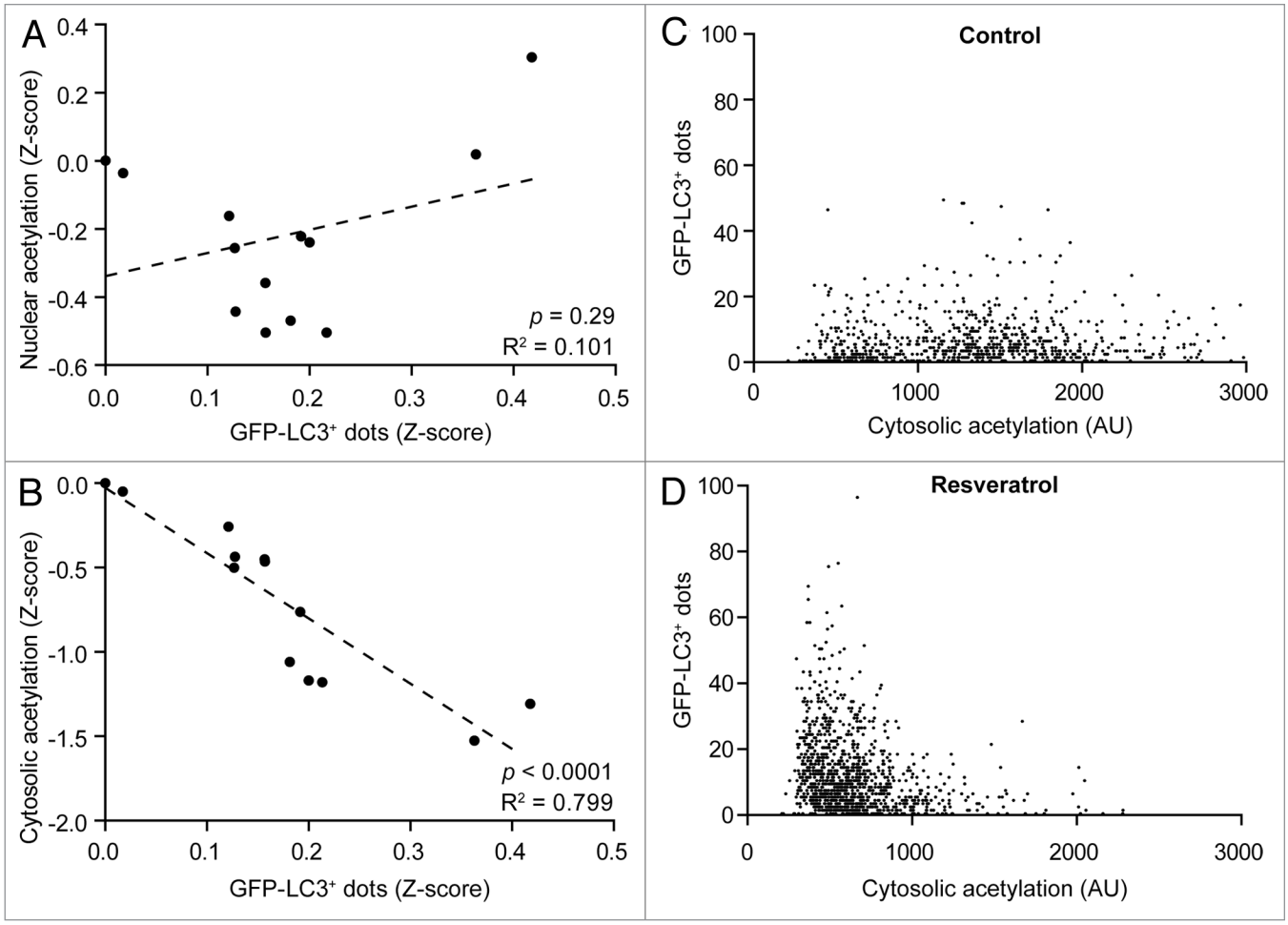

Figure 5. Negative correlation between the acetylation of cytoplasmic proteins and autophagy induction. GFP-LC3-expressing human osteosarcoma U2OS cells were left untreated or treated with 30 μM of the phenolic compounds used in this study, including resveratrol, for 6 h. Thereafter, cells were processed for the immunofluorescence microscopy-assisted quantification of GFP-LC3+ dots and nuclear (A) or cytoplasmic (B–D) protein acetylation levels. In (A and B), population-based results (each dot representing the mean of n = 500 cells) are reported, together with linear regression curves and the corresponding statistical indicators (p values and determination coefficients, R^2). In (C and D), results from one representative experiment are reported (each dot representing a single cell). In this latter scenario, p values and determination coefficients were invariably were > 0.2 and < 0.1, respectively.

binding sites were then blocked with 5% FBS (v:v in PBS), followed by overnight incubation at 4°C with a primary antibody specifically recognizing lysine residues that have been post-translationally modified by acetylation at the ε amino group (Cell Signaling Technology). Revelation was performed with appropriate AlexaFluor™ conjugates (Molecular Probes-Invitrogen). Nuclear counterstaining was obtained with 10 μ Hoechst 33342 (Molecular Probes-Invitrogen). Non-automated fluorescence microscopy assessments were performed on an IRE2 microscope (Leica Microsystems) equipped with a DC300F camera.

Automated immunofluorescence microscopy. Images from plates processed as described above were acquired using a BD pathway 855 automated microscope (BD Imaging Systems) equipped with a 40X objective (Olympus) and coupled to a robotized Twister II plate handler (Caliper Life Sciences). Images were then analyzed either for the presence of GFP-LC3+ (green) puncta in the cytoplasm or for the intensity of protein acetylation (red) in the cytoplasm and the nucleus by means of the BD Attovision software (BD Imaging Systems). To this aim, the surface of each cell was segmented and subdivided into a cytoplasmic and a nuclear region according to manufacturer's standard proceedings. The RB 2x2 and Marr-Hildreth algorithms were used to recognize cytoplasmic GFP-LC3+ dots.

Immunoblotting. Approximately 5×10^5 cells were washed with cold PBS and lysed following standard procedures.[73,74] Thereafter, 25 μg of proteins were separated according to molecular weight on NuPAGE Novex Bis-Tris 4–12% pre-cast gels (Invitrogen) and electrotransferred to Immobilon™ PVDF membranes (Bio-Rad). Non-specific binding sites were blocked with 5% non-fat powdered milk (w:v) plus 0.05% Tween 20 (v:v) in TBS for 1 h, followed by overnight incubation at 4°C with the following primary antibodies: anti-Acetylated-Lysine (Cell Signaling Technology), anti-Acetylated-Histone 3 (Lys9, Cell Signaling Technology), anti-Acetylated-Tubulin (Lys40, Cell Signaling Technology), anti-LC3B (Cell Signaling Technology) and anti-p62 (Abnova). Revelation was performed with appropriate

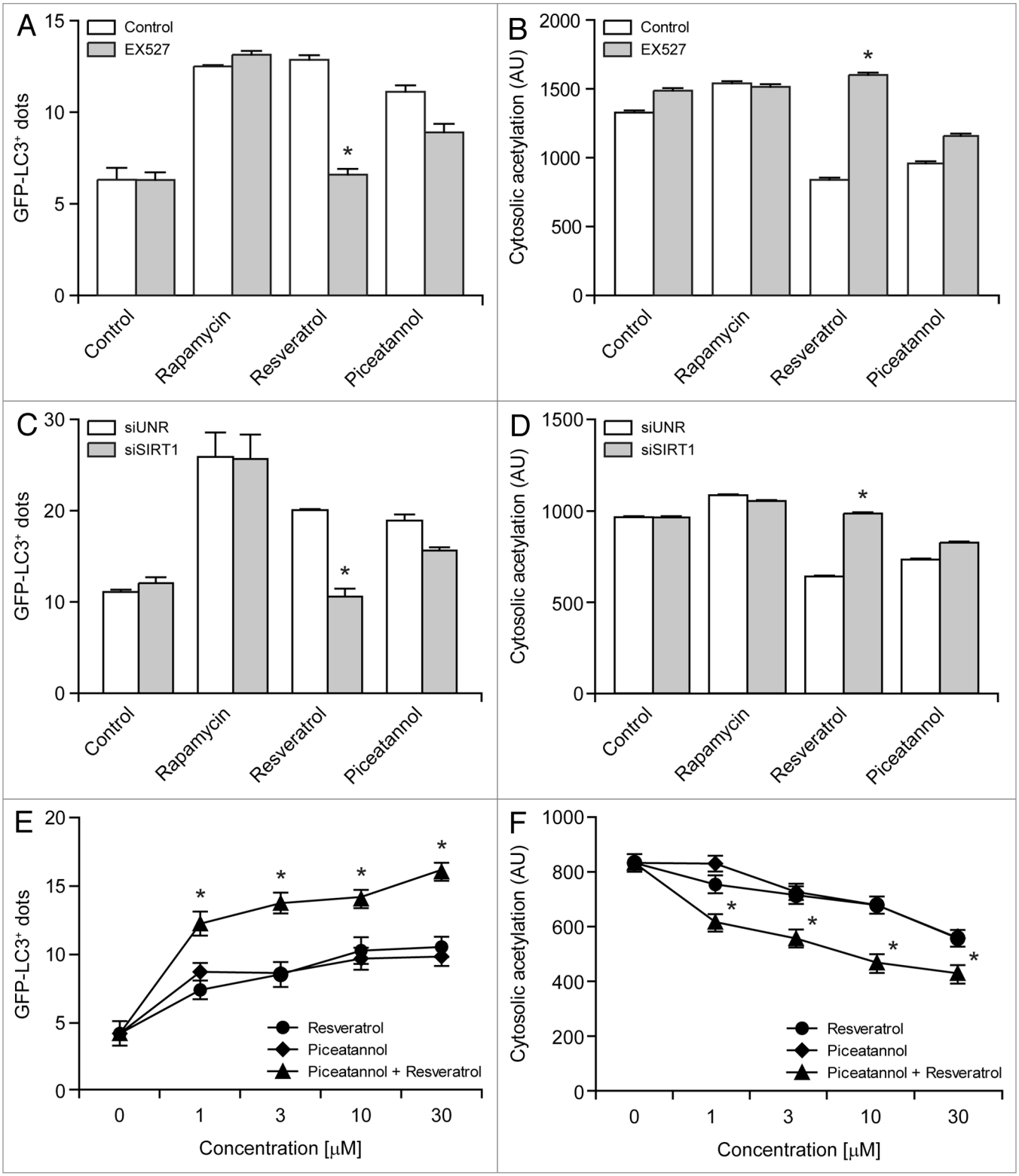

Figure 6. For figure legend, see page 3859.

horseradish peroxidase (HRP)-labeled secondary antibodies (Southern Biotech) coupled with the SuperSignal West Pico chemoluminiscent substrate (Thermo Scientific-Pierce). Ponceau Red staining or antibodies recognizing glyceraldehyde-3-phosphate dehydrogenase (GAPDH) (Chemicon International) or histone 3 (Cell Signaling Technology) were used to monitor equal loading of lanes. Densitometry was performed by means of the open-source software ImageJ (freely available at http://rsbweb.

Figure 6 (See opposite page). Resveratrol and piceatannol operate via distinct mechanisms and synergize in the induction of autophagy. (A–D) Differential effects of sirtuin 1 (SIRT1) inhibition on resveratrol- and piceatannol-induced autophagy. GFP-LC3-expressing human osteosarcoma U2OS cells were left untreated or treated with 1 μM rapamycin, 30 μM resveratrol and 30 μM piceatannol, alone or in combination with 10 μM EX527 for 6 h (A and B). Alternatively, GFP-LC3-expressing U2OS cells were transfected with a control siRNA (siUNR) or with a SIRT1-targeting siRNA (siSIRT1) for 24 h, and then left untreated or treated with 30 μM resveratrol or 30 μM piceatannol for additional 6 h (C and D). Finally, cells were processed for the immunofluorescence microscopy-assisted quantification of GFP-LC3$^+$ dots (A and C) or cytoplasmic protein acetylation (B and D). Results from n = 3 independent experiments are reported as means ± SEM *p < 0.05 (unpaired, two-tailed Student's t-test), as compared with cells treated with the same phenolic compound alone in control conditions (no EX527 or siUNR transfection). (E and F) Synergistic effects of resveratrol and piceatannol on the induction of autophagy and on the deacetylation of cytoplasmic proteins. U2OS cells were incubated with resveratrol and piceatannol, alone or in combination (the total concentration of polyphenols is indicated), for 6 h, followed by the immunofluorescence microscopy-assisted quantification of GFP-LC3$^+$ dots (E) or cytoplasmic protein acetylation (F). Results from n = 3 independent experiments are reported as means ± SEM *p < 0.05 (unpaired, two-tailed Student's t-test), as compared with cells receiving the same concentration of either compound alone.

nih.gov/ij/download.html). To this aim, the intensity of the band of interest was normalized to that of loading controls.

Statistical analysis. Unless otherwise specified, experiments invariably entailed triplicate parallel assessments and were repeated at least twice. Data were analyzed using the Prism 5 software (GraphPad Software) and statistical significance was assessed by means of unpaired, two-tailed Student's t-tests. The correlation between data sets was evaluated by means of determination coefficients (R^2). p values < 0.05 were considered statistically significant.

Disclosure of Potential Conflicts of Interest

No potential conflicts of interest were disclosed.

Acknowledgments

G.K. is supported by the Ligue Nationale contre le Cancer (LNC, Equipe labelisée), Agence Nationale pour la Recherche (ANR), European Commission (Active p53, Apo-Sys, ChemoRes, ApopTrain), Fondation pour la Recherche Médicale (FRM), Institut National du Cancer (INCa), Cancéropôle Ile-de-France, Fondation Bettencourt-Schueller and the LabEx Immuno-Oncology. G.M. and M.N.S. are supported by an EMBO fellowship and a postdoctoral contract from the Junta de Extremadura, respectively. S.A.K. is the recipient of a grant from the Higher Education Commission (HEC) of Pakistan. L.G. is financed by the LabEx Immuno-Oncology.

References

1. Mizushima N, Levine B. Autophagy in mammalian development and differentiation. Nat Cell Biol 2010; 12:823-30; PMID:20811354; http://dx.doi.org/10.1038/ncb0910-823.
2. Levine B, Kroemer G. Autophagy in the pathogenesis of disease. Cell 2008; 132:27-42; PMID:18191218; http://dx.doi.org/10.1016/j.cell.2007.12.018.
3. Mizushima N, Levine B, Cuervo AM, Klionsky DJ. Autophagy fights disease through cellular self-digestion. Nature 2008; 451:1069-75; PMID:18305538; http://dx.doi.org/10.1038/nature06639.
4. Karantza-Wadsworth V, Patel S, Kravchuk O, Chen G, Mathew R, Jin S, et al. Autophagy mitigates metabolic stress and genome damage in mammary tumorigenesis. Genes Dev 2007; 21:1621-35; PMID:17606641; http://dx.doi.org/10.1101/gad.1565707.
5. Tasdemir E, Maiuri MC, Galluzzi L, Vitale I, Djavaheri-Mergny M, D'Amelio M, et al. Regulation of autophagy by cytoplasmic p53. Nat Cell Biol 2008; 10:676-87; PMID:18454141; http://dx.doi.org/10.1038/ncb1730.
6. Mathew R, Kongara S, Beaudoin B, Karp CM, Bray K, Degenhardt K, et al. Autophagy suppresses tumor progression by limiting chromosomal instability. Genes Dev 2007; 21:1367-81; PMID:17510285; http://dx.doi.org/10.1101/gad.1545107.
7. Green DR, Galluzzi L, Kroemer G. Mitochondria and the autophagy-inflammation-cell death axis in organismal aging. Science 2011; 333:1109-12; PMID:21868666; http://dx.doi.org/10.1126/science.1201940.
8. Madeo F, Eisenberg T, Kroemer G. Autophagy for the avoidance of neurodegeneration. Genes Dev 2009; 23:2253-9; PMID:19797764; http://dx.doi.org/10.1101/gad.1858009.
9. Yip CK, Murata K, Walz T, Sabatini DM, Kang SA. Structure of the human mTOR complex I and its implications for rapamycin inhibition. Mol Cell 2010; 38:768-74; PMID:20542007; http://dx.doi.org/10.1016/j.molcel.2010.05.017.
10. Bjedov I, Toivonen JM, Kerr F, Slack C, Jacobson J, Foley A, et al. Mechanisms of life span extension by rapamycin in the fruit fly Drosophila melanogaster. Cell Metab 2010; 11:35-46; PMID:20074526; http://dx.doi.org/10.1016/j.cmet.2009.11.010.
11. Blagosklonny MV. Rapamycin and quasi-programmed aging: four years later. Cell Cycle 2010; 9:1859-62; PMID:20436272; http://dx.doi.org/10.4161/cc.9.10.11872.
12. Harrison DE, Strong R, Sharp ZD, Nelson JF, Astle CM, Flurkey K, et al. Rapamycin fed late in life extends lifespan in genetically heterogeneous mice. Nature 2009; 460:392-5; PMID:19587680.
13. Kapahi P, Zid BM, Harper T, Koslover D, Sapin V, Benzer S. Regulation of lifespan in Drosophila by modulation of genes in the TOR signaling pathway. Curr Biol 2004; 14:885-90; PMID:15186745; http://dx.doi.org/10.1016/j.cub.2004.03.059.
14. Anisimov VN, Zabezhinski MA, Popovich IG, Piskunova TS, Semenchenko AV, Tyndyk ML, et al. Rapamycin increases lifespan and inhibits spontaneous tumorigenesis in inbred female mice. Cell Cycle 2011; 10:4230-6; PMID:22107964; http://dx.doi.org/10.4161/cc.10.24.18486.
15. Alvers AL, Wood MS, Hu D, Kaywell AC, Dunn WA Jr., Aris JP. Autophagy is required for extension of yeast chronological life span by rapamycin. Autophagy 2009; 5:847-9; PMID:19458476.
16. Jia K, Levine B. Autophagy is required for dietary restriction-mediated life span extension in C. elegans. Autophagy 2007; 3:597-9; PMID:17912023.
17. Hartford CM, Ratain MJ. Rapamycin: something old, something new, sometimes borrowed and now renewed. Clin Pharmacol Ther 2007; 82:381-8; PMID:17728765; http://dx.doi.org/10.1038/sj.clpt.6100317.
18. Hidvegi T, Ewing M, Hale P, Dippold C, Beckett C, Kemp C, et al. An autophagy-enhancing drug promotes degradation of mutant alpha1-antitrypsin Z and reduces hepatic fibrosis. Science 2010; 329:229-32; PMID:20522742; http://dx.doi.org/10.1126/science.1190354.
19. Rose C, Menzies FM, Renna M, Acevedo-Arozena A, Corrochano S, Sadiq O, et al. Rilmenidine attenuates toxicity of polyglutamine expansions in a mouse model of Huntington's disease. Hum Mol Genet 2010; 19:2144-53; PMID:20190273; http://dx.doi.org/10.1093/hmg/ddq093.
20. Eisenberg T, Knauer H, Schauer A, Büttner S, Ruckenstuhl C, Carmona-Gutierrez D, et al. Induction of autophagy by spermidine promotes longevity. Nat Cell Biol 2009; 11:1305-14; PMID:19801973; http://dx.doi.org/10.1038/ncb1975.
21. Morselli E, Maiuri MC, Markaki M, Megalou E, Pasparaki A, Palikaras K, et al. Caloric restriction and resveratrol promote longevity through the Sirtuin-1-dependent induction of autophagy. Cell Death Dis 2010; 1:e10; PMID:21364612; http://dx.doi.org/10.1038/cddis.2009.8.
22. Knab B, Osiewacz HD. Methylation of polyphenols with vicinal hydroxyl groups: A protection pathway increasing organismal lifespan. Cell Cycle 2010; 9:3387-8; PMID:20703087; http://dx.doi.org/10.4161/cc.9.17.13016.
23. Lu JY, Lin YY, Zhu H, Chuang LM, Boeke JD. Protein acetylation and aging. Aging (Albany NY) 2011; 3:911-2; PMID:22067362.
24. Baur JA, Pearson KJ, Price NL, Jamieson HA, Lerin C, Kalra A, et al. Resveratrol improves health and survival of mice on a high-calorie diet. Nature 2006; 444:337-42; PMID:17086191; http://dx.doi.org/10.1038/nature05354.
25. Lagouge M, Argmann C, Gerhart-Hines Z, Meziane H, Lerin C, Daussin F, et al. Resveratrol improves mitochondrial function and protects against metabolic disease by activating SIRT1 and PGC-1alpha. Cell 2006; 127:1109-22; PMID:17112576; http://dx.doi.org/10.1016/j.cell.2006.11.013.
26. Scarlatti F, Maffei R, Beau I, Codogno P, Ghidoni R. Role of non-canonical Beclin 1-independent autophagy in cell death induced by resveratrol in human breast cancer cells. Cell Death Differ 2008; 15:1318-29; PMID:18421301; http://dx.doi.org/10.1038/cdd.2008.51.

27. Morselli E, Galluzzi L, Kepp O, Criollo A, Maiuri MC, Tavernarakis N, et al. Autophagy mediates pharmacological lifespan extension by spermidine and resveratrol. Aging (Albany NY) 2009; 1:961-70; PMID:20157579.
28. Stein S, Matter CM. Protective roles of SIRT1 in atherosclerosis. Cell Cycle 2011; 10:640-7; PMID:21293192; http://dx.doi.org/10.4161/cc.10.4.14863.
29. Pacholec M, Bleasdale JE, Chrunyk B, Cunningham D, Flynn D, Garofalo RS, et al. SRT1720, SRT2183, SRT1460, and resveratrol are not direct activators of SIRT1. J Biol Chem 2010; 285:8340-51; PMID:20061378; http://dx.doi.org/10.1074/jbc.M109.088682.
30. Vetterli L, Maechler P. Resveratrol-activated SIRT1 in liver and pancreatic β-cells: a Janus head looking to the same direction of metabolic homeostasis. Aging (Albany NY) 2011; 3:444-9; PMID:21483037.
31. Houtkooper RH, Pirinen E, Auwerx J. Sirtuins as regulators of metabolism and healthspan. Nat Rev Mol Cell Biol 2012; 13:225-38; PMID:22395773.
32. Kim GW, Yang XJ. Comprehensive lysine acetylomes emerging from bacteria to humans. Trends Biochem Sci 2011; 36:211-20; PMID:21075636; http://dx.doi.org/10.1016/j.tibs.2010.10.001.
33. Zhao S, Xu W, Jiang W, Yu W, Lin Y, Zhang T, et al. Regulation of cellular metabolism by protein lysine acetylation. Science 2010; 327:1000-4; PMID:20167786; http://dx.doi.org/10.1126/science.1179689.
34. Rolef Ben-Shahar T, Heeger S, Lehane C, East P, Flynn H, Skehel M, et al. Eco1-dependent cohesin acetylation during establishment of sister chromatid cohesion. Science 2008; 321:563-6; PMID:18653893; http://dx.doi.org/10.1126/science.1157774.
35. Perdiz D, Mackeh R, Poüs C, Baillet A. The ins and outs of tubulin acetylation: more than just a post-translational modification? Cell Signal 2011; 23:763-71; PMID:20940043; http://dx.doi.org/10.1016/j.cellsig.2010.10.014.
36. Kaidi A, Weinert BT, Choudhary C, Jackson SP. Human SIRT6 promotes DNA end resection through CtIP deacetylation. Science 2010; 329:1348-53; PMID:20829486; http://dx.doi.org/10.1126/science.1192049.
37. Muth V, Nadaud S, Grummt I, Voit R. Acetylation of TAF(I)68, a subunit of TIF-IB/SL1, activates RNA polymerase I transcription. EMBO J 2001; 20:1353-62; PMID:11250901; http://dx.doi.org/10.1093/emboj/20.6.1353.
38. Tang X, Gao JS, Guan YJ, McLane KE, Yuan ZL, Ramratnam B, et al. Acetylation-dependent signal transduction for type I interferon receptor. Cell 2007; 131:93-105; PMID:17923090; http://dx.doi.org/10.1016/j.cell.2007.07.034.
39. Wang Q, Zhang Y, Yang C, Xiong H, Lin Y, Yao J, et al. Acetylation of metabolic enzymes coordinates carbon source utilization and metabolic flux. Science 2010; 327:1004-7; PMID:20167787; http://dx.doi.org/10.1126/science.1179687.
40. Galluzzi L, Vitale I, Abrams JM, Alnemri ES, Baehrecke EH, Blagosklonny MV, et al. Molecular definitions of cell death subroutines: recommendations of the Nomenclature Committee on Cell Death 2012. Cell Death Differ 2012; 19:107-20; PMID:21760595; http://dx.doi.org/10.1038/cdd.2011.96.
41. Shulga N, Wilson-Smith R, Pastorino JG. Sirtuin-3 deacetylation of cyclophilin D induces dissociation of hexokinase II from the mitochondria. J Cell Sci 2010; 123:894-902; PMID:20159966; http://dx.doi.org/10.1242/jcs.061846.
42. Guan KL, Xiong Y. Regulation of intermediary metabolism by protein acetylation. Trends Biochem Sci 2011; 36:108-16; PMID:20934340; http://dx.doi.org/10.1016/j.tibs.2010.09.003.
43. Hirschey MD, Shimazu T, Capra JA, Pollard KS, Verdin E. SIRT1 and SIRT3 deacetylate homologous substrates: AceCS1,2 and HMGCS1,2. Aging (Albany NY) 2011; 3:635-42; PMID:21701047.
44. Salminen A, Kaarniranta K. SIRT1: regulation of longevity via autophagy. Cell Signal 2009; 21:1356-60; PMID:19249351; http://dx.doi.org/10.1016/j.cellsig.2009.02.014.
45. Zhao Y, Yang J, Liao W, Liu X, Zhang H, Wang S, et al. Cytosolic FoxO1 is essential for the induction of autophagy and tumour suppressor activity. Nat Cell Biol 2010; 12:665-75; PMID:20543840; http://dx.doi.org/10.1038/ncb2069.
46. Lee JY, Koga H, Kawaguchi Y, Tang W, Wong E, Gao YS, et al. HDAC6 controls autophagosome maturation essential for ubiquitin-selective quality-control autophagy. EMBO J 2010; 29:969-80; PMID:20075865; http://dx.doi.org/10.1038/emboj.2009.405.
47. Lee IH, Finkel T. Regulation of autophagy by the p300 acetyltransferase. J Biol Chem 2009; 284:6322-8; PMID:19124466; http://dx.doi.org/10.1074/jbc.M807135200.
48. Lee IH, Cao L, Mostoslavsky R, Lombard DB, Liu J, Bruns NE, et al. A role for the NAD-dependent deacetylase Sirt1 in the regulation of autophagy. Proc Natl Acad Sci USA 2008; 105:3374-9; PMID:18296641; http://dx.doi.org/10.1073/pnas.0712145105.
49. Kume S, Uzu T, Horiike K, Chin-Kanasaki M, Isshiki K, Araki S, et al. Calorie restriction enhances cell adaptation to hypoxia through Sirt1-dependent mitochondrial autophagy in mouse aged kidney. J Clin Invest 2010; 120:1043-55; PMID:20335657; http://dx.doi.org/10.1172/JCI41376.
50. Morselli E, Mariño G, Bennetzen MV, Eisenberg T, Megalou E, Schroeder S, et al. Spermidine and resveratrol induce autophagy by distinct pathways converging on the acetylproteome. J Cell Biol 2011; 192:615-29; PMID:21339330; http://dx.doi.org/10.1083/jcb.201008167.
51. Aires DJ, Rockwell G, Wang T, Frontera J, Wick J, Wang W, et al. Potentiation of dietary restriction-induced lifespan extension by polyphenols. Biochim Biophys Acta 2012; 1822:522-6; PMID:22265987; http://dx.doi.org/10.1016/j.bbadis.2012.01.005.
52. Burke MF, Khera AV, Rader DJ. Polyphenols and cholesterol efflux: is coffee the next red wine? Circ Res 2010; 106:627-9; PMID:20203311; http://dx.doi.org/10.1161/CIRCRESAHA.109.215855.
53. Pallauf K, Rimbach G. Autophagy, polyphenols and healthy ageing. Ageing Res Rev 2012; PMID:22504405; http://dx.doi.org/10.1016/j.arr.2012.03.008.
54. Klionsky DJ, Abeliovich H, Agostinis P, Agrawal DK, Aliev G, Askew DS, et al. Guidelines for the use and interpretation of assays for monitoring autophagy in higher eukaryotes. Autophagy 2008; 4:151-75; PMID:18188003.
55. Tasdemir E, Galluzzi L, Maiuri MC, Criollo A, Vitale I, Hangen E, et al. Methods for assessing autophagy and autophagic cell death. Methods Mol Biol 2008; 445:29-76; PMID:18425442; http://dx.doi.org/10.1007/978-1-59745-157-4_3.
56. Kepp O, Galluzzi L, Lipinski M, Yuan J, Kroemer G. Cell death assays for drug discovery. Nat Rev Drug Discov 2011; 10:221-37; PMID:21358741; http://dx.doi.org/10.1038/nrd3373.
57. Fass E, Shvets E, Degani I, Hirschberg K, Elazar Z. Microtubules support production of starvation-induced autophagosomes but not their targeting and fusion with lysosomes. J Biol Chem 2006; 281:36303-16; PMID:16963441; http://dx.doi.org/10.1074/jbc.M607031200.
58. Peck B, Chen CY, Ho KK, Di Fruscia P, Myatt SS, Coombes RC, et al. SIRT inhibitors induce cell death and p53 acetylation through targeting both SIRT1 and SIRT2. Mol Cancer Ther 2010; 9:844-55; PMID:20371709; http://dx.doi.org/10.1158/1535-7163.MCT-09-0971.
59. Schlicker C, Boanca G, Lakshminarasimhan M, Steegborn C. Structure-based development of novel sirtuin inhibitors. Aging (Albany NY) 2011; 3:852-72; PMID:21937767.
60. Ford J, Jiang M, Milner J. Cancer-specific functions of SIRT1 enable human epithelial cancer cell growth and survival. Cancer Res 2005; 65:10457-63; PMID:16288037; http://dx.doi.org/10.1158/0008-5472.CAN-05-1923.
61. Baur JA, Ungvari Z, Minor RK, Le Couteur DG, de Cabo R. Are sirtuins viable targets for improving healthspan and lifespan? Nat Rev Drug Discov 2012; 11:443-61; PMID:22653216; http://dx.doi.org/10.1038/nrd3738.
62. Howitz KT, Bitterman KJ, Cohen HY, Lamming DW, Lavu S, Wood JG, et al. Small molecule activators of sirtuins extend Saccharomyces cerevisiae lifespan. Nature 2003; 425:191-6; PMID:12939617; http://dx.doi.org/10.1038/nature01960.
63. Nair S, Ren J. Autophagy and cardiovascular aging: lesson learned from rapamycin. Cell Cycle 2012; 11:2092-9; PMID:22580468; http://dx.doi.org/10.4161/cc.20317.
64. Potter GA, Patterson LH, Wanogho E, Perry PJ, Butler PC, Ijaz T, et al. The cancer preventative agent resveratrol is converted to the anticancer agent piceatannol by the cytochrome P450 enzyme CYP1B1. Br J Cancer 2002; 86:774-8; PMID:11875742; http://dx.doi.org/10.1038/sj.bjc.6600197.
65. Galluzzi L, Kepp O, Kroemer G. TP53 and MTOR crosstalk to regulate cellular senescence. Aging (Albany NY) 2010; 2:535-7; PMID:20876940.
66. Martins I, Galluzzi L, Kroemer G. Hormesis, cell death and aging. Aging (Albany NY) 2011; 3:821-8; PMID:21931183.
67. Vitale I, Galluzzi L, Castedo M, Kroemer G. Mitotic catastrophe: a mechanism for avoiding genomic instability. Nat Rev Mol Cell Biol 2011; 12:385-92; PMID:21527953; http://dx.doi.org/10.1038/nrm3115.
68. Kroemer G, Galluzzi L, Brenner C. Mitochondrial membrane permeabilization in cell death. Physiol Rev 2007; 87:99-163; PMID:17237344; http://dx.doi.org/10.1152/physrev.00013.2006.
69. Kroemer G, Galluzzi L, Vandenabeele P, Abrams J, Alnemri ES, Baehrecke EH, et al.; Nomenclature Committee on Cell Death 2009. Classification of cell death: recommendations of the Nomenclature Committee on Cell Death 2009. Cell Death Differ 2009; 16:3-11; PMID:18846107; http://dx.doi.org/10.1038/cdd.2008.150.
70. de La Motte Rouge T, Galluzzi L, Olaussen KA, Zermati Y, Tasdemir E, Robert T, et al. A novel epidermal growth factor receptor inhibitor promotes apoptosis in non-small cell lung cancer cells resistant to erlotinib. Cancer Res 2007; 67:6253-62; PMID:17616683; http://dx.doi.org/10.1158/0008-5472.CAN-07-0538.
71. Galluzzi L, Vitale I, Senovilla L, Olaussen KA, Pinna G, Eisenberg T, et al. Prognostic impact of vitamin B6 metabolism in lung cancer. Cell Rep 2012; In press; PMID:22854025; http://dx.doi.org/10.1016/j.celrep.2012.06.017.
72. Morselli E, Tasdemir E, Maiuri MC, Galluzzi L, Kepp O, Criollo A, et al. Mutant p53 protein localized in the cytoplasm inhibits autophagy. Cell Cycle 2008; 7:3056-61; PMID:18818522; http://dx.doi.org/10.4161/cc.7.19.6751.
73. Criollo A, Galluzzi L, Maiuri MC, Tasdemir E, Lavandero S, Kroemer G. Mitochondrial control of cell death induced by hyperosmotic stress. Apoptosis 2007; 12:3-18; PMID:17080328; http://dx.doi.org/10.1007/s10495-006-0328-x.
74. Galluzzi L, Morselli E, Vitale I, Kepp O, Senovilla L, Criollo A, et al. miR-181a and miR-630 regulate cisplatin-induced cancer cell death. Cancer Res 2010; 70:1793-803; PMID:20145152; http://dx.doi.org/10.1158/0008-5472.CAN-09-3112.

Cell Cycle
Publication details, including instructions for authors and subscription information:
http://www.tandfonline.com/loi/kccy20

Coffee induces autophagy in vivo

Federico Pietrocola[abc], Shoaib Ahmad Malik[abcd], Guillermo Mariño[ab], Erika Vacchelli[abc], Laura Senovilla[e], kariman chaba[ab], Mireia Niso-Santano[ab], Maria Chiara Maiuri[ab], Frank Madeo[f] & Guido Kroemer[abgh]

[a] Equipe 11 labellisée par la Ligue Nationale Contre le Cancer; INSERM U1138; Centre de Recherche des Cordeliers; Paris, France

[b] Metabolomics and Molecular Cell Biology Platforms; Gustave Roussy; Villejuif, France

[c] Université de Paris Sud; Villejuif, France

[d] Directorate of Medical Sciences; Government College University; Faisalabad, Pakistan

[e] INSERM U1015; Gustave Roussy; Villejuif, France

[f] Institute of Molecular Biosciences; University of Graz; Graz, Austria

[g] Pôle de Biologie; Hôpital Européen Georges Pompidou; AP-HP; Paris, France

[h] Université Paris Descartes; Sorbonne Paris Cité; Paris, France

Published online: 25 Apr 2014.

To cite this article: Federico Pietrocola, Shoaib Ahmad Malik, Guillermo Mariño, Erika Vacchelli, Laura Senovilla, kariman chaba, Mireia Niso-Santano, Maria Chiara Maiuri, Frank Madeo & Guido Kroemer (2014) Coffee induces autophagy in vivo, Cell Cycle, 13:12, 1987-1994, DOI: 10.4161/cc.28929

To link to this article: http://dx.doi.org/10.4161/cc.28929

Cell Cycle 13:12, 1987–1994; June 15, 2014; © 2014 Landes Bioscience

Coffee induces autophagy in vivo

Federico Pietrocola[1,2,3,†], Shoaib Ahmad Malik[1,2,3,4,†], Guillermo Mariño[1,2], Erika Vacchelli[1,2,3], Laura Senovilla[5], Kariman Chaba[1,2], Mireia Niso-Santano[1,2], Maria Chiara Maiuri[1,2], Frank Madeo[6], and Guido Kroemer[1,2,7,8,*]

[1]Equipe 11 labellisée par la Ligue Nationale Contre le Cancer; INSERM U1138; Centre de Recherche des Cordeliers; Paris, France; [2]Metabolomics and Molecular Cell Biology Platforms; Gustave Roussy; Villejuif, France; [3]Université de Paris Sud; Villejuif, France; [4]Directorate of Medical Sciences; Government College University; Faisalabad, Pakistan; [5]INSERM U1015; Gustave Roussy; Villejuif, France; [6]Institute of Molecular Biosciences; University of Graz; Graz, Austria; [7]Pôle de Biologie; Hôpital Européen Georges Pompidou; AP-HP; Paris, France; [8]Université Paris Descartes; Sorbonne Paris Cité; Paris, France

[†]These authors contributed equally to this paper.

Keywords: acetyl-coenzyme A, acetylation, mTOR, macroautophagy

Epidemiological studies and clinical trials revealed that chronic consumption coffee is associated with the inhibition of several metabolic diseases as well as reduction in overall and cause-specific mortality. We show that both natural and decaffeinated brands of coffee similarly rapidly trigger autophagy in mice. One to 4 h after coffee consumption, we observed an increase in autophagic flux in all investigated organs (liver, muscle, heart) in vivo, as indicated by the increased lipidation of LC3B and the reduction of the abundance of the autophagic substrate sequestosome 1 (p62/SQSTM1). These changes were accompanied by the inhibition of the enzymatic activity of mammalian target of rapamycin complex 1 (mTORC1), leading to the reduced phosphorylation of $p70^{S6K}$, as well as by the global deacetylation of cellular proteins detectable by immunoblot. Immunohistochemical analyses of transgenic mice expressing a GFP–LC3B fusion protein confirmed the coffee-induced relocation of LC3B to autophagosomes, as well as general protein deacetylation. Altogether, these results indicate that coffee triggers 2 phenomena that are also induced by nutrient depletion, namely a reduction of protein acetylation coupled to an increase in autophagy. We speculate that polyphenols contained in coffee promote health by stimulating autophagy.

Introduction

Large epidemiological studies involving large cohorts of individuals have demonstrated that coffee consumption is inversely associated with total and cause-specific mortality, both in males and in females. The consumption of coffee is associated with a reduction of cancer, heart disease, respiratory disease, stroke, diabetes, and infections (both in males and females).[1-3] These effects are dose-dependent (with a plateau of 6 cups per day) and do not depend on caffeine content, because both decaffeinated and caffeinated coffee were similarly associated with improved health.[4,5] Independent surveys revealed that coffee consumption might have protective effects, among many, on highly penetrant tumors such as endometrial,[6,7] mammary[8] hepatocellular,[9] colorectal,[10] and prostatic cancer.[11] Although such studies cannot differentiate between causal and associational findings, they do suggest that chronic coffee consumption might have broad health-improving effects.

One of the general cell biological phenomena that has been attributed a global health-promoting and anti-aging property is autophagy,[12-14] a lysosomal degradation pathway responsible for the selective renewal of cytoplasmic organelles.[15,16] In macroautophagy (here referred to as "autophagy"), portions of the cytoplasm are sequestered in 2-membraned vesicles, the autophagosomes, which later fuse with lysosomes for the degradation of the luminal content by lysosomal hydrolases. Since autophagy preferentially targets damaged macromolecules (such as unfolded and aggregated proteins) and organelles (such as dysfunctional mitochondria),[17] it contributes to ridding the cytoplasm of aged structures and hence potentially "rejuvenates" non-nuclear portions of the cell.[18,19] Autophagy has also been suggested to participate in hormesis,[20] which consists in the adaptation of cells to low levels of stress, rendering them resistant to otherwise lethal effects of intense stress.[21,22] Several studies indicate that autophagy may act as a tumor-suppressive mechanism.[23-26] Based on these premises, we investigated the possibility that coffee might induce autophagy in vivo in mice. Here, we report that both natural and decaffeinated coffee similarly induce a broad organism-wide autophagic response.

Results and Discussion

Chronic administration of non-toxic doses of coffee induces autophagy in mice

Continuous administration of 1 or 3% coffee in the drinking water for 16 d did not affect the body weight of C57Bl/6

*Correspondence to: Guido Kroemer; Email: kroemer@orange.fr
Submitted: 03/27/2014; Accepted: 04/16/2014; Published Online: 04/25/2014
http://dx.doi.org/10.4161/cc.28929

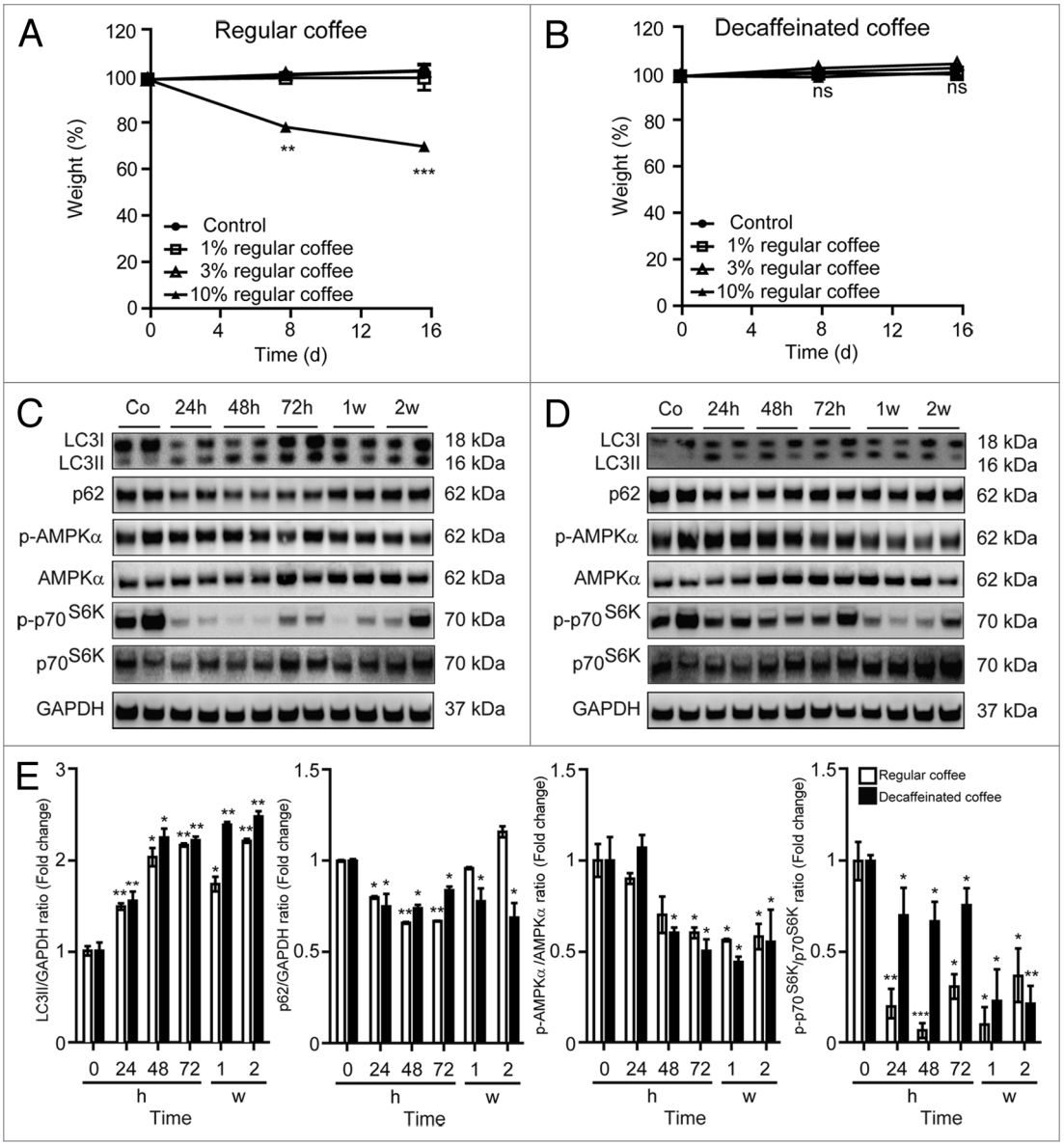

Figure 1. Long-term administration of regular and decaffeinated coffee at a dose not affecting body weight induces autophagy in the liver. (**A and B**). Effect of 2 wk administration of regular (**A**) or decaffeinated coffee (**B**) on body weight. C57BL/6 mice were administrated with the indicated doses of regular coffee (**A**) or decaffeinated coffee (**B**) diluted in drinking water, which was provided to mice ad libitum. The dose not affecting body weight (3% w/v) was designated for investigating pro-autophagic effects. Results from n = 3 independent experiments. (**C and D**). Immunoblotting analysis of long-term coffee administration on autophagy regulation in liver. Administration of both regular (**C**) and decaffeinated coffee (**D**) for up to 2 wk (w) resulted in activation of autophagy, as measured by LC3 lipidation and p62/SQSTM1 degradation (quantified in **E**). Autophagy activation was associated with a decrease in mTORC1 activity, as measured by the phosphorylation of $p70^{s6k}$, but not to an activation of AMPK (quantified in **E**). GAPDH levels were monitored to ensure equal loading. Representative images are reported in (**C and D**). Results from n = 3 independent experiments are presented as fold change ± SEM $^{*}P < 0.05$; $^{**}P < 0.01$; $^{***}P < 0.005$ (unpaired, 2-tailed Student *t* test), compared with untreated mice.

mice. In contrast, 10% of caffeinated (but not of decaffeinated) coffee did cause weight reduction over this period, suggesting some caffeine-associated effects (**Fig. 1A and B**). As a result, we evaluated the capacity of chronic treatment with 3% coffee to induce autophagy in vivo. This dose is well within the range of that absorbed by coffee-consuming persons. Three percent of either caffeinated or decaffeinated coffee induced similar signs of increased autophagic flux in the liver (**Fig. 1C–E**), heart (**Fig. S1**), and muscle (**Fig. S2**), namely lipidation of microtubule-associated protein 1 light chain 3 β (LC3B), leading to an increase in its electrophoretic mobility in sodium dodecyl sulfate PAGE (SDS-PAGE), generating the isoform II of LC3B, accompanied by a decrease in the overall abundance of the autophagic substrate sequestosome-1 (p62/SQSTM1) (**Fig. 1C–E**). These results were observable as early as 24 h after beginning of the treatment and lasted for the entire 2-wk experiment, indicating that chronic exposure to coffee can induce autophagy irrespective from its caffeine content.

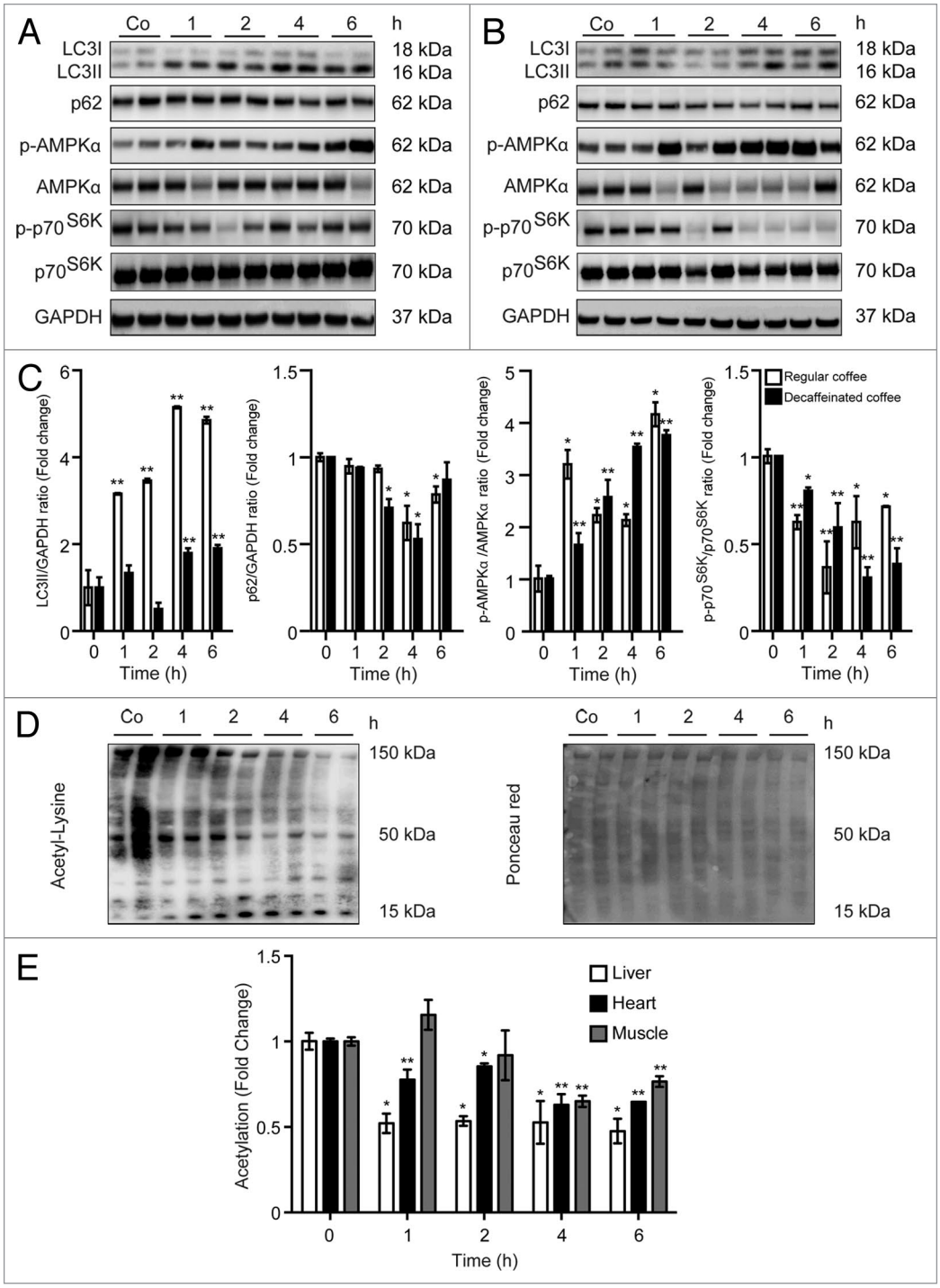

Figure 2. Short-term administration of both regular coffee and decaffeinated coffee induces autophagy accompanied by a reduction in global acetylation levels of proteins in the liver. (**A and B**). Immunoblotting analysis of short-term coffee administration on autophagy regulation in liver. Gavage of both regular coffee (**A**) and decaffeinated coffee (**B**) resulted in an activation of autophagy, although at different extent and timing, as measured by LC3 lipidation and p62 degradation (quantified in **C**). In both cases, autophagy induction was accompanied by an activation of AMPK and by a reduction in the activity of mTORC1, as measured by the phosphorylation of its substrate $p70^{s6k}$ (quantified in **C**). Representative images are depicted in (**A and B**). Results from n = 3 independent experiments are presented as fold change ± SEM $^{*}P < 0.05$; $^{**}P < 0.01$; (unpaired, 2-tailed Student *t* test), compared with untreated mice. (**D and E**) Immunoblot detection of protein acetylation in mice administered with regular coffee. Coffee administration (by gavage) resulted in a significant drop in the overall acetylation levels of proteins in liver, heart, and muscle (quantified in **E**) in a range of time of 1 to 6 h depending on the tissue. Panels in (**D**) refer to liver. Ponceau red staining was used to monitor equal loading of the lanes. Results from n = 3 independent experiments are presented as fold change ± SEM $^{*}P < 0.05$; $^{**}P < 0.01$ (unpaired, 2-tailed Student *t* test), compared with untreated mice.

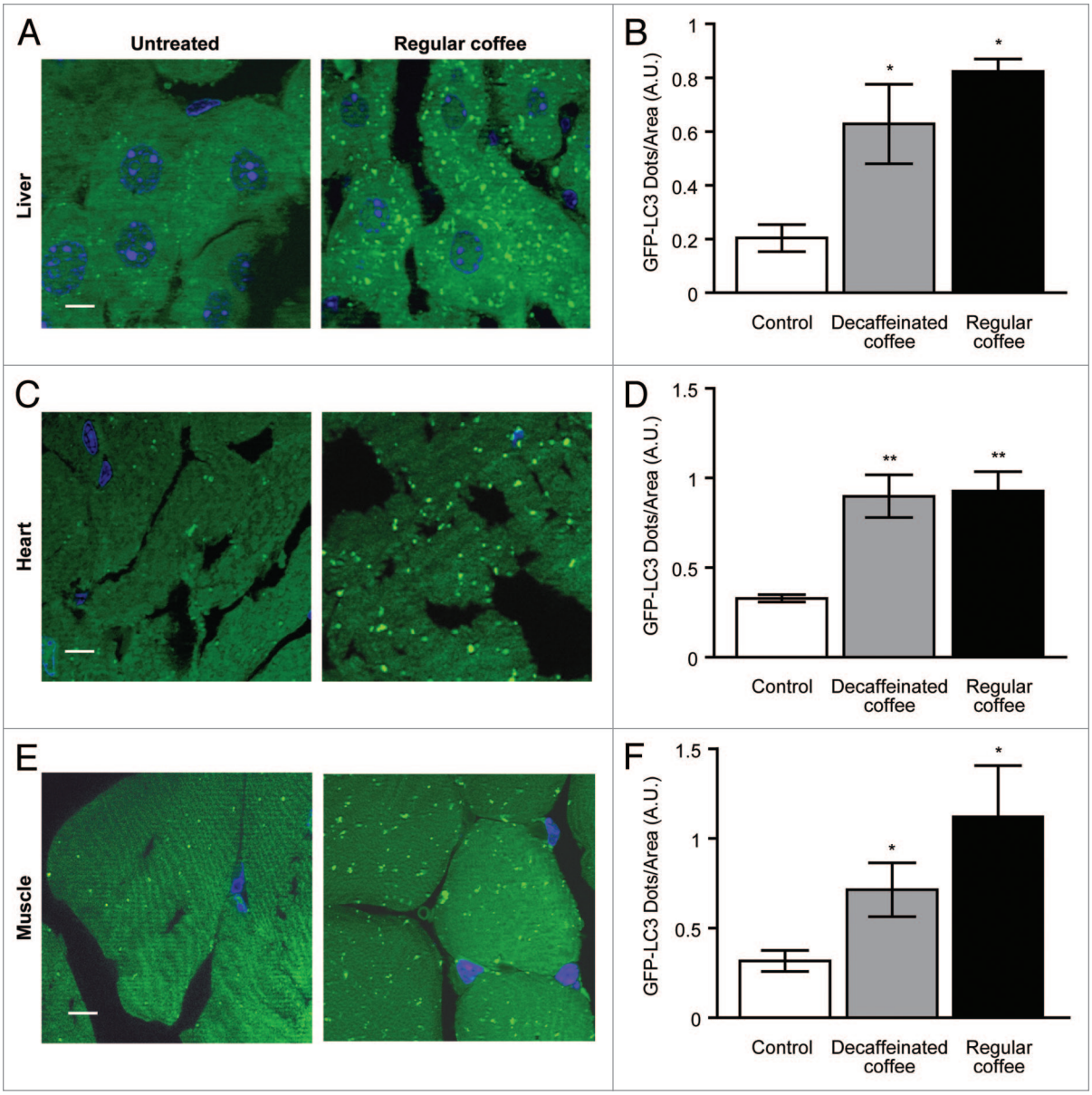

Figure 3. Autophagy induction mediated by short-term coffee administration is confirmed for liver, heart, and muscle from GFP-LC3 transgenic mice. GFP-LC3-expressing mice were administered with regular and decaffeinated coffee by gavage and analyzed for autophagy induction after 4 h. (**A–F**). Fluorescence microscopic analysis of liver (**A**), heart (**C**), and muscle (**E**) revealed a significant increase in the number of LC3II puncta per area of cells in all tissues (quantified in **B, D, and F**). Representative images of tissues from untreated vs. regular coffee-treated mice are depicted in (**A, C, and E**) (bar scale: 10 μm). Results from 3 independent experiments are presented as GFP-LC3 dots/area (means ± SEM). *$P < 0.05$; **$P < 0.01$; (unpaired, 2-tailed Student *t* test), compared with untreated mice.

Short-term administration of coffee induces autophagy in vivo

We next determined the kinetics with which coffee can stimulate autophagy in vivo. For this, coffee was administered by gavage to C57BL/6 mice, and autophagy was quantified by immunoblot determination of the conversion of native LC3B-I into lipidated, membrane-associated LC3B-II, as well as by measurements of p62/SQSTM1 degradation. Irrespective of the absence or presence of caffeine, coffee induced a rapid LC3B-I to LC3B-II conversion and a depletion of p62/SQSTM1 in the liver (**Fig. 2A and B**). Similarly, both regular and decaffeinated coffee induced signs of autophagy in the heart (**Fig. S3**) and in the muscle (**Fig. S4**). The kinetics of LC3B-I to LC3B-II conversion were similar in all organs. The depletion of p62/SQSTM1 occurred earlier (1 h) in the heart (**Fig. S3**) than in the liver (**Fig. 2**) and in the skeletal muscle (**Fig. S4**), where it was detectable only at 4 h, thus confirming an organ-specific and transcription-dependent behavior of p62, as recently described.[29] To further evaluate the capacity of coffee to induce autophagy in vivo, we next took advantage of transgenic mice expressing a chimeric GFP–LC3 protein under the control of the ubiquitous CAG promoter.[30] Microscopic detection of the GFP-dependent fluorescent signal allowed for

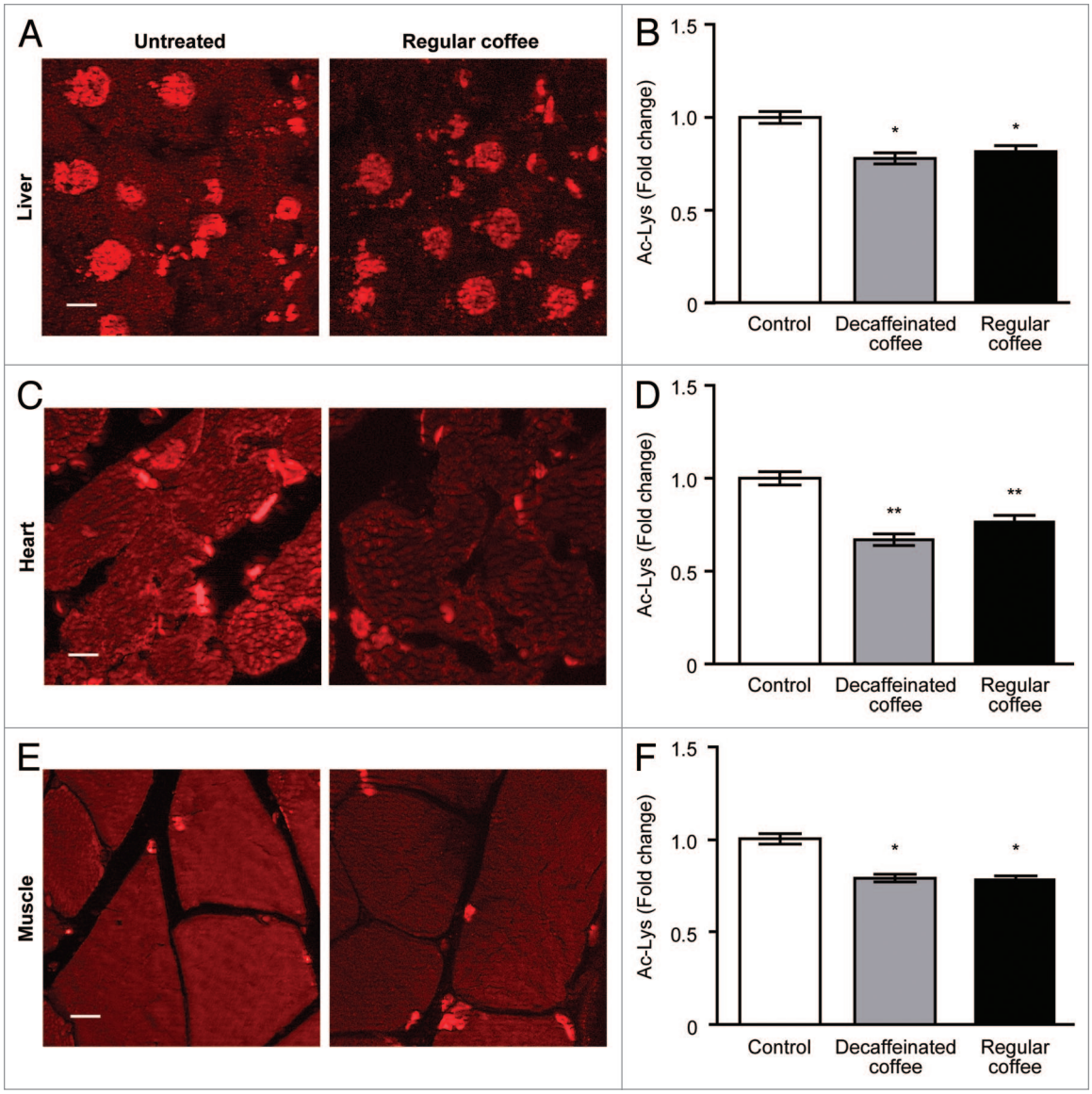

Figure 4. Reduction in global protein acetylation levels mediated by short-term coffee administration in liver, heart, and muscle. Livers, hearts, and muscles from C57Bl/6 mice were analyzed 4 h after treatment with regular and decaffeinated coffee to determine protein acetylatation by immunofluorescence. Fluorescence microscope analysis of liver (**A**), heart (**C**), and muscle (**E**) revealed a significant decrease in the acetylation of proteins in all tissues (quantified in **B, D, and F**). Representative images of untreated vs. regular coffee-treated mice are depicted in (**A, C, and E**) (bar scale: 10 μm). Results from n = 3 independent experiments are presented as acetylated lysine intensity fold change ± SEM, considering the values of tissues from untreated mice as 1. *$P < 0.05$; **$P < 0.01$; (unpaired, 2-tailed Student *t* test), compared with untreated mice.

the detection of coffee-induced autophagy, as GFP-LC3 relocated from a mostly diffuse distribution (in untreated animals) to cytoplasmic puncta (in treated animals). The accumulation of GFP-LC3$^+$ puncta was observed in liver, muscle, and heart 4 h after administration of either caffeinated or decaffeinated coffee (**Fig. 3**), confirming the notion that coffee does induce a significant induction of autophagy in multiple organs.

Coffee ingestion causes global deacetylation of proteins and hence mimics caloric restriction

To characterize the mechanisms through which coffee induces autophagy, we determined its capacity to activate prominent energy sensors such as AMP-activated protein kinase (AMPK) and mammalian target of rapamycin complex 1 (mTORC1). While acute (within hours) stimulation with caffeinated or decaffeinated coffee did induce the activating phosphorylation of AMPK (**Fig. 2A–C**), a more protracted exposure (days to weeks) failed to do so and actually reduced AMPK phosphorylation (**Fig. 1C–E**). Thus, the present data suggest that AMPK cannot be responsible for autophagy induced by long-term coffee administration. However, both acute and chronic administration of coffee did reduce the phosphorylation of the mTORC1 substrate p70^{S6K} (**Figs. 1C–E and 2A–C**), suggesting that this nutrient sensor might be involved in pro-autophagic signaling. Coffee contains multiple polyphenols,[31,32] and a range of chemically different

phenolic compounds have been demonstrated capable to stimulate the deacetylation of cellular proteins, correlating with their pro-autophagic activity.[33] We therefore investigated the possibility that in vivo treatment with coffee would reduce the acetylation of cellular proteins using 2 distinct methodologies designed to detect acetyl-lysine-modified proteins. First, extracts from liver (**Fig. 2D and E**), myocardium (**Fig. S3**), and skeletal muscle (**Fig. S4**) revealed a reduction in protein acetylation upon coffee treatment. This effect was detectable as soon as 1 h after coffee gavage in the liver and in the heart and 4 h post-gavage in the skeletal muscle (**Fig. 2E**). Second, the deacetylation of proteins was detectable by immunofluorescence staining with antibodies specific for acetyl-lysine-modified proteins, revealing a reduction in protein acetylation both in the cytoplasm and in nuclei from hepatocytes, cardiomyocytes, and skeletal myocytes 4 h post-gavage (**Fig. 4**). Again, these effects were similar for caffeinated and decaffeinated coffee. Altogether, these results support the notion that autophagy induction by coffee is linked to the deacetylation of cellular proteins as well as to the inhibition of mTORC1.

Concluding remarks

The data presented in this paper unequivocally demonstrate that coffee is a potent, rapid inducer of autophagy in multiple tissues in vivo in mice. This effect is independent of caffeine content. Although caffeine has been shown to inhibit mTORC1 and to induce autophagy in hepatocytes in vivo, thereby reducing intrahepatic lipid content and stimulating β-oxidation, as well as counteracting hepatosteatosis,[34] caffeine is apparently not required for coffee-induced autophagy. Rather, other coffee components that are not eliminated during the decaffeination process, presumably polyphenols, must be responsible for these effects. Autophagy induced by coffee is accompanied by the inhibition of mTORC1, which represses autophagy in conditions of nutrient availability (particularly amino acids and lipids).[35,36] Several polyphenols have been shown to induce autophagy, correlating with their capacity to reduce the acetylation levels of cellular proteins.[33,37,38] In theory, the reduction of acetylation levels may be explained by the depletion of the sole donor of acetyl groups, acetyl coenzyme A,[39,40] the suppression of the activity of acetyltransferases (for instance by spermidine or C646),[21,39] or the activation of deacetylatses (such as sirtuin 1, which can be activated by resveratrol).[37] Irrespective of the precise mechanism causing protein deacetylation, this phenomenon is broadly associated with the induction of autophagy by starvation[39] or by several pharmacological inducers including spermidine and resveratrol.[41] In the present report, we extend the list of agents able to trigger deacetylation reactions to coffee, correlating with its capacity to stimulate autophagy.

Based on the present data, the hypothesis that coffee reduces general mortality by inducing autophagy warrants further experimental and clinical scrutiny.

Materials and Methods

Reagents

The results presented refer to a single commercial brand (Belle France) of 100% regular and decaffeinated hydro soluble coffee. Results were confirmed using other 2 commercial brands (Nestle, Lavazza). Concentrations are expressed in % (weight per volume).

Mouse experiments and tissue processing

Six-weeks-aged female C57BL/6 mice (Charles River Laboratory) and transgenic C57BL/6 mice expressing the fusion protein GFP-LC3 under the control of CAG (cytomegalovirus immediate-early [CMVie] enhancer and chicken β-actin promoter) promoter, were bred and maintained according to both the FELASA and the European Community regulations for animal use in research (2010/63UE) as well as the local Ethics Committee for Animal Welfare (project number: 2012–065, 2012–067). Mice were housed in a temperature-controlled environment with 12-h light/dark cycles and received food and water ad libitum. For long-term coffee experiments, mice were first administered with 1%, 3%, and 10% w/v of regular and decaffeinated coffee in drinking water ad libitum in order to select a dose not affecting body weight; mice were then administrated with 3% w/v of coffee for 2 wk. Mice were sacrificed, and tissues were recovered and immediately frozen in liquid nitrogen 24, 48, or 72 h, 1 wk and 2 wk after treatment. For short-term coffee experiments, mice were administered with 3% w/v dose of regular and decaffeinated coffee by gavage and sacrificed after 1, 2, 4, and 6 h, when tissues were immediately frozen in liquid nitrogen. After extraction, tissues were homogenized during 2 cycles for 20 s at 5500 rpm using a Precellys 24 tissue homogenator (Bertin Technologies) in a 20 mM Tris buffer (pH 7.4) containing 150 mM NaCl, 1% Triton X-100, 10 mM EDTA, and Complete® protease inhibitor cocktail (Roche Applied Science). Tissue extracts were then centrifuged at 12 000 g at 4 °C, and supernatants were collected. Protein concentration in the supernatants was evaluated by the bicinchoninic acid technique (BCA protein assay kit, Pierce Biotechnology).

Quantitative analysis of GFP-LC3 dots in mouse tissue sections and immunofluorescence

To avoid postmortem autophagy induction, dead mice were immediately perfused with 4% paraformaldehyde (w:v in PBS, pH 7.4). Tissues were then harvested and further fixed with the same solution for at least 4 h, followed by treatment with 15% sucrose (w:v in PBS) for 4 h and with 30% sucrose (w:v in PBS) overnight. Tissue samples were embedded in Tissue-Tek OCT compound (Sakura Finetechnical Co, Ltd) and stored at -80 °C. Five micrometer (5 μm) thick tissue sections were prepared with a CM3050 S cryostat (Leica Microsystems), air-dried for 1 h, washed in PBS for 5 min, dried at RT for 30 min, and mounted with VECTASHIELD anti-fading medium. For acetylation staining, 5-μm-thick tissue sections were prepared. Tissues were permeabilized with 0.1% Triton and blocked with 5% BSA, then incubated overnight at 4 °C with primary antibody in 2% BSA. After 1 h RT incubation with secondary-HRP conjugated antibody, tissues were mounted as described above. For each organ, approximately 10 pictures of 5 independent visual fields from at least 3 mice were acquired using an Axio Observer inverted fluorescence microscope equipped with Apotome confocal-like system (Carl Zeiss). GFP-LC3 dots per area of cells and acetylation intensity were quantified by means of Metamorph (Molecular Devices) software.

Fluorescence microscopy

For the analysis of GFP-LC3 mice tissue sections, a Leica APO 63× NA 1.15 immersion objective was employed. For acetylation analysis, a Leica APO 40× NA 1.15 immersion objective was used. Zeiss Immersol® immersion oil was used for all microscopic analyses. Images were acquired with a Leica DFC 350 Fx camera (version 1.8.0) using Leica LAS AF software and processed with Adobe Photoshop (version CS5) software.

Immunoblotting

For immunoblotting, 25 μg of proteins were separated on 4–12% bis-tris acrylamide (Invitrogen) or 12% tris-glycine SDS-PAGE precast gels (Biorad) and electrotransferred to Immobilon™ membranes (Millipore Corporation). Membranes were then sliced horizontally in different parts according to the molecular weight of the protein of interest to allow simultaneous detection of different antigens within the same experiment.[27,28] Unspecific binding sites were saturated by incubating membranes for 1 h in 0.05% Tween 20 (v:v in TBS) supplemented with 5% non-fat powdered milk (w:v in TBS), followed by an overnight incubation with primary antibodies specific for acetylated-lysine, LC3B, phospho-AMPK (Thr172), AMPK, phospho-ribosomal protein S6 kinase (Thr421/Ser424), ribosomal protein S6 kinase, (Cell Signaling Technology), or STQM/p62 (Santa Cruz Biotechnology). Development was performed with appropriate horseradish peroxidase (HRP)-labeled secondary antibodies (Southern Biotech) plus the SuperSignal West Pico chemoluminescent substrate (Thermo Scientific-Pierce). An anti-glyceraldehyde-3-phosphate dehydrogenase antibody (Chemicon International) was used to control equal loading of lanes. Immunoblotting quantifications were performed through densitometric analysis by means of ImageJ software in 3 independent experiments.

Disclosure of Potential Conflicts of Interest

No potential conflicts of interest were disclosed.

Acknowledgments

We thank Noboru Mizushima for the generous gift of GFP-LC3 transgenic mice. G.K. is supported by the Ligue contre le Cancer (équipe labelisée); Agence National de la Recherche (ANR); Association pour la recherche sur le cancer (ARC); Cancéropôle Ile-de-France; Institut National du Cancer (INCa); Fondation Bettencourt-Schueller; Fondation de France; Fondation pour la Recherche Médicale (FRM); the European Commission (ArtForce); the European Research Council (ERC); the LabEx Immuno-Oncology; the SIRIC Stratified Oncology Cell DNA Repair and Tumor Immune Elimination (SOCRATE); the SIRIC Cancer Research and Personalized Medicine (CARPEM); and the Paris Alliance of Cancer Research Institutes (PACRI). F.M. is supported by FWF grants LIPOTOX, P23490-B12, I1000, and P24381-B20.

Supplemental Materials

Supplemental materials may be found here:
www.landesbioscience.com/journals/cc/article/28929

References

1. Kempf K, Herder C, Erlund I, Kolb H, Martin S, Carstensen M, Koenig W, Sundvall J, Bidel S, Kuha S, et al. Effects of coffee consumption on subclinical inflammation and other risk factors for type 2 diabetes: a clinical trial. Am J Clin Nutr 2010; 91:950-7; PMID:20181814; http://dx.doi.org/10.3945/ajcn.2009.28548
2. Vinson JA, Burnham BR, Nagendran MV. Randomized, double-blind, placebo-controlled, linear dose, crossover study to evaluate the efficacy and safety of a green coffee bean extract in overweight subjects. Diabetes Metab Syndr Obes 2012; 5:21-7; PMID:22291473; http://dx.doi.org/10.2147/DMSO.S27665
3. Greenberg JA, Boozer CN, Geliebter A. Coffee, diabetes, and weight control. Am J Clin Nutr 2006; 84:682-93; PMID:17023692
4. Freedman ND, Park Y, Abnet CC, Hollenbeck AR, Sinha R. Association of coffee drinking with total and cause-specific mortality. N Engl J Med 2012; 366:1891-904; PMID:22591295; http://dx.doi.org/10.1056/NEJMoa1112010
5. Malerba S, Turati F, Galeone C, Pelucchi C, Verga F, La Vecchia C, Tavani A. A meta-analysis of prospective studies of coffee consumption and mortality for all causes, cancers and cardiovascular diseases. Eur J Epidemiol 2013; 28:527-39; PMID:23934579; http://dx.doi.org/10.1007/s10654-013-9834-7
6. Terry P, Vainio H, Wolk A, Weiderpass E. Dietary factors in relation to endometrial cancer: a nationwide case-control study in Sweden. Nutr Cancer 2002; 42:25-32; PMID:12235647; http://dx.doi.org/10.1207/S15327914NC421_4
7. Gunter MJ, Schaub JA, Xue X, Freedman ND, Gaudet MM, Rohan TE, Hollenbeck AR, Sinha R. A prospective investigation of coffee drinking and endometrial cancer incidence. Int J Cancer 2012; 131:E530-6; PMID:22021096; http://dx.doi.org/10.1002/ijc.26482
8. Kotsopoulos J, Ghadirian P, El-Sohemy A, Lynch HT, Snyder C, Daly M, Domchek S, Randall S, Karlan B, Zhang P, et al. The CYP1A2 genotype modifies the association between coffee consumption and breast cancer risk among BRCA1 mutation carriers. Cancer Epidemiol Biomarkers Prev 2007; 16:912-6; PMID:17507615; http://dx.doi.org/10.1158/1055-9965.EPI-06-1074
9. Bravi F, Bosetti C, Tavani A, Bagnardi V, Gallus S, Negri E, Franceschi S, La Vecchia C. Coffee drinking and hepatocellular carcinoma risk: a meta-analysis. Hepatology 2007; 46:430-5; PMID:17580359; http://dx.doi.org/10.1002/hep.21708
10. Sinha R, Cross AJ, Daniel CR, Graubard BI, Wu JW, Hollenbeck AR, Gunter MJ, Park Y, Freedman ND. Caffeinated and decaffeinated coffee and tea intakes and risk of colorectal cancer in a large prospective study. Am J Clin Nutr 2012; 96:374-81; PMID:22695871; http://dx.doi.org/10.3945/ajcn.111.031328
11. Lu Y, Zhai L, Zeng J, Peng Q, Wang J, Deng Y, Xie L, Mo C, Yang S, Li S, et al. Coffee consumption and prostate cancer risk: an updated meta-analysis. Cancer Causes Control 2014; 25:591-604; PMID:24584929; http://dx.doi.org/10.1007/s10552-014-0364-8
12. Blagosklonny MV. Answering the ultimate question "what is the proximal cause of aging?". Aging (Albany NY) 2012; 4:861-77; PMID:23425777
13. Blagosklonny MV. Hypoxia, MTOR and autophagy: converging on senescence or quiescence. Autophagy 2013; 9:260-2; PMID:23192222; http://dx.doi.org/10.4161/auto.22783
14. Blagosklonny MV. Rapamycin extends life- and health span because it slows aging. Aging (Albany NY) 2013; 5:592-8; PMID:23934728
15. Levine B, Kroemer G. Autophagy in the pathogenesis of disease. Cell 2008; 132:27-42; PMID:18191218; http://dx.doi.org/10.1016/j.cell.2007.12.018
16. Murrow L, Debnath J. Autophagy as a stress-response and quality-control mechanism: implications for cell injury and human disease. Annu Rev Pathol 2013; 8:105-37; PMID:23072311; http://dx.doi.org/10.1146/annurev-pathol-020712-163918
17. Youle RJ, van der Bliek AM. Mitochondrial fission, fusion, and stress. Science 2012; 337:1062-5; PMID:22936770; http://dx.doi.org/10.1126/science.1219855
18. Rubinsztein DC, Mariño G, Kroemer G. Autophagy and aging. Cell 2011; 146:682-95; PMID:21884931; http://dx.doi.org/10.1016/j.cell.2011.07.030
19. López-Otín C, Blasco MA, Partridge L, Serrano M, Kroemer G. The hallmarks of aging. Cell 2013; 153:1194-217; PMID:23746838; http://dx.doi.org/10.1016/j.cell.2013.05.039
20. Martins I, Galluzzi L, Kroemer G. Hormesis, cell death and aging. Aging (Albany NY) 2011; 3:821-8; PMID:21931183
21. Eisenberg T, Knauer H, Schauer A, Büttner S, Ruckenstuhl C, Carmona-Gutierrez D, Ring J, Schroeder S, Magnes C, Antonacci L, et al. Induction of autophagy by spermidine promotes longevity. Nat Cell Biol 2009; 11:1305-14; PMID:19801973; http://dx.doi.org/10.1038/ncb1975

22. Madeo F, Tavernarakis N, Kroemer G. Can autophagy promote longevity? Nat Cell Biol 2010; 12:842-6; PMID:20811357; http://dx.doi.org/10.1038/ncb0910-842
23. Kroemer G, Jäättelä M. Lysosomes and autophagy in cell death control. Nat Rev Cancer 2005; 5:886-97; PMID:16239905; http://dx.doi.org/10.1038/nrc1738
24. Morselli E, Galluzzi L, Kepp O, Mariño G, Michaud M, Vitale I, Maiuri MC, Kroemer G. Oncosuppressive functions of autophagy. Antioxid Redox Signal 2011; 14:2251-69; PMID:20712403; http://dx.doi.org/10.1089/ars.2010.3478
25. White E. Deconvoluting the context-dependent role for autophagy in cancer. Nat Rev Cancer 2012; 12:401-10; PMID:22534666; http://dx.doi.org/10.1038/nrc3262
26. Ma Y, Galluzzi L, Zitvogel L, Kroemer G. Autophagy and cellular immune responses. Immunity 2013; 39:211-27; PMID:23973220; http://dx.doi.org/10.1016/j.immuni.2013.07.017
27. Criollo A, Niso-Santano M, Malik SA, Michaud M, Morselli E, Mariño G, Lachkar S, Arkhipenko AV, Harper F, Pierron G, et al. Inhibition of autophagy by TAB2 and TAB3. EMBO J 2011; 30:4908-20; PMID:22081109; http://dx.doi.org/10.1038/emboj.2011.413
28. Shen S, Niso-Santano M, Adjemian S, Takehara T, Malik SA, Minoux H, Souquere S, Mariño G, Lachkar S, Senovilla L, et al. Cytoplasmic STAT3 represses autophagy by inhibiting PKR activity. Mol Cell 2012; 48:667-80; PMID:23084476; http://dx.doi.org/10.1016/j.molcel.2012.09.013
29. Sahani MH, Itakura E, Mizushima N. Expression of the autophagy substrate SQSTM1/p62 is restored during prolonged starvation depending on transcriptional upregulation and autophagy-derived amino acids. Autophagy 2014; 10:431-41; PMID:24394643; http://dx.doi.org/10.4161/auto.27344
30. Hashimoto D, Ohmuraya M, Hirota M, Yamamoto A, Suyama K, Ida S, Okumura Y, Takahashi E, Kido H, Araki K, et al. Involvement of autophagy in trypsinogen activation within the pancreatic acinar cells. J Cell Biol 2008; 181:1065-72; PMID:18591426; http://dx.doi.org/10.1083/jcb.200712156
31. Wang Y, Ho CT. Polyphenolic chemistry of tea and coffee: a century of progress. J Agric Food Chem 2009; 57:8109-14; PMID:19719133; http://dx.doi.org/10.1021/jf804025c
32. Lecour S, Lamont KT. Natural polyphenols and cardioprotection. Mini Rev Med Chem 2011; 11:1191-9; PMID:22070680
33. Pietrocola F, Mariño G, Lissa D, Vacchelli E, Malik SA, Niso-Santano M, Zamzami N, Galluzzi L, Maiuri MC, Kroemer G. Pro-autophagic polyphenols reduce the acetylation of cytoplasmic proteins. Cell Cycle 2012; 11:3851-60; PMID:23070521; http://dx.doi.org/10.4161/cc.22027
34. Sinha RA, Farah BL, Singh BK, Siddique MM, Li Y, Wu Y, Ilkayeva OR, Gooding J, Ching J, Zhou J, et al. Caffeine stimulates hepatic lipid metabolism by the autophagy-lysosomal pathway in mice. Hepatology 2014; 59:1366-80; PMID:23929677
35. Kroemer G, Mariño G, Levine B. Autophagy and the integrated stress response. Mol Cell 2010; 40:280-93; PMID:20965422; http://dx.doi.org/10.1016/j.molcel.2010.09.023
36. Sengupta S, Peterson TR, Sabatini DM. Regulation of the mTOR complex 1 pathway by nutrients, growth factors, and stress. Mol Cell 2010; 40:310-22; PMID:20965424; http://dx.doi.org/10.1016/j.molcel.2010.09.026
37. Morselli E, Mariño G, Bennetzen MV, Eisenberg T, Megalou E, Schroeder S, Cabrera S, Bénit P, Rustin P, Criollo A, et al. Spermidine and resveratrol induce autophagy by distinct pathways converging on the acetylproteome. J Cell Biol 2011; 192:615-29; PMID:21339330; http://dx.doi.org/10.1083/jcb.201008167
38. Bennetzen MV, Mariño G, Pultz D, Morselli E, Færgeman NJ, Kroemer G, Andersen JS. Phosphoproteomic analysis of cells treated with longevity-related autophagy inducers. Cell Cycle 2012; 11:1827-40; PMID:22517431; http://dx.doi.org/10.4161/cc.20233
39. Mariño G, Pietrocola F, Eisenberg T, Kong Y, Malik SA, Andryushkova A, Schroeder S, Pendl T, Harger A, Niso-Santano M, et al. Regulation of autophagy by cytosolic acetyl-coenzyme A. Mol Cell 2014; 53:710-25; PMID:24560926; http://dx.doi.org/10.1016/j.molcel.2014.01.016
40. Eisenberg T, Schroeder S, Andryushkova A, Pendl T, Küttner V, Bhukel A, Mariño G, Pietrocola F, Harger A, Zimmermann A, et al. Nucleocytosolic depletion of the energy metabolite acetyl-coenzyme a stimulates autophagy and prolongs lifespan. Cell Metab 2014; 19:431-44; PMID:24606900; http://dx.doi.org/10.1016/j.cmet.2014.02.010
41. Mariño G, Morselli E, Bennetzen MV, Eisenberg T, Megalou E, Schroeder S, Cabrera S, Bénit P, Rustin P, Criollo A, et al. Longevity-relevant regulation of autophagy at the level of the acetylproteome. Autophagy 2011; 7:647-9; PMID:21460620; http://dx.doi.org/10.4161/auto.7.6.15191

Cell Death and Differentiation (2015) 22, 509–516

www.nature.com/cdd

Spermidine induces autophagy by inhibiting the acetyltransferase EP300

F Pietrocola[1,2,8], S Lachkar[1,2], DP Enot[3], M Niso-Santano[1,2], JM Bravo-San Pedro[1,2], V Sica[1,2], V Izzo[1,2], MC Maiuri[1,2], F Madeo[4,5], G Mariño*[,1,2,8] and G Kroemer*[,1,2,3,6,7]

Several natural compounds found in health-related food items can inhibit acetyltransferases as they induce autophagy. Here we show that this applies to anacardic acid, curcumin, garcinol and spermidine, all of which reduce the acetylation level of cultured human cells as they induce signs of increased autophagic flux (such as the formation of green fluorescent protein-microtubule-associated protein 1A/1B-light chain 3 (GFP-LC3) puncta and the depletion of sequestosome-1, p62/SQSTM1) coupled to the inhibition of the mammalian target of rapamycin complex 1 (mTORC1). We performed a screen to identify the acetyltransferases whose depletion would activate autophagy and simultaneously inhibit mTORC1. The knockdown of only two acetyltransferases (among 43 candidates) had such effects: EP300 (E1A-binding protein p300), which is a lysine acetyltranferase, and NAA20 (*N*(α)-acetyltransferase 20, also known as NAT5), which catalyzes the N-terminal acetylation of methionine residues. Subsequent studies validated the capacity of a pharmacological EP300 inhibitor, C646, to induce autophagy in both normal and enucleated cells (cytoplasts), underscoring the capacity of EP300 to repress autophagy by cytoplasmic (non-nuclear) effects. Notably, anacardic acid, curcumin, garcinol and spermidine all inhibited the acetyltransferase activity of recombinant EP300 protein *in vitro*. Altogether, these results support the idea that EP300 acts as an endogenous repressor of autophagy and that potent autophagy inducers including spermidine *de facto* act as EP300 inhibitors.
Cell Death and Differentiation (2015) **22,** 509–516; doi:10.1038/cdd.2014.215; published online 19 December 2014

Macroautophagy (herein referred to as 'autophagy') consist in the sequestration of cytoplasmic material in autophagosomes, followed by their fusion with lysosomes for the bulk degradation of autophagic cargo by lysosomal hydrolases.[1] This phenomenon can be measured by following the redistribution of green fluorescent protein-microtubule-associated protein 1A/1B-light chain 3 (GFP-LC3) fusion proteins from a diffuse location to autophagosomes (that results in the formation of the so-called GFP-LC3 'puncta'), the diminution of the overall abundance of autophagic substrates (such as sequestosome-1, p62/SQSTM1), and the stereotyped activation of proautophagic signals (such as the inhibition of the mammalian target of rapamycin complex 1, mTORC1).[2]

There is growing consensus that the induction of autophagy by nutritional, pharmacological or genetic interventions can reduce age-related pathologies (such as neurodegenerative diseases or type 2 diabetes) and/or extend longevity.[3–6] This applies to caloric restriction or intermediate fasting,[7] continuous or intermittent medication of rapamycin,[8–10] administration of the sirtuin 1-activator resveratrol,[11,12] external supply of the polyamine spermidine,[13] or genetic ablation of p53.[14] In all these cases, inhibition of autophagy by deleting or silencing relevant genes abolishes the extension of health span and/or lifespan.[13–17] Moreover, direct induction of autophagy by transgenic expression of autophagy-relevant genes such as *ATG5* in mice is sufficient to increase lifespan.[18]

Recently, acetyltransferases have emerged as a potential target for the pharmaceutical induction of autophagy. Thus, depletion of the sole donor of acetyl groups, acetyl-coenzyme A (acetyl-CoA), is sufficient to reduce the acetylation of cytoplasmic and nuclear proteins coupled to the induction of autophagy.[19–22] Culture of mammalian cells in nutrient-free (NF) conditions or starvation of mice for 24 h reduced the intracellular nucleocytosolic concentrations of acetyl-CoA at the same time as autophagy was induced, and replenishment of acetyl-CoA by external sources (for instance, by providing a membrane-permeant precursor of α-ketoglutarate for anaplerotic reactions or by microinjection of acetyl-CoA) was sufficient to inhibit starvation-induced autophagy.[19–22] Beyond the inhibition of acetyltransferases by acetyl-CoA depletion, direct pharmacological inhibition of acetyltransferases might also contribute to the induction of autophagy. A close correlation between autophagy induction and deacetylation of cytoplasmic proteins was observed in a screen conceived to identify autophagy-stimulating polyphenols[23] as well as in

[1]Equipe 11 labellisée par la Ligue Nationale contre le cancer, INSERM U1138, Centre de Recherche des Cordeliers, Paris 75006, France; [2]Université Paris Descartes, Sorbonne Paris Cité, Paris, France; [3]Metabolomics and Molecular Cell Biology Platforms, Gustave Roussy, Villejuif 94805, France; [4]Institute of Molecular Biosciences, University of Graz, Graz 8010, Austria; [5]BioTechMed Graz, Graz 8010, Austria; [6]Université de Paris Sud, Villejuif 94805, France and [7]Pôle de Biologie, Hôpital Européen Georges Pompidou, AP-HP, Paris 75015, France

*Corresponding authors: G Mariño or G Kroemer, Equipe 11 labellisée par la Ligue Nationale contre le cancer, INSERM U1138, Centre de Recherche des Cordeliers, 15 rue de l'ecole de medecine, Paris 75006, France. Tel: +33 1 44 27 76 67; Fax: +33 1 44 27 76 74; E-mail: gmg.marino@gmail.com or kroemer@orange.fr

[8]These authors contributed equally to this work.

Abbreviations: EP300; E1A-binding protein p300; GFP, green fluorescent protein; LC3, microtubule-associated protein 1A/1B-light chain 3; mTORC1, mammalian target of rapamycin complex 1; NAA20, *N*(α)-acetyltransferase 20; ATG, autophagy-related; S6RP, S6 ribosomal protein

Received 03.8.14; revised 14.11.14; accepted 19.11.14; Edited by M Piacentini; published online 19.12.14

in vivo experiments designed to explore the health-improving effects of coffee.[24] Spermidine turned out to be an efficient inhibitor of histone acetyltransferases *in vitro*[13] and reduced the global protein acetylation levels in cultured cells.[25,26]

Driven by these premises, we investigated the hypothesis that several health-related compounds including anacardic acid, curcumin, garcinol and spermidine might induce autophagy by inhibition of acetyltranferases. Here we report results supporting this hypothesis. Moreover, we demonstrate that one particular acetyltransferase, EP300 (E1A-binding protein p300), negatively controls autophagy and that anacardic acid, curcumin, garcinol and spermidine may induce autophagy by directly inhibiting EP300.

Results and discussion

Anacardic acid, curcumin, garcinol and spermidine induce autophagy and deacetylation of cellular proteins. Anacardic acid (6-pentadecyl-salicylic acid from the nutshell of the cashew, *Anacardium occidentale*), curcumin (from the South Asian spice turmeric, *Curcuma longa*, one of the principal ingredients of curry powder), garcinol (from the fruit of the Kokum tree, *Garcina indica*) or spermidine (a polyamine contained in all organisms, but found at particularly high concentrations in some health-related products such as durian fruit, fermented soybeans and wheat germs) were all able to stimulate the formation of GFP-LC3 puncta when added to human U2OS cells stably expressing this fluorescent biosensor (Figures 1a and b). Induction of GFP-LC3 puncta was also observed in the presence of bafilomycin A1, a specific inhibitor of the vacuolar ATPase required for the fusion between autophagosomes and lysosomes (Figure 1c), supporting the notion that these agents induce autophagic flux.[2] When added to non-transfected U2OS cells, anacardic acid, curcumin, garcinol and spermidine also stimulated the autophagy-associated lipidation of LC3, which increases its electrophoretic mobility to create the LC3-II form, in both the absence and presence of bafilomycin A1 (Figure 1d), confirming that they induce autophagy. These results were confirmed in additional human cancer cell lines as well as in primary, non-transformed murine embryonic fibroblasts (Supplementary Figure 1). Anacardic acid, curcumin, garcinol and spermidine also reduced the overall lysine acetylation of cellular proteins (Figures 2a and b), determined by means of a protocol in which cells were fixed in such a way that the plasma membrane but not the nuclear envelope would be permeabilized, allowing a fluorescence-labeled antibody-recognizing proteins with acetylated lysines to gain access to the cytoplasm but not the nucleus.[23] The magnitude of deacetylation induced by these compounds correlated with their potential to induce autophagy (Figure 2c). Anacardic acid, curcumin, garcinol and spermidine also reduced the phosphorylation of S6RP (S6 ribosomal protein), a substrate of p70S6K (p70S6 kinase), which operates downstream of mTORC1, correlating with their autophagy-inducing capacity (Figures 2d–f). Moreover, all the mentioned acetyltransferase inhibitors induced a significant reduction of p62/SQSTM1 levels, thus confirming (together with the results shown in

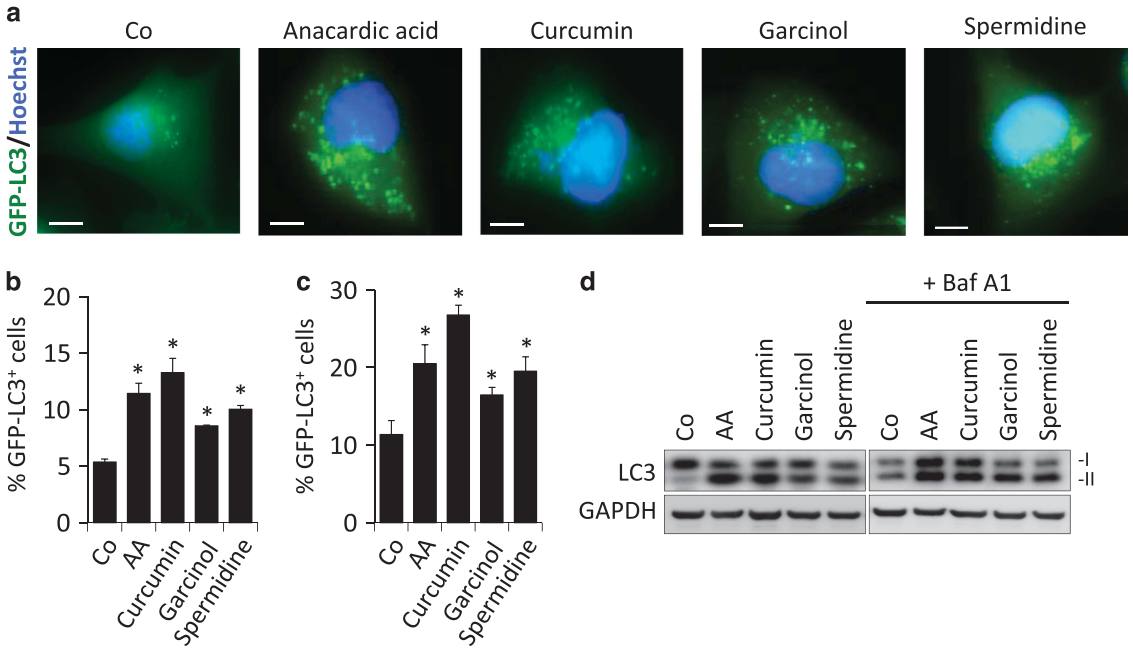

Figure 1 Chemical inhibition of acetyltransferases increases autophagic flux. (**a**) Representative fluorescence pictures of human U2OS cells stably expressing the autophagosome marker GFP-LC3 after treatment with the indicated acetyltransferase inhibitors for 4 h in a complete culture media (Co). (**b** and **c**) Quantification of GFP-LC3 dots for the data depicted in (**a**) either in the absence (**b**) or presence (**c**) of the lysosomal inhibitor bafilomycin A1 (Baf A1), to measure autophagic flux. (**d**) Representative immunoblots of total cell lysates showing an increase in LC3-II formation (LC3 lipidation) upon treatment with the indicated acetyltransferase inhibitors either in the presence or absence of Baf A1. Graphic bars represent average and S.E.M. values for at least three independent experiments. **P*-values <0.05 in two-tailed Student's *T*-test as compared with control. Scale bars, 5 μm

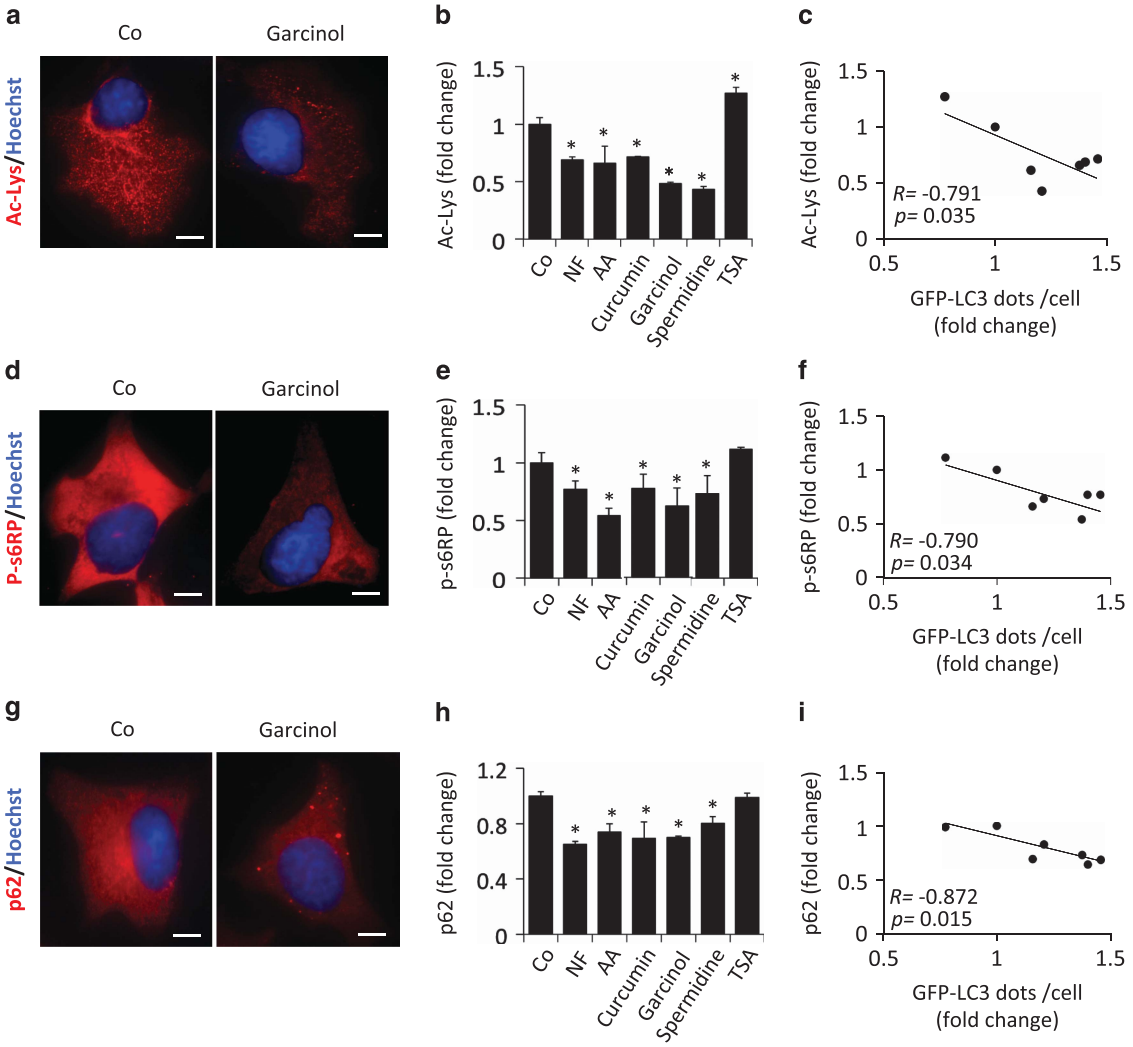

Figure 2 Inhibition of acetyltransferase reduces both cytoplasmic protein acetylation and mTORC1 activity. (**a**) Representative microphotographs of human U2OS cells either untreated (Co) or treated with acetyltransferase inhibitors (garcinol as an example) after staining for the detection of cytoplasmic acetylated lysine epitopes. (**b**) Quantification of the average lysine acetylation of cytoplasmic proteins after treatment with different acetyltransferase inhibitors. (**c**) Scatter graph showing the correlation between the number of GFP-LC3 dots per cell and the average level of cytoplasmic protein lysine acetylation upon treatment with the indicated acetyltransferase inhibitors. NF and trichostatin A (TSA), which were used as controls for decreased (NF) or increased (TSA) cytoplasmic protein acetylation. (**d**) Representative pictures of U2OS cells treated as in (**a**) after staining for the detection of phosphorylated ribosomal protein S6 (p-S6RP). (**e**) Quantification of the average phosphorylation level of p-S6RP after treatment with acetyltransferase inhibitors. (**f**) Scatter graph showing the correlation between an increase of GFP-LC3 dots per cell and a decrease of cytoplasmic protein lysine acetylation. (**g**) Representative pictures of U2OS cells treated as in (**a**) after staining for the detection of p62/SQSTM1. (**h**) Quantification of the average cellular level of p62/SQSTM1 after treatment with acetyltransferase inhibitors. (**i**) Scatter graph showing the correlation between an increase in GFP-LC3 dots per cell and a decrease in p62/SQSTM1 cellular levels. Graphic bars represent average and S.E.M. values for at least three independent experiments. **P*-values <0.05 in two-tailed Student's *T*-test as compared with control. Scale bars, 10 μm

Figure 1) the induction of a *bona fide* autophagic flux (Figures 2g and h). In this regard, we could observe that the reduction of cellular p62/SQSTM1 levels significantly correlated with the increase of GFP-LC3 puncta accumulation (Figure 2i). Altogether, these results reveal the ability of anacardic acid, curcumin, garcinol and spermidine to stimulate a stereotyped molecular cascade of biochemical events that resembles that induced by NF conditions: deacetylation of cellular proteins, inhibition of the mTORC1 pathway and induction of autophagy.

Identification of the acetyltransferase EP300 as a major endogenous repressor of autophagy. To identify the acetyltransferase(s) that control(s) autophagy, we systematically compared the capacity of pharmacological autophagy inducers to the small interfering RNA (siRNA)-mediated knockdown of 43 distinct gene products annotated as protein acetyltransferases with regard to four parameters: (i) induction of GFP-LC3 puncta in the presence of bafilomycin A1, (ii) reduction in the expression of the autophagic substrate p62/SQSTM1 in the absence of bafilomycin A1, (iii) dephosphorylation of s6RP and (iv) protein lysine deacetylation. Knockdown of only two acetyltransferases was able to induce the triad of GFP-LC3 puncta, p62/SQSTM1 depletion, and s6RP dephosphorylation. This applies to EP300, which is a lysine acetyltranferase, and NAA20, (*N*(α)-acetyltransferase 20,

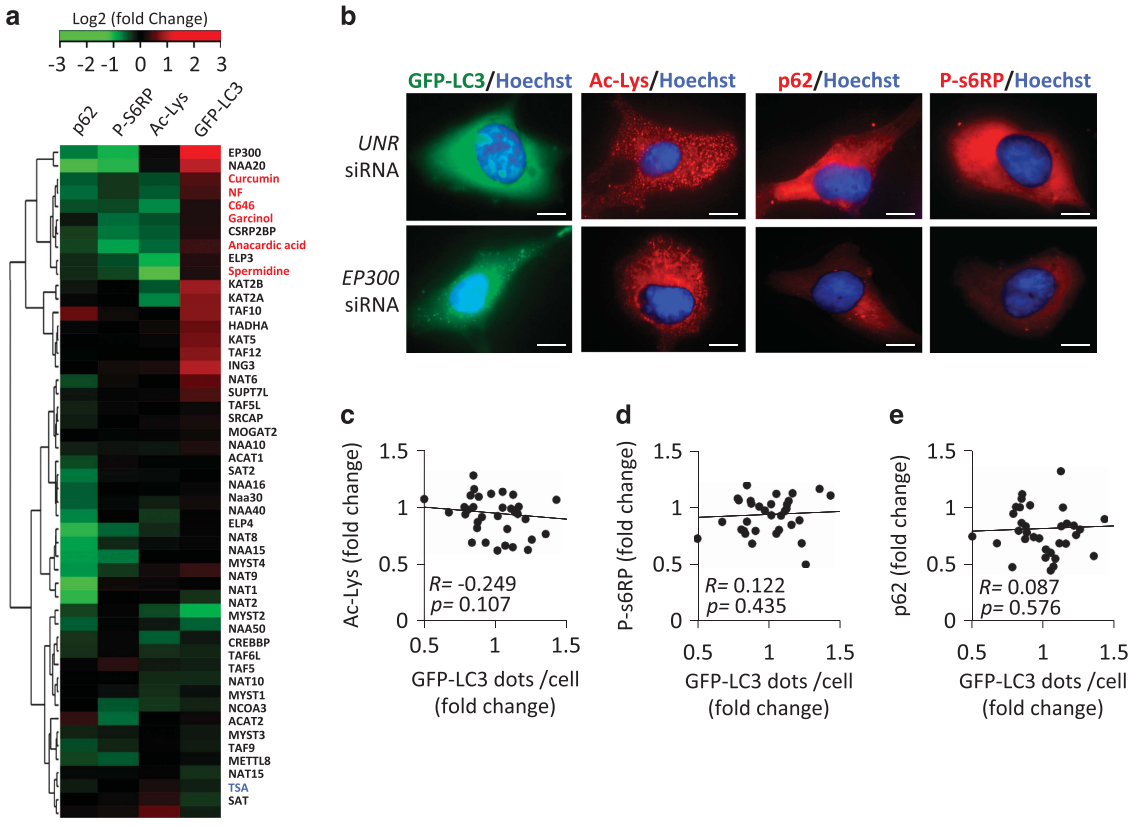

Figure 3 Specific knockdown of a single acetyltransferase has no major impact on the lysine acetylation of cytoplasmic protein. (**a**) Hierarchical clustering and heat map depicting relative intensity values for immunofluorescence analyses against either p62/SQSTM1, phospho-s6-ribosomal protein (p-s6RP) or acetyl-lysine (Ac-lys) epitopes and GFP-LC3 puncta accumulation in the presence of bafilomycin A1 (Baf A1) after systematic knockdown of 43 distinct acetyltransferases and treatment with different acetyltransferase inhibitors in U2OS cells. In the case of gene knockdown, each square from the heat map represents the average fold change value of two siRNAs targeting each of the acetyltransferase genes. Gene names are depicted in black, whereas chemical acetyltransferase inhibitors and NF conditions are shown in red. Trichostatin A (TSA) used as a positive control for increase in proteins acetylation is shown in blue. (**b**) Representative pictures of U2OS cells either untreated (Co), treated with acetyltransferase inhibitors (curcumin as an example) or after single knockdown of acetyltransferase genes (EP300 as an example). (**c**–**e**) Scatter graph showing the correlation between the number of GFP-LC3 dots per cell and the average level of cytoplasmic protein lysine acetylation (**c**) or s6RP phosphorylation (**d**) or p62/SQSTM1 degradation (**e**) upon specific knockdown of single acetyltransferase genes. Scale bars, 5 μm

also known as NAT5), which catalyzes the N-terminal acetylation of methionine residues, an irreversible posttranscriptional modification, and not the reversible acetylation of *N*-ε-lysine groups. The absence of antibodies recognizing acetylated methionine prompted us to focus our studies on the characterization of EP300 activity. Knockdown of EP300 however failed to cause a significant decrease of protein lysine deacetylation (Figures 3a and b). Moreover, we were unable to detect a correlation between overall protein acetylation levels, s6RP phosphorylation or p62/SQSTM1 cellular content and autophagy induction by the knockdown of individual acetyltransferases (Figures 3c–e). This finding that may reflect the high specificity of such inhibitory manipulations, which target only one single acetyltransferase, compared with the chemical inhibitors, which likely target multiple acetyltransferases. Although knockdown of EP300 failed to reduce the overall acetylation status of cellular proteins (Figures 3a and b), inhibition of EP300 by a 'specific' antagonist, C646,[27] did cause such an effect if used at a concentration of 10 μM (Figure 4a). Careful dose–response studies, however, allowed us to dissociate the capacity of C646 to reduce protein acetylation and to induce GFP-LC3 puncta. At doses ranging from 300 nM to 1 μM, C646 did induce significant levels of LC3B puncta without causing detectable deacetylation of cellular proteins (Figures 4a and b). Thus, the available data indicate that this compound is a more potent autophagy inducer (operating at an ED_{50} of ~1 μM) than any of the other chemicals used in this study, in line with the fact that C646 can inhibit EP300 at an ED_{50} of ~1 μM.[27] Moreover, truly selective inhibition of EP300 (by depletion with two non-overlapping siRNAs or by low-dose C646) could induce autophagy without causing global protein deacetylation. Importantly, C646 potently induced GFP-LC3 puncta with a similar efficiency in intact cells and in cytoplasts, that is, cells that have been enucleated (Figures 5a and b), underscoring the possibility that EP300 mediates autophagy inhibition by cytoplasmic (non-nuclear, transcription-independent) effects.[28]

Spermidine induces autophagy by inhibiting the acetyltransferase activity of EP300. Several of the chemical autophagy inducers used in this study have been described to inhibit EP300. This applies to anacardic acid,[29] curcumin,[30] garcinol[31] and C646.[27] However, spermidine,

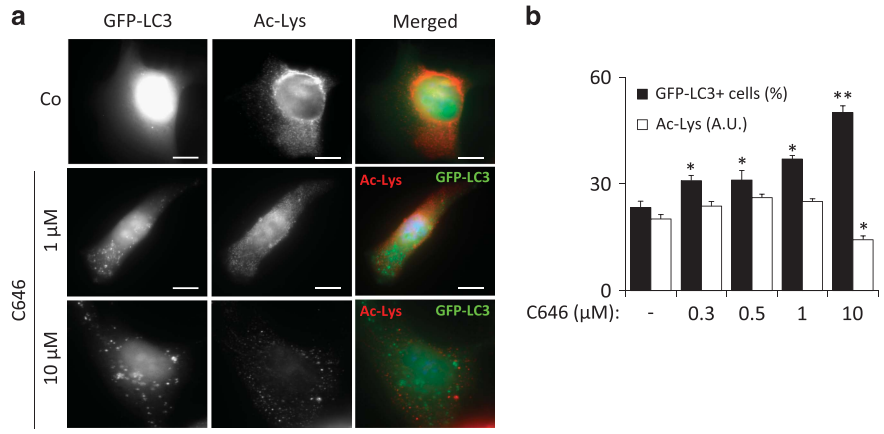

Figure 4 Chemical inhibition of EP300 acetyltransferase increases autophagic flux without affecting general protein acetylation levels. (**a**) Representative fluorescence pictures of human U2OS cells stably expressing the autophagosome marker GFP-LC3 that were either untreated (Co) or treated with EP300-specific inhibitor C646 at the depicted concentrations after staining for the detection of cytoplasmic acetylated lysine epitopes. (**b**) Graph showing the percentage of GFP-LC3$^+$ cells (cells with more than 25 GFP-LC3 puncta) as well as the average lysine acetylation of cytoplasmic proteins after treatment with different concentrations of the EP300 inhibitor C646. Graphic bars represent average and S.E.M. values for at least three independent experiments. *P-values <0.05 in two-tailed Student's T-test as compared with control. Scale bars, 5 μm

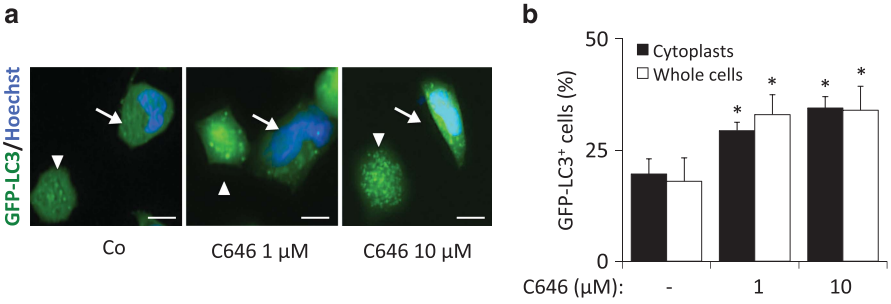

Figure 5 The effects of chemical inhibition of EP300 acetyltransferase are nucleus-independent. (**a**) Representative pictures for GFP-LC3 puncta accumulation in both enucleated (cytoplasts, arrowheads) and nucleated cells (arrows) treated with C646 at the depicted concentrations. (**b**) Quantification of the percentage of GFP-LC3$^+$ cells or cytoplasts (showing more than 25 GFP-LC3 puncta) after treatment with C646 for 4 h in the presence of bafilomycin A1 (Baf A1). Graphic bars represent average and S.E.M. values for at least three independent experiments. *P-values <0.05 in two-tailed Student's T-test as compared with control. Scale bars, 5 μm

which is known to inhibit histone acetyltransferases in yeast (that lacks an EP300 ortholog), has not yet been evaluated for its capacity to interfere with the catalytic activity of EP300. In a cell-free system, spermidine inhibited the capacity of recombinant human EP300 protein to acetylate its substrate histone H3 (Figures 6a and b). This effect was obtained at a physiological concentration of the acetyl donor acetyl-CoA of 10 μM, yet was attenuated when acetyl-CoA levels were raised 10-fold to 100 μM (Figures 6c and d and Supplementary Figure 2), suggesting that spermidine acts as a competitive inhibitor, similar to the aforementioned agents.[27,29–31]

Concluding remarks. The results in this paper underscore the notion that inhibitors of acetyltransferases act as potent autophagy inducers. Among the agents evaluated in this work, spermidine may represent the most attractive agent for therapeutic use, for multiple reasons. First, spermidine is a natural compound contained in all cells, including those of our body, which means that all mammals, including humans, physiologically dispose of an endogenous pool of this polyamine. Second, to date no adverse effects of exogenous supply of spermidine have been reported to the best of our knowledge. Third, spermidine has a broad longevity-extending activity in multiple species from yeast to rodents.[13,32–35] Spermidine retards the manifestation of several major age-associated diseases including arterial aging,[36] colon cancer[37] and neurodegenerative processes in mice,[19,38,39] suggesting that it may be used for the prophylaxis of major age-related pathologies.

Here we report the evidence that spermidine may act as an autophagy inducer by virtue of its capacity to inhibit acetyltransferases. Beyond its capacity to reduce the overall levels of protein acetylation, spermidine also inhibits EP300, the acetyltransferase that physiologically acts as a sensor of nutrient-dependent acetyl-CoA levels[19] and that directly acetylates and inhibits several core autophagy proteins including ATG5, ATG7, ATG12 and LC3.[28] Thus, the autophagy-repressive activity of EP300 may not only depend on the intracellular concentration of acetyl-CoA but may also be regulated by the presence of spermidine (and likely other polyamines) that acts as a competitive inhibitor or its

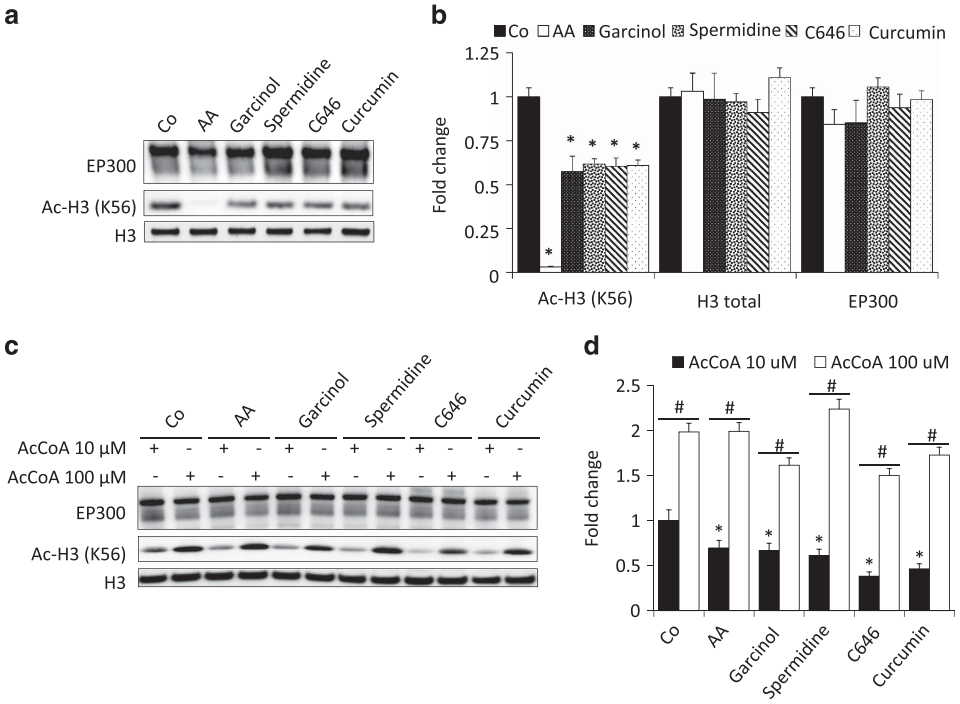

Figure 6 Spermidine competitively inhibits EP300 acetyltransferase activity in a cell-free system. (**a**) Representative blots showing the inhibition of EP300 *in vitro* acetyltransferase activity against histone H3, one of EP300 preferred substrates. Anacardic acid (AA) was used as a positive control for EP300 inhibition. (**b**) Quantification of the data obtained in several independent experiments. (**c**) EP300 inhibition by different acetyltransferase inhibitors, including spermidine, was reverted by raising the acetyl-CoA (AcCoA) concentration from 10 to 100 μM, suggesting the competitive nature of EP300 inhibition. (**d**) Quantification of the data corresponding to several replicate experiments similar to that shown in (**c**). Graphic bars in (**b** and **d**) represent average and S.E.M. values for at least three independent experiments. **P*-value <0.05 in two-tailed Student's *T*-test as compared with control in the absence of inhibitors; $^{\#}$*P*-value <0.05 in two-tailed Student's *T*-test as compared with the same condition in the presence of 100 μM of AcCoA

acetyltransferase activity. In fact, this is the first insight into the molecular mechanism(s) by which spermidine stimulates autophagic flux in mammalian cells. Further analyses on the capacity of spermidine to inhibit acetyltransferases should elucidate the mechanisms through which this polyamine exerts beneficial effects in diverse pathophysiological contexts. Furthermore, it may be tempting to develop new, truly specific EP300 inhibitors as investigational drugs and – perhaps – new lead compounds for the therapeutic induction of autophagy.

Materials and Methods

Chemicals, cell lines and culture conditions. Unless otherwise specified, chemicals were purchased from Sigma-Aldrich (St. Louis, MO, USA), culture media and supplements for cell culture were from Gibco-Invitrogen (Carlsbad, CA, USA) and plasticware was from Corning (Corning, NY, USA). Human osteosarcoma U2OS cells and their GFP-LC3-expressing derivatives were cultured in DMEM medium containing 10% fetal bovine serum, 100 mg/l sodium pyruvate, 10 mM HEPES buffer, 100 U/ml penicillin G sodium and 100 mg/ml streptomycin sulfate (37 °C, 5% CO_2). Cells were seeded in 6- and 12-well plates or in 10 and 15 cm dishes and grown for 24 h before treatment with 100 μM curcumin, 50 μM anacardic acid, 3 μM garcinol, 1 or 10 μM C646, 100 μM spermidine and 50 μM TSA. For serum and nutrient deprivation, cells were cultured in serum-free Earle's balanced salt solution.

RNA interference in human cell cultures. siRNAs were reverse transfected with the help of the RNAi MaxTM transfection reagent (Invitrogen, Eugene, OR, USA) according to the manufacturer's instructions. Sequences of the different siRNAs used in this study have been published previously.[19]

Preparation of cytoplasts. U2OS cells stably expressing GFP-LC3 were trypsinized and incubated in 3 ml of complete medium supplemented with 7.5 mg/ml cytochalasin B for 45 min at 37 °C. This cell suspension was layered onto a discontinuous Ficoll density gradient (3 ml of 55%, 1 ml of 90% and 3 ml of 100% Ficoll-Paques; GE Healthcare, Buckinghamshire, UK) in complete medium containing 7.5 mg/ml cytochalasin B. Gradients were prepared in ultracentrifuge tubes and pre-equilibrated at 37 °C in a CO_2 incubator overnight. Gradients containing cell suspensions were centrifuged in a prewarmed rotor (SW41; Beckman Coulter, Brea, CA, USA) at 30 000 × *g* for 30 min at 32 °C. The cytoplast-enriched fraction was collected from the interface between 55 and 90% Ficoll layers, washed in complete medium and incubated for 4 h at 37 °C before treatments.

Immunoblotting. For immunoblotting, 25 μg of proteins were separated on 4–12% Bis-Tris acrylamide (Invitrogen) or 12% Tris-Glycine SDS-PAGE precast gels (Bio-Rad, Hercules, CA, USA) and electrotransferred to Immobilon membranes (Millipore Corporation, Billerica, MA, USA). Membranes were then sliced into different parts according to the molecular weight of the protein of interest to allow simultaneous detection of different antigens within the same experiment. Unspecific binding sites were saturated by incubating membranes for 1 h in 0.05% Tween-20 (v : v in TBS) supplemented with 5% non-fat powdered milk (w : v in TBS), followed by an overnight incubation with primary antibody. Development was performed with appropriate horseradish peroxidase (HRP)-labeled secondary antibodies (Southern Biotech, Birmingham, USA) plus the SuperSignal West Pico chemoluminescent substrate (Thermo Scientific-Pierce). An anti-glyceraldehyde-3-phosphate dehydrogenase antibody (Chemicon International, Temecula, CA, USA) was used to control equal loading of lanes.

Automated microscopy. U2OS cells stably expressing GFP-LC3 were seeded in 96-well imaging plates (BD Falcon, Sparks, MD, USA) 24 h before stimulation. Cells were treated with the indicated agents for 4 h. Subsequently, cells were fixed with 4% PFA and counterstained with 10 μM Hoechst 33342. Images were acquired using a BD pathway 855 automated microscope (BD Imaging

Systems, San Jose, USA) equipped with a ×40 objective (Olympus, Center Valley, PA, USA) coupled to a robotized Twister II plate handler (Caliper Life Sciences, Hopkinton, MA, USA). Images were analyzed for the presence of GFP-LC3 puncta in the cytoplasm by means of the BD Attovision software (BD Imaging Systems). Cell surfaces were segmented and divided into cytoplasmic and nuclear regions according to standard proceedings. RB 2×2 and Marr-Hildreth algorithms were used to detect cytoplasmic GFP-LC3-positive dots.

Statistical analyses were conducted using the R software (http://www.r-project.org/). For quantitative analyses of protein acetylation, cell surfaces were segmented into cytoplasmic and nucleic regions, and average staining intensity of each individual cell was measured for statistical analysis.

Immunofluorescence. Cells were fixed with 4% PFA for 15 min at room temperature and permeabilized with 0.1% Triton X-100 for 10 min, except for staining of cytoplasmic acetyl-lysine-containing proteins, in which any permeabilization step further than PFA fixation was avoided. Nonspecific binding sites were blocked with 5% bovine serum albumin in PBS, followed by incubation with primary antibodies overnight at 4 °C. Later, the cells were incubated with appropriate Alexa Fluor conjugates (Molecular Probes-Invitrogen, Eugene, OR, USA). In the case of cytoplasmic acetyl-lysine staining, an additional step of blocking using anti-acetylated-tubulin antibody (1 : 200) was applied. Ten micromoles of Hoechst 33342 (Molecular Probes-Invitrogen) was used for nuclear counterstaining. Fluorescence wide-field and confocal microscopy assessments were performed on an DM IRE2 microscope (Leica Microsystems, Wetzlar, Germany) equipped with a DC300F camera and with an LSM 510 microscope (Carl Zeiss, Jena, Germany), respectively.

Fluorescence microscopy. Confocal fluorescence images were captured using a Leica TCS SPE confocal fluorescence microscope (Leica Microsystems). Non-confocal images were acquired with an Axio Observer inverted fluorescence microscope (Carl Zeiss). For experiments with human cell lines, a Leica APO x63 NA 1.3 immersion objective was used, whereas for the analysis of GFP-LC3 mice tissue sections, a Leica APO x40 NA 1.15 immersion objective was used. Zeiss Immersol immersion oil (Zeiss, Jena, Germany) was used for all microscopic analyses. Images were acquired with a Leica DFC 350 Fx camera (version 1.8.0) using Leica LAS AF software and processed with Adobe Photoshop (version CS2) software (Adobe Systems, San Jose, CA, USA).

***In vitro* acetylation assay.** Recombinant GST-EP300 fusion protein, corresponding to amino acids 1066–1707 (14–418; Millipore, Billerica, MA, USA) was assessed for its acetyltransferase activity on the EP300 natural substrate recombinant histone H3 protein (M2503S; New England Biolabs, Ipswich, MA, USA). Briefly, 1 μg of EP300 HAT domain was incubated in the presence of an HAT assay buffer (250 mM Tris-HCl, pH 8.0, 50% glycerol, 0.5 mM EDTA and 5 mM dithiothreitol), 1 μg of histone H3 protein and 10 or 100 μM of acetyl-CoA (A2056; Sigma-Aldrich) for 1 h at 30 °C. The reaction was stopped by adding 4x SDS buffer and boiling the samples. Acetylation of substrate proteins was measured by immunoblotting using specific antibodies against H3K56 (Cell Signaling, Danvers, MA, USA).

Statistical analyses. Unless otherwise mentioned, experiments were performed in triplicate and repeated at least two times. Data were analyzed using the GraphPad Prism 5 software (Graphpad software, La Jolla, CA, USA) and statistical significance was assessed by means of two-tailed Student's *t*-test or ANOVA tests, as appropriate.

Conflict of Interest

The authors declare no conflict of interest.

Acknowledgements. GK is supported by the Ligue contre le Cancer (équipe labelisée); Agence National de la Recherche (ANR); Association pour la recherche sur le cancer (ARC); Cancéropôle Ile-de-France; Institut National du Cancer (INCa); Fondation Bettencourt-Schueller; Fondation de France; Fondation pour la Recherche Médicale (FRM); the European Commission (ArtForce); the European Research Council (ERC); the LabEx Immuno-Oncology; the SIRIC Stratified Oncology Cell DNA Repair and Tumor Immune Elimination (SOCRATE); the SIRIC Cancer Research and Personalized Medicine (CARPEM); and the Paris Alliance of Cancer Research Institutes (PACRI). FM is supported by FWF Grants LIPOTOX, P23490-B12, I1000 and P24381-B20. MN-S. is supported by the Fondation pour la Recherche Médicale (FRM).

1. Feng Y, He D, Yao Z, Klionsky DJ. The machinery of macroautophagy. *Cell Res* 2014; **24**: 24–41.
2. Klionsky DJ, Abdalla FC, Abeliovich H, Abraham RT, Acevedo-Arozena A, Adeli K *et al.* Guidelines for the use and interpretation of assays for monitoring autophagy. *Autophagy* 2012; **8**: 445–544.
3. Levine B, Kroemer G. Autophagy in the pathogenesis of disease. *Cell* 2008; **132**: 27–42.
4. Madeo F, Tavernarakis N, Kroemer G. Can autophagy promote longevity? *Nat Cell Biol* 2010; **12**: 842–846.
5. Rubinsztein DC, Marino G, Kroemer G. Autophagy and aging. *Cell* 2011; **146**: 682–695.
6. Lopez-Otin C, Blasco MA, Partridge L, Serrano M, Kroemer G. The hallmarks of aging. *Cell* 2013; **153**: 1194–1217.
7. Longo VD, Mattson MP. Fasting: molecular mechanisms and clinical applications. *Cell Metab* 2014; **19**: 181–192.
8. Harrison DE, Strong R, Sharp ZD, Nelson JF, Astle CM, Flurkey K *et al.* Rapamycin fed late in life extends lifespan in genetically heterogeneous mice. *Nature* 2009; **460**: 392–395.
9. Anisimov VN, Zabezhinski MA, Popovich IG, Piskunova TS, Semenchenko AV, Tyndyk ML *et al.* Rapamycin increases lifespan and inhibits spontaneous tumorigenesis in inbred female mice. *Cell cycle* 2011; **10**: 4230–4236.
10. Blagosklonny MV. Linking calorie restriction to longevity through sirtuins and autophagy: any role for TOR. *Cell Death Dis* 2010; **1**: e12.
11. Hubbard BP, Sinclair DA. Small molecule SIRT1 activators for the treatment of aging and age-related diseases. *Trends Pharmacol Sci* 2014; **35**: 146–154.
12. Sinclair DA, Guarente L. Small-molecule allosteric activators of sirtuins. *Annu Rev Pharmacol Toxicol* 2014; **54**: 363–380.
13. Eisenberg T, Knauer H, Schauer A, Buttner S, Ruckenstuhl C, Carmona-Gutierrez D *et al.* Induction of autophagy by spermidine promotes longevity. *Nat Cell Biol* 2009; **11**: 1305–1314.
14. Tavernarakis N, Pasparaki A, Tasdemir E, Maiuri MC, Kroemer G. The effects of p53 on whole organism longevity are mediated by autophagy. *Autophagy* 2008; **4**: 870–873.
15. Jia K, Levine B. Autophagy is required for dietary restriction-mediated life span extension in *C. elegans*. *Autophagy* 2007; **3**: 597–599.
16. Morselli E, Maiuri MC, Markaki M, Megalou E, Pasparaki A, Palikaras K *et al.* Caloric restriction and resveratrol promote longevity through the Sirtuin-1-dependent induction of autophagy. *Cell Death Dis* 2010; **1**: e10.
17. Bjedov I, Toivonen JM, Kerr F, Slack C, Jacobson J, Foley A *et al.* Mechanisms of life span extension by rapamycin in the fruit fly *Drosophila melanogaster*. *Cell Metab* 2010; **11**: 35–46.
18. Pyo JO, Yoo SM, Ahn HH, Nah J, Hong SH, Kam TI *et al.* Overexpression of Atg5 in mice activates autophagy and extends lifespan. *Nat Commun* 2013; **4**: 2300.
19. Marino G, Pietrocola F, Eisenberg T, Kong Y, Malik SA, Andryushkova A *et al.* Regulation of autophagy by cytosolic acetyl-coenzyme A. *Mol Cell* 2014; **53**: 710–725.
20. Schroeder S, Pendl T, Zimmermann A, Eisenberg T, Carmona-Gutierrez D, Ruckenstuhl C *et al.* Acetyl-coenzyme A: a metabolic master regulator of autophagy and longevity. *Autophagy* 2014; **10**: 1335–1337.
21. Eisenberg T, Schroeder S, Buttner S, Carmona-Gutierrez D, Pendl T, Andryushkova A *et al.* A histone point mutation that switches on autophagy. *Autophagy* 2014; **10**: 1143–1145.
22. Eisenberg T, Schroeder S, Andryushkova A, Pendl T, Kuttner V, Bhukel A *et al.* Nucleocytosolic depletion of the energy metabolite acetyl-coenzyme a stimulates autophagy and prolongs lifespan. *Cell Metab* 2014; **19**: 431–444.
23. Pietrocola F, Marino G, Lissa D, Vacchelli E, Malik SA, Niso-Santano M *et al.* Pro-autophagic polyphenols reduce the acetylation of cytoplasmic proteins. *Cell Cycle* 2012; **11**: 3851–3860.
24. Pietrocola F, Malik SA, Marino G, Vacchelli E, Senovilla L, Chaba K *et al.* Coffee induces autophagy *in vivo*. *Cell Cycle* 2014; **13**: 1987–1994.
25. Morselli E, Marino G, Bennetzen MV, Eisenberg T, Megalou E, Schroeder S *et al.* Spermidine and resveratrol induce autophagy by distinct pathways converging on the acetylproteome. *J Cell Biol* 2011; **192**: 615–629.
26. Marino G, Morselli E, Bennetzen MV, Eisenberg T, Megalou E, Schroeder S *et al.* Longevity-relevant regulation of autophagy at the level of the acetylproteome. *Autophagy* 2011; **7**: 647–649.
27. Bowers EM, Yan G, Mukherjee C, Orry A, Wang L, Holbert MA *et al.* Virtual ligand screening of the p300/CBP histone acetyltransferase: identification of a selective small molecule inhibitor. *Chem Biol* 2010; **17**: 471–482.
28. Lee IH, Finkel T. Regulation of autophagy by the p300 acetyltransferase. *J Biol Chem* 2009; **284**: 6322–6328.
29. Devipriya B, Kumaradhas P. Probing the effect of intermolecular interaction and understanding the electrostatic moments of anacardic acid in the active site of p300 enzyme via DFT and charge density analysis. *J Mol Graphics Modell* 2012; **34**: 57–66.

30. Devipriya B, Kumaradhas P. Molecular flexibility and the electrostatic moments of curcumin and its derivatives in the active site of p300: a theoretical charge density study. *Chem-Biol Interact* 2013; **204**: 153–165.
31. Balasubramanyam K, Altaf M, Varier RA, Swaminathan V, Ravindran A, Sadhale PP *et al.* Polyisoprenylated benzophenone, garcinol, a natural histone acetyltransferase inhibitor, represses chromatin transcription and alters global gene expression. *J Biol Chem* 2004; **279**: 33716–33726.
32. Madeo F, Eisenberg T, Buttner S, Ruckenstuhl C, Kroemer G. Spermidine: a novel autophagy inducer and longevity elixir. *Autophagy* 2010; **6**: 160–162.
33. Minois N, Carmona-Gutierrez D, Bauer MA, Rockenfeller P, Eisenberg T, Brandhorst S *et al.* Spermidine promotes stress resistance in *Drosophila melanogaster* through autophagy-dependent and -independent pathways. *Cell Death Dis* 2012; **3**: e401.
34. Gupta VK, Scheunemann L, Eisenberg T, Mertel S, Bhukel A, Koemans TS *et al.* Restoring polyamines protects from age-induced memory impairment in an autophagy-dependent manner. *Nat Neurosci* 2013; **16**: 1453–1460.
35. Kibe R, Kurihara S, Sakai Y, Suzuki H, Ooga T, Sawaki E *et al.* Upregulation of colonic luminal polyamines produced by intestinal microbiota delays senescence in mice. *Scientific Rep* 2014; **4**: 4548.
36. LaRocca TJ, Gioscia-Ryan RA, Hearon Jr CM, Seals DR. The autophagy enhancer spermidine reverses arterial aging. *Mech Ageing Dev* 2013; **134**: 314–320.
37. Soda K, Kano Y, Chiba F, Koizumi K, Miyaki Y. Increased polyamine intake inhibits age-associated alteration in global DNA methylation and 1,2-dimethylhydrazine-induced tumorigenesis. *PLoS One* 2013; **8**: e64357.
38. Velloso NA, Dalmolin GD, Gomes GM, Rubin MA, Canas PM, Cunha RA *et al.* Spermine improves recognition memory deficit in a rodent model of Huntington's disease. *Neurobiol Learn Mem* 2009; **92**: 574–580.
39. Wang IF, Guo BS, Liu YC, Wu CC, Yang CH, Tsai KJ *et al.* Autophagy activators rescue and alleviate pathogenesis of a mouse model with proteinopathies of the TAR DNA-binding protein 43. *Proc Natl Acad Sci USA* 2012; **109**: 15024–15029.

Supplementary Information accompanies this paper on Cell Death and Differentiation website (http://www.nature.com/cdd)